UiT
THE ARCTIC
UNIVERSITY
OF NORWAY

Faculty of Science and Technology

Department of Geosciences

Holocene glacier history of Svalbard:

Retracing the style of (de-)glaciation

—

Wesley R. Farnsworth

A dissertation for the degree of Philosophiae Doctor – December 2018

Holocene glacier history of Svalbard: Retracing the style of (de-)glaciation

Wesley R. Farnsworth

Holocene glacier history of Svalbard: Retracing the style of (de-)glaciation

Wesley Randall Farnsworth

A dissertation submitted to the Faculty of Science and Technology,
UiT The Arctic University of Norway
for the degree of Philosophiae Doctor (PhD)

Department of Arctic Geology
The University Centre in Svalbard (UNIS)

And

Department of Geosciences
UiT, The Arctic University of Norway

December 2018

Title: Holocene glacier history of Svalbard: Retracing the style of (de-)glaciation

Author: Wesley Randall Farnsworth

Supervision by:

Prof. Ólafur Ingólfsson (University Centre in Svalbard & University of Iceland)
Prof. Michael Retelle (Bates College & University Centre in Svalbard)
Prof. Anders Schomacker (UiT, The Arctic University of Norway)

ISBN (print):
ISBN (online):

Print in Norway:

Front cover illustration: *Modified oblique aerial photograph (ID: S38_1850) taken in 1938 by the Norwegian Polar Institute from an altitude of 2900 m a.s.l. above the eastern margin of Valhallfonna with a view to the south down Lomfjorden. The bay of De Geerbukta and the Fakse moraine system are located in the foreground.*

Abstract

Identifying the key factors that influence the global cryosphere and eustatic sea level are critical in today's populated world characterized by a changing climate. Within the Arctic, which has recently experienced amplified warming, and located between the Polar Northern Atlantic and the Arctic seasonal sea-ice, the Svalbard archipelago experiences a heightened sensitivity to climate change. Studying the processes, dynamics and historic fluctuations of Svalbard's glaciers and climate is critical. Understanding these elements allows us to place current rates of change into longer-term perspective and ultimately to better model future climatic conditions. This study synthesizes the state of the art of Svalbard's Holocene glacial and climate history. Chapters (i) introduce new findings of Holocene glaciers and climate; (ii) discuss the factors influencing Svalbard ice margins; (iii) summarize accumulated knowledge in the perspective of today's paradigm; and (iv) outline potential approaches to address further unknowns regarding the Holocene on Svalbard.

Through the Holocene, Svalbard glaciers have exhibited at least two phases of widespread re-advances, one during the Early Holocene and another throughout the entire Late Holocene. No geomorphological features have been identified corresponding to glacier re-advances between 9.0 – 4.5 ka BP. The Early Holocene glacier re-advances are identified across Svalbard and correspond to a diverse range of glacier sizes. With our current level of age constraint, these ice marginal fluctuations do not appear synchronous. Furthermore, the Early Holocene climate is believed to have been warm, unfavorable for glacier growth, and characterized by deglaciation. Early Holocene glacier re-advances appear to relate to the time-transgressive nature of deglaciation. Thus, the re-advances correspond to glacio-dynamics (not mass balance) and reflect the complex style of ice-mass-loss during a changing climate.

Landforms and deposits from glaciers re-advancing during the Late Holocene have been the primary focus of Holocene glacial studies. Glacier re-advances and corresponding deposits have been attributed to episodic Neoglacial cooling and the Little Ice Age (LIA). The majority of Late Holocene glacier re-advances have been dated to between 4.0 – 0.5 ka BP with the highest frequency of re-advances constrained to 1.0 – 0.5 ka BP, during the first half of the LIA. It has been suggested that glacial landforms and deposits from LIA re-advances indicate rapid and dynamic glacier behavior, and in some cases surge-type events.

During the 20th century (i.e. post-LIA), Svalbard glaciers have exhibited widespread negative mass balance, ice marginal retreat, and glacier thinning. This phase of retreat has had a direct influence on glacier thermal regime, hydrologic system and surface profile. Through the 20th century, some Svalbard glaciers have continued to exhibit surge-type re-advances. Several glaciers have surged numerous times. These glacio-dynamic re-advances have been un-sustained and each subsequent surge has been less extensive then prior surges. Consequently, and despite re-advance, glaciers reflect a continual phase of ice-mass-loss in a periodic fashion.

Our understanding of Svalbard's Holocene glaciers and climate has progressed but critical components remain obscure. For example, although our understanding of the timing of the Holocene glacial minimum has improved, we lack detailed constraints on the extent of ice retreat across Svalbard during the Mid-Holocene. As reconstructions of palaeo-temperatures develop, the improvement of palaeo-precipitation proxies (e.g., leaf wax hydrogen isotopes) should continue. Additionally, as we approach further unknowns of Svalbard's Holocene history, it is evident that studies must take a holistic approach. Combining a mixture of archives, geochronological methods and emerging techniques will enhance the accuracy of reconstructions detailing Svalbard's glacial history.

Acknowledgements

Working under the supervision of Ólafur Ingólfsson, Michael Retelle and Anders Schomacker has been a highlight of this project. The experience, knowledge and encouragement I have been exposed to through last years in this team has exceeded all belief. I feel so fortunate to have the support, guidance and perspective of such an inspiring group of scientists, educators and leaders.

During my doctoral, I have also had privilege to be surrounded by outstanding mentors and role models. I am grateful for the boundless motivation, support and discussions fostered by; Helena Alexanderson, Ívar Örn Benediktsson, Skafti Brynjólfsson, Anders Bjørk, Max Eckerstorfer, Mark Furze, Graham L. Gilbert, Sten-Andreas Grundvåg, Anne Hormes, Ole Humlum, Kristian Kjeldsen, Kurt Kjær, Harold Lovell, Marc Macias-Fauria, Jordan Mertes, Hreggviður Norðdahl, Lena Rubensdotter, Heïdi Sevestre and Alan Werner. Thank you.

The development of this doctoral thesis has been greatly aided by a group of individuals whom have donated time, data, energy and expertise. I would like to thank all co-authors for their contributions and improvements to the manuscripts. Additionally, the thesis text has benefited from constructive feedback from Graham L. Gilbert, David C. Farnsworth and supervisors.

I have been fortunate enough to develop this project in the Arctic Geology Department at the University Centre in Svalbard. The hallway is my home and I am grateful for the community that evolves within it. Thank you for the company, encouragement, coffees (beers) and cakes. This doctoral project has also benefited from great support in the field (Sveinn Brynjólfssson & Sara Mollie Cohen), and internally at UNIS; from the Library (Berit Jakobsen & Catherine Fjeldstad) and from Logistics. Thank you for your support. This project has also greatly benefited from the open doors and inviting research communities at The Natural History Museum of Denmark, University of Copenhagen and the School of Engineering and Natural Science at the University of Iceland.

This doctoral project has been generously supported by the UNIS internal research fund, Svalbard Environmental Protection Fund, Carlsberg Foundation, Arctic Research and Studies, ResClim Research School, Arctic Field Grant from the Svalbard Science Forum and Letterstedtska Föreningen.

The ever-evolving community of Svalbard friends that has anchored me since January 2010, up until today, is the most valuable aspect of my life up here. I cannot image these last years without the love, laughs and strength that has come from you all. We have also had a pretty nice time. Thank you.

Finally, I would like to thank my family for their limitless love, support and encouragement. I also am endlessly grateful for my partner, Hrefna Dögg Gunnarsdóttir, for her love, patience and balance.

Thanks to you all.

Preface

This dissertation is submitted in partial fulfillment of the requirements for the Degree of Philosophiae Doctor (PhD) in Science. This thesis is a product of a four-year PhD study carried out at the University Centre in Svalbard (UNIS) between December 2014 and December 2018. The doctoral project was conducted in collaboration with UiT The Arctic University of Norway in Tromsø. The project was supervised by Ólafur Ingólfsson (University of Iceland and UNIS), Michael Retelle (Bates College and UNIS) and Anders Schomacker (UiT and the Natural History Museum of Denmark, University of Copenhagen).

While the four-year doctoral position was funded by the University Centre in Svalbard, additional funding for field work, data analysis, conference attendance and mobility was sought through different funding agencies. This doctoral project was financially supported primarily by the UNIS internal research fund (to Ingólfsson), Svalbard Environmental Protection Fund (16/35 to Farnsworth), Carlsberg Foundation (CF14-0756 to Schomacker), Arctic Research and Studies (to Schomacker & Farnsworth), ResClim Research School (to Farnsworth), Arctic Field Grant from the Svalbard Science Forum (to Schomacker) and Letterstedtska Föreningen (to Farnsworth).

In fulfillment of the 25% teaching and duty work written into the doctoral contract, Farnsworth gave lectures, ran exercises, instructed during field excursions and assisted in eight UNIS courses. Since spring 2015, Farnsworth contributed to 13 different classes including bachelor courses AG-204, AG-210, AG-220, as well as graduate courses AG-326/826, AG-330/830, AG-346, AG-348/848 and AS-301.

In addition to teaching, research findings from this doctoral project were disseminated through oral and poster presentations at 12 international conferences throughout the Nordic countries and North America. Oral presentations were given at all conferences unless otherwise noted. **2018**: PAST Gateways Durham, United Kingdom April; 33rd Nordic Geological Winter Meeting Copenhagen, Denmark January; **2017**: Geological Society of America, GSA Annual Meeting Seattle, USA October; International Quaternary Webinar October; PAST Gateways Kristineberg, Sweden May; **2016**: PAST Gateways Trondheim, Norway May; 32nd Nordic Geological Winter Meeting Helsinki, Finland January; **2015**: American Geophysical Union Annual Meeting, AGU San Francisco, USA December (Poster); ResClim PhD. Forum Askö, Sweden November; Nordic International Glaciological Symposia, IGS Copenhagen, Denmark October; International Glaciological Society, IGS Symposia Höfn, Iceland June (Poster); 45th International Arctic Workshop Bergen, Norway May (Poster).

This doctoral thesis is a synopsis of five research manuscripts:

***Farnsworth, W.R.,** Ingólfsson, Ó., Retelle, M., Allaart, L., Håkansson, L., Schomacker, A. (2018): Svalbard glaciers re-advanced during the Pleistocene-Holocene transition. *Boreas 47,* 1022-1032. DOI:10.1111/bor.12326.

Larsen, E., Lyså, A., Rubensdotter, L., **Farnsworth, W.R., Jensen, M., Nadeau, M. Ottesen, D. (2018): Lateglacial and Holocene glacier activity in the Van Mijenfjorden area, western Svalbard. *arktos.* DOI: 10.1007/s41063-018-0042-2.

***Farnsworth, W.R.,** Ingólfsson, Ó., Noormets, R., Allaart, L., Alexanderson, H., Henriksen, M., Schomacker, A. (2017): Dynamic Holocene glacial history of St. Jonsfjorden, Svalbard. *Boreas 46,* 585-603. DOI: 10.1111/bor.12269.

*****Farnsworth, W.R.,** Ingólfsson, Ó., Schomacker, A., Retelle, M. (2016): Over 400 previously undocumented Svalbard surge-type glaciers identified. *Geomorphology 264*, 52-60. DOI: 10.1016/j.geomorph.2016.03.025.

Farnsworth, W.R., Ingólfsson, Ó., Schomacker, A., Retelle, M. *in prep.* Holocene glacial and climate history of Svalbard - status, perspectives and challenges.

*Reprints were made with permission from *John Wiley & Sons, **Springer and ***Elsevier.*

CONTENTS

1. INTRODUCTION **1**
1.0.1 The Holocene 2
1.1 Svalbard 2
1.1.1 Regional setting and modern climate 2
1.1.2 Glacial history and relative sea level 3
1.1.3 Landscape and glaciers 6
1.1.4 Surge-type glaciers, behavior and landform assemblages 8
1.1.5 Aims and research objectives 9

2. METHODS **11**
2.0.1 Terrestrial stratigraphy and mapping 11
2.0.2 Marine data acquisition and processing 11
2.0.3 Sampling and radiocarbon dating 12

3. AUTHOR CONTRIBUTIONS AND MANUSCRIPT SUMMARIES **13**
3.1 Chapter I Farnsworth *et al.* 2018 14
3.2 Chapter II Larsen *et al.* 2018 15
3.3 Chapter III Farnsworth *et al.* 2017 16
3.4 Chapter IV Farnsworth *et al.* 2016 17
3.5 Chapter V Farnsworth *et al. in prep* 18

4. DISCUSSION **19**
4.1 Svalbard Holocene climate and the unknowns 19
4.1.1 Atlantic waters control the temperature 19
4.1.2 Palaeo-precipitation remains unknown 19
4.2 Drivers of Holocene glacier re-advances 20
4.2.1 Early Holocene re-advances 20
4.2.2 Neoglacial – Little Ice Age re-advances 21
4.2.3 Post-Little Ice Age re-advances 22
4.2.4 Early vs. Late Holocene ice cover variations 23
4.3 Advances in deglaciation 24
4.3.1 Restrained rebound and ice caps chasing the equilibrium line 24
4.3.2 Late Pleistocene – Early Holocene ice shelves on Svalbard 27
4.3.3 Modern glacier behavior as a model for past glacier dynamics 28

5. SUMMARY AND CONCLUSIONS **33**

6. FUTURE PERSPECTIVES **35**

References **36**

Research papers
Chapter I Farnsworth *et al.* 2018
Chapter II Larsen *et al.* 2018
Chapter III Farnsworth *et al.* 2017
Chapter IV Farnsworth *et al.* 2016
Chapter V Farnsworth *et al. in prep*

Appendices **187**

1. INTRODUCTION

Present geologic processes provide insight into past geological events, and a window into the future (Lyell 1830; Hume 1955). Therefore, studying glaciers and their history is crucial for extending our relatively short observational record, putting our process understanding into a long-term perspective, and better anticipating future climatic conditions (Ingólfsson & Landvik 2013; Hughes *et al.* 2016). Arctic glaciers are valuable indicators of past climate variations given their sensitivity to winter precipitation and summer temperatures (Oerlemans 2005). Investigations of past changes in high-latitude glaciers and climate allow us to better understand the role of the Arctic in the global climate system (McKay & Kaufman 2014). Today, climatic shifts are occurring with an amplified effect in the Arctic and did so following the last deglaciation as well (Hald *et al.* 2007; Hartmann *et al.* 2013). Current climatic conditions are driving negative glacier net mass balance and reduction in the global cryosphere (Kaser et al. 2006; Kjeldsen *et al.* 2015; Huss & Hock 2015). These changes in ice volume have a direct impact on global sea level (DeConto & Pollard 2016; Shepherd *et al.* 2018; Bamber *et al.* 2018).

Understanding the dynamics that govern the stability of marine based ice sheets like the West Antarctic Ice Sheet (WAIS) is critical, given the (potential) sea level equivalent stored within them (Schoof 2007; Joughin *et al.* 2014). While we now have decadal-scale observational records for modern ice sheets, the past ice sheet records can offer a detailed long-term perspective on the style and characteristics of ice sheet behavior (Patton *et al.* 2015; Gandy *et al.* 2018). The Svalbard Barents Sea Ice Sheet (SBSIS) is a palaeo-analogue for the WAIS and can provide valuable insights into the dynamics and style of deglaciation that can be expected from a marine-based ice sheet in a rapidly changing climate (Mercer 1969, 1970; Patton *et al.* 2015, 2017; Esteves *et al.* 2017). Understanding the processes, controls, and dynamics acting on the SBSIS during the Late Pleistocene and Early Holocene allow us to better predict the future evolution of the WAIS (Winsborrow *et al.* 2012).

Investigations of ice sheet dynamics commonly target ice streams, the rapidly flowing rivers of ice that drain disproportionately large volumes of the ice sheet (Stokes & Clark 1999; Bennett *et al.* 2003; Briner 2016; Stokes *et al.* 2016; Larsen *et al.* 2018). Ice stream behavior and dynamics have been investigated in contemporary glacier systems and reconstructed from palaeo-drainage networks based on their geomorphological traces (Andreassen & Winsborrow 2009; Winsborrow *et al.* 2012; Joughin *et al.* 2014; Kleman & Applegate 2014; Margold *et al.* 2015; Stokes *et al.* 2016). Distinct landsystem models have been developed to identify and categorize past ice streams (Stokes & Clark 1999; Evans *et al.* 2008; Andreassen *et al.* 2014). Interestingly, similarities exist between the geomorphological assemblages developed for ice streams and surge-type glaciers, which may indicate a dynamic commonality (Kjær *et al.* 2008; Winsborrow *et al.* 2012; Andreassen *et al.* 2014; Ingólfsson *et al.* 2016; Newton & Huuse 2017).

Svalbard and the surrounding marine environment are an ideal region to investigate glaciers and climate history. The terrestrial and marine archives are fingerprinted with the final stages of deglaciation of the marine based SBSIS (Ingólfsson & Landvik 2013, 2014; Flink *et al.* 2017; Hogan *et al.* 2017). Furthermore, investigations of Svalbard glaciers are particularly important due to the region's climatic sensitivity, amplified response to global shifts in atmospheric and oceanic temperatures, as well as the high density of documented surge-type glaciers (Jiskoot *et al.* 2000; Benestad *et al.*, 2003; Hagen *et al.* 2003; Hald *et al.* 2007; Sevestre & Benn 2015; Isaksen *et al.* 2016).

1.0.1 The Holocene

The end of the Pleistocene, characterized by a cold period known as the Younger Dryas (YD), ended at 11.7 ka BP and transitioned rapidly into the warmer Holocene period (Dansgaard *et al.*, 1993; Cohen *et al.* 2013; updated). The global climate during the Holocene has traditionally been regarded as relatively stable, compared to the preceding Late Pleistocene (Dansgaard *et al.* 1993; Steffensen *et al.* 2008; Rockström *et al.* 2009). However, this paradigm of a relatively uneventful Holocene is being increasingly challenged (Bond *et al.* 2001; Mayewski *et al.* 2004; Wanner *et al.* 2011). The Holocene period is separated into three sub-divisions or stages; Early, Mid and Late Holocene, which correspond to the Greenlandian, Northgrippian and Meghalayan stages, respectively (Walker et al. 2012; Cohen *et al.* 2013; updated). The timing of these stages is partitioned as follows: from 11.7 – 8.2, 8.2 – 4.2 and 4.2 to present. In this text, the Late Holocene stage is, in turn, broken into three time periods, Neoglacial (4.2 ka BP – 1920 AD), Little Ice Age (LIA; 1250 – 1920 AD), and Post-LIA (1920 – present).

1.1 Svalbard

1.1.1 Regional setting and contemporary climate

Located along the dominant corridor of atmospheric moisture between the Atlantic and the Arctic Basin, the Svalbard archipelago spans from 74° – 81° N and 10° – 35° E (Fig. 1; Drange *et al.* 2013). The region has a sensitive climate due to its position at the northern extent of the North Atlantic Drift (West Spitsbergen Current; Fig. 1) and the southern border of the Arctic sea-ice front (Rogers *et al.* 2005). Svalbard is categorized as having a dry, high-Arctic climate with periglacial conditions, extreme winter temperatures and warm continuous permafrost (French 2007;

Christiansen *et al.* 2010). Despite its northerly latitude, Spitsbergen, the largest of Svalbard's islands, (followed in size by Nordaustlandet, Edgeøya and Barentsøya), currently experiences a relatively mild climate. The warm West Spitsbergen Current travels off the western extent of Svalbard and influences weather patterns and sea-ice distribution (Fig. 1B; Førland *et al.* 1997). Regional climate is controlled by the interactions between the Icelandic Low and the Siberian High pressure systems where high temperatures (and precipitation) are driven north over Svalbard by the North Atlantic cyclone track (Hanssen-Bauer *et al.* 1990; Humlum 2002). Svalbard precipitation is closely coupled to the mode of the North Atlantic Oscillation (Dickson *et al.* 2000) and falls predominantly in solid form. The interactions of these air masses along the western flank of Svalbard result in relatively warmer and wetter winter conditions than are typical for such latitudes (Førland *et al.* 1997; Eckerstorfer & Christiansen 2011). Over the last century, most of the annual variability seen in mean annual air temperature (roughly 4 – 5 °C on an annual – decadal scale) is a result of fluctuations occurring during the winter and shoulder-season months (September – November and March – May). Summertime (June, July and August) temperature averages since the start of the Longyearbyen record in 1912 have gradually increased from roughly 4 °C to 5.5 °C, but exhibit minimal variability, i.e. in between 0.5 – 1.0 °C (Christiansen *et al.* 2013).

1.1.2 Glacial history and relative sea level

Today, it is widely accepted that the Svalbard Barents Sea region has undergone repeated glaciations through the Late Quaternary (Mangerud *et al.* 1998; Landvik *et al.* 1998; Svendsen *et al.* 2004; Larsen *et al.* 2006). The concept of an ice sheet covering Svalbard, the Barents Sea and extending as far south as Scandinavia has developed for over a century (De Geer 1900). In 1860, raised marine beaches with fossil bearing marine sediments were described in Norway and were suggested to relate to uplift of the earth's crust following the unloading of an ice mass (Kjerulf & Sars 1860). In the late 1800s raised marine beaches with varying maximum elevations were likewise observed across Svalbard, in some locations extending up to 100 m a.s.l. (Pike 1898; Nathorst 1899, 1901; Salvigsen 1981).

The early studies that dated these raised marine shorelines and examined the signatures of relative sea level changes form the foundation of current understanding of the former center of ice load over Svalbard and the Barents Sea as well as the rates of glacio-isostatic rebound (Feyling-Hanssen & Olsson 1960; Blake 1961, 1962; Schytt *et al.* 1968; Hoppe 1972). More recent radiocarbon dated relative sea level curves from across Svalbard and the Barents Sea have enhanced our understanding of the pattern of uplift introduced by the earlier studies (Salvigsen 1981; Forman 1990; Bondevik *et al.* 1995; Landvik *et al.* 1998; Forman *et al.* 2004).

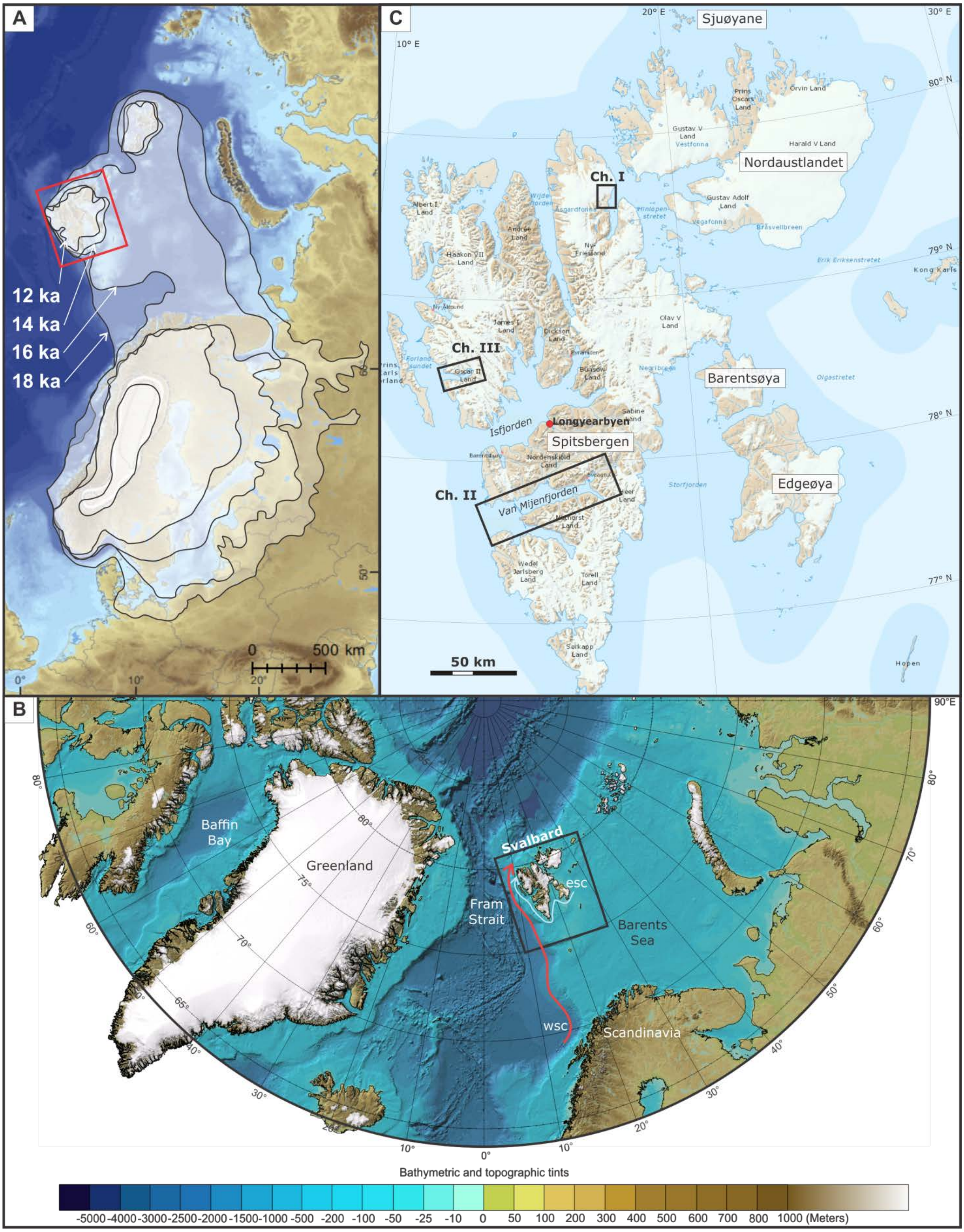

Fig. 1 A) Map of North Atlantic with the most-credible time-slice reconstructions (18, 16, 14 & 12 ka BP) of ice cover over Scandinavia, Svalbard and the Barents Sea from DATED1 (modified from Hughes et al. 2016). Extensive ice retreat occurs around Svalbard between 15 – 10 ka BP. B) Bathymetry of the North Atlantic, with Svalbard located at the northwestern extent of the Eurasian plate and the Barents Sea. The warm West Spitsbergen Current (WSC) runs up along Svalbard's western margin while the cool East Spitsbergen Current (ESC) traces down and around from the east (map modified from IBCAO). C) Topographic map of Svalbard with place names. Site

locations presented in Chapters I – III. Chapters IV and V target the whole region. The islands of Kvitøya located to the northeast of Nordaustlandet and Bjørnøya located between Norway and Spitsbergen are not shown on the map (modified from the Norwegian Polar Institute).

Although the maximum elevations of raised marine sediments outline a general region influenced by substantial ice cover, large uncertainties remained around the geometry and extent of the ice. For decades, investigations focused on and debated the extent of ice cover across Svalbard during the Late Weichselian or Last Glacial Maximum (25 – 15 ka BP; LGM; Ingólfsson & Landvik 2013; Hughes *et al.* 2016). Opposing positions developed regarding the recent glacial history of the Svalbard region. The "maximalist" school of thought argued extensive ice cover based on correlations of terrestrial and marine stratigraphic records, suggesting Weichselian ice reached the shelf west of Svalbard with limited ice-free areas existing (Mangerud *et al.* 1992; Mangerud & Svendsen 1992; Svendsen *et al.* 1992, 1996). The "minimalists" argued for substantially less extensive LGM ice, based on the apparent lack of Late Weichselian glacial deposits as well as the preservation of sediments and landforms of pre-LGM age which had been identified across the west coast of Spitsbergen (Salvigsen 1977; Boulton 1979; Miller 1982; Forman & Miller 1984; Lehman & Forman 1987; Forman 1989; Houmark-Nielsen & Funder 1999; Andersson *et al.* 1999, 2000).

As additional marine geological data have been collected for the region, it has become evident that the extent of LGM ice cover was closer to the view supported the maximalist reconstructions. However, the observations of preserved old landforms by the minimalists reflects the complexity and dynamics of the SBSIS fingerprinted between its regions of streaming and non-streaming ice (Lehman & Forman 1992; Mangerud *et al.* 1992; Landvik *et al.* 1998; Ottesen *et al.* 2007; Landvik *et al.* 2005, 2013; Ingólfsson & Landvik 2013). At present, there is a firm understanding of the extent of Late Weichselian glaciation and general timing of deglaciation (Fig. 1A; Hormes *et al.* 2013; Hughes *et al.* 2016), but knowledge of the thickness, dynamics and behavior remain less clear (Landvik *et al.* 2014).

While the ice thickness of the SBSIS is unknown, submarine glacial landforms and geomorphological evidence indicate grounded ice identified beneath 500 m water depth suggest minimum ice thickness values (Landvik *et al.* 1998). Numerical ice sheet models suggest ice thickness on the order of 1500 – 3000 m thick (Lambeck 1995; Patton *et al.* 2015). As the SBSIS is often compared to the WAIS, measured ice thickness on the contemporary ice sheet can be used as a gauge for the potential ice thickness over the SBSIS during the Late Weichselian (Mercer 1970). In the West Antarctic grounded ice has been identified 2 km beneath contemporary sea level and ice thicknesses range from 1.5 – 3 km thick (Fretwell *et al.* 2012; Jamieson *et al.* 2014).

As the current vision of the SBSIS has developed, reconstructions of the size, shape and behavior of the ice sheet have evolved. What was once a concentric mono-domed slow-moving ice sheet, regulated by large-scale northern hemisphere climatic oscillations, has become a multi-domed, dynamic ice sheet characterized by regions of streaming ice with intermittent zones of non-erosive slow creeping ice cover. Furthermore, the complex behavior is influenced by not just climate fluctuations, but additional factors including relative sea level, subglacial topography, substrate characteristics, basal temperature, and hydrological conditions (Ingólfsson & Landvik 2013).

1.1.3 Landscape and glaciers

Svalbard is 62,000 km^2 of glaciated mountainous terrain interrupted by low-lying open fjord-valleys leading into over-deepened fjords systems (Ottesen *et al.* 2007; Gilbert *et al.* 2018). Svalbard exhibits geologic strata ranging from Precambrian to Quaternary (Hisdal 1985; Dallman *et al.* 2015). Lithologic and structural controls govern topography and mountain morphology. Topography of the western and northern coasts of Spitsbergen are characterized by high relief alpine terrain while the central and northeastern regions exhibiting gentle plateau-shaped highlands with intersecting incised valleys (Humlum 2002; Dallman *et al.* 2015). Large portions of northern Spitsbergen exceed 1200 m a.s.l. with many peaks extending over 1600 m a.s.l., while mountain summits further south range around 1000 m a.s.l. The island of Nordaustlandet reaches up to between 600 – 700 m a.s.l. while peaks on Barentsøya and Edgeøya are closer to 500 m a.s.l. (Fig. 1C). Strand-flats and low lying regions are overlain by post-glacial raised marine sediment are commonly found along the outer coasts of Svalbard (Fig. 2A). Higher elevations are generally ice covered with exceptions existing around interior regions of Spitsbergen, which are located in a precipitation shadow (Humlum 2002).

Glaciers cover roughly 57% of Svalbard at present and over 65% of that area drains into tidewater glaciers (Blaszczyk *et al.* 2009; Nuth *et al.* 2013). The total volume of Svalbard's glaciers is estimated at 6700 ± 835 km^3 or 17 ± 2 mm of sea level equivalent (Martin-Español *et al.* 2015). Estimates derived from aerial imagery from the early 1990s suggest ice cover ranged around 60% (Hagen *et al.* 1993) while estimates of glacier extent during the end of the LIA c. 1920, indicate over 70% of Svalbard was glaciated (Martin-Moreno *et al.* 2017). Glacier types on Svalbard include cirque, valley, and fjord glaciers systems, thin alpine ice caps and extensive ice caps, unconstrained by regional topography and grounded below sea level (Fig. 2B, C & D).

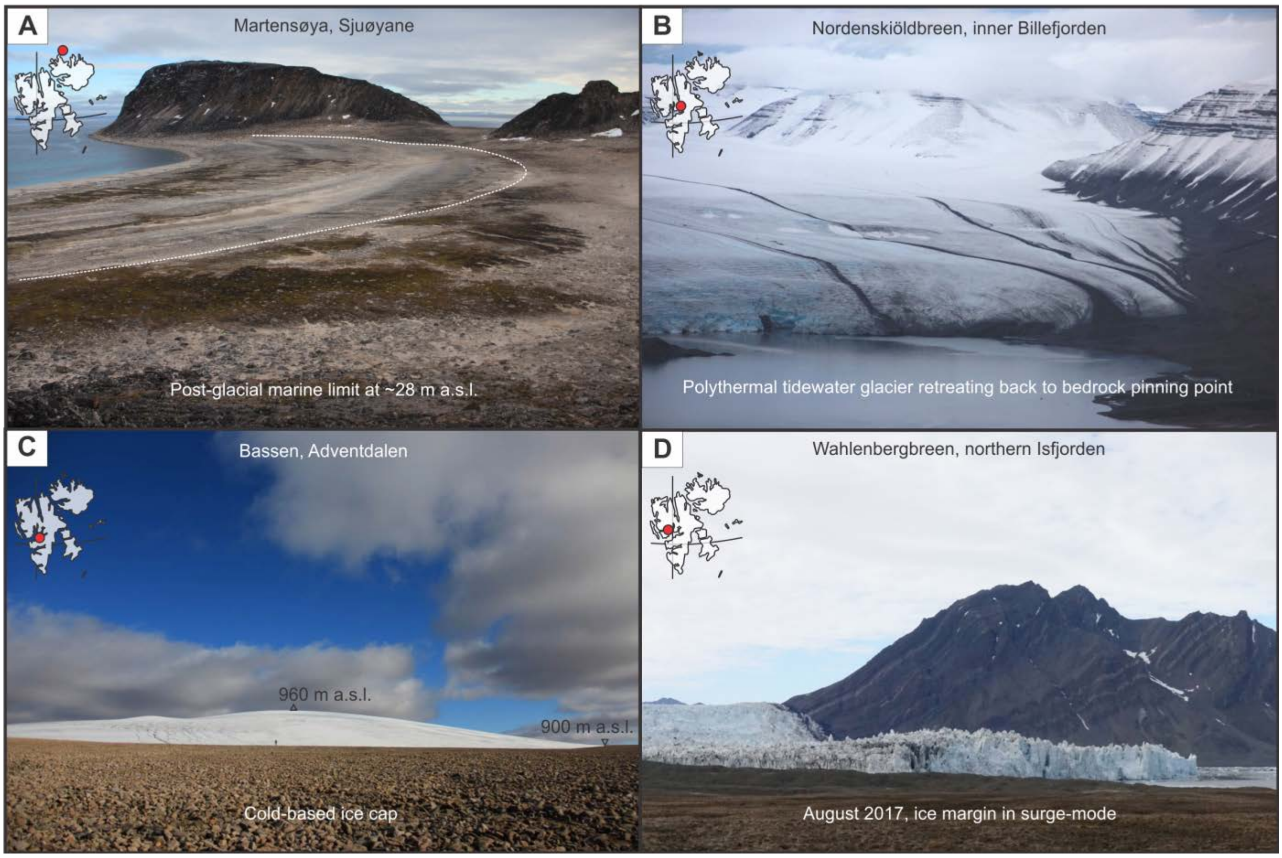

Fig. 2 Photo-mosaic of Svalbard landscape and glaciers; A) raised marine shorelines on eastern Sjuøyane (northern Svalbard) with a post-glacial marine limit approximately 28 m a.s.l., B) polythermal, tidewater margin of Nordenskiöldbreen (inner Isfjorden) retreating back from its Late Holocene maximum, C) thin, cold-based alpine ice cap located to the northeast of Longyearbyen, central Spitsbergen, D) Wahlenbergbreen heavily crevassed and surging into Isfjorden, Aug. 2017.

As a function of the size, thickness, and local climate, Svalbard glaciers exhibit a range of thermal regimes. The majority of glaciers and ice caps on Svalbard are polythermal suggesting areas of the ice are temperate (i.e., thick enough to exceed the pressure melting point) while other areas are cold-based (i.e., frozen to the substrate beneath the glacier; Björnsson *et al.* 1996). Some of the smallest glaciers systems are entirely cold based. These glacier systems have a low erosive impact on underlying substrate, as they do not flow across the substratum and often exhibit annual ice velocities on the mm – cm scale moving slowly due to internal deformation (Liestøl 1993; Hagen *et al.* 2003). Small cirque and valley glaciers characterize north central and central Spitsbergen reflecting the low precipitation there (Humlum 2002). Glacier equilibrium line altitudes (ELA) range from less than 200 m to over 700 m a.s.l. and are closely linked to precipitation patterns as well as regional summer temperatures and ice velocities (Hagen *et al.* 2003). In northeastern Spitsbergen and Nordaustlandet, glacier thickness has been measured and modeled to exceed 600 m (van Pelt *et al.* 2013; Navarro *et al.* 2014, 2016; Fürst *et al.* 2017). In numerous locations, up-stream of tidewater glacier termini, some of this grounded ice is believed to extend down to 200 meters below sea level (Fürst *et al.* 2017).

1.1.4 Surge-type glaciers, behavior and landform assemblages

Svalbard has the greatest density of surge-type glaciers in the world (Hagen *et al.* 1993; Sevestre & Benn 2015). A glacier "surges" when it undergoes a rapid increase in velocity (order of magnitude greater than normal) and often also increases in length over a relatively short duration of a time i.e., months to a decade (Meier & Post 1969; Kamb *et al.* 1985; Sharp 1988; Sevestre & Benn 2015; Ingólfsson *et al.* 2016). A glacier that exhibits surge-type behavior typically displays these dynamic phases of ice flow, followed by a quiescent phase, a period of slow flow, and ice stagnation lasting decades to centuries (Kamb *et al.* 1985; Harrison & Post 2003; Dowdeswell *et al.* 1991).

The classic model of a surge-type glacier is characterized by a regularly timed, surge event and a quiescent phase cycle. In a typical cycle a bulge of long-collected ice mass in the accumulation zone, is passed down glacier in a kinematic wave resulting in extensional stresses. The surge is followed by ice front retreat, profile steepening and slow regaining of ice mass in the accumulation zone (Clarke *et al.* 1984; Kamb *et al.* 1985; Murray *et al.* 2000). Traditional theory of surge-type glaciers suggests that ice front fluctuations are a result of internal dynamics and are unrelated to climatic conditions (Meier & Post 1969; Sharp 1988). These internal dynamics have been associated with the reorganization of the basal hydrological system (Kamb *et al.* 1985), switching of glacier thermal regime (Fowler *et al.* 2001; Sevestre *et al.* 2015), as well as sediment deformation and/or decoupling at the base of the glacier (Clarke *et al.* 1984; Björnsson 1998; Kjær *et al.* 2006). A conceptual, unifying theory regarding the controlling factors has been proposed based on the enthalpy balance of a glacier system (Sevestre & Benn 2015).

Despite the theoretical strength and simplicity of this traditional surge-type glacier model, glacier surges do not always follow it. Svalbard tidewater glaciers have been observed to exhibit surge behavior that is inconsistent with the traditional model (Sevestre *et al.* 2018). For example, numerous marine-terminating glaciers in Svalbard have exhibited a snout destabilization where surge-type behavior initiates at the terminus and propagates upward through the glacier system (Rolstad *et al.* 1997; Luckman *et al.* 2002; Dowdeswell & Benham 2003; Murray *et al.* 2012; Flink *et al.* 2015; Dunse *et al.* 2015; Strozzi *et al.* 2017; Sevestre *et al.* 2018). Furthermore recent studies have highlighted a connection between surge cyclicity and mass balance (Dowdeswell *et al.* 1995; Striberger *et al.* 2011), as well as surge-type glacier distribution and climatic conditions (Sevestre & Benn 2015). These observations suggest greater complexity of surge cyclicity, dynamics and glacier front fluctuations in a warming climate (Sevestre *et al.* 2018; Willis *et al.* 2018).

Glacier surges are infrequently observed, as glaciers spend the majority of their time in the quiescent phase. Thus, the identification of a surge-type glacier can be challenging. Consequently, studies have developed varying approaches to identify these types of glaciers during the quiescent phase. Studies from Iceland have highlighted how surge-type glaciers respond uniquely to climatically favorable conditions (a period of positive mass balance) compared to non-surge-type glaciers (Björnsson 1998; Sigurðsson 1998; Björnsson *et al.* 2003). The studies conclude that the outlet glaciers known to exhibit surge-type behavior move too slowly, relative to accumulation rates, to stay in balance. In contrast, non-surge-type glaciers exhibit velocities similar to steady-state or balanced velocities (Björnsson *et al.* 2003). Thus, during a period of prolonged positive mass balance, typical glaciers advance, while surge-type glaciers accumulate mass and exhibit gradual steepening of surface profiles. Additionally, studies suggest that surge-type glacier behavior can be interpreted based on a distinguishable landform assemblage with specific landforms indicative of rapid ice flow (Evans & Rea 1999, 2003; Ottesen *et al.* 2008; Brynjólfsson *et al.* 2012; Schomacker *et al.* 2014; Flink *et al.* 2015; Farnsworth *et al.* 2016; Ingólfsson *et al.* 2016). Landform assemblages include streamlined features (flutes, drumlins and mega-scale glacial lineations) as well as deposits oriented oblique or perpendicular to ice flow (crevasse squeeze ridges, concertina eskers and glaciotectonized end moraines; Ingólfsson *et al.* 2016). This "landform assemblage" approach allows for the identification of surge behavior during the prolonged quiescent phase, as a glacier snout downwastes and upper accumulation zone regains mass. However, as geomorphological record is effective at identifying glacier systems that have exhibited rapid ice flow, it is less helpful at providing evidence for surge cyclicity (unless linked to stratigraphy; Schomacker *et al.* 2014).

Landform assemblages similar to those of surge-type glaciers have been investigated at the margins of Greenland and Antarctic ice sheets as well as in regions covered by past ice sheets in North America, Iceland and the Barents Sea (Ó Cofaigh *et al.* 2002; Andreassen & Winsborrow 2009; Jakobsson *et al.* 2011; Dowdeswell *et al.* 2014; Principato *et al.* 2016). The combinations of streamlined and oblique landforms that have been mapped at present (and past) ice margins are associated with streaming glacier ice (Stokes *et al.* 2013; Spagnolo *et al.* 2014; Jakobsson *et al.* 2018). The similarities between the geomorphological assemblages of surge-type glaciers and ice streams may suggest a dynamic commonality (Kjær *et al.* 2008; Andreassen *et al.* 2014; Ingólfsson *et al.* 2016). The abundance and relative accessibility of surge-type glaciers on Svalbard allow for the potential to investigate analogs to large ice streams both modern and past (Flink *et al.* 2017).

1.1.5 Aims, and research Objectives

The broad purpose of this doctoral project is to investigate the history of Svalbard glaciers through the Holocene (Fig. 3). Mapping and dating glacier marginal fluctuations allows one to estimate when and where a glacier advanced or retreated. Furthermore, the comparison of palaeoclimate conditions and patterns in glacier activity may indicate the potential driving factors controlling ice marginal fluctuations. Through detailed stratigraphic and geomorphological investigations of glacier forelands, it is possible to trace the style and dynamics of (de-)glaciation. This study uses a suite of data from marine, terrestrial and lacustrine archives in order to reconstruct a mosaic of glacier and climate history for the Holocene on Svalbard.

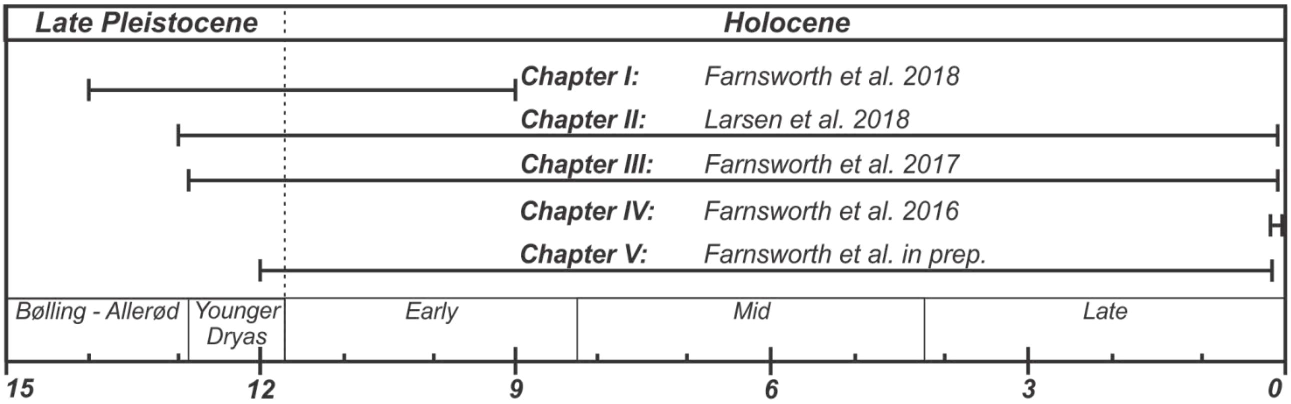

Fig. 3 Timeline of Late Pleistocene and Holocene with targeted time span for each manuscript (Cohen et al. 2013; updated). Note manuscripts from chapters II, III and V span the entire Holocene including the end of the Late Pleistocene (Farnsworth et al. 2017, in prep.; Larsen et al. 2018). The studies presented in chapters I and IV focus on the transition into the Holocene (Farnsworth et al. 2018) and the most recent period of the Holocene (Farnsworth et al. 2016).

Holocene studies have long targeted the unknown aspects of the glacier and climate history of Svalbard. This doctoral thesis addresses several of these outstanding research questions: (1) Is there evidence of Younger Dryas cooling and glacier re-advances on Svalbard? (2) Did meltwater from the collapsing Laurentide Ice Sheet (LIS) influence climate on Svalbard during the 8.2 ka BP event? (3) When was the Holocene (glacial) minimum and how extensive was the glacier cover during this period? (4) When was glacier cover most extensive during the Holocene period and was the LIA the climax of the Neoglacial during the Late Holocene? (5) Which sedimentary archives provide the deepest understanding of Holocene glaciers and climate? (6) What factors control glacier fluctuations on Svalbard through the Holocene?

This thesis is comprised of five chapters that detail Holocene glacier history on Svalbard. Chapters II, III and V span the entire Holocene period. Chapters I and IV target the transition from Late Pleistocene into the Holocene and glacial conditions at the end of the Holocene, respectively (Fig. 3). Chapters II and III are case studies of western Spitsbergen fjords (Van Mijenfjorden and St. Jonsfjorden) where marine and terrestrial data are used to detail glacier history. Chapters I and IV survey the entire Svalbard region targeting Early Holocene and Late Holocene glacial deposits respectively. Chapter V is a synthesis of all Holocene studies from Svalbard.

2. METHODS

2.0.1 Terrestrial stratigraphy and mapping

Field sites were selected based on detailed investigation of aerial imagery, topographic data and digital elevation models provided by the Norwegian Polar Institute on the TopoSvalbard website. Sites were prioritized based on cross-cutting relationships of large-scale geomorphic features such as: beach ridges, glacial deposits, and drainage pathways in addition to the potential for natural geological sections cleared by hand. Lithostratigraphic logging was conducted in natural sections, and documented by sedimentological field logs, photographs, and GPS waypoints.

Field mapping was conducted using computers equipped with and integrated GPS and ArcGIS software (Larsen *et al.* 2018) as well as aerial image prints and a hand-held Garmin GPS (Farnsworth *et al.* 2017, 2018). Terrestrial maps were constructed using digital ortho-rectified imagery produced by the Norwegian Polar Institute in ArcGIS 10.3. The landforms and surface sediment mapped in Van Mijenfjorden were based on 3D projected digital aerial photographs using ESRI ArcMap software with the Stereo Analyst plugin. The maps of Quaternary geology generally follow standard methodology for the Geological Survey of Norway, with some features unique to the Svalbard region (Farnsworth *et al.* 2017, 2018; Larsen *et al.* 2018).

2.0.2 Marine data acquisition and processing

Sea floor data are presented from Van Mijenfjorden and St. Jonsfjorden (Farnsworth *et al.* 2017; Larsen *et al.* 2018). Data from Van Mijenfjorden was collected in 2001 by the Norwegian Hydrographic Service with an EM-1002 Simrad multibeam echo-sounder using 111 beams. The data from inner Van Mijenfjorden (Rindersbukta) were collected in July 2006 by a portable Geoswath system with a 250 kHz transducer mounted in front of a small vessel. The data from Van Mijenfjorden were gridded with a cell size of 5 m and from Rindersbukta with 1 or 5 m.

Sea-floor data were collected throughout St. Jonsfjorden in June 2013. Bathymetric data were collected on board UNIS R/V 'Viking Explorer' with a Kongsberg EM2040 multibeam echosounder. Sea-floor sediment surface and subbottom acoustic sediment structures were studied with the Edgetech 2000 CSS combined side-scan sonar and subbottom profiler systems. The data from all surveys were tidal corrected and spikes were removed (Farnsworth *et al.* 2017; Larsen *et al.* 2018). The marine geological maps from St. Jonsfjorden were produced with QPS Fledermaus Software package based on high-resolution seafloor data.

2.0.3 Sampling and radiocarbon dating

Following field sampling, shell, driftwood, terrestrial plant remains and whalebone subsamples were cleaned, weighed, photographed, identified and subsequently sent for dating at a laboratory with accelerator mass spectrometry (AMS). Samples presented in this thesis were radiocarbon dated at the Ångström Laboratory (Uppsala University, Sweden, Ua) the GeoBiosphere Science Centre (Lund University, Sweden, LuS), the National Laboratory for Age Determination in Trondheim (Norwegian University of Science and Technology, Tra), and at the Scottish Universities Environmental Research Centre (University of Glasgow, SUERC). See chapter V for details on previously published ages from additional laboratories (Farnsworth *et al.* in prep.).

New and previously published radiocarbon ages are presented in tabularized form with metadata in accordance to Hughes *et al.* (2016; Farnsworth *et al.* 2017, 2018, in prep.; Larsen *et al.* 2018). While radiocarbon ages are given as conventional ages relative to 1950 (Stuiver & Polach 1977; Farnsworth *et al.* in prep.) all ages presented in text or figures are in calibrated median ages in kilo-years before present (cal. ka BP) unless otherwise noted. All terrestrial radiocarbon dates have been (re-)calibrated with IntCal13, either using the OXCAL v4.2 or the Calib Rev. 7.0.4 programs (Ramsey & Lee 2013; Reimer *et al.* 2013). Additionally, each ^{14}C age of a marine organism has been (re-)corrected for a marine reservoir effect by selecting 'MARINE13' and inputting a 'Delta R' or implementing a reservoir correction. A ΔR of 70 ± 30 which corresponding to a marine reservoir of 450 years was used to correct for the marine reservoir in the first and final chapters according to Mangerud & Svendsen (2017) and Farnsworth *et al.* (2018; in prep.). In Chapter II a ΔR of 20 ± 30 (recommended for Svalbard; Mangerud *et al.* 2006) was utilized, while a reservoir age of 440 years was subtracted from marine samples in Chapter III (according to Mangerud & Gulliksen 1975; Mangerud *et al.* 2006). The variation in analysis is partially due to Mangerud *et al.* (2006) not concluding on a single approach for North Atlantic marine reservoir corrections, but rather presenting two different views on how to analyze the marine reservoir for the region. It is suggested that Atlantic Water from Scotland to Svalbard has nearly the same marine reservoir age (Mangerud *et al.* 2006; Mangerud & Svendsen 2017), although this may have varied through time depending on the mixture of water masses entering south of Scotland. On the Holocene timescale, variations are believed to be negligible (Bondevik *et al.* 1995).

3. AUTHOR CONTRIBUTIONS AND CHAPTER SUMMARIES

All co-authors contributed to the writing of each manuscript. Farnsworth led the production of the manuscripts in Ch. I and III – V with support from co-authors. Researcher Eiliv A. Larsen from the Geological Survey of Norway led the production of the manuscript presented in Ch. II, while Farnsworth assisted with fieldwork, mapping, figure development, literature review, data interpretation and writing. All co-authors support the use of these manuscripts in this thesis.

Table 1 summarizes the work conducted by the authors of each study (Chapters I – V).

Task:	***Ch. I***	***Ch. II***	***Ch. III***	***Ch. IV***	***Ch. V***
Logistics / preparation	*Farnsworth Ingólfsson Schomacker*	*Larsen Lyså Rubensdotter*	*Farnsworth Ingólfsson Noormets Alexanderson Henriksen*	*-NA*	*-NA*
Fieldwork	*Farnsworth Ingólfsson Allaart Schomacker*	*Larsen Lyså Rubensdotter Farnsworth*	*Farnsworth Ingólfsson Noormets Allaart Alexanderson Henriksen*	*-NA*	*-NA*
Funding	*Ingólfsson Retelle Håkansson Schomacker*	*Larsen Lyså Jensen*	*Ingólfsson Noormets*	*-NA*	*-NA*
Mapping	*-NA*	*Larsen Lyså Rubensdotter Farnsworth*	*Farnsworth Allaart Noormets Schomacker*	*Farnsworth*	*-NA*
Figures	*Farnsworth*	*Larsen Lyså Rubensdotter Farnsworth Ottesen*	*Farnsworth Allaart*	*Farnsworth*	*Farnsworth*
Literature Review	*Farnsworth*	*Larsen Lyså Rubensdotter Farnsworth*	*Farnsworth Ingólfsson*	*Farnsworth Ingólfsson*	*Farnsworth Alexanderson*
Data interpretation	*Farnsworth Ingólfsson Retelle Schomacker*	*Larsen Lyså Rubensdotter Farnsworth Nadeau Ottesen*	*Farnsworth Ingólfsson Noormets Alexanderson Henriksen Schomacker*	*Farnsworth Ingólfsson Retelle Schomacker*	*Farnsworth*
Text prep.	*All authors*	*All authors*	*All authors*	*All authors*	*All authors*

3.1 Chapter I

Farnsworth, W.R., Ingólfsson, Ó., Retelle, M., Allaart, L., Håkansson, L., Schomacker, A. (2018): Svalbard glaciers re-advanced during the Pleistocene-Holocene transition. Boreas 47, 1022-1032. DOI:10.1111/bor.12326.

The goal of this study was to feature the extensive and widespread moraines formed by glacier re-advances across Svalbard during the transition from the end of the Pleistocene to Early Holocene. In this manuscript we introduce the first well-dated end moraine formed during the Late-glacial Early Holocene (LGEH) in De Geerbukta, NE Spitsbergen. This landform was deposited by an outlet glacier re-advancing into a fjord extending 4.4 km beyond the Late Holocene (LH) maximum. Furthermore, we introduce six additional locations where glacier moraines have been wave-washed or cut by postglacial raised marine shorelines, suggesting the landforms were deposited before or during high relative sea-level stands, thus exhibiting a similar LGEH age. Our new evidence suggests that the LGEH glaciers were more dynamic, exhibited re-advances, and extended well beyond the extensively studied LH glacial expansion. The timing of the De Geerbukta glacier re-advance compared to a synthesis of existing data including four palaeoclimate records and 15 other proposed glacier advances from Svalbard does not suggest clear synchronicity in glacial and climatic events. The widespread occurrence of the LGEH glacier deposits on Svalbard, suggests that the culmination of the Neoglacial advances during the Little Ice Age does not mark the maximum extent of most Svalbard glaciers since regional deglaciation; it is just the most studied and most visible in the geological record. This study contributes to our understanding of the style of deglaciation during Late Pleistocene - Early Holocene on Svalbard by introducing a period in time characterized by glacier re-advances and discussing the complexities that exist between past glacier behavior and climate.

3.2 Chapter II

Larsen, E., Lyså, A., Rubensdotter, L., Farnsworth, W.R., Jensen, M., Nadeau, M., Ottesen, D. (2018): Lateglacial and Holocene glacier activity in the Van Mijenfjorden area, western Svalbard. arktos. DOI: 10.1007/s41063-018-0042-2.

The aim of this study was to detail the Late Weichselian and Holocene glacial history for the entire Van Mijenfjorden system, through sedimentological, morphological and chronological investigations of both terrestrial as well as marine archives. This study describes ice marginal glacier deposits related to re-advances spanning from Late Pleistocene to post Little Ice Age from the mouth of the fjord into the inner tributaries of the Van Mijenfjorden-system. The fjord exhibits a record of glacier fluctuations related to the episodic break-down of Late Weichselian ice in the catchment during the Late Pleistocene and Early Holocene as well as the episodic growth of re-advancing glacier systems throughout the Neoglacial, Little Ice Age and 20th century during the Late Holocene. Several interesting observations are made in this study: i) the glacier filling the entire Van Mijenfjorden system retreated during the Younger Dryas period without leaving evidence of regressive retreat, ii) numerous (Early Holocene and Neoglacial) glacier re-advances are described where ice margins extended well beyond their Little Ice Age maximum positions and, iii) the Paulabreen glacier system surged at least five times in the last 650 years, with each subsequent surge advance exhibiting a less extensive maximum than the previous, resulting in an overall decrease in mass since the early LIA. This manuscript contributes to our understanding of the deglaciation and Holocene glacier fluctuations observed from within the mouth, to the head of an entire fjord-system by detailing the complexities of glacier fluctuations and climate. This study additionally documents the diversity in the maximum position of glacier margins during the Holocene.

3.3 Chapter III

Farnsworth, W.R., Ingólfsson, Ó., Noormets, R., Allaart, L., Alexanderson, H., Henriksen, M., Schomacker, A. (2017): Dynamic Holocene glacial history of St. Jonsfjorden, Svalbard. Boreas 46, 585-603. DOI: 10.1111/bor.12269.

The objective of this study was to reconstruct the Holocene glacial history of inner St. Jonsfjorden, western Spitsbergen, by constructing detailed geomorphological maps of marine and terrestrial environments as well as constraining the chronological sequence of glacier events. Stratigraphic and geomorphology evidence indicate an Early Holocene tributary glacier advance constrained to the transition from Late Pleistocene to Early Holocene. Identification and ^{14}C dating of the thermophilous bivalve *Modiolus modiolus* to 10.0 $\pm$ 0.12 cal. ka BP constrains the minimum age of deglaciation for the inner fjord, and suggests a rapid northward migration of the species during the Early Holocene. Furthermore, evidence from the Late Holocene enhances our understanding of the onset and subsequent climax of the Neoglacial-Little Ice Age in inner St. Jonsfjorden. The present-day terminus of Osbornebreen, the dominating glacier system in St. Jonsfjorden, is located over 8.5 km up-fjord of its Neoglacial maximum extent. Cross-cutting relationships suggest subsequent advances of all the smaller glaciers in the inner fjord following the break-up of the Osbornebreen tidewater glacier. Glacial deposits, landforms and their cross-cutting relationships observed in both terrestrial and marine settings imply a complex and highly dynamic environment through the later part of the Holocene. Similar to Van Mijenfjorden, much of St. Jonsfjorden becomes ice-free during the Late Pleistocene and Early Holocene. Additionally, a large dynamic re-advance from the main tidewater glacier Osbornebreen occurs during the early LIA. Since this re-advance Osbornebreen has exhibited a series of retrogressive ice marginal advances characterized by each maximum position less extensive than the subsequent. This study contributes to our understanding of the Holocene glacier history by describing evidence of dynamic glacier behavior preserved in the terrestrial and marine archives of St. Jonsfjorden.

3.4 Chapter IV

Farnsworth, W.R., Ingólfsson, Ó., Schomacker, A., Retelle, M. (2016): Over 400 previously undocumented Svalbard surge-type glaciers identified. Geomorphology 264, 52-60. DOI: 10.1016/j.geomorph.2016.03.025.

The purpose of this study was to identify glaciers that likely exhibited surge-type behavior during the culmination of the Little Ice Age by identifying crevasse squeeze ridges in an aerial image survey of glacier forelands throughout Svalbard. Crevasse squeeze ridges are landforms indicative of rapid-dynamic ice flow and are suggested to be unique to surging glacier land systems. Estimates vary greatly as to the actual percentage of surge-type glaciers in Svalbard, and consequently their distribution pattern is poorly understood. Recent (2008–2012), high-resolution aerial imagery from TopoSvalbard, provided by the Norwegian Polar Institute, was surveyed targeting all the terrestrial glacier forelands in Svalbard. Prior to our study, less than 280 individual glaciers in Svalbard had been documented to exhibit surge behavior. By using crevasse squeeze ridges as indicators of surge behavior, we have identified 431 additional glaciers that have exhibited surge-like advances. This is probably a modest value as the unique surge landforms were not visible in approximately one-third of the forelands with documented surge histories. Limits to the crevasse squeeze ridge technique are presented and potential controlling factors for crevasse squeeze ridge formation and preservation are discussed. This study contributes to our understanding of the extent of glacio-dynamic behavior experienced during the end of the LIA and early 20th century across Svalbard by surveying glacier forelands in search of a landform indicative of rapid ice-velocities and suggestive of previous surge-type behavior.

3.5 Chapter V

Farnsworth, W.R., Ingólfsson, Ó., Alexanderson, H., Forwick, M., Noormets, R., Retelle, M., Schomacker, A. (in prep.): Holocene glacial and climate history of Svalbard - status, perspectives and challenges.

We review published literature of Holocene glacier and climate history from Svalbard. This review endeavors to establish the state of the art regarding the Holocene history of Svalbard, by synthesizing findings from all Holocene studies and creating a geochronological database of all ages (^{14}C, TCN and Lum.) spanning 12.0 ka BP to present sampled on Svalbard and the surrounding region. A database of ages has been constructed, quality assessed, and categorized by archive (marine, terrestrial and lacustrine). No review has yet been compiled despite over a century of ice front observations, hundreds of Holocene glacier studies and an ever-developing understanding of ice dynamics and the Arctic climate system. This overview: (1) presents a brief summary of major shifts in climate and glacier cover across the Svalbard region throughout the Holocene; (2) introduces a quality assessed database of published ages that constrain glacier fluctuations (deglaciation, ice free, re-advance and marginal position) and climatic conditions (warming, cooling, wetter, and drier); (3) discusses challenges in methodology as well as potentials regarding sedimentary archives and; (4) addresses the complexities of glacier systems in response to changes in climate. This synthesis establishes the state of the art regarding Holocene glacier and climate history by summarizing all Holocene literature from Svalbard and discussing findings within a modern perspective.

4. DISCUSSION

4.1 Svalbard Holocene climate and the unknowns

While orbital conditions and the northern hemisphere summer insolation have often been linked with the Holocene thermal optimum and the subsequent Neoglacial cooling, observations of Holocene glaciers and climate from Svalbard deviate in two key ways (Laskar *et al.* 2004). The marine thermal optimum on Svalbard pre-dates the peak in summer insolation (Hald *et al.* 2007; Mangerud & Svendsen 2017). Furthermore, Svalbard glaciers are found to have exhibited marked re-advances throughout both the Early and the Late Holocene (Farnsworth *et al.* 2018; in prep.). These two characteristics of the Holocene climate and glacier history suggest that more than orbital forcing is controlling the temperature, precipitation and glacier behavior in Svalbard during the Holocene. In this section, the importance of Atlantic waters around Svalbard with regard to sea-ice cover, temperature, and precipitation is discussed further.

4.1.1 Atlantic waters control the temperature

Today, mean annual air temperatures recorded on Svalbard (Longyearbyen) are at least 5 °C higher than other high-Arctic meteorological stations (Eckerstorfer & Christiansen 2011). Svalbard's mild, high-Arctic climate is a direct result of the oceanic currents arriving to and traveling around the archipelago today (Førland *et al.* 1997; Drange *et al.* 2013). Furthermore, current sea-ice cover conditions (i.e., ice-free conditions on the west coast and the sea-ice dominated east coast) drive a strong temperature gradient across Svalbard (Isaksen *et al.* 2016). Thus, the West Spitsbergen Current sea surface temperature anomalies influence regional sea-ice extent which, in turn, impacts regional and local variations in air temperature and precipitation (Jung *et al.* 2017). Svalbard's Holocene climate, and by association its glaciers, are linked to the effects of North Atlantic waters arriving to the region. Further modeling investigations are needed to address the controls and robustness of the West Spitsbergen Current. This will improve knowledge of the over-arching factors governing Holocene climate on Svalbard.

4.1.2 Palaeo-precipitation remains unknown

There is no direct means of measuring precipitation during the majority of the Holocene on Svalbard. The oldest ice core records showing snow accumulation extend back to roughly 1 ka BP (Isaksson *et al.* 2005; Divine *et al.* 2011). The greatest potential for reconstructing Holocene precipitation on Svalbard is through detailed investigations of lake catchments and sedimentary archives (Røthe *et al.* 2018). The first hydrogen isotope leaf wax study from Svalbard has recently been conducted on a Holocene lake record and provides insight in to past hydroclimate (Balascio *et al.* 2018). The analysis of leaf wax hydrogen isotopes from lake sediments is a developing proxy associated with hydroclimate, palaeo-precipitation and sedimentation within lake catchments (Thomas *et al.* 2012, 2016). As this method further develops and studies target lakes across Svalbard, our understanding of past precipitation across the region will improve (Farnsworth *et al.* in prep.).

Although precipitation patterns on Svalbard through the Holocene are not well understood, the knowledge of modern processes can help contextualize Holocene precipitation (Humlum 2002). Thus, the better the understanding of the intricacies of modern precipitation processes, more effective models will be developed for both past and future conditions. Numerous studies of modern field observations and modeling suggest interconnection between increased temperature, decreasing sea-ice extent, and increased precipitation for the Norwegian High Arctic (Nowak & Hodson 2013; Bitanja & Selten 2014; Isaksen *et al.* 2016; Kopec *et al.* 2016). Increased rates of precipitation recorded in Svalbard have been associated with warmer autumn seasons and the associated delay of sea-ice formation (Christiansen *et al.* 2013; Nowak & Hodson 2013). Relatively warm and wet conditions have driven strong negative mass balance on low elevation cirque and valley glaciers (Möller & Kohler 2018). Alternatively, continental high-elevation glacier accumulation zones, which remain above the freezing point, may gain mass and benefit from the increased precipitation. Consequently, precipitation during the Early Holocene, due to the rapid increase of ocean temperatures (Hald *et al.* 2004), and decrease in sea-ice cover (Müller & Stein 2012), likely had a large, but as of yet unquantifiable influence on the regional hydro-climate and glacier mass balance (Mangerud & Svendsen 2017; Farnsworth *et al.* 2018; Balascio *et al.* 2018).

4.2 Drivers of Holocene glacier re-advance

Svalbard glaciers re-advanced throughout the Early Holocene (as late as 9 ka BP) and through the entire Late Holocene (Larsen *et al.* 2018; Farnsworth *et al.* 2017, 2018, in prep.). However, the rate of glacier growth during these periods of re-advances is poorly constrained and not fully understood (Farnsworth *et al.* 2018). There is currently no evidence to suggest that glaciers re-advanced through the Mid Holocene on Svalbard (Farnsworth *et al.* in prep.).

4.2.1 Early Holocene re-advances

One must consider what evidence suggests that Early Holocene glacier re-advances are controlled by mass balance and hence are climatically forced. Ice-marginal oscillations during the Early Holocene are asynchronous, and appear to occur during an unfavorable climate (warm oceans, high summer insolation, variable sea-ice conditions; Larsen *et al.* 2018; Farnsworth *et al.* 2017, 2018, in prep.). Although the percentage of glacier cover across Svalbard may have theoretically increased at periods during the deglaciation (due to the re-advancing glacier margins), general ice volume was probably in continuous decline during this period (Farnsworth *et al.* 2018; in prep.). Unless increased precipitation during the Early Holocene out-weighed the present reconstructed climatic factors, ice marginal re-advances were probably controlled by glacio-dynamic behavior.

4.2.2 Neoglacial – Little Ice Age re-advances

Svalbard glaciers re-advanced throughout the Neoglacial period (Werner 1993; Reusche *et al.* 2014; Røthe *et al.* 2015; van der Bilt *et al.* 2016; Philipps *et al.* 2017) and during the LIA (Svendsen & Mangerud 1997; Snyder *et al.* 2000; Humlum *et al.* 2005; de Wet *et al.* 2018). The combination of low summer insolation (Laskar *et al.* 2004) and explosive volcanic activity (Miller *et al.* 2012) influenced cooling in the northern hemisphere and may have been key factors in creating conditions favorable for glacier growth during the Late Holocene. As introduced in the last section, little is known about patterns of Holocene precipitation across Svalbard.

One alkenone-based (summer) temperature reconstruction from western Spitsbergen lake sediments suggests the Little Ice Age was "mild" (D'Andrea *et al.* 2013). The authors go on to suggest that precipitation played a larger contribution to regional glacier re-advances than previously acknowledged (D'Andrea *et al.* 2013). While it is important to note the limited knowledge of past precipitation, there is ample evidence suggesting that air and ocean temperatures were relatively cool and also favored glaciers growth during the late Neoglacial and LIA (Divine *et al.* 2011; Bartels *et al.* 2017; Ojala *et al.* 2018; Røthe *et al.* 2018; van der Bilt *et al.* 2018; Balascio *et al.* 2018). The Kongressvatnet lake sediment record suggests that, in the 18th and 19th centuries, reconstructed summer temperatures were 2 °C to 3 °C cooler during the later LIA by comparison to the 20th century. Based on the 100-year-plus temperature record from Longyearbyen, an increase of 1.5 °C in summer temperatures have had a substantial influence on glaciers. Furthermore, annual variability reflected in the record's mean annual air temperature (seen on an annual-decadal scale) is dominantly derived from fluctuations during the winter and shoulder seasons (Christiansen *et al.* 2013; Farnsworth *et al.* in prep.). Consequently, it is not clear how much impact 2 – 3 °C (average summer) temperature increase would have on Svalbard glaciers. However, it is roughly twice the increase recorded during the last century in Longyearbyen.

The reconstructed summer temperatures from the Kongressvatnet lake sediment record also suggest the Neoglacial and early LIA was even cooler than the late LIA. Accordingly, most Late Holocene glacier re-advances (dated by overridden vegetation or mollusc shells) date to the early (between 1.0 – 0.5 ka BP), not the late LIA (Farnsworth *et al.* in prep.). Early observations from the

1900s, describing glaciers proximal to their Late Holocene maxima does not suggest anything about the timing of glacier re-advance. It just suggests the glaciers were slowly starting to retreat. The D'Andrea *et al.* (2013) summer temperature record is particularly interesting as it does not reflect a clear or defined cooling excursion during the LIA, but rather an extended and pronounced phase of Neoglacial. Furthermore, the study raises the question, are average summer temperatures sensitive "first responders" to climatic shifts in Svalbard?

Sea-ice conditions during the Neoglacial and LIA are characterized by increasing but variable ice extent around Svalbard (Müller & Stein 2012; Müller *et al.* 2014; Bartels *et al.* 2017). Although increasing sea-ice cover reconstructed through most of the Late Holocene is presumed to favor glacier growth (suppressing summer temperatures, minimizing the number of positive degree days and decreasing frontal ablation) it is unclear how much this restricts precipitation (Farnsworth *et al.* in prep.).

In phase with climatic favorability, several glacier re-advances constrained to the Neoglacial – LIA have been characterized as surges based on size, extent of glacial deposits and preservation of landforms (related to rapid ice advances) corresponding to associated ice-margins (Ottesen *et al.* 2008; Kristensen *et al.* 2009; Kempf *et al.* 2013; Farnsworth *et al.* 2016, 2017; Lovell & Boston 2017; Flink *et al.* 2017; Lyså *et al.* 2018). While the most extensive Late Holocene glacier deposits have been associated with surge-type behavior especially near the culmination of the LIA (Kristensen *et al.* 2009; Kempf *et al.* 2013; Flink *et al.* 2015; Lyså *et al.* 2018), an increasing number of studies have identified both complete and fragmented moraine ridges outboard of the LIA maxima (Werner 1993; Sletten *et al.* 2001; Reusche *et al.* 2014; Philipps *et al.* 2017; Larsen *et al.* 2018). The classical perspective of the (Late) Holocene glacial maximum occurring during the culmination of the LIA is being challenged (Svendsen & Mangerud 1997; Snyder *et al.* 2000).

4.2.3 Post Little Ice Age re-advances

Despite trends in negative mass balance throughout the later 20th century (Hagen *et al.* 2003; Nuth *et al.* 2013; Martin-Moreno *et al.* 2017; Østby *et al.* 2017) glacier re-advances have been observed after the LIA. However, these glacier re-advances are not sustained in the long-term and are attributed to short-lived changes in glacio-dynamic conditions such as surging (Lefauconnier & Hagen 1991; Hagen *et al.* 1993, 2003; Dunse *et al.* 2015; Lovell *et al.* 2015; Sevestre & Benn 2015; Sevestre *et al.* 2018).

4.2.4 Early vs. Late Holocene glacier cover variation

Although the percent of glacier cover from the LIA through the 20th century may be similar to the percentage during the Early Holocene (c. 10.0 ka BP), the spatial distribution of glacier ice across Svalbard is different (Fig. 4). At numerous sites on Svalbard, Late Holocene glaciers have re-advanced over shorelines of Late Pleistocene-Early Holocene age (Fig. 4A, C & E).

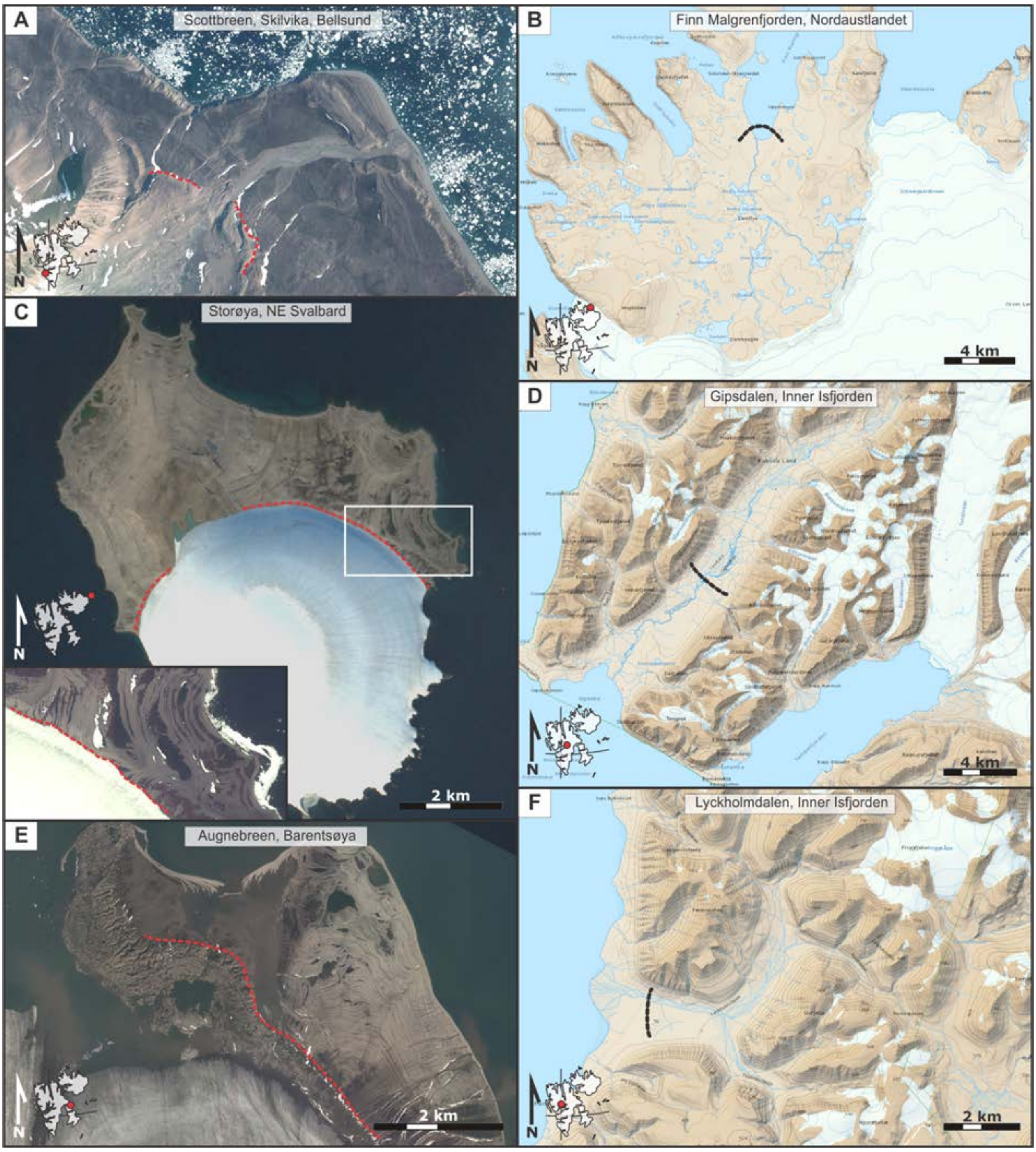

Fig. 4 The distribution of glacier-cover across Svalbard is different during the Early Holocene compared to the Late Holocene. A, C & E) Examples of aerial imagery and Landsat data where Late Holocene glaciers overlay or have overridden shorelines of Late Pleistocene and Early Holocene age; A) Scottbreen (Mangerud & Landvik 2007), B) Storøya, (Jonsson 1983) and Augnebreen (Bondevik et al. 1995). B, D & F) Examples of topographic maps from selected regions

with previously described Early Holocene ice margins. At present, catchments are ice-free with no indications of Late Holocene glaciation in; B) Finn Malgrenfjorden (Ulfstedt 1987), D) Gipsdalen (Tolgensbakk 1990) and F) Lyckholmdalen (Farnsworth et al. 2018).

In some cases, raised beaches from high relative sea levels (of Early Holocene age) are seen melting out from cold-based ice margins (Fig. 4C). Evidence from these sites implies that these areas were ice-free at the time of shoreline formation and that subsequent climatic changes effectively reinvigorated glaciers during the Late Holocene. In contrast, there are examples of unglaciated regions today where Early Holocene ice margins re-advanced, suggesting that the residual SBSIS-ice persisted in these regions and subsequent Holocene climate was not conducive to re-glaciate these catchments. The present general distribution of glaciers ice and prevailing winds suggests that these regions are dry and shadowed from precipitation (Fig. 4; Humlum 2002). It is unclear if these variations in ice cover relate to dynamic behavior during the Early Holocene, trends in Late Holocene precipitation patterns or some combination of the two.

4.3 Advances in Deglaciation

Through the 20th century, Svalbard glaciers have undergone widespread retreat (Blaszczyk *et al.* 2009; Nuth *et al.* 2013; Martin-Moreano *et al.* 2017). Air temperatures have risen (Christiansen *et al.* 2013; Isaksen *et al.* 2016); sea-ice cover has declined (Muckenhuber *et al.* 2016; Petty *et al.* 2018); and ocean temperatures have increased, as evidenced by the reappearance of thermophilous marine molluscs around Svalbard (Berge *et al.* 2005; Mangerud & Svendsen 2017). Despite these trends, some Svalbard glaciers continue to re-advance.

Current conditions, regarding atmospheric and ocean temperatures, are similar to those reconstructed from the period of glacier retreat during the Early Holocene (Hald *et al.* 2004; Muller & Stein 2012; Hormes *et al.* 2013; Bartels *et al.* 2017; Mangerud & Svendsen 2017). However, there are two clear contrasts between these periods generally characterized by glacier retreat. First, northern hemisphere summer insolation approached its maximum during the Early Holocene (Fig. 4; Laskar *et al.* 2004). Second, post-glacial isostatic rebound rates were at their peak during the Early Holocene, while, at present, sea level in most regions on Svalbard has stabilized or is transgressing (Bondevik *et al.* 1995; Forman *et al.* 2004; Fjeldskaar *et al.* 2018). In the following section several hypothetical scenarios, which may have influenced glacier dynamics during the Early Holocene on Svalbard, are discussed.

4.3.1 Restrained rebound and ice caps chasing the equilibrium line

Relative sea level curves from Svalbard suggest that half of the total glacio-isostatic uplift occurs during the first 2 – 2.5 ka after deglaciation (Landvik *et al.* 1998; Forman *et al.* 2004). Unlike postglacial relative sea level curves constructed from dated raised marine shorelines, the rate and extent of uplift prior to local deglaciation is invisible in our raised marine records (Fig. 5A). The majority of the sea level curves from Svalbard do not project “restrained rebound” as described by Andrews (1970), but rather rapid post-glacial uplift (Bondevik *et al.* 1995; Forman *et al.* 2004). While raised shorelines provide visual geomorphological evidence of postglacial uplift, restrained rebound is the term used to describe pre-deglacial rebound. Thus, some extent of uplift presumably initiated prior to the majority of Svalbard shoreline formation (coastlines becoming ice-free). This section speculates about the amount of (restrained) rebound that occurred during Svalbard’s deglaciation prior to the formation of shorelines, and the start of the geomorphological record.

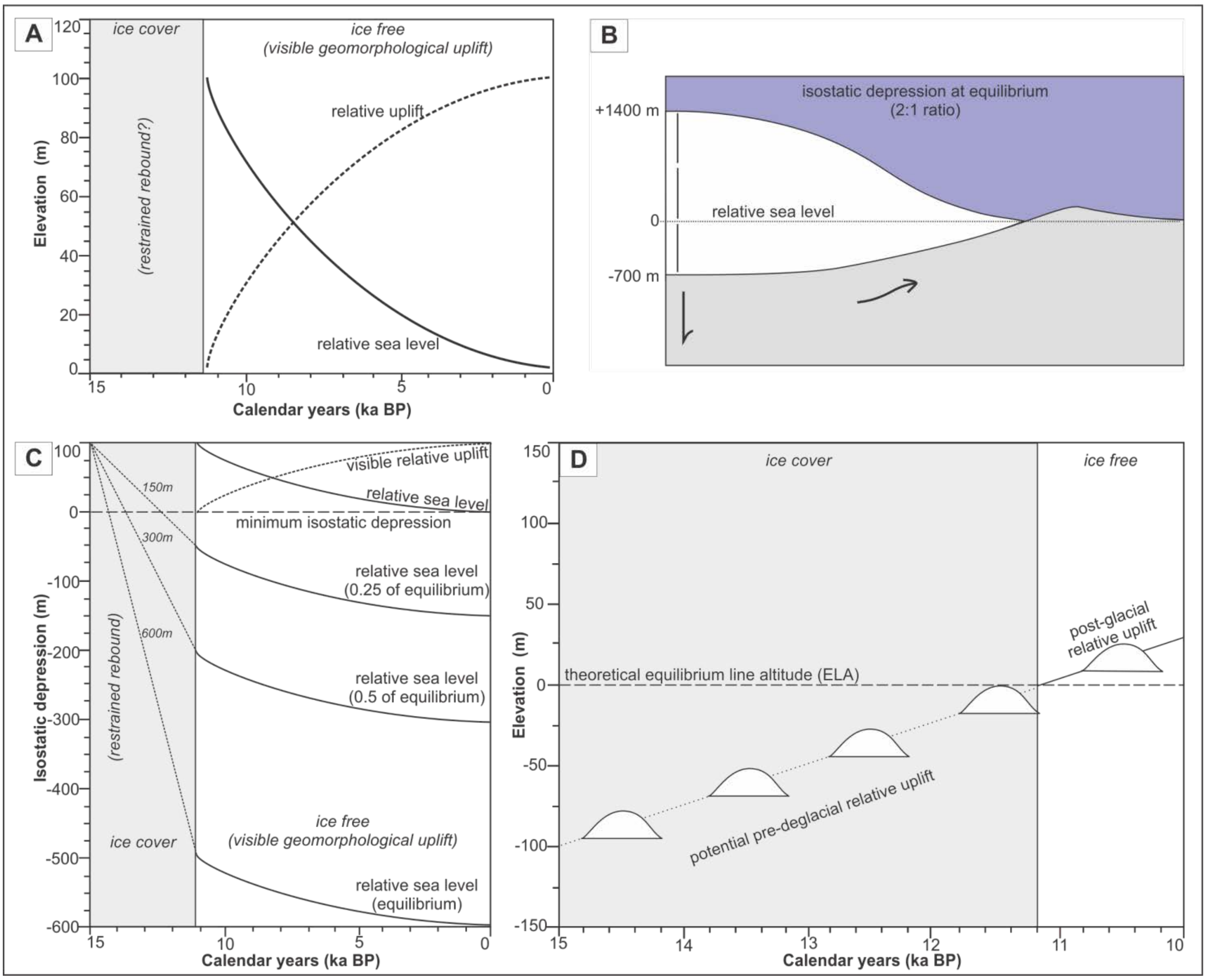

Fig. 5 Introduction and estimates of pre-deglacial (restrained) rebound. (A) Schematic relative sea level curve from Svalbard with the inverse relative uplift of 100 m after shorelines became ice-free slightly before 11 ka BP (Forman et al. 2004). (B) Model of the distribution ratio of ice sheet situated above to below sea level once isostatic depression reaches equilibrium (modified from Wolcott 1970; Andrews 1974). (C) Estimates of the extent of restrained rebound prior to an 11 ka BP deglaciation based on an ice sheet thickness of 2100 m and varying levels of isostatic equilibrium. (D) Minimum estimate of restrained rebound (1/6th of equilibrium = 100 m) projecting a schematic ice cap traveling through a constant palaeo-equilibrium line altitude.

Assuming ice thickness around Svalbard and the Barents Sea was on the order of 2000 m thick, at equilibrium, a ratio of 2:1 would reflect the distribution of ice above to ice below sea level (Andrews 1974; Lambeck, 1995; Landvik *et al.* 1998; Fig. 5B). Additionally, Svalbard is one of the regions glaciated longest throughout the last glacial cycle (~18 ka; Patton *et al.* 2015). If the ice mass persisted for long enough to arrive at equilibrium, theory would suggest roughly 700 m of the ice was located below sea level, while 1400 m of it would remain above the relative sea level. Given the assumptions of the thickness, duration and thinning of the ice sheet around Svalbard, it is only possible to speculate if equilibrium was reached regarding ice load over the (20 km) thick continental crust (Ritzmann & Jokat 2003; Patton *et al.* 2015).

The SBSIS lost the bulk of its mass between 18 – 14 ka BP (Fig. 1; Hughes *et al.* 2016). While thinning may have initiated early in southwestern Spitsbergen, the Svalbard region held ice later than the Barents Sea, with the majority of the ice loss occurring between 15 – 10 ka BP (Fig. 1C; Hughes *et al.* 2016; Young *et al.* 2018). Various schematic scenarios of linear uplift (restrained rebound) are projected between 15 – 11 ka BP based on an ice thickness of 2100 m and varying levels of isostatic equilibrium (Fig. 5C). These projections are linked to a schematic relative sea level curve with 100 meters of post-glacial isostatic uplift between 11.2 ka BP and present. Isostatic adjustment presumably reached at least 1/6th of equilibrium, thus there was a minimum of a 100 m of hidden uplift between 15 – 11 ka BP, prior to shorelines becoming ice free.

Similar to Ruddiman's (2006) schematic model of glaciation, isostatic adjustment and equilibrium line altitude (ELA), the model focuses on the interval of deglaciation (Fig. 5D). Although neither deglaciation nor uplift was linear, a model ice cap is plotted uplifting through a constant theoretical equilibrium line altitude (ELA). This schematic diagram represents what could have occurred during the period of pre-deglacial rebound, prior to Svalbard shorelines becoming ice free. The minimum projected restrained rebound (100 m) is nearly double the rise in ELA (but in the opposite direction) estimated for the 20th century (1900 – present; Røthe *et al.* 2015). The mass loss exhibited during the post-LIA period on Svalbard suggests that a 60 m rise in ELA can have a profound influence on glacier extent and mass balance. Consequently, if the relative ELA descended roughly 100 m (or if land rose up through an ELA), glaciers would exhibit strong positive mass balance. Furthermore, depending on the elevation of the ELA and the regional terrain, even a small shift in ELA can have substantial impact. Regions characterized by highland plateaus can undergo near instantaneous glaciation if terrain surpasses the threshold of the ELA (Ives *et al.* 1975; Lie *et al.* 2003).

Although there are broad assumptions regarding these estimates of pre-deglacial, restrained rebound (ice thickness, duration, age of deglaciation etc.), it is possible that hidden geomorphological uplift may have impacted Svalbard glaciers and ice dynamics during the deglaciation. The regions characterized by high-elevation plateaus, such as northeastern Spitsbergen and Nordaustlandet, could have benefited the most from this pre-deglacial rebound. Although the rate of uplift is only a fraction of uplift projected from records in Iceland during deglaciation (Norðdahl & Ingólfsson 2016) this process, coupled with enhanced precipitation patterns maybe one of the contributing factors influencing glacial re-advances during the Late Pleistocene and Early Holocene (Farnsworth *et al.* 2018).

4.3.2 Late Pleistocene – Early Holocene ice shelves on Svalbard

As the WAIS provides a modern analogue for what conditions might have been like around Svalbard and the Barents Sea during the transition from Late Pleistocene to Early Holocene (Mercer *et al.* 1970; Esteves *et al.* 2017), it is important to consider how an ice shelf may have influenced regional climate and glaciers. Ice shelves or palaeocrystic ice leave subtle morphological and sedimentological fingerprints (Hjort *et al.* 2001; Roberts *et al.* 2008; Bradly & England 2008; Fitzsimmon *et al.* 2012; Davies *et al.* 2017; Furze *et al.* 2017). Therefore relatively few palaeo-ice shelves have been described (Hodgson 1994; England *et al.* 2009; Furze *et al.* 2018).

No evidence for Holocene ice shelves has yet been identified on Svalbard. Nor, at this point, have ice shelves been the focus of any Svalbard studies. However, as ice shelves are currently an important component of the WAIS, it is possible that floating ice shelves or tongues existed during the transition from the Late Pleistocene and Early Holocene (Farnsworth *et al.* in prep.). The implications of the presence of ice shelves and their potential destabilization can have substantial consequences for glacier mass balance and dynamics, related to buttressing, back-stress, as well as precipitation (Cook & Vaughan 2010; Davies *et al.* 2017). Where ice shelves in the western Antarctic have thinned, retreated, and collapsed (Cook & Vaughan 2010), tributary glaciers have exhibited accelerated ice discharge and dynamic unsustainable advances reflective of surge-type behavior (De Angelis & Skvarca 2003; Scambos *et al.* 2003; Rignot *et al.* 2004; Berthier *et al.* 2012).

Recent studies from Svalbard have speculated that if ice shelves could have developed from a concentrated iceberg mélange or paleocrystic ice in Van Mijenfjorden and Storfjorden during deglaciation, and influenced Early Holocene glacier dynamics (Larsen *et al.* 2018; Nielsen & Rasmussen 2018). Despite the mouths of Svalbard fjords becoming ice-free prior to the onset of the Younger Dryas, there are minimal ice marginal deposits identified from this period. Furthermore, marine sedimentation rates increase only at the start of the Early Holocene (Forwick & Vorren 2010; Larsen *et al.* 2018; Nielsen & Rasmussen 2018). More work is needed in these regions that targets sediment archives spanning the Late Pleistocene to Early Holocene. Studies should investigate the geomorphological fingerprints related to ice shelves, like epi-shelf lake deposits and ice-shelf moraines (Hjort *et al.* 2001; Bentley *et al.* 2005; Furze *et al.* 2018).

4.3.3 Modern glacier behavior as a model for past glacier dynamics

Through the 20th century, Arctic glaciers and sea-ice extent have been in a general decline (Bintanja & Selten 2014; Huss and Hock 2015). At present, Arctic glacier ice surface velocities are generally increasing (Strozzi *et al.* 2017) resulting in increased rates of frontal ablation (Luckman *et al.* 2016). Since the onset of the 20th century, the rise in both atmospheric and oceanic temperatures is observed from around the Svalbard archipelago (Pavlov *et al.* 2013; Isaksen *et al.* 2016). Frontal ablation of Svalbard tidewater glaciers is closely linked to fjord water temperatures at depth which drive ice-front undercutting by oceanic melt (Luckman *et al.* 2016; Vallot *et al.* 2018). This process is apparent from enhanced surficial crevassing (Luckman *et al.* 2016). Crevasses can greatly influence the glacier hydrological system allowing for increased passage ways for supra-glacial run-off to enter the glacier system, and increasing the probability of meltwater lubricating the glacier bed (Dunse *et al.* 2015; How *et al.* 2017).

Recently, several tidewater glaciers in Svalbard have exhibited a snout destabilization, when surge-type behavior initiates at the terminus and propagates upward through the glacier system (Dunse *et al.* 2015; Strozzi *et al.* 2017; Sevestre *et al.* 2018). This development in process understanding complicates our over-simplified view of surge dynamics and glacier front fluctuations in a warming climate (Sevestre *et al.* 2018).

Traditional surge-type glacier theory suggests that ice front fluctuations (i.e., surge events) are a result of internal dynamics and are unrelated to climatic conditions (Meier & Post 1969; Sharp 1988). However, other studies have highlighted a connection between surge cyclicity and mass balance (Dowdeswell *et al.* 1995; Striberger *et al.* 2011), as well as surge-type glacier distribution and climatic conditions (Sevestre & Benn 2015). Furthermore, glaciers can exhibit surge-type behavior both in and out of phase with climate favorable for glacier growth, given the correct mass balance and basal conditions (Dowdeswell *et al.* 1995; Striberger *et al.* 2011; Philipps *et al.* 2017).

Svalbard glaciers re-advanced during deglaciation in the Early Holocene as well as through the 20th century, and both periods have been generally characterized as climatically unfavorable for glaciers (Farnsworth *et al.* 2018, in prep.). Surge-type behavior has been suggested for numerous Late Holocene glacier re-advances on Svalbard, based on (1) the extent of the glacier deposits (Liestøl 1977; Kristensen *et al.* 2009), (2) the landforms (assemblages) associated with rapid ice flow (Schomacker *et al.* 2014; Copland *et al.* 2011; Paul 2015; Farnsworth *et al.* 2016; Lovell &

Boston 2017) and (3) the internal deformation structures preserved within residual dead-ice (Lovell *et al.* 2015). However, these indicators of surge behavior are not always preserved from older events due to the erosion of glacier deposits (Kirkbride & Winkler 2012; Landvik *et al.* 2014).

Given the absence of knowledge about past precipitation patterns, unknown rates of hidden uplift, the fingerprints of ice shelves, and our poor constraint on the chronology of Holocene glacier re-advances, we are unable to positively conclude whether climate or glacier dynamics is the driving factor of Holocene ice-front fluctuations (Farnsworth *et al.* 2018, in prep). However, on a Holocene time-scale, the difference of a surge-type glacier's response to climate compared to a non-surge-type glacier maybe negligible as the assumed variability fits within the margins of error of our current dating techniques (Philipps *et al.* 2017).

It is critical to recognize how the style of subsequent ice loss following the glacier re-advances may vary given the two different types of glacier behavior. Oerlemans & van Pelt (2015) suggest one of the key results of a surge is lowering the mean surface elevation, which increases the ablation area and subsequently causes a negative perturbation in the mass budget of the glacier system. Thus, a glacier that surges into a warming climate will exhibit a greater rate of retreat in comparison to a non-surge-type glacier (retreating under the same unfavorable climatic forcing; Dowdeswell *et al.* 1995; Oerlemans & van Pelt 2015; Farnsworth *et al.* 2018). The process of a dynamic unsustainable re-advance into a warming climate is an efficient means of shedding a large mass of ice in a short period of time. Potentially, this could result in a retreat so extensive the glacier system is not able to return to an active surge phase (Dowdeswell *et al.* 1995; Striberger *et al.* 2011).

For most Svalbard's glaciers where numerous surges have been documented, each successive surge is less extensive than the previous (Fig. 6A & B; Flink *et al.* 2015; Lønne 2016; Farnsworth *et al.* 2017; Flink *et al.* 2017; Larsen *et al.* 2018), a documented exception to this is Nathorstbreen (Sund *et al.* 2014). These recessive surge moraines have been mapped and described across Svalbard with the most frequent series of events identified in front of Tunabreen and Paulabreen (Fig. 6A & B; Flink *et al.* 2015; Larsen *et al.* 2018). Eight separate surge events have been documented in front of both glacier systems (four each) where submarine moraine ridges indicated the outer-most ice extent for each event (Flink *et al.* 2015; Larsen *et al.* 2018). Additionally, recent surges have been observed at both glacier systems where submarine morphology is yet to be investigated, but ice extent was less extensive than the four earlier events (Kristensen & Benn 2012; Larsen *et al.* 2018; St. Andrews Glaciology and C. Borstad personal comm.). In some locations on Svalbard, where postglacial uplift has raised once-shallow fjords above the modern coast, similar ice marginal deposits can be identified in series (Fig. 6C & D).

Given the relation between the high relative sea level and the glacier deposits, the timing of the formation of these landforms must have been rapid and shortly after deglaciation (Farnsworth *et al.* 2018).

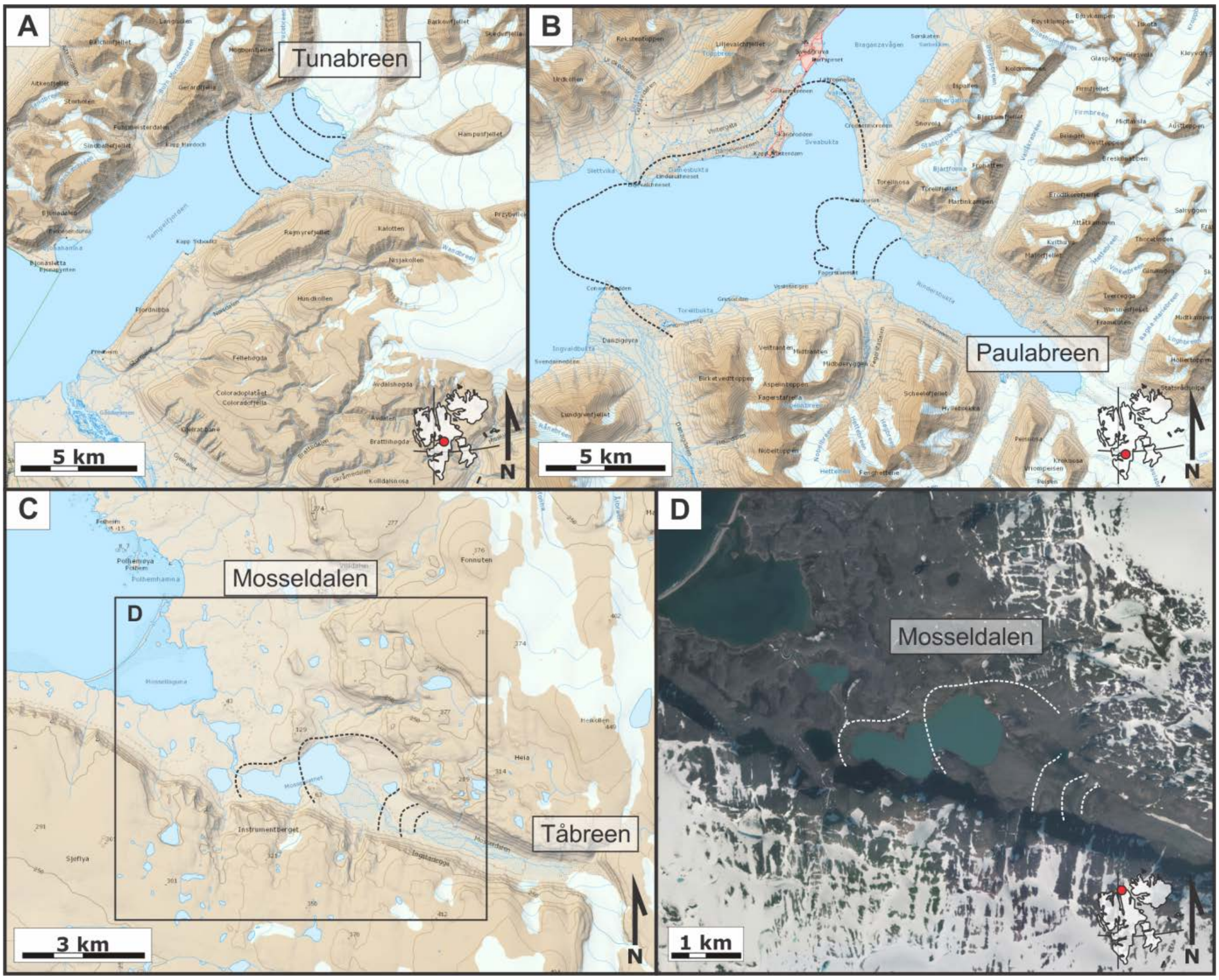

Fig. 6A & B) Topographic maps of documented end moraines from surges indicating retrogressive surge extent for Tunabreen and Paulabreen, respectively (Flink et al. 2015; Larsen et al. 2018). C) Topographic map with a series of ice marginal deposits preserved in Mosseldalen that were deposited successively into a high relative sea level during the Late Pleistocene and Early Holocene. Landforms from all three sites seem to have been deposited into a shallow fjord environment during a period characterized by a transition from cool to warm climate. D) Inset aerial image of Mosseldalen with ice marginal deposits indicated modified from TopoSvalbard.

Model projections of ELA for the rest of the 20th century suggest ELAs will rise above most of the summits and ice fields in Svalbard (Førland *et al.* 2011; Østby *et al.* 2017). This will lead to considerable mass change as well as shifts in the glacier thermal and hydrological regimes, directly influencing glacier dynamics (Dunse *et al.* 2015; Østby *et al.* 2017; Willis *et al.* 2018). Given the processes detailed in recent Svalbard surge studies, it appears that warming oceans could continue to trigger instabilities at tidewater margins (Dunse *et al.* 2015; Strozzi *et al.* 2017; Sevestre *et al.* 2018; Willis *et al.* 2018). Considering the climatic similarities between the transitions of the Younger Dryas to Early Holocene and the LIA to the 20th century, it is possible that these processes have acted on Svalbard glaciers in the past. The deglaciation at the onset of the Holocene may better reflect current ice dynamics than previously acknowledged. These findings from Svalbard compliment earlier studies documenting the dynamic and complex pattern of deglaciation, which appears time transgressive across the Barents Sea (Winsborrow *et al.* 2010; Andreassen *et al.* 2014; Bjarnadóttir *et al.* 2014; Newton & Huuse 2017).

As comparisons are made between the WAIS and the SBSIS, it is increasingly important to consider unsustainable glacio-dynamic behavior regarding the style of ice loss in a warming climate (Mercer 1970; Oerlemans & van Pelt 2015; Newton & Huuse 2017; Willis *et al.* 2018; Farnsworth *et al.* 2018). Evidence of this dynamic style of deglaciation is emerging from the Svalbard Barents Sea region, during both the last deglaciation and at present. Are we beginning to see this glacio-dynamic behavior in the West Antarctic (De Angelis & Skvarca 2003; Scambos *et al.* 2003; Berthier *et al.* 2012)?

5. SUMMARY AND CONCLUSIONS

Through the Holocene, Svalbard glaciers have exhibited (at least) two phases of widespread glacier re-advance, during the Early Holocene and throughout the entire Late Holocene. No geomorphological features have been identified corresponding to glacier re-advances between 9.0 – 4.5 ka BP. Consequently, relatively little is known about the extent of Svalbard glaciers during the Mid Holocene.

Early Holocene glacier re-advances are identified across Svalbard, corresponding to a diverse range of glacier sizes. With our current level of age constraint, these ice marginal fluctuations do not appear synchronous in time. Furthermore, the Early Holocene climate is believed to have been warm, unfavorable for glacier growth and characterized by deglaciation. Early Holocene glacier re-advances appear to relate to the time-transgressive nature of deglaciation. Glacier re-advances likely corresponded to glacier dynamics (not mass balance) and reflect the complex style of ice-mass-loss during a changing climate.

Landforms and deposits from glaciers re-advancing during the Late Holocene have been the primary focus of Holocene glacial studies. Glacier re-advances and corresponding deposits have been attributed to episodic Neoglacial cooling and the Little Ice Age (LIA). The majority of Late Holocene glacier re-advances have been dated to between 4.0 – 0.5 ka BP. The highest frequency of re-advances are constrained to 1.0 – 0.5 ka BP, during the first half of the LIA. Glacial landforms and deposits from LIA re-advances have been suggested to indicate rapid and dynamic glacier behavior (in some cases characteristic of surge-type events).

During the 20th century (post-LIA), Svalbard glaciers have exhibited widespread negative mass balance, ice marginal retreat, and glacier thinning. This phase of retreat has had a direct influence on glacier thermal regime, hydrologic system and surface profile. Through the 20th century, some Svalbard glaciers have continued to exhibit surge-type re-advances. Several glaciers have exhibited this behavior numerous times. These glacio-dynamic re-advances have been un-sustained and each subsequent surge has been less extensive then the previous. Consequently, and despite re-advance, glaciers reflect a continual phase of ice-mass-loss in a periodic fashion.

- Throughout the Holocene, Svalbard glaciers have responded to a varying combination of climatic, environmental and dynamic driving factors which influence both the extent and behavior of ice margins.

- Glaciers during the Late Pleistocene and Early Holocene were dynamic, exhibited re-advances and extended well beyond Late Holocene glacier maxima in many locations across Svalbard.
- The marine Holocene thermal optimum on Svalbard, marked by the early arrival of warm water species to the coasts of Svalbard during the onset of the Holocene, pre-dates the peak in northern hemisphere summer insolation and the terrestrial thermal optimum.
- During the Holocene glacial minimum, glaciers covered a small, but unknown percentage of Svalbard. Marine sediment cores from Svalbard fjords suggest some tidewater glacier fronts persisted through the glacial minimum.
- Evidence of episodic Neoglacial glacier re-advances is being identified more commonly across Svalbard, suggesting a stepped and variable phase of conditions favorable for glacier growth during the Late Holocene.
- The Little Ice Age maximum does not reflect the glacial maximum extent across Svalbard; since the deglaciation, the onset of the Holocene or even during the Late Holocene, in most locations.
- Svalbard glaciers exhibited widespread glacio-dynamic re-advances at some point during the Little Ice Age, in some cases developing (and preserving) landforms indicative of surge-type behavior.
- Following the Little Ice Age, the majority of Svalbard glaciers have undergone extensive retreat and thinning which has led to changes in the thermal regime, hydrological system, and surface profile of glaciers.
- Some glaciers on Svalbard have continued to exhibit dynamic re-advances characterized as surges-type behavior, however each surge-event is less extensive than the previous exhibiting a trend of continual ice loss.

6. FUTURE PROSPECTS

All studies of glacier and climate history should strive to have a holistic approach to systems and processes; taking into account a mixture of methods, archives and disciplines. Future Svalbard studies should endeavor to:

- Enhance our understanding of the range of variability as well as factors governing the arrival and strength of the West Spitsbergen Current to Svalbard. As the impact of these warm Atlantic waters around Svalbard has a strong control on regional temperatures and precipitation, these conditions are critical for predicting future climatic conditions as well as glacier extent and dynamics.
- Better address past precipitation patterns both through proxy studies (e.g., leaf wax hydrogen isotopes) and better understanding recent shifts and current processes in order to constrain models used to project precipitation in a changing climate.
- Target lakes corresponding to larger glacier systems which persisted throughout more of the (or the entire) Holocene. This would close the gap in knowledge regarding the Holocene glacier minimum and the early onset of the Neoglacial. Furthermore, defining a Holocene tephrochronology for Svalbard, based on pan-Arctic volcanism, would improve high-Arctic lake sediment chronologies as well as put volcanic events into climatic perspective.
- Focus on regions around Svalbard (e.g. Van Mijenfjorden, Storfjorden, Isfjorden and Hinlopen Strait) where ice shelves or palaeocristic ice may have formed during the transition from the Late Pleistocene to the Early Holocene. By combining stratigraphic and morphological data from marine and terrestrial archives it may be possible to suggest if these features existed around Svalbard and whether they had an influence on glacier dynamics or environmental conditions.
- Further constrain the timing of Late Pleistocene – Early Holocene glacier re-advances. Additionally, attempts to model this transitional period based on estimates of oceanic/atmospheric temperatures, precipitation and relative uplift would be valuable.
- Improve our understanding of post-glacial (and pre-deglacial) uplift around Svalbard. Studies should continue to detail sea level curves to better resolve Holocene transgressions and rebound intricacies. Further studying crustal rheology and characteristics of the response of the Earth’s crust to isostatic loading and unloading (return rate/size of area influenced) would be valuable.

References

Andersson, T., Forman, S.L., Ingólfsson, Ó., Manley, W.F. (1999): Late Quaternary environmental history of central Prins Karls Forland, western Svalbard. *Boreas 28*, 292–307.

Andersson, T., Forman, S.L., Ingólfsson, Ó., Manley, W.F. (2000): Stratigraphic and morphologic constraints on the Weichselian glacial history of northern Prins Karls Forland, Western Svalbard. *Geografiska Annaler Series A 82*, 455–470.

Andreassen, K., Winsborrow, M.C.M. (2009): Signature of ice streaming in Bjørnøyarenna, Polar North Atlantic, through the Pleistocene and implications for ice-stream dynamics. *Annals of Glaciology 50*, 17–26.

Andreassen, K., Winsborrow, M.C.M., Bjarnadóttir, L.R., Rüther, D.C. (2014): Ice stream retreat dynamics inferred from an assemblage of landforms in the northern Barents Sea. *Quaternary Science Reviews 92*, 246–257.

Andrews, J.T. (1970): A Geomorphological Study of postglacial uplift with particular Reference to Arctic Canada, Institute of British Geographers, London, Special Publication, 2.

Andrews, J.T., (1974): Glacial isostasy. Hutchinson and Ross, Inc., Stroudsburg, Pennsylvania, Dowden, USA, 1–491.

Balascio, N.L., D'Andrea, W.J., Gjerde, M., Bakke, J. (2018): Hydroclimate variability of High Arctic Svalbard during the Holocene inferred from hydrogen isotopes of leaf waxes. *Quaternary Science Reviews 183*, 177–187.

Jonathan, L.B., Richard, M.W., Ben, M., Bert, W. (2018): The land ice contribution to sea level during the satellite era. *Environmental Research Letters 13*, 063008.

Bartels, M., Titschack, J., Fahl, K., Stein, R., Seidenkrantz, M.S., Hillaire-Marcel, C., Hebbeln, D. (2017): Atlantic water advection vs. glacier dynamics in northern Spitsbergen since early deglaciation. *Climate of the Past 13*, 1717–1749.

Benestad, R.E., Hanssen-Bauer, I., Skaugen, T.E., Førland, E.J. (2003): Associations between sea-ice and the local climate on Svalbard. Norwegian Meteorological Institute. *KLIMA Report 1–07/02*, 1–13.

Bennett, M.R. (2003): Ice streams as the arteries of an ice sheet: their mechanics, stability and significance *Earth Science Reviews 61*, 309–339.

Bentley, M.J., Hodgson, D.A., Sugden, D.E., Roberts, S.J., Smith, J.A., Leng, M.J., Bryant, C. (2005): Early Holocene retreat of the George VI Ice Shelf, Antarctic Peninsula. *Geology 33*, 173–176.

Berge, J., Johnsen, G., Nilsen, F., Gulliksen, B., Slagstad, D. (2005): Ocean temperature oscillations enable reappearance of blue mussels Mytilus edulis in Svalbard after 1000 year absence. *Marine Ecology Progress Series 303*, 167–175.

Berthier, E., Scambos, T., Schuman, C.A. (2012): Mass loss of Larsen B tributary glaciers (Antarctic Peninsula) unabated since 2002. *Geophysical Research Letters 39*, L13501.

van der Bilt, W.G.M., Bakke, J., Vasskog, K., D'Andrea, W.J., Bradley, R.S., Olafsdóttir, S. (2015): Reconstruction of glacier variability from lake sediments reveals dynamic Holocene climate in Svalbard. *Quaternary Science Reviews 126*, 201–218.

van der Bilt, W.G.M., D'Andrea, W.J., Bakke, J., Balascio, N.L., Werner, J.P., Gjerde, M., Bradley, R.S. (2018): Alkenone-based reconstructions reveal four-phase Holocene temperature evolution for High Arctic Svalbard. *Quaternary Science Reviews 183*, 204–213.

Bintanja, R., Selten, F.M. (2014): Future increases in Arctic precipitation linked to local evaporation and sea-ice retreat. *Nature 509*, 479–482.

Bjarnadóttir, L.R., Winsborrow, M.C.M., Andreassen, K. (2014): Deglaciation of the central Barents Sea. *Quaternary Science Reviews 92*, 208–226.

Björnsson, H., Gjessing, Y., Hamran, S.E., Hagen, J.O. (1996): The thermal regime of sub-polar glaciers mapped by multi-frequency radio-echo sounding. *Journal of Glaciology 42*, 23–32.

Björnsson, H. (1998): Hydrological characteristics of the drainage system beneath a surging glacier. *Nature 395*, 771–774.

Björnsson, H., Pálsson, F., Sigurdsson, O., Flowers, G.E. (2003): Surges of glaciers in Iceland. *Annals of Glaciology 36,* 82–90.
Blake, W.J. (1961): Russian settlement and land rise in Nordaustlandet, Spitsbergen. *Arctic 14,* 101–111.
Blake, W.J. (1962): Geomorphology and Glacial Geology in Nordaustlandet, Spitsbergen. PhD thesis, Department of Geology, Ohio State University, Columbus, 1–477.
Blaszczyk, M., Jania, J.A., Hagen, J.O. (2009): Tidewater glaciers of Svalbard: Recent changes and estimates of calving fluxes. *Polish Polar Research 30,* 85–142.
Bond, G., Kromer, B., Beer, J., Muscheler, R., Evans, M.N., Showers, W., Hoffmann, S., Lotti-Bond, R., Hajdas, I., Bonani, G. (2001): Persistent solar influence on north Atlantic climate during the Holocene. *Science 294,* 2130–2136.
Bondevik, S., Mangerud, J., Ronnert, L., Salvigsen, O. (1995): Postglacial sea-level history of Edgeoya and Barentsoya, eastern Svalbard. *Polar Research 14,* 153–180.
Boulton, G.S. (1979): Glacial history of the Spitsbergen archipelago and the problem of a Barents Shelf ice sheet. *Boreas 8,* 31–57.
Bradley, R.S., England, J.H. (2008): The Younger Dryas and the sea of ancient ice: *Quaternary Research 70,* 1–10.
Briner, J.P. (2016): Ice streams waned as ice sheets shrank. *Nature 530,* 287–288.
Brynjólfsson, S., Ingólfsson, Ó., Schomacker, A. (2012): Surge fingerprinting of cirque glaciers at the Tröllaskagi peninsula, North Iceland. *Jökull 62,* 151–166.
Christiansen, H.H., Etzelmüller, B., Isaksen, K., Juliussen, H., Farbrot, H., Humlum, O., Johansson, M., Ingeman-Nielsen, T., Kristensen, L., Hjort, J., Holmlund, P., Sannel, A.B.K., Sigsgaard, C., Åkerman, H.J., Foged, N., Blikra, L.H., Pernosky, M.A., Ødegård, R.S. (2010): The thermal state of permafrost in the nordic area during the international polar year 2007–2009. *Permafrost and Periglacial Processes 21,* 156–181.
Christiansen, H.H., Humlum, O., Eckerstorfer, M. (2013): Central Svalbard 2000–2011 Meteorological Dynamics and Periglacial Landscape Response. *Arctic, Antarctic, and Alpine Research 45,* 6–18.
Clarke, G.K.C., Collins, S.G., Thompson, D.E. (1984): Flow, thermal structure, and subglacial conditions of a surge-type glacier. *Canadian Journal of Earth Sciences 21,* 232–240.
Cohen, K.M., Finney, S.C., Gibbard, P.L., Fan, J.X. (2013; updated): The ICS international chronostratigraphic chart. Episodes 36, 199–204.
Cook, A.J., Vaughan, D.G. (2010): Overview of areal changes of the ice shelves on the Antarctic Peninsula over the past 50 years. *The Cryosphere 4,* 77–98.
Copland, L., Sylvestre, T., Bishop, M., Shroder, J., Seong, Y., Owen, L., Bush, A., Kamp, U. (2011): Expanded and recently increased glacier surging in the karakoram. *Arctic, Antarctic and Alpine Research 43,* 503–516.
Dallmann, W.K., Elvevold, S. (2015): Geoscience atlas of Svalbard. In Dallmann,W. K. (ed.): Geoscience Atlas of Svalbard, 133–174. Norsk Polarinstitutt Rapport serie 148, Oslo.
D'Andrea, W.J., Vaillencourt, D.A., Balascio, N.L., Werner, A., Roof, S.R., Retelle, M., Bradley R.S. (2012): Mild little ice age and unprecedented recent warmth in an 1800 year lake sediment record from Svalbard. *Geology 40,* 1007–1010.
Dansgaard, W., Johnsen, S.J., Clausen, H.B., Dahl-Jensen, D., Gundestrup, N.S., Hammer, C.U., Hvidberg, C.S., Steffensen, J.P., Sveinbjörnsdottir, A.E., Jouzel, J. Bond, G. (1993): Evidence for general instability of past climate from a 250-kyr ice-core record. *Nature 364,* 218–220.
Davies, B.J., Hambrey, M.J., Glasser, N.F., Holt, T., Rodés, A., Smellie, J.L., Carrivick, J.L., Blockley, S.P.E. (2017): Ice-dammed lateral lake and epishelf lake insights into Holocene dynamics of Marguerite Trough Ice Stream and George VI Ice Shelf, Alexander Island, Antarctic Peninsula. *Quaternary Science Reviews 177,* 189–219.
De Angelis, H., Skvarca, P. (2003): Glacier surge after ice shelf collapse. *Science 299,* 1560–1562.

DeConto, R.M., Pollard, D. (2016): Contribution of Antarctica to past and future sea-level rise. *Nature 531,* 591–597.
De Geer, G. (1900): Om östra Spitsbergens glaciation under istiden. *Geologiska Föreningens i Stockholm Förhandlingar 22,* 427–436.
Dickson, R.R., Osborn, T.J., Hurrell, J.W., Meincke, J., Blindheim, J., Adlandsvik, B., Vinje, T., Alekseev, G., Maslowski, W. (2000): The Arctic Ocean response to the North Atlantic Oscillation. *Journal of Climate 13,* 2671–2696.
Divine, D., Isaksson, E., Martma, T., Meijer, H.A.J., Moore, J., Pohjola, V., van de Wal, R.S.W., Godtliebsen, F. (2011): Thousand years of winter surface air temperature variations in Svalbard and northern Norway reconstructed from ice-core data. *Polar Research 30,* 73–79.
Dowdeswell, J.A., Hamilton, G.S., Hagen, J.O. (1991): The duration of the active phase on surge-type glaciers: contrasts between Svalbard and other regions. *Journal of Glaciology 37,* 388–400.
Dowdeswell, J.A., Hodgkins, R., Nuttall, A.M., Hagen, J.O., Hamilton, G.S. (1995): Mass balance change as a control on the frequency and occurrence of glacier surges in Svalbard, Norwegian High Arctic. *Geophysical Research Letters 22,* 2909–2912.
Dowdeswell, J.A., Benham, T.J. (2003): A surge of Perseibreen, Svalbard, examined using aerial photography and ASTER high resolution satellite imagery. *Polar Research 22,* 373–383.
Dowdeswell, J.A., Hogan, K.A., Ó Cofaigh, C., Fugelli, E.M.G., Noormets, R. (2014): Late Quaternary ice flow in a West Greenland fjord and cross-shelf trough system: submarine landforms from Rink Isbrae to Uummannaq shelf and slope. *Quaternary Science Reviews 92*, 292–309.
Drange H, Dokken T, Furevik T Gerdes, R., Berger, W., Nesje, A., Orvik, K.A., Skagseth, Ø., Skjelvan, I., Østerhus, S. (2005): The Nordic Seas: an overview. In: Drange H, Dokken T, Furevik T et al (eds) The Nordic seas: an integrated perspective. American Geophysical Union, Washington, DC, 1–10.
Dunse, T., Schellenberger, T., Hagen, J., Kääb, A., Schuler, T., Reijmer, C. (2015): Glacier-surge mechanisms promoted by a hydro-thermodynamic feedback to summer melt. *The Cryosphere 9,* 197–215.
Eckerstorfer, M., Christiansen, H.H. (2011): The “High Arctic Maritime Snow Climate” in Central Svalbard. *Arctic, Antarctic, and Alpine Research 43,* 11–21.
England, J., Furze, M.F.A., Doupe, J.P. (2009): Revision of the NW Laurentide Ice Sheet: implications for paleoclimate, the northeast extremity of Beringia, and Arctic Ocean sedimentation. *Quaternary Science Reviews 28,* 1573–1596.
Esteves, M., Bjarnadóttir, L.R., Winsborrow, M.C.M., Shackleton, C.S., Andreassen, K. (2017): Retreat patterns and dynamics of the Sentralbankrenna glacial system, central Barents Sea. *Quaternary Science Reviews 169,* 131–147.
Evans, D.J.A., Rea, B.R. (1999): Geomorphology and sedimentology of surging glaciers: a land-systems approach. *Annals of Glaciology 28,* 75–82.
Evans, D.J.A., Rea, B.R. (2003): Surging glacier landsystem. In: Evans, D.J.A. (Ed.), Glacial Landsystems. Arnold, London, 259–288.
Evans, D.J.A., Clark, C.D., Rea, B.R. (2008): Landform and sediment imprints of fast glacier flow in the southwest Laurentide Ice Sheet. *Journal of Quaternary Science 23,* 249–272.
Farnsworth, W.R., Ingólfsson, Ó., Retelle, M., Schomacker, A. (2016): Over 400 previously undocumented Svalbard surge-type glaciers identified. *Geomorphology 264,* 52–60.
Farnsworth, W.R., Ingólfsson, Ó., Noormets, R., Allaart, L., Alexanderson, H., Henriksen, M., Schomacker, A. (2017): Dynamic Holocene glacial history of St. Jonsfjorden, Svalbard. *Boreas 46,* 585–603.
Farnsworth, W.R., Ingólfsson, Ó., Retelle, M., Allaart, L., Håkansson, L., Schomacker, A. (2018): Svalbard glaciers re-advanced during the Pleistocene-Holocene transition. *Boreas 47,* 1022–1032.

Farnsworth, W.R., Ingólfsson, Ó., Alexandersson, H., Forwick, M., Noormets, R., Retelle, M., Schomacker, A. (*in prep.)*: Holocene glacial and climate history of Svalbard – status, perspectives and challenges.

Feyling-Hanssen, R.W., Olsson, I.U. (1960): Five radiocarbon datings of Post Glacial shorelines in Central Spitsbergen. *Norsk Geografisk Tidsskrift 17,* 122–131.

Fitzsimons, S. J., Mager, S., Frew, R., Clifford, A., Wilson, G. (2012): Formation of ice-shelf moraines by accretion of seawater and marine sediment at the southern margin of the McMurdo Ice Shelf, Antarctica. *Annals of Glaciology 53,* 211–220.

Fjeldskaar, W., Bondevik, S., Amantov, A. (2018): Glaciers on Svalbard survived the Holocene thermal optimum. *Quaternary Science Reviews 199,* 18–29. DOI: 10.1016/j.quascirev.2018.09.003.

Flink, A.E., Noormets, R., Kirchner, N., Benn, D.I., Luckman, A., Lovell, H. (2015): The evolution of a submarine landform record following recent and multiple surges of Tunabreen glacier, Svalbard. *Quaternary Science Reviews 108,* 37–50.

Flink, A.E., Noormets, R., Fransner,O., Hogan, K.A., O'Regan, M., Jakobsson, M. (2017): Past ice flow in Wahlenbergfjorden and its implications for late Quaternary ice sheet dynamics in northeastern Svalbard. *Quaternary Science Reviews 163,* 162–179.

Forman, S.L., Miller, G.H. (1984): Time-dependent soil morphologies and pedogenetic processes on raised beaches, Brøggerhalvøya, Spitsbergen, Svalbard archipelago. *Arctic and Alpine Research 16,* 381–394.

Forman, S.L. (1989): Late Weichselian glaciation and deglaciation of Forlandsundet area, western Spitsbergen, Svalbard. *Boreas 18,* 51–60.

Forman, S.L. (1990): Post-glacial relative sea-level history of northwestern Spitsbergen, Svalbard. *Geological Society of America Bulletin 102,* 1580–1590.

Forman, S.L., Lubinski, D.J., Ingólfsson, Ó., Zeeberg, J.J., Snyder, J.A., Siegert, M.J., Matishov, G.G. (2004): A review of postglacial emergence on Svalbard, Franz Josef Land and Novaya Zemlya, northern Eurasia. *Quaternary Science Reviews 23,* 1391–1434.

Forwick, M., Vorren, T. O., Hald, M., Korsun, S., Roh, Y., Vogt, C., Yoo, K.-C. (2010): Spatial and temporal influence of glaciers and rivers on the sedimentary environment in Sassenfjorden and Tempelfjorden, Spitsbergen. *Geological Society, London, Special Publications 344,* 163–193.

Fowler, A.C., Murray, T., Ng, F.S.L. (2001): Thermally controlled glacier surging. *Journal of Glaciology 47,* 527–538.

French, M.H. (2007): The Periglacial Environment. Third edition. Chichester, U.K. and Hoboken, New Jersey John Wiley & Sons, 1–458.

Fretwell, P., Pritchard, H.D., Vaughan, D.G., Bamber, J.L., Barrand, N.E., Bell, R., Bianchi, C., Bingham, R.G., Blankenship, D.D., Casassa, G., Catania, G., Callens, D., Conway, H., Cook, A.J., Corr, H.F.J., Damaske, D., Damm, V., Ferraccioli, F., Forsberg, R., Fujita, S., Gogineni, P., Griggs, J.A., Hindmarsh, R.C.A., Holmlund, P., Holt, J.W., Jacobel, R.W., Jenkins, A., Jokat, W., Jordan, T., King, E.C., Kohler, J., Krabill, W., Riger-Kusk, M., Langley, K.A., Leitchenkov, G., Leuschen, C., Luyendyk, B.P., Matsuoka, K., Nogi, Y., Nost, O.A., Popov, S.V., Rignot, E., Rippin, D.M., Riviera A., Roberts, J., Ross, N., Siegert, M.J., Smith, A.M., Steinhage, D., Studinger, M., Sun, B., Tinto, B.K., Welch, B.C., Young, D.A., Xiangbin, C., Zirizzotti, A. (2012): Bedmap2: Improved ice bed, surface and thickness datasets for Antarctica. *The Cryosphere 6,* 375–393.

Fürst, J.J., Gillet-Chaulet, F., Benham, T.J., Dowdeswell, J.A., Grabiec, M., Navarro, F., Pettersson, R., Moholdt, G., Nuth, C., Sass, B., Aas, K., Fettweis, X., Lang, C., Seehaus, T., Braun, M. (2017): Application of a two-step approach for mapping ice thickness to various glacier types on Svalbard. *The Cryosphere 11,* 2003–2032.

Furze, M.F.A., Pieńkowski, A.J., McNeely, M.A., Bennett, R., Cage, A.G. (2018): Deglaciation and ice shelf development at the northeast margin of the Laurentide Ice Sheet during the Younger Dryas chronozone. *Boreas 47*, 271–296.
Førland, E.J., Hanssen-Bauer, I., Nordli, P.Ø. (1997): Climate statistics and longterm series of temperature and precipitation at Svalbard and Jan Mayen. Rapport 21/97 - *Report Series of the Norwegian Meteorological Institute* 92 pp.
Førland, E.J., Benestad, R, Hanssen-Bauer, I. (2011): Temperature and precipitation development at Svalbard 1900–2100. *Advances in Meteorology 2011*, 1-14.
Gandy, N., Gregoire, L.J., Ely, J.C., Clark, C.D., Hodgson, D.M., Lee, V., Bradwell, T., Ivanovic, R.F. (2018): Marine Ice Sheet Instability and Ice Shelf Buttressing Influenced Deglaciation of the Minch Ice Stream, Northwest Scotland. *The Cryosphere Discuss 2018,* 1–24. DOI: 10.5194/tc-2018-116.
Gilbert, G.L., O'Neill, H.B., Nemec, W., Thiel, C., Christiansen, H.H., Buylaert, J.-P. (2018): Late Quaternary sedimentation and permafrost development in a Svalbard fjord-valley, Norwegian high Arctic. *Sedimentology 65*, 1-28. DOI:10.1111/sed.12476.
Hagen, J.O., Liestøl, O., Roland, E., Jørgensen, T. (1993): Glacier atlas of Svalbard and Jan Mayen. Meddelelser vol 129. Norsk Polarinstitutt, Oslo, 1–143.
Hagen, J.O., Melvold, K., Pinglot, J.F., Dowdeswell, J.A. (2003): On the net mass balance of the glaciers and ice caps of Svalbard, Norwegian Arctic. *Arctic, Antarctic and Alpine Research 35*, 264–270.
Hald, M., Ebbesen, H., Forwick, M., Godtliebsen, F., Khomenko, L., Korsun, S., Ringstad Olsen, L., Vorren, T.O. (2004): Holocene paleoceanography and glacial history of the West Spitsbergen area, Euro-Arctic margin. *Quaternary Science Reviews 23*, 2075–2088.
Hald, M., Andersson, C., Ebbesen, H., Jansen, E., Klitgaard-Kristensen, D., Risebrobakken, B., Salomonsen, G.R., Sarnthein, M., Sejrup, H.P., Telford, R.J., (2007): Variations in temperature and extent of Atlantic Water in the northern North Atlantic during the Holocene. *Quaternary Science Reviews 26*, 3423–3440.
Hanssen-Bauer, I., Kristensen Solås, M., Steffensen, E.L. (1990): The climate of Spitsbergen. *Norwegian Meteorological Institute Report 39/90*, 1–40.
Hartmann, D.L., Klein Tank, A.M.G., Rusticucci, M., Alexander, L.V., Brönnimann, S., Charabi, Y., Dentener, F.J., Dlugokencky, E.J., Easterling, D.R., Kaplan, A., Soden, B.J., Thorne, P.W., Wild, M. Zhai, P.M. (2013): Observations: atmosphere and surface. In Stocker, T.F., Qin, D., Plattner, G.-K., Tignor, M., Allen, S.K., Boschung, J., Nauels, A., Xia, Y., Bex, V. Midgley, P.M. (eds.): Climate Change 2013 the Physical Science Basis: Working Group I Contribution to the Fifth Assessment Report of the Intergovernmental Panel on Climate Change, 159–254. Cambridge University Press, Cambridge.
Harrison, W.D., Post, A.S. (2003): How much do we really know about glacier surging? *Annals of Glaciology 26*, 1–6.
Hisdal, V. (1985): Geography of Svalbard, Polar handbook No. 2. Oslo: *Norsk Polarinstitutt.*
Hjort, C., Bentley, M.J., Ingólfsson, Ó. (2001): Holocene and pre-Holocene temporary disappearance of the George VI Ice Shelf, Antarctic Peninsula. *Antarctic Science 13,* 296–301.
Hodgson, D.A. (1994): Episodic ice streams and ice shelves during retreat of the north western most sector of the Late Wisconsinan Laurentide Ice Sheet over the central Canadian Arctic Archipelago. *Boreas 23,* 14–28.
Hogan, K.A., Dowdeswell, J.A., Hillenbrand, C.-D., Ehrmann, W., Noormets, R. Wacker, L. (2017): Subglacial sediment pathways and deglacial chronology of the northern Barents Sea Ice Sheet. *Boreas 46,* 750–771.
Hoppe, G. (1972): Ice sheets around the Norwegian Sea during the Würm glaciation. *Ambio Special Report 2,* 25–29.

Hormes, A., Gjermundsen, E.F., Rasmussen, T.L. (2013): From mountain top to the deep sea—deglaciation in 4D of the northwestern Barents Sea ice sheet. *Quaternary Science Reviews 75,* 78–99.

Houmark-Nielsen, M., Funder, S. (1999): Pleistocene stratigraphy of Kongsfjordhallet, Spitsbergen, Svalbard. *Polar Research 18,* 39–49.

How, P., Benn, D.I., Hulton, N.R.J., Hubbard, B., Luckman, A., Sevestre, H., van Pelt, W.J.J., Lindbäck, K., Kohler, J., Boot, W. (2017): Rapidly changing subglacial hydrological pathways at a tidewater glacier revealed through simultaneous observations of water pressure, supraglacial lakes, meltwater plumes and surface velocities. *The Cryosphere 11,* 2691–2710.

Hughes, A.L.C., Gyllencreutz, R., Lohne, Ø.S., Mangerud, J., Svendsen, J.I. (2016): The last Eurasian ice sheets – a chronological database and time-slice reconstruction, DATED-1. *Boreas 45,* 1–45.

Hume, D. (1955): An enquiry concerning human understanding. In: S.M. Cahn (Ed.), The Monist. Oxford University Press, 1–112.

Humlum, O. (2002): Modelling late 20th-century precipitation in Nordenskiöld Land, Svalbard, by geomorphic means. Norsk Geografisk Tidsskrift. *Norwegian Journal of Geography 56,* 96–103.

Humlum, O., Elberling, B., Hormes, A., Fjordheim, K., Hansen, O.H., Heinemeier, J. (2005): Late-Holocene glacier growth in Svalbard, documented by subglacial relict vegetation and living soil microbes. *The Holocene 15,* 396–407.

Huss, M., Hock, R., (2015): A new model for global glacier change and sea-level rise. *Frontiers in Earth Science 3,* 1-22.

Ingólfsson, Ó., Landvik, J.Y. (2013): The Svalbard-Barents Sea ice sheet– Historical, current and future perspectives. *Quaternary Science Reviews 64,* 33–60.

Ingólfsson, Ó., Benediktsson, Í.Ö., Schomacker, A., Kjær, K.H., Brynjólfsson, S., Jónsson, S.A., Korsgaard, N.J., Johnson, M.D. (2016): Glacial geological studies of surge-type glaciers in Iceland – research status and future challenges. *Earth-Science Reviews 152,* 37–69.

Isaksen, K., Nordli, Ø., Førland, E.J., Łupikasza, E., Eastwood, S., Niedźwiedź, T. (2016): Recent warming on Spitsbergen—Influence of atmospheric circulation and sea ice cover. *Journal of Geophysical Research: Atmospheres 121,* 11913–11931.

Isaksson, E., Divine, D., Kohler, J., Martma, T., Pohjola, V., Motoyama, H., Watanabe, O. (2005): Climate oscillations as recorded in Svalbard ice core delta^{18}O records between AD 1200 and 1997. *Geografiska Annaler Series A 87,* 203–214.

Ives, J.D., Andrews, J.T., Barry, R.G. (1975): Growth and decay of the Laurentide ice sheet and comparison with Fenno-Scandinavia. *Naturwissenschaften 62,* 118–25.

Jakobsson, M., Anderson, J.B., Nitsche, F.O., Dowdeswell, J.A., Gyllencreutz, R., Kirchner, N., Mohammad, R., O'Regan, M., Alley, R.B., Anandakrishnan, S., Eriksson, B., Kirshner, A., Fernandez, R., Stolldorf, T., Minzoni, R., Majewski, W. (2011): Geological record of ice shelf break-up and grounding line retreat, Pine Island Bay, West Antarctica. *Geology 39,* 691–694.

Jakobsson, M., Hogan, K.A., Mayer, L.A., Mix, A., Jennings, A., Stoner, J., Eriksson, B., Jerram, K., Mohammad, R., Pearce, C., Reilly, B., Stranne, C. (2018): The Holocene retreat dynamics and stability of Petermann Glacier in northwest Greenland. *Nature Communications 9,* 1-11.

Jamieson, S.S., Vieli, A., Ó Cofaigh, C., Stokes, C.R., Livingstone, S.J., Hillenbrand, C.-D. (2014): Understanding controls on rapid ice-stream retreat during the last deglaciation of Marguerite Bay, Antarctica, using a numerical model. *Journal of Geophysical Research Earth Surface 119,* 247–263.

Jiskoot, H., Murray, T., Boyle, P. (2000): Controls on the distribution of surge-type glaciers in Svalbard. *Journal of Glaciology 46,* 412–422.

Jonsson, S. (1983): On the geomorphology and past glaciation of Storøya, Svalbard. *Geografiska Annaler Series A 65,* 1–17.

Joughin, I., Smith, B.E., Medley, B. (2014): Marine Ice Sheet Collapse Potentially Under Way for the Thwaites Glacier Basin, West Antarctica. *Science 344,* 735–738.

Jung, O., Sung, M.-K. Sato, K. Lim, Y.-K. Kim, S.-J. Baek, E.-H., Kim, B.-M. (2017): How does the SST variability over the western North Atlantic Ocean control Arctic warming over the Barents-Kara Seas? *Environmental Research Letters 12,* 1-8.

Kamb, B., Raymond, C.F., Harrison, W.D., Engelhardt, H., Echelmeyer, K.A., Humphrey, N., Brugman, M.M., Pfeffer, T. (1985): Glacier surge mechanism: 1982–1983 surge of variegated glacier, Alaska. *Science 227,* 469–479.

Kaser, G., Cogley, J.G., Dyurgerov, M.B., Meier, M.F., Ohmura, A. (2006): Mass balance of glaciers and ice caps: Consensus estimates for 1961–2004, *Geophysical Research Letters 33,* 1-5.

Kempf, P, Forwick, M, Laberg, J.S., Vorren, T.O. (2013): Late Weichselian and Holocene sedimentary palaeoenvironment and glacial activity in the high-arctic van Keulenfjorden, Spitsbergen. *The Holocene 23,* 1607–1618.

Kirkbride, M.P., Winkler, S. (2012): Correlation of Late Quaternary moraines: impact of climate variability, glacier response, and chronological resolution. *Quaternary Science Reviews 46,* 1–29.

Kjeldsen, K.K., Korsgaard, N.J., Bjørk, A.A., Khan, S.A., Box, J.E., Funder, S., Larsen, N.K., Bamber, J.L., Colgan, W., van den Broeke, M., Siggaard-Andersen, M.-L., Nuth, C., Schomacker, A., Andresen, C.S., Willerslev, E., Kjær, K.H. (2015): Spatial and temporal distribution of mass loss from the Greenland Ice Sheet since AD 1900. *Nature 528,* 396–400.

Kjerulf, T., Sars, M. (1860): Iagtagelser over den postpliocene eller glaciale Formation i en del of det sydlige Norge, Universitets-program for første halvaar, *Christiania,*1–66.

Kjær, K.H., Larsen, E., van der Meer, J., Ingólfsson, Ó., Krüger, J., Benediktsson, Í.Ö., Knudsen, C. Schomacker, A. (2006): Subglacial decoupling at the sediment/bedrock interface: a new mechanism for rapid flowing ice. *Quaternary Science Reviews* 25, 2704–2712.

Kjær, K.H., Korsgaard, N.J., Schomacker, A. (2008): Impact of multiple glacier surges — a geomorphological map from Brúarjökull, East Iceland. *Journal of Maps 2008,* 5–20.

Kleman, J., Applegate, P.J. (2014): Durations and propagation patterns of ice sheet instability events. *Quaternary Science Reviews 92,* 32–39.

Kopec, B.G., Feng, X., Michel, F.A., Posmentier, E.S. (2016): Influence of sea ice on Arctic precipitation. *Proceedings of the National Academy of Sciences 113,* 46–51.

Kristensen, L., Benn, D.I., Hormes, A., Ottesen, D. (2009): Mud aprons in front of Svalbard surge moraines: evidence of subglacial deforming layers or proglacial glaciotectonics? *Geomorphology 111*, 206–221.

Kristensen, L., Benn, D.I. (2012): A surge of the glaciers Skobreen-Paulabreen, Svalbard, observed by time-lapse photographs and remote sensing data. *Polar Research 31,* 1751–8369.

Lambeck, K. (1995): Constraints on the Late Weichselian ice sheet over the Barents Sea from observations of raised shorelines. *Quaternary Science Reviews 14,* 1–16.

Landvik, J.Y., Bondevik, S., Elverhøi, A., Fjeldskaar, W., Mangerud, J., Salvigsen, O., Siegert, M.J., Svendsen, J.I., Vorren, T.O. (1998): The last glacial maximum of Svalbard and the Barents Sea area: ice sheet extent and configuration. *Quaternary Science Reviews 17,* 43–75.

Landvik, J.Y., Ingólfsson, Ó., Mienert, J., Lehman, S.J., Solheim, A., Elverhøi, A., Ottesen, D. (2005): Rethinking Late Weichselian ice-sheet dynamics in coastal NW Svalbard. *Boreas 34,* 7–24.

Landvik, J.Y., Brook, E.J., Gualtieri, L., Linge, H., Raisbeck, G., Salvigsen, O., Yiou, F. (2013): ^{10}Be exposure age constraints on the LateWeichselian ice-sheet geometry and dynamics in inter-ice-stream areas, western Svalbard. *Boreas 42,* 43–56.

Landvik, J.Y., Alexanderson, H., Henriksen, M., Ingólfsson, Ó. (2014): Landscape imprints of changing glacial regimes during ice-sheet build-up and decay: a conceptual model from Svalbard. *Quaternary Science Reviews 92,* 258–268.

Larsen, E.A., Lyså, A., Rubensdotter, L., Farnsworth, W.R., Jensen, M., Nadeau, M.J., Ottesen, D. (2018): Late-Glacial and Holocene glacier activity in the Van Mijenfjorden area, western Svalbard. *arktos 4,* 1–9. DOI: 10.1007/s41063-018-0042-2.

Larsen, E.A., Kjær, K.H., Demidov, I.N., Funder, S., Grøsfjeld, K., Houmark-Nielsen, M., Jensen, M., Linge, H., Lyså, A. (2006): Late Pleistocene glacial and lake history of northwestern Russia. *Boreas 35,* 394–424.

Larsen, N.K., Levy, L.B., Carlson, A.E., Buizert, C., Olsen, J., Strunk, A., Bjørk, A.A., Skov, D.S. (2018): Instability of the Northeast Greenland Ice Stream over the last 45,000 years. *Nature Communications 9,* 1–8. DOI: 10.1038/s41467-018-04312-7.

Laskar, J., Correia, A.C.M., Gastineau, M., Joutel, F., Levrard, B., Robutel, P. (2004): Long term evolution and chaotic diffusion of the insolation quantities of Mars. *Icarus 170,* 343–364.

Lefauconnier, B., Hagen, J.O. (1991): Surging and Calving Glaciers in Eastern Svalbard. *Norsk Polarinstitutt, Meddeleler*, 116.

Lehman, S.J., Forman, S.L. (1987): Glacier extent and sea level variation during the Late Weichselian on northwest Spitsbergen, Svalbard. *Polar Research 5,* 271–272.

Lehman, S.J., Forman, S.L. (1992): Late Weichselian glacier retreat in Kongsfjorden, West Spitsbergen, Svalbard. *Quaternary Research 37,* 139–154.

Lie, Ø., Dahl, S.O., Nesje, A. (2003): A theoretical approach to glacier equilibrium-line altitudes using meteorological data and glacier mass balance records from southern Norway. *The Holocene 13,* 365–372.

Liestøl, O. (1993): Glaciers of Europe – Glaciers of Svalbard, Norway. In: Satellite Image Atlas of Glaciers of the World. In: R.S. Williams, J.G. Ferrigno (eds.) *U.S. Geological Survey Professional Paper* 1386-E-5, *Satellite Image Atlas of Glaciers of the World:* E127–E151.

Lovell, H., Fleming, E.J., Benn, D.I., Hubbard, B., Lukas, S., Naegeli, K. (2015): Former dynamic behavior of a cold-based valley glacier on Svalbard revealed by basal ice and structural glaciology investigations. *Journal of Glaciology 61,* 309–328.

Lovell, H., Boston, C.M. (2017): Glacitectonic composite ridge systems and surge-type glaciers: an updated correlation based on Svalbard, Norway. *arktos 3,* 1–16.

Luckman, A., Murray, T., Strozzi, T. (2002): Surface flow evolution throughout a glacier surge measured by satellite radar interferometry. *Geophysical Research Letters 29,* 101–104.

Luckman, A., Benn, D. I., Cottier, F., Bevan, S., Nilsen, F., Inall, M. (2015): Calving rates at tidewater glaciers vary strongly with ocean temperature. *Nature Communications 6,* 1–7. DOI: 10.1038/ncomms9566.

Luoto, T.P., Ojala, A.E.K., Arppe, L., Brooks, S.J., Kurki, E., Oksman, M., Wooller, M.J., Zajączkowski, M. (2018): Synchronized proxy-based temperature reconstructions reveal mid- to late Holocene climate oscillations in High Arctic Svalbard. *Journal of Quaternary Science 33,* 93–99.

Lyell, C. (1830–1833): Principles of Geology, 3 vols. Murray, London. Reprinted 1990, University of Chicago Press, Chicago.

Lyså, A., Larsen, E., Høgaas, F., Jensen, M.A., Klug, M., Rubensdotter, L., Szczucinski, W. (2018): A temporary glacier-surge ice-dammed lake, Braganzavågen, Svalbard. *Boreas* 47, 837–854.

Lønne, I. (2016): A new concept for glacial geological investigations of surges, based on high-Arctic examples (Svalbard). *Quaternary Science Reviews 132*, 74–100.

Mangerud, J., Gulliksen, S. (1975): Apparent radiocarbon ages of recent marine shells from Norway, Spitsbergen, and Arctic Canada. *Quaternary Research 5,* 263–273.

Mangerud, J., Bolstad, M., Elgersma, A., Helliksen, D., Landvik, J.Y., Lønne, I., Lycke, A. K., Salvigsen, O., Sandahl, T., Svendsen, J.I. (1992): The last glacial maximum on Spitsbergen, Svalbard. *Quaternary Research 38,* 1–31.
Mangerud, J., Svendsen, J.I. (1992): The last interglacial-glacial period on Spitsbergen, Svalbard. *Quaternary Science Reviews 11,* 633–664.
Mangerud, J., Dokken, T., Hebbeln, D., Heggen, B., Ingólfsson, Ó., Landvik, J.Y., Mejdahl, V., Svendsen, J.I. Vorren, T.O. (1998): Fluctuations of the Svalbard Barents Sea Ice Sheet during the last 150 000 years. *Quaternary Science Reviews 17,* 11–42.
Mangerud, J., Bondevik, S., Gulliksen, S., Hufthammer, A., Høisæter, T. (2006): Marine ^{14}C reservoir ages for 19th century whales and molluscs from the North Atlantic. *Quaternary Science Reviews 25,* 3228–3245.
Mangerud, J., Landvik, J.Y. (2007): Younger Dryas cirque glaciers in western Spitsbergen: smaller than during the Little Ice Age. *Boreas 36,* 278–285.
Mangerud, J., Svendsen, J.I. (2017): The Holocene Thermal Maximum around Svalbard, Arctic North Atlantic; molluscs show early and exceptional warmth. *The Holocene 28,* 65–83.
Margold, M., Stokes, C.R., Clark, C.D. (2015): Ice streams in the Laurentide Ice Sheet: identification, characteristics and comparison to modern ice sheets. *Earth-Science Reviews 143,* 117–146.
Martín-Español, A., Navarro, F., Otero, J., Lapazaran, J., Błaszczyk, M. (2015): Estimate of the total volume of Svalbard glaciers, and their potential contribution to sea-level rise, using new regionally based scaling relationships. *Journal of Glaciology 61,* 29–41.
Martín-Moreno, R., Allende Álvarez, F., Hagen, J.O. (2017): ‘Little Ice Age’ glacier extent and subsequent retreat in Svalbard archipelago. *The Holocene 27,* 1379–1390.
Mayewski, P.A., Rohling, E.E., Curt Stager, J., Karlen, W., Maasch, K.A., David Meeker, L., Meyerson, E.A., Gasse, F., van Kreveld, S., Holmgren, K., Lee-Thorp, J., Rosqvist, G., Rack, F., Staubwasser, M., Schneider, R.R., Steig, E.J. (2004): Holocene climate variability. *Quaternary Research 62,* 243–255.
McKay, N.P., Kaufman, D.S. (2014): An extended Arctic proxy temperature database for the past 2,000 years. *Scientific Data 1,* 1-10.
Meier, M.F., Post, A. (1969): What are glacier surges? *Canadian Journal of Earth Sciences 6,* 807–817.
Mercer, J.H. (1970): A former ice sheet in the Arctic Ocean? *Palaeogeography, Palaeoclimatology, Palaeoecology 8,* 19–27.
Miller, G.H. (1982): Quaternary depositional episodes, western Spitsbergen, Norway - aminostratigraphy and glacial history. *Arctic and Alpine Research 14,* 321–340.
Miller, G.H., Geirsdóttir, Á., Zhong, Y., Larsen, D.J., Otto-Bliesner, B.L., Holland, M.M., Bailey, D.A., Refsnider, K.A., Lehman, S.J., Southon, J.R., Anderson, C., Björnsson, H., Thordarson, T. (2012): Abrupt onset of the Little Ice Age triggered by volcanism and sustained by sea-ice/ocean feedbacks. *Geophysical Research Letters 39,* 1-5.
Möller, M., Kohler, J. (2018): Differing Climatic Mass Balance Evolution Across Svalbard Glacier Regions Over 1900–2010. *Frontiers in Earth Science 6*, 1–20.
Muckenhuber, S., Nilsen, F., Korosov, A., Sandven, S. (2016): Sea ice cover in Isfjorden and Hornsund, Svalbard (2000–2014) from remote sensing data. *The Cryosphere 10,* 149-158.
Müller, J., Stein, R. (2014): High-resolution record of late glacial and deglacial sea ice changes in Fram Strait corroborates ice–ocean interactions during abrupt climate shifts. *Earth and Planetary Science Letters 403,* 446–455.
Müller, J., Werner, K., Stein, R., Fahl, K., Moros, M., Jansen, E. (2012): Holocene cooling culminates in sea ice oscillations in Fram Strait. *Quaternary Science Reviews 47,* 1–14.
Murray, T., Stuart, G.W., Miller, P. J., Woodward, J., Smith, A.M., Porter, P.R., Jiskoot, H. (2000): Glacier surge propagation by thermal evolution at the bed. *Journal of Geophysical Research, 105,* 13491–13507.

Murray, T., James, T.D., Macheret, Y.Y., Lavrentiev, I., Glazovsky, A., Sykes, H. (2012): Geometric changes in a tidewater glacier in Svalbard during its surge cycle. *Arctic, Antarctic, and Alpine Research 44,* 359–367.

Nathorst, A.G. (1899): The Swedish arctic expedition of 1898. *The Geographical Journal 14,* 51-76 and 155–176.

Navarro, F.J., Martín-Español, A., Lapazaran, J.J., Grabiec, M., Otero, J., Vasilenko, E.V., Puczko, D. (2014): Ice Volume Estimates from Ground-Penetrating Radar Surveys, Wedel Jarlsberg Land Glaciers, Svalbard. *Arctic, Antarctic, and Alpine Research 46,* 394–406.

Navarro, F.J., Lapazarán, J., Martín-Español, A., Otero, J. (2016): Ground penetrating radar studies in Svalbard aimed to the calculation of the ice volume of its glaciers. *Cuadernos de Investigación Geográfica 42,* 399–414.

Newton, A.M.W., Huuse, M. (2017): Glacial geomorphology of the central Barents Sea: implications for the dynamic deglaciation of the Barents Sea Ice Sheet. *Marine Geology 387,* 114–131.

Nielsen, T., Rasmussen, T.L. (2018): Reconstruction of ice sheet retreat after the Last Glacial maximum in Storfjorden, southern Svalbard. *Marine Geology 402,* 228–243.

Norðdahl, H., Ingólfsson, Ó. (2015): Collapse of the Icelandic ice sheet controlled by sea-level rise? *arktos 1,* 1–18.

Nowak, A., Hodson, A., (2013): Hydrological response of a High-Arctic catchment to changing climate over the past 35 years: a case study of Bayelva watershed, Svalbard. *Polar Research 32,* 1–16.

Nuth, C., Kohler, J., König, M., von Deschwanden, A., Hagen, J.O., Kääb, A., Moholdt, G., Pettersson, R. (2013): Decadal changes from a multitemporal glacier inventory of Svalbard. *The Cryosphere 7,* 1603–1621

Ó Cofaigh, C., Pudsey, C.J., Dowdeswell, J.A., Morris, P. (2002): Evolution of subglacial bedforms along a paleo-ice stream, Antarctic Peninsula continental shelf. *Geophysical Research Letters 29,* 411–414.

Oerlemans, J. (2005): Atmospheric science: extracting a climate signal from 169 glacier records. *Science 308,* 675–677.

Oerlemans, J., van Pelt, W.J.J. (2015): A model study of Abrahamsenbreen, a surging glacier in northern Spitsbergen. *The Cryosphere 9,* 767–779.

Ottesen, D., Dowdeswell, J.A., Landvik, J.Y., Mienert, J. (2007): Dynamics of the Late Weichselian ice sheet on Svalbard inferred from high-resolution sea-floor morphology. *Boreas 36,* 286–306.

Ottesen, D., Dowdeswell, J.A., Benn, D.I., Kristensen, L., Christiansen, H.H., Christensen, O., Hansen, L., Lebesbye, E., Forwick, M., Vorren, T.O. (2008): Submarine landforms characteristic of glacier surges in two Spitsbergen fjords. *Quaternary Science Review 27,* 1583–1599.

Patton, H., Andreassen, K., Bjarnadóttir, L.R., Dowdeswell, J.A., Winsborrow, M.C.M. Noormets, R., Polyak, L., Auriac, A., Hubbard, A. (2015): Geophysical constraint on the dynamics and retreat of the Barents Sea Ice Sheet as a palaeo-benchmark for models of marine ice-sheet deglaciation. *Reviews of Geophysics 53,* 1051–1098.

Patton, H., Hubbard, A., Andreassen, K., Auriac, A., Whitehouse, P.L., Stroeven, A.P., Shackleton, C., Winsborrow, M.C.M., Heyman, J., Hall, A.M. (2017): Deglaciation of the Eurasian ice sheet complex. *Quaternary Science Reviews 169,* 148–172.

Paul, F. (2015): Revealing glacier flow and surge dynamics from animated satellite image sequences: examples from the Karakoram. *The Cryosphere 9,* 2201–2214.

Pavlov, A.K., Tverberg, V., Ivanov, B.V., Nilsen, F., Falk-Petersen, S., Granskog, M.A. (2013): Warming of Atlantic Water in two west Spitsbergen fjords over the last century (1912–2009). *Polar Research 32,* 1–14.

van Pelt, W.J.J., Oerlemans, J., Reijmer, C.H., Pettersson, R., Pohjola, V.A., Isaksson, E., Divine, D. (2013): An iterative inverse method to estimate basal topography and initialize ice flow models. *The Cryosphere 7,* 987–1006.

Petty, A.A. (2018): A possible link between winter Arctic sea ice decline and a collapse of the Beaufort High? *Geophysical Research Letters 45*, 2879–2882.

Philipps, W., Briner, J.P., Gislefoss, L., Linge, H., Koffman, T., Fabel, D., Xu, S., Hormes, A. (2017): Late Holocene glacier activity at inner Hornsund and Scottbreen, southern Svalbard. *Journal of Quaternary Science 32*, 501–515.

Pike, A. (1898): A Cruise on the East of Spitsbergen. *The Geographical Journal 11*, 365–371.

Principato, S.M., Moyer, A.N., Hampsch, A.G., Ipsen, H.A. (2016): Using GIS and streamlined landforms to interpret palaeo-ice flow in northern Iceland. *Boreas 45,* 470–482.

Ramsey, C., Lee, S. (2013): Recent and Planned Developments of the Program OxCal. *Radiocarbon 55*, 720–730.

Reimer, P.J., Bard, E., Bayliss, A., Beck, J.W., Blackwell, P.G., Bronk Ramsey, C., Buck, C. E., Cheng, H., Edwards, R.L., Friedrich, M., Grootes, P.M., Guilderson, T.P., Haflidason, H., Hajdas, I., Hatte, C., Heaton, T.J., Hoffmann, D.L., Hogg, A.G., Hughen, K.A., Kaiser, K.F., Kromer, B., Manning, S.W., Niu, M., Reimer, R.W., Richards, D.A., Scott, E.M., Southon, J.R., Staff, R.A., Turney, C.S.M., van der Plicht, J. (2013): IntCal13 and Marine13 Radiocarbon Age Calibration Curves 0–50,000 Years cal BP. *Radiocarbon 55,* 1869–1887.

Reusche, M., Winsor, K., Carlson, A.E., Marcott, S.A., Rood, D.H., Novak, A., Roof, S., Retelle, M., Werner, A., Caffee, M., Clark, P.U. (2014): ^{10}Be surface exposure ages on the late-Pleistocene and Holocene history of Linnébreen on Svalbard. *Quaternary Science Reviews 89,* 5–12.

Rignot, E., Casassa, G., Gogineni, P., Krabill, W., Rivera, A., Thomas, R. (2004): Accelerated ice discharge from the Antarctic Peninsula following the collapse of Larsen B ice shelf. *Geophysical Research Letters 31*, 1–4.

Ritz, C., Edwards, T.L., Durand, G., Payne, A.J., Peyaud, V., Hindmarsh, R.C.A. (2015): Potential sea-level rise from Antarctic ice-sheet instability constrained by observations. *Nature 528,* 115–118.

Ritzmann, O., Jokat, W. (2003): Crustal structure of northwestern Svalbard and the adjacent Yermak Plateau: Evidence for Oligocene simple shear rifting and non-volcanic break-up. *Geophysical Journal International 152*, 139–159.

Roberts, S.J., Hodgson, D.A., Bentley, M.J., Smith, J.A., Millar, I.L., Olive, V., Sugden, D.E. (2008): The Holocene history of George VI Ice Shelf, Antarctic Peninsula from clast-provenance analysis of epishelf lake sediments. *Palaeogeography, Palaeoclimatology, Palaeoecology 259*, 258–283.

Rockström, J., Steffen, W., Noone, K., Persson, A., Chapin, F.S., Lambin, E.F., Lenton, T.M., Scheffer, M., Folke, C., Schellnhuber, H.J., Nykvist, B., de Wit, C.A., Hughes, T., van der Leeuw, S., Rodhe, H., Sorlin, S., Snyder, P.K., Costanza, R., Svedin, U., Falkenmark, M., Karlberg, L., Corell, R.W., Fabry, V.J., Hansen, J., Walker, B. Liverman, D., Richardson, K., Crutzen, P., Foley, J.A. (2009): A safe operating space for humanity. *Nature 461*, 472–475.

Rogers, J.C., Yang, L., Li, L. (2005): The role of Fram Strait winter cyclones on sea ice flux and on Spitsbergen air temperatures. *Geophysical Research Letters 32*, 1–4.

Rolstad, C., Amlien, J., Hagen, J.O., Lundén, B. (1997): Visible and near-infrared digital images for determination of ice velocities and surface elevation during a surge on Osbornebreen, a tidewater glacier in Svalbard. *Annals of Glaciology 24*, 255–261.

Ruddiman, W.F. (2006): Orbital changes and climate. *Quaternary Science Reviews 25*, 3092-3112.

Røthe, T.O., Bakke, J., Vasskog, K., Gjerde, M., D'Andrea, W.J., Bradley, R.S. (2015): Arctic Holocene glacier fluctuations reconstructed from lake sediments at Mitrahalvøya, Spitsbergen. *Quaternary Science Reviews 109*, 111–125.

Røthe, T.O., Bakke, J., Støren, E.W.N., Bradley, R.S. (2018): Reconstructing Holocene Glacier and Climate Fluctuations From Lake Sediments in Vårfluesjøen, Northern Spitsbergen. *Frontiers in Earth Science 6,* 1–20.

Salvigsen, O. (1977): Radiocarbon datings and the extension of the Weichselian icesheet in Svalbard. *Norsk Polarinstitutt Årbok 1976,* 209–224.

Salvigen, O. 1981: Radiocarbon dated raised beaches in Kong Karls Land, Svalbard, and their consequences for the glacial history of the Barents Sea area. *Geografiska Annaler Series A* 63, 283–291.

Salvigsen, O., Nydal, R. (1981): The Weichselian glaciation in Svalbard before 15000 BP. *Boreas 10,* 433–446.

Sato, K., Inoue, J., Watanabe, M. (2014): Influence of the Gulf Stream on the Barents Sea ice retreat and Eurasian coldness during early winter. *Environmental Research Letters 9*, 1–9.

Scambos, T.A., Bohlander, J.A., Shuman, C.A. Skvarca, P. (2004): Glacier acceleration and thinning after ice shelf collapse in the Larsen B embayment, Antarctica. *Geophysical Research Letters 31,* 1–4.

Schomacker, A., Benediktsson, Í.Ö. Ingólfsson, Ó (2014): The Eyjabakkajökull glacial landsystem, Iceland: geomorphic impact of multiple surges. *Geomorphology 218,* 98–107.

Schoof, C. (2007): Ice sheet grounding line dynamics: steady states, stability, and hysteresis. *Journal of Geophysical Research: Earth Surface 112,* 1–19.

Schytt, V., Hoppe, G., Blake, W.J., Grosswald, M.G. (1968): The extent of the Würm glaciation in the European Arctic. *International Association of Scientific Hydrology General Assembly of Bern 1967 79,* 207–216.

Sevestre, H. Benn, D.I. (2015): Climatic and geometric controls on the global distribution of surge-type glaciers: implications for a unifying model of surging. *Journal of Glaciology 61,* 646–662.

Sevestre, H., Benn, D.I., Hulton, N.R.J., Bælum, K. (2015): Thermal structure of Svalbard glaciers and implications for thermal switch models of glacier surging. *Journal of Geophysical Research: Earth Surface 120,* 2220–2236.

Sevestre, H., Benn, D.I., Luckman, A., Nuth, C., Kohler, J., Lindbäck, K., Pettersson, R. (2018): Tidewater Glacier Surges Initiated at the Terminus. *Journal of Geophysical Research: Earth Surface 123*, 1035-1051.

Sharp, M. (1988): Surging glaciers: behaviour and mechanisms. *Progress in Physical Geography 12,* 349–370.

Shepherd, A., Ivins, E., Rignot, E., Smith, B., van den Broeke, M., Velicogna, I., Whitehouse, P., Briggs, K., Joughin, I., Krinner, G., Nowicki, S., Payne, T., Scambos, T., Schlegel, N., A,G., Agosta, C., Ahlstrøm, A., Babonis, G., Barletta, V., Blazquez, A., Bonin, J., Csatho, B., Cullather, R., Felikson, D., Fettweis, X., Forsberg, R., Gallee, H., Gardner, A., Gilbert, L., Groh, A., Gunter, B., Hanna, E., Harig, C., Helm, V., Horvath, A., Horwath, M., Khan, S., Kjeldsen, K.K., Konrad, H., Langen, P., Lecavalier, B., Loomis, B., Luthcke, S., McMillan, M., Melini, D., Mernild, S., Mohajerani, Y., Moore, P., Mouginot, J., Moyano, G., Muir, A., Nagler, T., Nield, G., Nilsson, J., Noel, B., Otosaka, I., Pattle, M.E., Peltier, W.R., Pie, N., Rietbroek, R., Rott, H., Sandberg-Sørensen, L., Sasgen, I., Save, H., Scheuchl, B., Schrama, E., Schröder, L., Seo, K.-W., Simonsen, S., Slater, T., Spada, G., Sutterley, T., Talpe, M., Tarasov, L., van der Berg, W.J., van der Wal, W., van Wessem, M., Vishwakarma, B.D., Wiese, D., Wouters, B. (2018): Mass balance of the Antarctic Ice Sheet from 1992 to 2017. *Nature 558,* 219–222.

Sigurðsson, O., (1998): Glacier variations in Iceland 1930–1995. *Jökull 45,* 3–24.

Sletten, K., Lyså, A., Lønne, I. (2001): Formation and disintegration of a high-Arctic ice-cored moraine complex, Scott Turnerbreen, Svalbard. *Boreas 30,* 272–284.

Snyder, J.A., Werner, A., Miller, G.H. (2000): Holocene cirque glacier activity in western Spitsbergen, Svalbard: sediment records from proglacial Linnévatnet. *The Holocene 10,* 555–563.

Spagnolo, M., King, E.C., Ashmore, D.W., Rea, B.R., Ely, J.C., Clark, C.D. (2014): Looking through drumlins: testing the application of ground-penetrating radar. *Journal of Glaciology 60,* 1126–1134.

Steffensen, J.P., Andersen, K.K., Bigler, M., Clausen, H.B., Dahl-Jensen, D., Fischer, H., Goto-Azuma, K., Hansson, M., Johnsen, S.J., Jouzel, J., Masson-Delmotte, V., Popp, T., Rasmussen, S.O., Röthlisberger, R., Ruth, U., Stauffer, B., Siggaard-Andersen, M.-L., Sveinbjörnsdóttir, A.E., Svensson, A., White, J.W.C. (2008): High resolution Greenland ice core data show abrupt climate change happens in few years. *Science 321,* 680–684.

Stokes, C.R. Clark, C.D. (1999): Geomorphological criteria for identifying Pleistocene ice streams. *Annals of Glaciology 28,* 67–74.

Stokes, C.R., Fowler, A.C., Clark, C.D., Hindmarsh, R.C.A., Spagnolo, M. (2013): The instability theory of drumlin formation and its explanation of their varied composition and internal structure. *Quaternary Science Reviews 62,* 77–96.

Stokes, C.R., Margold, M., Clark, C.D., Tarasov, L. (2016): Ice stream activity scaled to ice sheet volume during Laurentide Ice Sheet deglaciation. *Nature 530,* 322–326.

Striberger, J., Björck, S., Benediktsson, Í.Ö., Snowball, I., Uvo, C.B., Ingólfsson, Ó., Kjær, K.H. (2011): Climatic control of the surge periodicity of an Icelandic outlet glacier. *Journal of Quaternary Science 26,* 561–565.

Strozzi, T., Kääb, A., Schellenberger, T. (2017): Frontal destabilization of Stonebreen, Edgeøya, Svalbard. *The Cryosphere 11,* 553–566.

Stuiver, M., Polach, H., (1977): Discussion reporting of ^{14}C data. *Radiocarbon 19,* 355–363.

Sund, M., Lauknes, T.R., Eiken, T. (2014): Surge dynamics in the Nathorstbreen glacier system, Svalbard. *The Cryosphere 8,* 623–638.

Svendsen, J.I., Mangerud, J., Elverhøi, A., Solheim, A., Schüttenhelm, R.T.E. (1992): The Late Weichselian glacial maximum on western Spitsbergen inferred from offshore sediment cores. *Marine Geology 104,* 1–17.

Svendsen, J.I., Elverhøi, A., Mangerud, J. (1996): The retreat of the Barents Sea Ice Sheet on the western Svalbard margin. *Boreas 25,* 244–256.

Svendsen, J.I., Mangerud, J. (1997): Holocene glacial and climatic variations on Spitsbergen, Svalbard. *The Holocene 7,* 45–57.

Svendsen, J.I., Alexanderson, H., Astakhov, V.I., Demidov, I., Dowdeswell, J.A., Funder, S., Gataullin, V., Henriksen, M., Hjort, C., Houmark-Nielsen, M., Hubberten, H.W., Ingólfsson, Ó., Jakobsson, M., Kjær, K.H., Larsen, E., Lokrantz, H., Lunkka, J.P., Lyså, A., Mangerud, J., Matiouchkov, A., Murray, A., Möller, P., Niessen, F., Nikolskaya, O., Polyak, L., Saarnisto, M., Siegert, C., Siegert, M.J., Spielhagen, R.F., Stein, R. (2004): Late Quaternary ice sheet history of northern Eurasia. *Quaternary Science Reviews 23,* 1229–1271.

Thomas, E.K., McGrane, S., Briner, J.P., Huang, Y. (2012): Leaf wax δ^2H and varve-thickness climate proxies from proglacial lake sediments, Baffin Island, Arctic Canada. *Journal of Paleolimnology 48,* 193–207.

Thomas, E.K., Briner, J.P., Ryan-Henry, J.J., Huang, Y. (2016): A major increase in winter snowfall during the middle Holocene on western Greenland caused by reduced sea ice in Baffin Bay and the Labrador Sea. *Geophysical Research Letters 43,* 5302–5308.

Tolgensbakk, J. (1990): Gipsdalen, Svalbard. Quaternary geology and geomorphology 1:40,000. Department of Physical Geography, University of Oslo. Norwegian Polar Institute.

Ulfstedt A-C., (1987): Geomorfologin på Glenhalvöya med omgivningar. *Ymer, 80 report 1987,* 109-112.

Vallot, D., Åström, J., Zwinger, T., Pettersson, R., Everett, A., Benn, D., Luckman, A., van Pelt, W., Nick, F., Kohler, J. (2018): Effects of undercutting and sliding on calving: a global approach applied to Kronebreen, Svalbard. *The Cryosphere 12,* 609–625.

Walker, M.J.C., Berkelhammer, M., Björck, S., Cwynar, L.C., Fisher, D.A., Long, A.J., Lowe, J.J. Newnham, R.M., Rasmussen, S.O., Weiss, H. (2012): Formal subdivision of the Holocene Series/Epoch: a Discussion Paper by a Working Group of INTIMATE (Integration of ice-core, marine and terrestrial records) and the Subcommission on Quaternary Stratigraphy (International Commission on Stratigraphy). *Journal of Quaternary Science 27,* 649-659.

Wanner, H., Solomina, O., Grosjean, M., Ritz, S. P., Jetel, M. (2011): Structure and origin of Holocene cold events. *Quaternary Science Reviews 30,* 3109–3123.

Werner, A. (1993): Holocene moraine chronology, Spitsbergen, Svalbard: lichenometric evidence for multiple Neoglacial advances in the Arctic. *The Holocene 3,* 128–137.

de Wet, G.A., Balascio, N.L., D'Andrea, W.J., Bakke, J., Bradley, R.S., Perren, B. (2018): Holocene glacier activity reconstructed from proglacial lake Gjøavatnet on Amsterdamøya, NW Svalbard. *Quaternary Science Reviews 183,* 188–203.

Willis, M.J., Zheng, W., Durkin, W.J., Pritchard, M.E., Ramage, J.M., Dowdeswell, J.A., Benham, T.J., Bassford, R.P., Stearns, L.A., Glazovsky, A.F., Macheret, Y.Y., Porter, C.C. (2018): Massive destabilization of an Arctic ice cap. *Earth and Planetary Science Letters 502,* 146–155.

Winsborrow, M.C.M., Andreassen, K., Corner, G.D. Laberg, J.S. (2010): Deglaciation of a marine-based ice sheet: late Weichselian palaeo-ice dynamics and retreat in the southern Barents Sea reconstructed from onshore and offshore glacial geomorphology. *Quaternary Science Reviews 29,* 424–442.

Winsborrow, M.C.M., Stokes, C.R., Andreassen, K. (2012): Ice-stream flow switching during deglaciation of the southwestern Barents Sea. *GSA Bulletin 124,* 275–290.

Wolcott, R.I. 1970. Isostatic response to loading of the crust in Canada. *Canadian Journal of Earth Sciences 7,* 716-726.

Wuite, J., Rott, H., Hetzenecker, M., Floricioiu, D., De Rydt, J., Gudmundsson, G. H., Nagler, T., Kern, M. (2015): Evolution of surface velocities and ice discharge of Larsen B outlet glaciers from 1995 to 2013. *The Cryosphere 9,* 957–969.

Young, N.E., Lamp, J., Koffman, T., Briner, J.P., Schaefer, J., Gjermundsen, E.F., Linge, H., Zimmerman, S., Guilderson, T.P., Fabel, D., Hormes, A. (2018): Deglaciation of coastal south-western Spitsbergen dated with in situ cosmogenic ^{10}Be and ^{14}C measurements. *Journal of Quaternary Science 33*. DOI: 10.1002/jqs.3058.

Østby, T.I., Schuler, T.V., Hagen, J.O., Hock, R., Kohler, J., Reijmer, C.H. (2017): Diagnosing the decline in climatic mass balance of glaciers in Svalbard over 1957–2014. *The Cryosphere 11,* 191–215.

Research papers

Chapter	I	Farnsworth *et al.* 2018
Chapter	II	Larsen *et al.* 2018
Chapter	III	Farnsworth *et al.* 2017
Chapter	IV	Farnsworth *et al.* 2016
Chapter	V	Farnsworth *et al. in prep.*

Chapter I

Svalbard glaciers re-advanced during the Pleistocene-Holocene transition

Farnsworth, W.R., Ingólfsson, Ó., Retelle, M., Allaart, L., Håkansson, L., Schomacker, A. (2018): Svalbard glaciers re-advanced during the Pleistocene-Holocene transition. *Boreas 47,* 1022-1032. DOI:10.1111/bor.12326.

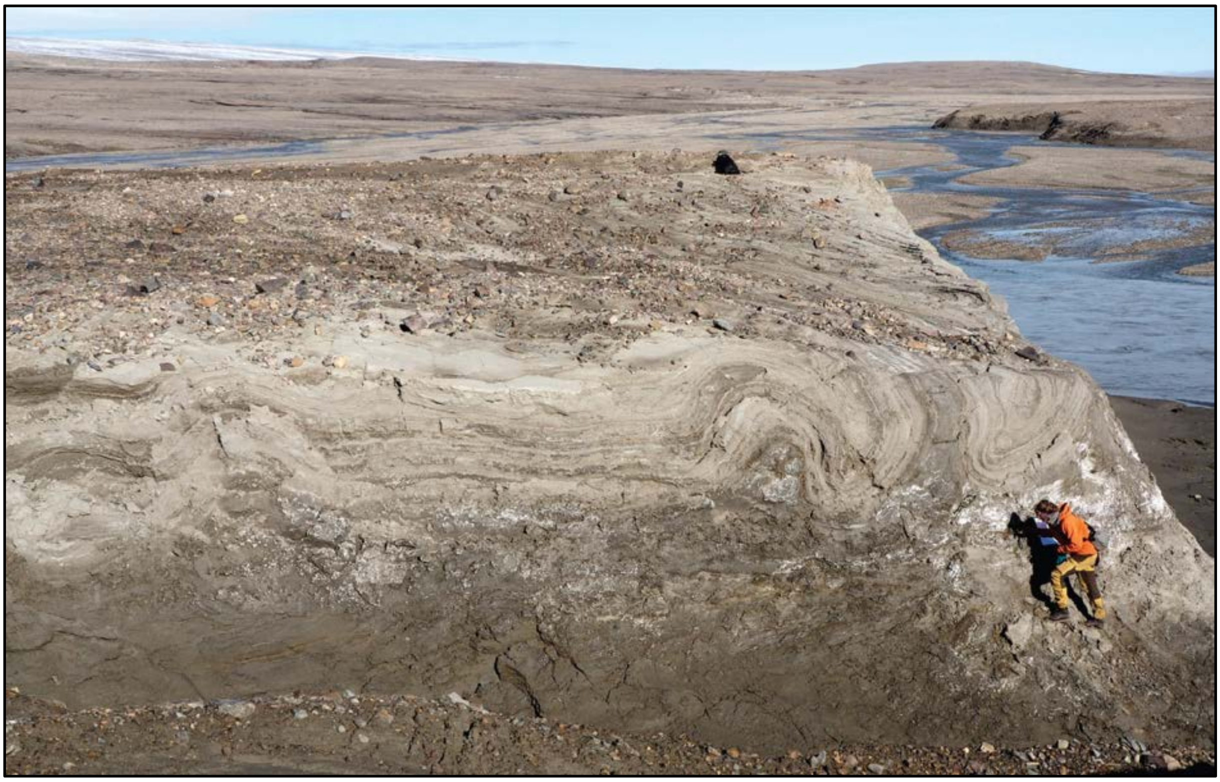

Glaciotectonized shallow marine sediments on the northern side of the Fakse moraine, De Geerbukta, northeastern Spitsbergen (photo from Ingólfsson).

BOREAS An international journal of Quaternary research

Svalbard glaciers re-advanced during the Pleistocene–Holocene transition

WESLEY R. FARNSWORTH, ÓLAFUR INGÓLFSSON, MICHAEL RETELLE, LIS ALLAART, LENA M. HÅKANSSON AND ANDERS SCHOMACKER

BOREAS

Farnsworth, W. R., Ingólfsson, Ó., Retelle, M., Allaart, L., Håkansson, L. M. & Schomacker, A.: Svalbard glaciers re-advanced during the Pleistocene–Holocene transition. *Boreas*. https://doi.org/10.1111/bor.12326. ISSN 0300-9483.

Despite warming regional conditions and our general understanding of the deglaciation, a variety of data suggest glaciers re-advanced on Svalbard during the Lateglacial–early Holocene (LGEH). We present the first well-dated end moraine formed during the LGEH in De Geerbukta, NE Spitsbergen. This landform was deposited by an outlet glacier re-advancing into a fjord extending 4.4 km beyond the late Holocene (LH) maximum. Comparing the timing of the De Geerbukta glacier re-advance to a synthesis of existing data including four palaeoclimate records and 15 other proposed glacier advances from Svalbard does not suggest any clear synchronicity in glacial and climatic events. Furthermore, we introduce six additional locations where glacier moraines have been wave-washed or cut by postglacial raised marine shorelines, suggesting the landforms were deposited before or during high relative sea-level stands, thus exhibiting a similar LGEH age. Contrary to current understanding, our new evidence suggests that the LGEH glaciers were more dynamic, exhibited re-advances and extended well beyond the extensively studied LH glacial expansion. Given the widespread occurrence of the LGEH glacier deposits on Svalbard, we suggest that the culmination of the Neoglacial advances during the Little Ice Age does not mark the maximum extent of most Svalbard glaciers since deglaciation; it is just the most studied and most visible in the geological record.

Wesley R. Farnsworth (WesleyF@unis.no), Ólafur Ingólfsson, Michael Retelle and Lena M. Håkansson, University Centre in Svalbard (UNIS), Longyearbyen N-9171, Norway; Wesley R. Farnsworth, Lis Allaart and Anders Schomacker, UiT The Arctic University of Norway, Tromsø N-9037, Norway; Ólafur Ingólfsson, University of Iceland, Askja, Sturlugata 7, Reykjavík IS-101, Iceland; Michael Retelle, Bates College, Lewiston, ME 04240, USA; Anders Schomacker, Natural History Museum of Denmark, University of Copenhagen, Øster Voldgade 5-7, Copenhagen K DK-1350, Denmark; *received 14th March 2018, accepted 3rd May 2018.*

Studying past changes in high latitude glaciers and climate allows us to better understand the role of the Arctic in the global climate system and to more effectively predict antecedent climate scenarios (McKay & Kaufman 2014). Climatic shifts are occurring with an amplified effect in the Arctic at present and also did so following the last deglaciation (Hald *et al.* 2007; Hartmann *et al.* 2013). Arctic glaciers can be valuable indicators for past climate given their sensitivity to summer temperatures and winter precipitation (Huss & Hock 2015). Due to Svalbard's high Arctic location between the northern extent of the North Atlantic Drift and the seasonal sea ice, the region is an ideal location to study the European Arctic's sensitivity to global climate change (Fig. 1; Rogers *et al.* 2005).

Based on evidence from cirque glaciers on the west coast of Spitsbergen, Svalbard, glaciers during the Little Ice Age (LIA), culminating *c.* 1920 CE, were believed to be at their greatest extent since before the Younger Dryas (YD; Svendsen & Mangerud 1997; Mangerud & Landvik 2007). Studies from western Spitsbergen suggest minimal glacier activity during the Lateglacial and early Holocene (LGEH), while the Neoglacial (*c.* 4.5 ka BP) cooling, which culminated during the LIA, has been interpreted to represent the Holocene glacial maximum in most locations (Werner 1993; Svendsen & Mangerud 1997; Reusche *et al.* 2014; Miller *et al.* 2017). It is assumed that if glaciers had extended further than their late Holocene (LH) maximum, it would have been during the YD (Svendsen & Mangerud 1992). In a review of the deglaciation of Svalbard, Hormes *et al.* (2013) suggested that one of the key research questions still remaining is whether there is any evidence of YD climatic cooling seen in Svalbard. Until now, few pre-LH moraines have been identified and only one has been dated, where two moraine ridge boulders provide ambiguous cosmogenic exposure ages (12.1 and 9.2 ka BP; Henriksen *et al.* 2014). Additionally, a couple of early Holocene glacier re-advances (following deglaciation) have been inferred from stratigraphical data of geological sections (Lønne 2005) or lake sediments (van der Bilt *et al.* 2015).

With few exceptions, current evidence (and lack thereof) suggests that since the deglaciation of Svalbard, the most extensive glacier positions occurred in the LH and in most cases roughly 100 years ago (Werner 1993; Humlum *et al.* 2005; Mangerud & Landvik 2007). The majority of Holocene glacier studies from Svalbard have focused on LH landforms, i.e. Neoglacial and Little Ice Age glacial deposits, which occur prominently and widespread throughout the landscape (Werner 1988, 1993; Reusche *et al.* 2014; Philipps *et al.* 2017). However, as a result of 'erosional censoring' the preservation of glacial deposits in Svalbard is strongly biased towards the youngest deposits (Kirkbride & Winkler 2012; Landvik *et al.* 2014).

We present evidence of a re-advance of Gullfaksebreen into De Geerbukta in northeast Spitsbergen constrained in time to the LGEH transition (Fig. 1). We summarize the glacial and palaeoclimatic conditions on Svalbard during the transition from glacial to interglacial mode between 14–9 ka BP (Landvik *et al.* 2014) and compare

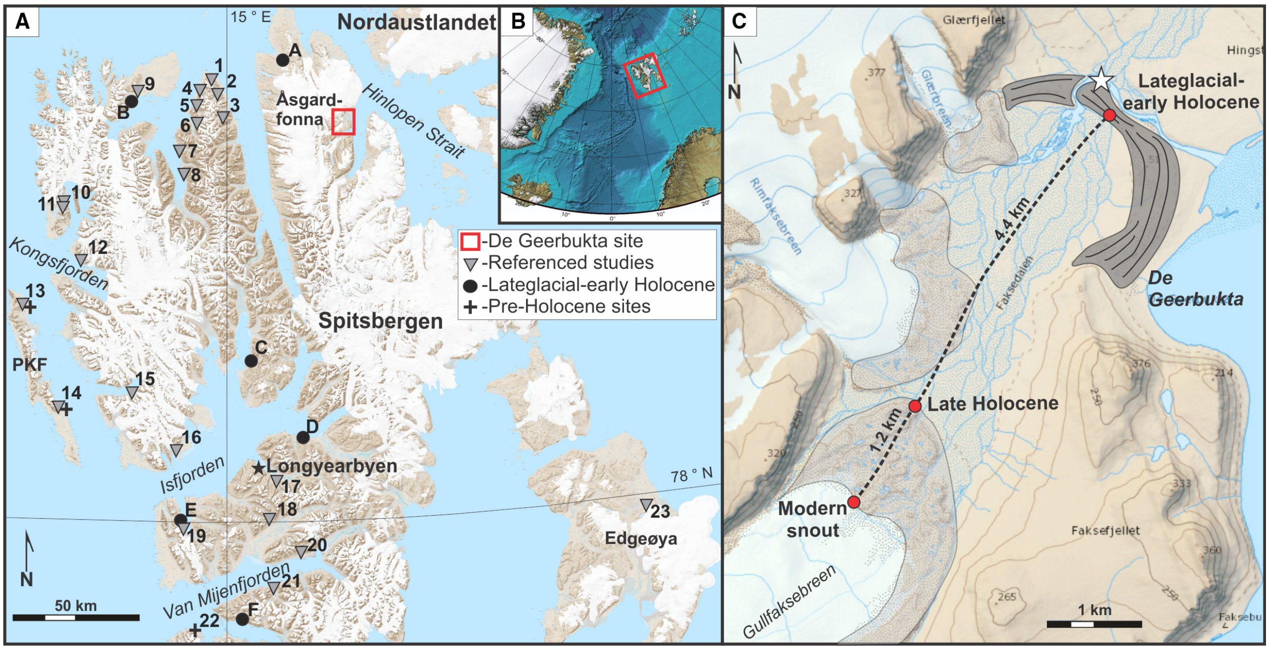

Fig. 1. A. Overview map of northern Spitsbergen. Symbols indicate sites with Lateglacial–early Holocene moraine ridges (see legend; referenced studies marked by grey triangles while Lateglacial–early Holocene glacier deposits marked by black dots, data presented in Tables S1, S2. B. Inset map of the North Atlantic, Svalbard marked by red box. C. Topographic map of Faksedalen with moraine deposits shaded grey. The entire Fakse moraine has been wave-washed indicated by dark lines while late Holocene deposits have not. Red circles and dotted line indicate distance measurements. White star marks the study site with proglacial glaciotectonized marine sediments presented in Fig. 2. Base maps in (A) and (C) modified from TopoSvalbard, (B) modified from IBCAO.

the Gullfaksebreen re-advance to the timing of previously published studies implying other LGEH glacier advances. We further up-scale this study by highlighting six additional sites on Svalbard where glacier deposits are cut by relatively high raised shorelines suggesting a similar LGEH age to the Faksebreen advance (Fig. 1A).

Material and methods

De Geerbukta fieldwork and sampling was conducted in August 2015, with focus on geomorphological and sedimentological mapping. Following field sampling, shell and whalebone subsamples were cleaned, weighed, photographed, identified and subsequently sent for dating at the Ångström Laboratory at Uppsala University. We present four new radiocarbon ages of shells and whalebone from De Geerbukta (Table 1).

Additional LGEH glacier marginal deposits (moraines) have been identified on the open access website TopoSvalbard, provided by the Norwegian Polar Institute. Access to modern (2008–12) high-resolution aerial imagery, digital elevation models and 1936 oblique aerial photographs provided the opportunity to thoroughly inspect the unglaciated landscape from numerous perspectives (Fig. S1). Cross-cutting relationships between raised marine shorelines and glacier moraines indicate that deposits left at previous glacial margins occurred during a high relative sea-level stand (Ingólfsson & Landvik 2013) while maximum constraining ages are inferred from the deglaciation ages of the fjord or region. The principle of parsimony thus suggests the moraines were deposited following the deglaciation and prior to significant drop in relative sea level; thus, the age of the moraines roughly straddle the interval of time corresponding to the LGEH. Modern glacier lengths were extracted from Svalbardkartet (König *et al.* 2014) while palaeo-glacier lengths were measured in TopoSvalbard (Table S1).

Each ^{14}C age of a marine organism presented in this study has been corrected and calibrated with IntCal13 (Reimer *et al.* 2013) using the Calib Rev. 7.0.4 program. A marine reservoir age has been implemented by selecting 'MARINE13' and inputting a 'Delta R' of 70±30 (Table 1; Mangerud & Svendsen 2018). All dates (of marine organisms) presented in previous studies have been re-(corrected and) calibrated accordingly (Table S2). The ages presented in text and figures are calibrated median ages in kilo-years before present (cal. ka BP).

Results

The Fakse moraine, De Geerbukta

Gullfaksebreen is an outlet glacier of the Åsgardfonna icecap located in NE Spitsbergen, extending 20 km and draining into De Geerbukta (Fig. 1A–C). Substantial ice-cored LH moraines protrude into Faksedalen from Gullfaksebreen and other outlet glaciers from Åsgard-

Table 1. De Geerbukta radiocarbon dates. Dates corrected for marine reservoir age with ΔR = 70±30 (Mangerud & Svendsen 2018) and calibrated with Marine13 on Calib Rev 7.0.4.

Lab. ID	Location	Date	Sample	Deposit	Elevation (m a.s.l.)	Lat./Long. (°)	^{14}C age (a BP)	δ^{13}C corr. (‰)	Cal. age (a BP) Median	Cal. age (a BP) 1σ
Ua-52521	De Geerbukta	12.8.2015	*M. truncata* frag.	Beach sand and gravel	45	79.60140′N, 17.65500′Eice	9725±42	1	10 553	10 484–10 622
Ua-52520	De Geerbukta	12.8.2015	Whalebone	Beach sand and gravel	28	79.61320′N, 17.68600′E	9020±35	−18.5	9591	9530–9652
Ua-52522	De Geerbukta	12.8.2015	*M. calcarea* paired shell	Deformed sand	8	79.61948′N, 17.67215′E	10 686±43	−0.1	11 933	11 826–12 039
Ua-52523	De Geerbukta	12.8.2015	*M. calcarea* paired shell	Deformed sand	7	79.61948′N, 17.67215′E	10 827±44	−1.5	12 193	12 059–12 326
Ua-52518	Palanderbukta	10.8.2015	*H. arctica* frag.	Beach sand and gravel	53	79.56044′N, 20.62425′E	9894±40	1.4	10 742	10 655–10 829

fonna (Fig. 1C). A 3.5-km-long arcuate moraine system ('Fakse moraine') with its highest point 52 m a.s.l. is located outside of the LH moraines at the mouth of Faksedalen (Fig. 2A–C; ArcticDEM). The Fakse moraine system is cut by the Fakse meltwater stream. Bedrock protrudes through the moraine material along the north-eastern part of the ridge. Glaciotectonized marine sediments are exposed in a geological section in the distal flank, outboard of the Fakse moraine (Figs 2D–F, 3). The glaciotectonized marine sediments were proximal to the ice margin but the sample site was not over-ridden (Figs 1C, 2D–F, 3). Following the retreat of Gullfaksebreen, the entire surface of the moraine was wave-washed, depositing shells and whalebones in the beach sediments (Fig. 2G–I; Table 1).

The younger bivalve found in living position in the deformed soft marine (silts and sands) sediments on the distal side of the Fakse moraine dates to 11.9 cal. ka BP (11 930 cal. a BP), effectively constraining a maximum age for the deposition of the Fakse moraine (Fig. 2G). We suggest these marine sediments were deposited in a shallow fjord environment (45–55 m water depth) with glaciers in the catchment but not directly proximal to a tidewater ice margin. The bivalve shells from the glaciotectonized marine sediments pre-date the moraine and suggest that Gullfaksebreen advanced into De Geerbukta sometime after 11.9 cal. ka BP (Table 1). Shell fragments at 45 m a.s.l. and a whalebone at 28 m a.s.l. sampled from beach sediments overlaying the Fakse moraine give minimum constraining ages for the deposit, dating to 10.6 and 9.6 cal. ka BP, respectively (10 550 and 9590 cal. a BP; Fig. 2H, I). Although the mollusc age dates that specific shoreline, the Fakse moraine, which has been entirely wave-washed, suggests the glacier had not only deposited the moraine, but retreated from its maximum position during the formation of the shoreline. Because the entire Fakse moraine has been inundated during a high relative sea level (above 52 m a.s.l.), we assume the glacier advanced into the fjord during or shortly after the maximum postglacial relative sea-level stand, sometime between 11.9–10.6 cal. ka BP (Fig. 3).

The older bivalve found in living position in the glaciotectonized marine sediments has a median age of 12.2 cal. ka BP (12 190 cal. a BP; Fig. 3, Table 1). The shells sampled from the deformed sediments are close in age, making it unclear how long the outer extent of De Geerbukta was ice-free before the Gullfaksebreen re-advance. Interestingly, the median age of the older bivalve extends the minimum age of the deglaciation of the Hinlopen Strait from roughly 11.3 to 12.2 ka BP (Hogan *et al.* 2017; Flink *et al.* 2017).

Extended Lateglacial–early Holocene glaciers

Based on the interpretation of surficial deposits visible in aerial imagery and digital elevation models of TopoSvalbard we introduce six locations where LGEH glaciers re-

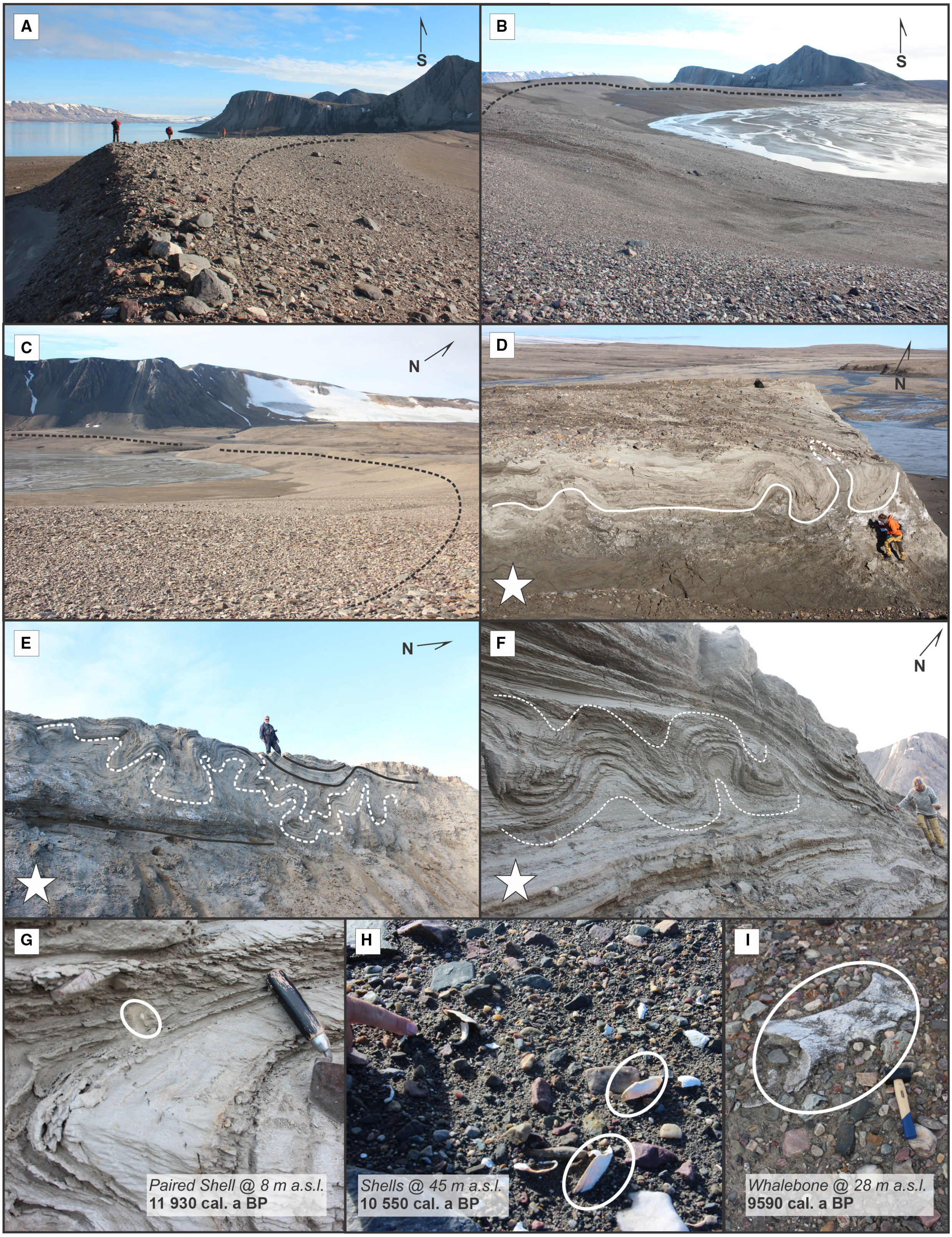

Fig. 2. A–C. Overview of the Fakse moraine with alluvial system and De Geerbukta on the glacial proximal and distal side respectively. D–F. Glaciotectonized marine sediments located on the distal side of the Fakse moraine. Deformed structures outlined for clarity. Location of the proglacial deformed sediments marked by white star in Fig. 1. G–I. Sampled paired shells in glaciotectonized marine sediments as well as shell fragments and whalebone in beach sediments overlaying the Fakse moraine, respectively. Corrected/calibrated ages and elevations indicated.

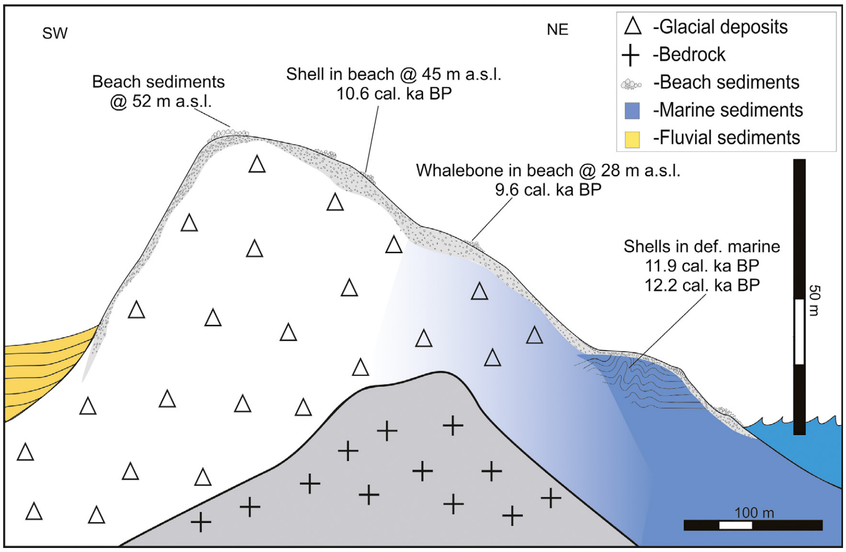

Fig. 3. Schematic cross-section of the Fakse moraine. Corrected/calibrated radiocarbon ages constrain the glacier advance in time.

advanced or exhibited stillstands substantial enough to leave remnant moraine ridges (Figs 1A, 4, S1; Table S1). Similar to the Fakse moraine in De Geerbukta, identified ridge deposits are interpreted to represent ice-marginal deposits often in the form of terminal (or frontal-lateral) moraines. In all cases, the moraine ridges are located at or around the marine limit. Glacial deposits have been partially or entirely wave-washed allowing for the potential to constrain the event with detailed sea-level curves (Forman 1989; Fig. S1).

Palaeo-glacier lengths for these six glaciers as well as De Geerbukta extended between roughly 2–8 km beyond their LH margins (Figs 1C, 5). On average, the LGEH glacial deposits that we introduce are ~4 km outboard of the LH moraines (Figs 1C, 5; Table S1). The sites with glacial deposits of suggested LGEH age are found across Spitsbergen and correspond to glaciers of all sizes with modern lengths ~1–20 km (Fig. 5). The two larger glaciers, Gullfaksebreen and Tåbreen, drain from the high plateau icecap, Åsgardfonna. Glaciers Heftybreen and Albertbreen correspond to small cirques, while Flowerbreen and Richterbreen today are small cirque glaciers; but during the LGEH both were most likely valley glaciers. The glacier that filled Lyckholmdalen during the LGEH probably was an outlet glacier from an icecap, which may correspond to the modern Friggkåpa (Fig. S1). In some cases, glacial deposits correlate to empty catchments, like Heftybreen, where at present the cirque is almost entirely ice-free (Fig. S1). Although an unknown amount of ice, remnant from the degrading Svalbard Barents Sea Ice Sheet (SBIS) probably still existed, all sites with LGEH moraines suggest transitional or local flow styles confining within topography and overprinting maximum ice-flow directions (Landvik *et al.* 2014).

Discussion

Lateglacial–early Holocene conditions and glacier deposits

Between 14–12 cal. ka BP, extensive regions of the marine-based sectors of the SBIS collapsed, resulting in a retreat of the northwestern margin from the shelf to positions inside the modern coastline of Svalbard (Mangerud *et al.* 1992; Hormes *et al.* 2013). Deglaciation was time transgressive and initially occurred in major troughs and fjords and subsequently in the inter-trough and terrestrial realms (Ingólfsson & Landvik 2013). The Holocene Thermal Optimum (HTO) is characterized by the migration and presence of warm water molluscs and foraminifera to waters around Svalbard between 11.2–5.5 cal. ka BP (Fig. 5; Salvigsen 2002; Hald *et al.* 2004). Proxy records from lake sediments collected in northwestern Spitsbergen suggest warm, moist conditions as early as 12.8 cal. ka BP (Balascio *et al.* 2018; van der Bilt *et al.* 2018) while a recent review of thermophilous molluscs suggests early warm conditions with peak warming (6 °C greater than at present) from 10.2–9.2 cal. ka BP (Mangerud & Svendsen 2018). Marine terminating glaciers responded to the warming by retreating back to terrestrial margins while some cirque glaciers disappeared completely (Snyder *et al.* 2000; Forwick & Vorren 2009).

A study highlighting transitional deposits on Spitsbergen suggests that there are numerous terrestrial and subaqueous glacial deposits that could be related to glacier advances during this period, traditionally associated with the deglaciation (Landvik *et al.* 2014). The LGEH glacier advances have been noted in some stratigraphical studies from Spitsbergen, but have been the

Fig. 4. High-resolution aerial imagery of six selected sites where glacier deposits (marked by white dotted lines) have been remotely constrained to Lateglacial–early Holocene age. Glacier deposits labelled A–F corresponding to the Tåbreen, Albertbreen, Lyckholmdalen, Flowerbreen, Heftybreen and Richterbreen glaciers/valleys, respectively. Glacier deposits presented in (A) and (C) correspond to outlet glaciers from plateau icecaps and (B) and (E) from cirque glaciers, while (D) and (F) highlight glacier deposits from valley glaciers. Imagery from TopoSvalbard. For topographic data and larger images see Figs S1, S2.

focus of fewer studies compared to the LH glacier deposits (Table S1). Studies in central Spitsbergen describe poorly constrained LGEH glacial deposits in Bromelldalen (Fig. 1A; site 18) and Gangdalen (Fig. 1A; site 21) but focus on regional sea levels, marine sediments and the deglaciation (Landvik & Salvigsen 1985; Mangerud *et al.* 1992). Additionally, shoreline studies from north central Spitsbergen partly constrain LGEH glacial deposits for several catchments (Fig. 1A; sites 1–8; Brückner *et al.* 2002; Eitel *et al.* 2002). More recently, stratigraphical sections near Longyearbyen (Fig. 1A; site 17) have been interpreted to represent a valley glacier advance between 10.6–10.4 cal. ka BP (Fig. 6; Lønne 2005). The deposits are located ~7 km outside of the present ice margin, and are at the regional Holocene marine limit (63 m a.s.l.). Lønne (2005) links this advance to a regional climatic

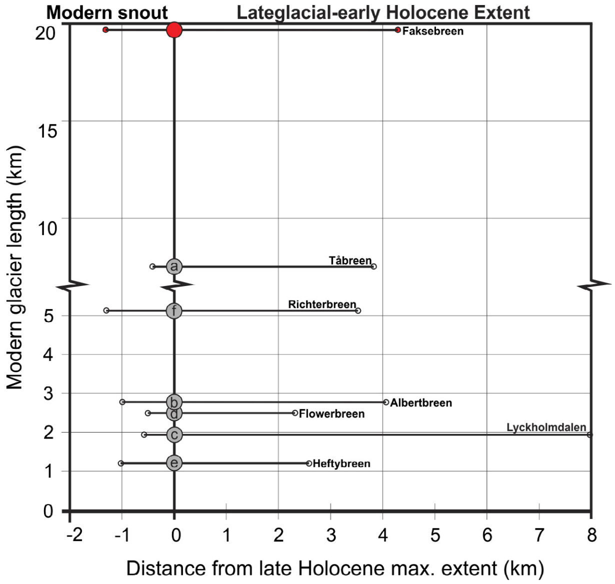

Fig. 5. Distances of Lateglacial–early Holocene glacier margins compared in length to the late Holocene maximum extent and the modern ice front (König *et al.* 2014). Red dots represent Faksedalen (introduced in Fig. 1C). Grey dots represent the six glacial systems introduced in Fig. 4. In all cases Lateglacial–early Holocene ice-marginal deposits are located several km outboard of the late Holocene glacier margins suggesting larger glaciers systems during the Lateglacial–early Holocene. For data see Table S1.

event, comparing other local advances in the Isfjorden area such as an advance of Aldegondabreen (SW Isfjorden) subsequent to 10.9 cal. ka BP and an advance of Esmarkbreen (N Isfjorden) subsequent to 10.3 cal. ka BP (Salvigsen *et al.* 1990; Lønne 2005). New data from St. Jonsfjorden suggest a tributary glacier advanced between 12.8–10.1 cal. ka BP (Fig. 5; site 15; Farnsworth *et al.* 2017). The oldest maximum constraining ages of reported glacier deposits reflecting postglacial re-advances correspond to two studies on north and south Prince Karls Forland with dates of 14 and 13.1 ka BP, respectively (Fig. 1A, sites 13, 14; Andersson *et al.* 1999, 2000). The youngest date reported as a maximum constraining age is from Edgeøya, located in the east of Svalbard where glacial sediments (with a whale rib) outboard of the Albrechtbreen Neoglacial deposits date to 9.2 cal. ka BP (Fig. 1A; site 23; Ronnert & Landvik 1993). Recent mapping in the Van Mijenfjorden identifies glacial deposits connected to a delta remnant from a high relative sea level, also suggested to be early Holocene in age (site 20; Larsen *et al.* in press).

Van der Bilt *et al.* (2015) suggest a Holocene (glacial) maximum between 9.6–9.5 cal. ka BP, based on a lake sediment core from NW Spitsbergen and suggest links to a meltwater pulse from the melting Laurentide Ice Sheet (LIS) via the Hudson Strait influencing regional climate (Fig. 1A; site 10). In contrast with the suggested early Holocene glacial maximum interpreted from the lake Hajeren sedimentary record, several studies suggest this period in time coincides with peak warming in Svalbard fjords and regional waters (Hald *et al.* 2004; Mangerud & Svendsen 2018). Although van der Bilt *et al.* (2015) assume that the peak in minerogenic-rich sediments dating from 9.6 to 9.5 ka BP in the lacustrine chronology reflects glacier advances from two snow patches driven by a large-scale connection to the melting LIS, other deposits in the catchment may also influence the Hajeren lake record. Interestingly, a study from Kløsa, the lake just one kilometer to the southwest of Hajeren suggests the outer Karlbreen moraine pre-dates the HTO. Interestingly, a study from Kløsa, the lake just one kilometer to the southwest of Hajeren suggests the outer Karlbreen moraine pre-dates the HTO. Given the mapped catchment boundary for lake Hajeren was drawn over the Karlbreen moraine in the southern end of the drainage (van der Bilt *et al.* 2015, 2016); it seems a simpler solutions for the peak in minerogenic sediments from Hajeren are sourced from the degradation of the Karlbreen moraine driven by warm regional conditions (Hald *et al.* 2004; Mangerud & Svendsen 2018). Although the interpretation of the chronology from Hajeren may not be sound, this would still suggest the Karlbreen moraine pre-dates the early Holocene glacier maximum and formed some-time during the LGEH (van der Bilt *et al.* 2015; Røthe *et al.* 2015).

In summary, most of these deposits are poorly constrained in age and seem to have formed between 14.0–9.0 cal. ka BP without clear synchronicity or prominent terminal moraines (Fig. 6). Thus, if they are related, it is not directly through one specific climatic event, but indirectly owing to environmental or external factors. Additionally, marine palaeoclimate records suggest that regional conditions were much warmer than at present (Hald *et al.* 2004; Mangerud & Svendsen 2018).

Glacier re-advances during deglaciation

Our current understanding of the regional deglaciation and Holocene history of Svalbard has only involved terminal moraines of re-advancing glaciers during the LH (Mangerud & Landvik 2007; Hormes *et al.* 2013). We revise this reconstruction by presenting the first well-constrained end moraine complex formed during the Lateglacial–early Holocene in De Geerbukta, NE Svalbard. We propose that the Fakse moraine was deposited in a fjord during a re-advance between 11.9–10.6 cal. ka BP. At that time, the palaeo-Gullfaksebreen extended over 5.5 km downvalley from the modern ice margin (4.4 km past the LH), marking the outermost glacier extent since the deglaciation.

The age constraint of the Fakse moraine and respective re-advance straddling the transition from the Pleistocene to Holocene equates to either the largest Holocene glacier extent occurring during the early Holocene (not during the LIA), or stands as the best candidate for a glacier re-advance on Svalbard occurring during the YD chronozone. Both scenarios improve our understanding of the

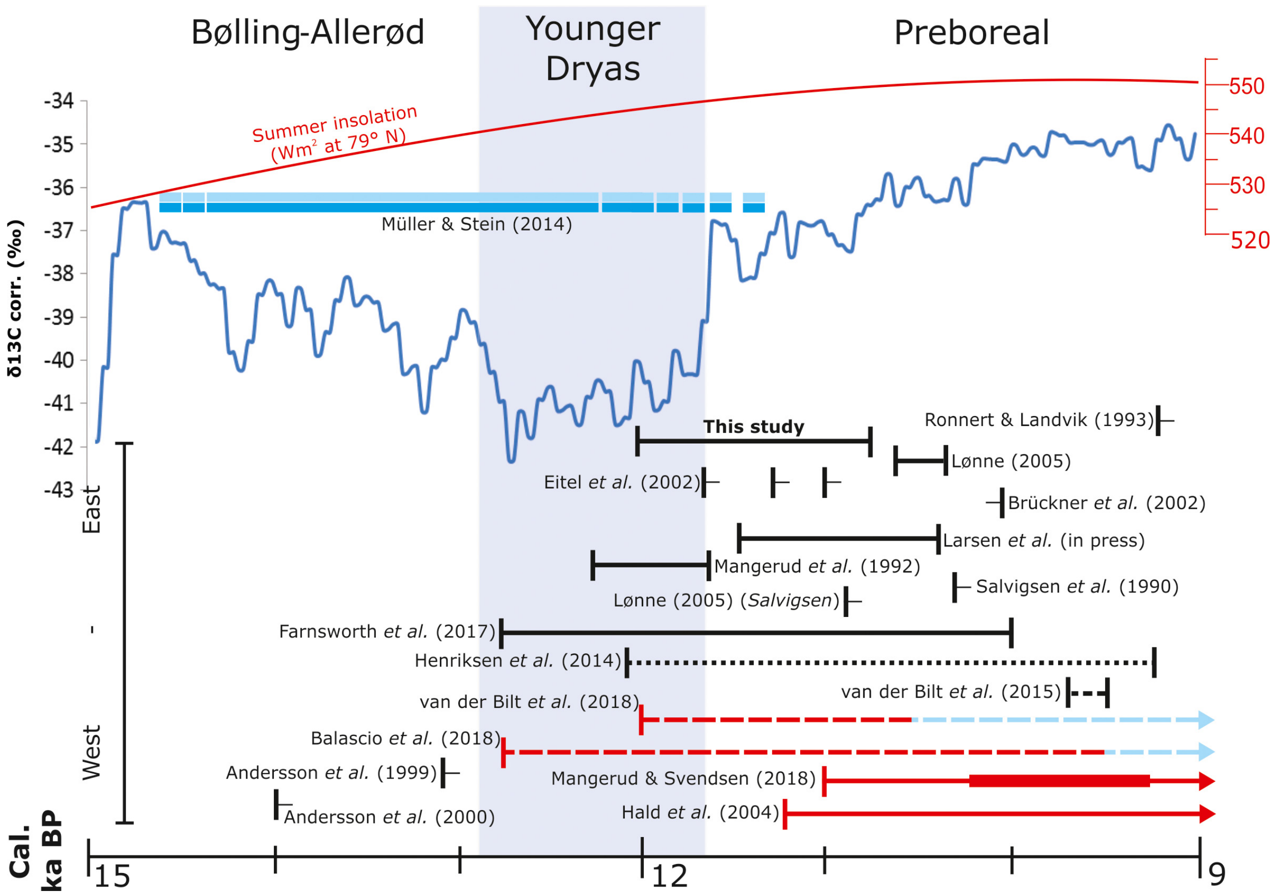

Fig. 6. Diagram summarizing Lateglacial–early Holocene climate and glacier deposits in Svalbard. $\delta^{18}O$ from NGRIP plotted in blue (Andersen *et al.* 2004). Summer insolation at 79°N indicated by red curve and sea-ice extent indicated by horizontal solid and fragmented blue lines based on proxy IP25 (Müller & Stein 2014). Black bars mark constrained glacier events, dashed lines indicate lacustrine studies and dotted lines indicate age range of dated glacial deposits. Partially constrained events marked by T-forms. Red/light blue bars indicate warm/cool conditions based on warm water species and proxies. Thick red line indicates maximum fjord temperatures at least 6 °C greater then present (Mangerud & Svendsen 2018). Shaded vertical bar marks the Younger Dryas period. See Table S2 for raw data and references.

recent history of glaciers and icecaps on Svalbard. Furthermore, the maximum constraining ages of bivalves from the glaciotectonized shallow marine sediments in De Geerbukta are the oldest radiocarbon ages inside of the Hinlopen Strait, pushing back the age of deglaciation a millennium in time (Table 1; Hogan *et al.* 2017; Flink *et al.* 2017).

Additionally, in this study we summarize the synchronicity of our well-constrained end moraine to an additional 15 other sites mentioned in the literature. We further upscale these findings by highlighting six other locations where geomorphologically similar deposits exist terrestrially on Svalbard. These LGEH glacier deposits correspond to glaciers of all sizes, and the deposits often extend several kilometres beyond LH maxima. Three of these six sites, which were identified remotely (in addition to De Geerbukta), have been ground-truthed, and as of yet, all lack the age constraint of the LGEH re-advance of Gullfaksebreen. We are confident in the general morphology of the moraine ridges and their location at the mouth of catchments, as well as their relationship to older postglacial sea levels.

Similar to the referenced study sites, the glacier deposits commonly occur proximal to the postglacial high relative sea-level stands. More research is needed to determine whether the marine tidewater setting played a dynamic role or was merely a result of the environment at the time. Studies of the sea-floor morphology would be complementary and potentially indicate whether these deposits are strictly linked to the LGEH relative sea level. However, unlike the terrestrial LGEH glacier deposits that can be indirectly constrained in age remotely, the submarine glacier deposits do not exhibit cross-cutting morphological evidence of a high relative sea level (constituting a minimum constraining age of deposition). Recent work from eastern Spitsbergen suggests glaciers may have extended further than the traditional Neoglacial–LIA maxima during the early Holocene, but the moraines are yet to be well constrained in time (Flink & Noormets 2017; Flink *et al.* 2018).

Glacier re-advances of LGEH age are not unique to Svalbard and have been identified at other North Atlantic ice-sheet margins during the last deglaciation. Some outlet glacier re-advances have been identified in Iceland shortly following the collapse of the marine-terminating Icelandic Ice Sheet between 13.4–11.7 cal. ka BP (Norðdahl & Ingólfsson 2015; Patton *et al.* 2017; Sigfúsdóttir *et al.* 2018). Local glaciers in North Greenland re-advanced in response to the YD cooling as interpreted from the GRIP ice-cores (Larsen *et al.* 2016), whereas most other glaciers in Greenland did not advance during the YD period (Denton *et al.* 2005; Funder *et al.* 2011). An extremely dynamic deglaciation is visible in offshore data from northern Scandinavia and the Barents Sea, where the interplay between rising eustatic sea level and grounding-line conditions influenced retreat, re-advances and stagnation (Newton & Huuse 2017). Furthermore, a non-linear deglaciation of the NW margin of the Laurentide Ice Sheet is suggested to have been interrupted by numerous re-advances and variable retreat rates (Stokes *et al.* 2009). It appears that as ice flow transitions from maximum to local flow style (Landvik *et al.* 2014) at the margins of ice sheets during deglaciation, glacier behaviour is increasingly being characterized by not just retreat, but by unsustainable (dynamic) re-advances, stagnation and episodic retreat. It is possible this may reflect the style of deglaciation and provide an analogue for how large bodies of ice rapidly shed mass, thus furthering our understanding of deglaciation.

As most glacier advances are mass balance controlled, driven by increased winter precipitation and/or lower summer temperatures, deposits from advancing glaciers constrained in age are associated with periods of cooler summer temperatures and/or abundant snowfall (Solomina *et al.* 2015). But, is this always the case? With our current understanding of the palaeoclimate of Svalbard one cannot test whether palaeo-glacier advances are forced by winter precipitation, summer temperatures, or internal glacier dynamics. If mass balance is the key driver of these glacier advances, a rough regional synchronicity in glacier fluctuations would be expected (which is not yet visible). Thus, it is crucial to constrain more than a single glacier to effectively infer past climatic conditions.

As it now appears, the time transgressive deglaciation of the fjord-systems may play an indirect role in the timing of the glacier re-advances. Thus, a re-advance located near the mouth of the fjord (i.e. Heftybreen, Site E) may be older than the age of the moraine located in an inner tributary fjord (Lyckholmdalen, Site C). And in this model, a mid-fjord tributary like Bolterdalen (Lønne 2005) may have re-advanced at some point in between the timing of the other two glaciers' re-advances.

On Svalbard, the LGEH deposits correspond to glaciers of all sizes. Additionally, numerous glacier deposits relate to currently empty cirques and valleys suggesting a connection to the deglaciation dynamics, and the subsequent Holocene climate not being favourable enough to reinvigorate the glaciers following their unsustainable advances (Figs 4, S1). Given the high frequency of surge-type behaviour seen on Svalbard (Sevestre & Benn 2015; Farnsworth *et al.* 2016), the simplest reasoning would suggest that during the LGEH glaciers also may have exhibited surge-type behaviour. Furthermore, several stratigraphical studies from western Spitsbergen have highlighted glacial re-advances from earlier in the Pleistocene during periods assumed to be warm and characterized by deglaciation (Fig. 1A; sites 13, 14 and 22; Landvik *et al.* 1992; Andersson *et al.* 1999, 2000).

At present, the lack of synchronicity and the unknown rate of glacier advance/retreat corresponding to most LGEH glacier moraines make it challenging to discern whether the glacial oscillations that left the deposits were controlled by climate, internal glacier dynamics (surges), or a combination of these factors. We need to better understand: (i) past winter precipitation and summer temperatures, (ii) rapid glacio-isostatic uplift rates and their potential influence on mass balance, (iii) sea ice–glacier interactions, and (iv) the dynamics of the break-up of an ice sheet, to identify casual linkages to climate or internal dynamics. The transition from the Lateglacial to early Holocene resulted in glacier re-advances, stillstands and complex behaviour at many ice-sheet margins during the past deglaciation. It is reasonable to expect the reorganizing of glacier hydrological systems, shifting thermal regimes and fluctuating glacier surface profiles during the LGEH on Svalbard (Ingólfsson & Landvik 2013; Landvik *et al.* 2013, 2014). Considering the increasing extent of open water, warm fjords, relatively high sea levels and summer insolation characteristic of the deglaciation, it is not surprising that glaciers exhibited complex behaviour.

Conclusions

Glacier deposits of LGEH age are present across Svalbard, correspond to glaciers of all sizes and suggest a period of much more active glaciodynamic behaviour than previously understood. These LGEH moraines extend significantly further than LH deposits that were previously believed to reflect the most extensive glacier extent on Svalbard since the last deglaciation. The LGEH deposits described here provide insight into deglaciation dynamics and the behaviour of marine-terminating ice sheets in the changing climate of the Pleistocene to the Holocene transition. These deposits reflect hiccups in the overall deglaciation on Svalbard. Although it is unknown whether these glacier deposits relate to climatic or dynamic forcing, they do suggest the style of the deglaciation of ice sheets may be more complex than our current understanding. Thus, deglaciation may not reflect a simple and continuous retreat, but rather be characterized by re-advance, stagnation and subsequent recession (Newton & Huuse 2017).

Acknowledgements. – The authors acknowledge Sveinn Brynjólfsson and Sara Mollie Cohen for assistance in the field. Fieldwork and radiocarbon dates were funded by the Carlsberg Foundation (CF14-0756 to AS) and UNIS, respectively. Geospatial support was provided by the Polar Geospatial Center under NSF PLR awards 1043681 and 1559691. Finally, the authors would like to gratefully acknowledge the constructive reviews provided by Mona Henriksen and Jan Mangerud.

References

Andersen, K. K., Azuma, N., Barnola, J. M. & Bigler, M. 2004: High-resolution record of Northern Hemisphere climate extending into the last interglacial period. *Nature 431*, 147–151.

Andersson, T., Forman, S. L., Ingólfsson, Ó. & Manley, W. F. 1999: Late Quaternary environmental history of central Prins Karls Forland, western Svalbard. *Boreas 28*, 292–307.

Andersson, T., Forman, S. L., Ingólfsson, Ó. & Manley, W. F. 2000: Stratigraphic and morphologic constraints on the Weichselian glacial history of northern Prins Karls Forland, Western Svalbard. *Geografiska Annaler A 82*, 455–470.

Balascio, N. L., D'Andrea, W. J., Gjerde, M. & Bakke, J. 2018: Hydroclimate variability of High Arctic Svalbard during the Holocene inferred from hydrogen isotopes of leaf waxes. *Quaternary Science Reviews 183*, 177–187, https://doi.org/10.1016/j.quascirev.2016.11.036.

van der Bilt, W. G. M., Bakke, J. & Balascio, N. L. 2016: Mapping sediment–landform assemblages to constrain lacustrine sedimentation in a glacier-fed lake catchment in northwest Spitsbergen. *Journal of Maps 12*, 985–993.

van der Bilt, W. G. M., Bakke, J., Vasskog, K., D'Andrea, W. J., Bradley, R. S. & Ólafsdóttir, S. 2015: Reconstruction of glacier variability from lake sediments reveals dynamic Holocene climate in Svalbard. *Quaternary Science Reviews 126*, 201–218.

van der Bilt, W. G. M., D'Andrea, W. J., Bakke, J., Balascio, N. L., Werner, J. P., Gjerde, M. & Bradley, R. S. 2018: Alkenone-based reconstructions reveal four-phase Holocene temperature evolution for High Arctic Svalbard. *Quaternary Science Reviews 183*, 204–213.

Brückner, H., Schellmann, G. & van der Borg, K. 2002: Uplifted beach ridges in Northern Spitsbergen as indicators for glacio-isostasy and palaeo-oceanography. *Zeitschrift für Geomorphologie 46*, 309–336.

Denton, G. H., Alley, R. B., Comer, G. C. & Broecker, W. S. 2005: The role of seasonality in abrupt climate change. *Quaternary Science Reviews 24*, 1159–1182.

Eitel, B., van der Borg, K., Eberle, J. & Megies, H. 2002: Late Pleistocene/Early Holocene glacial history of northern Andreeland (northern Spitsbergen/Svalbard Archipelago): evidence from glacial and fluvio-glacial deposits. *Zeitschrift für Geomorphologie 46*, 337–364.

Farnsworth, W. R., Ingólfsson, Ó., Noormets, R., Allaart, L., Alexanderson, H., Henriksen, M. & Schomacker, A. 2017: Dynamic Holocene glacial history of St. Jonsfjorden, Svalbard. *Boreas 46*, 585–603.

Farnsworth, W. R., Ingólfsson, Ó., Retelle, M. & Schomacker, A. 2016: Over 400 previously undocumented Svalbard surge-type glaciers identified. *Geomorphology 264*, 52–60.

Flink, A. E. & Noormets, R. 2017: Submarine glacial landforms and sedimentary environments in Vaigattbogen, northeastern Spitsbergen. *Marine Geology*, https://doi.org/10.1016/j.margeo.2017.07.019.

Flink, A. E., Hill, P., Noormets, R. & Kirchner, N. 2018: Holocene glacial evolution of Mohnbukta, in eastern Spitsbergen. *Boreas 47*, 390–409.

Flink, A. E., Noormets, R., Fransner, O., Hogan, K. A., Ó'Regan, M. & Jakobsson, M. 2017: Past ice flow in Wahlenbergfjorden and its implications for late Quaternary ice sheet dynamics in northeastern Svalbard. *Quaternary Science Reviews 163*, 162–179.

Forman, S. L. 1989: Late Weichselian glaciation and deglaciation of Forlandsundet area, western Spitsbergen, Svalbard. *Boreas 18*, 51–60.

Forwick, M. & Vorren, T. O. 2009: Late Weichselian and Holocene sedimentary environments and ice rafting in Isfjorden, Spitsbergen. *Palaeogeography, Palaeoclimatology, Palaeoecology 280*, 258–274.

Funder, S., Kjeldsen, K. K., Kjær, K. H. & Ó Cofaigh, C. 2011: The Greenland Ice Sheet during the past 300,000 years: a review. *Developments in Quaternary Science 15*, 699–713.

Hald, M., Andersson, C., Ebbesen, H., Jansen, E., Klitgaard-Kristensen, D., Risebrobakken, B., Salomonsen, G. R., Sarnthein, M., Sejrup, H. P. & Telford, R. J. 2007: Variations in temperature and extent of Atlantic Water in the northern North Atlantic during the Holocene. *Quaternary Science Reviews 26*, 3423–3440.

Hald, M., Ebbesen, H., Forwick, M., Godtliebsen, F., Khomenko, L., Korsun, S., Ringstad Olsen, L. & Vorren, T. O. 2004: Holocene paleoceanography and glacial history of the West Spitsbergen area, Euro-Arctic margin. *Quaternary Science Reviews 23*, 2075–2088.

Hartmann, D. L., Klein Tank, A. M. G., Rusticucci, M., Alexander, L. V., Brönnimann, S., Charabi, Y., Dentener, F. J., Dlugokencky, E. J., Easterling, D. R., Kaplan, A., Soden, B. J., Thorne, P. W., Wild, M. & Zhai, P. M. 2013: Observations: atmosphere and surface. *In* Stocker, T. F., Qin, D., Plattner, G.-K., Tignor, M., Allen, S. K., Boschung, J., Nauels, A., Xia, Y., Bex, V. & Midgley, P. M. (eds.): *Climate Change 2013 the Physical Science Basis: Working Group I Contribution to the Fifth Assessment Report of the Intergovernmental Panel on Climate Change*, 159–254. Cambridge University Press, Cambridge.

Henriksen, M., Alexanderson, H., Landvik, J. Y., Linge, H. & Peterson, G. 2014: Dynamics and retreat of the Late Weichselian Kongsfjorden ice stream, NW Svalbard. *Quaternary Science Reviews 92*, 235–245.

Hogan, K. A., Dowdeswell, J. A., Hillenbrand, C.-D., Ehrmann, W., Noormets, R. & Wacker, L. 2017: Subglacial sediment pathways and deglacial chronology of the northern Barents Sea Ice Sheet. *Boreas 46*, 750–771.

Hormes, A., Gjermundsen, E. F. & Rasmussen, T. L. 2013: From mountain top to the deep sea – Deglaciation in 4D of the northwestern Barents Sea ice sheet. *Quaternary Science Reviews 75*, 78–99.

Humlum, O., Elberling, B., Hormes, A., Fjordheim, K., Hansen, O. H. & Heinemeier, J. 2005: Late-Holocene glacier growth in Svalbard, documented by subglacial relict vegetation and living soil microbes. *The Holocene 15*, 396–407.

Huss, M. & Hock, R. 2015: A new model for global glacier change and sea-level rise. *Frontiers in Earth Science 3*, 1–54.

Ingólfsson, Ó. & Landvik, J. Y. 2013: The Svalbard-Barents Sea ice-sheet – Historical, current and future perspectives. *Quaternary Science Reviews 64*, 33–60.

Kirkbride, M. P. & Winkler, S. 2012: Correlation of Late Quaternary moraines: impact of climate variability, glacier response, and chronological resolution. *Quaternary Science Reviews 46*, 1–29.

König, M., Nuth, C., Kohler, J., Moholdt, G. & Pettersen, R. 2014: A digital glacier database for Svalbard. *In* Kargel, S. J., Leonard, J. G., Bishop, P. M., Kääb, A. & Raup, H. B. (eds.): *Global Land Ice Measurements from Space*, 229–239. Springer, Berlin.

Landvik, J. Y. & Salvigsen, O. 1985: Glaciation development and interstadial sea-level on central Spitsbergen, Svalbard. *Polar Research 3*, 1–10.

Landvik, J. Y., Alexanderson, H., Henriksen, M. & Ingólfsson, Ó. 2014: Landscape imprints of changing glacial regimes during ice-sheet build-up and decay: a conceptual model from Svalbard. *Quaternary Science Reviews 92*, 258–268.

Landvik, J. Y., Bolstad, M., Lycke, A. K., Mangerud, J. & Sejrup, H. P. 1992: Weichselian stratigraphy and palaeoenvironments at Bellsund, western Svalbard. *Boreas 21*, 335–358.

Landvik, J. Y., Brook, E. J., Gualtieri, L., Linge, H., Raisbeck, G., Salvigsen, O. & Yiou, F. 2013: ^{10}Be exposure age constraints on the Late Weichselian ice-sheet geometry and dynamics in inter-ice-stream areas, western Svalbard. *Boreas 42*, 43–56.

Larsen, E. A., Lyså, A., Rubensdotter, L., Farnsworth, W. R., Jensen, M., Nadeau, M. J. & Ottesen, D. in press: Late-Glacial and Holocene glacier activity in the Van Mijenfjorden area, western Svalbard. *Arctos 4*, https://doi.org/10.1007/s41063-018-0042-2.

Larsen, N. K., Funder, S., Linge, H., Möller, P., Schomacker, A., Fabel, D., Xu, S. & Kjær, K. H. in press: Younger Dryas re-advance of local glaciers in north Greenland. *Quaternary Science Reviews 147*, 47–58.

Lønne, I. 2005: Faint traces of high Arctic glaciations: an early Holocene ice-front fluctuation in Bolterdalen, Svalbard. *Boreas 34*, 308–323.

Mangerud, J. & Landvik, J. Y. 2007: Younger Dryas cirque glaciers in western Spitsbergen: smaller than during the Little Ice Age. *Boreas 36*, 278–285.

Mangerud, J. & Svendsen, J. I. 2018: The Holocene thermal optimum around Svalbard, Arctic North Atlantic; molluscs show early and exceptional warmth. *The Holocene 28*, 65–83.

Mangerud, J., Bolstad, M., Elgersma, A., Helliksen, D., Landvik, J. Y., Lønne, I., Lycke, A. K., Salvigsen, O., Sandahl, T. & Svendsen, J. I. 1992: The last glacial maximum on Spitsbergen, Svalbard. *Quaternary Research 38*, 1–31.

McKay, N. P. & Kaufman, D. S. 2014: An extended Arctic proxy temperature database for the past 2,000 years. *Scientific Data 1*, 140026, https://doi.org/10.1038/sdata.2014.26.

Miller, G. H., Landvik, J. Y., Lehman, S. J. & Southon, J. R. 2017: Episodic Neoglacial snowline descent and glacier expansion on Svalbard reconstructed from the ^{14}C ages of ice-entombed plants. *Quaternary Science Reviews 155*, 67–78.

Müller, J. & Stein, R. 2014: High-resolution record of late glacial and deglacial sea ice changes in Fram Strait corroborates ice–ocean interactions during abrupt climate shifts. *Earth and Planetary Science Letters 403*, 446–455.

Newton, A. M. W. & Huuse, M. 2017: Glacial geomorphology of the central Barents Sea: implications for the dynamic deglaciation of the Barents Sea Ice Sheet. *Marine Geology 387*, 114–131.

Norðdahl, H. & Ingólfsson, Ó. 2015: Collapse of the Icelandic ice sheet controlled by sea-level rise? *Arctos 1*, https://doi.org/10.1007/s41063-015-0020-x.

Patton, H., Hubbard, A., Bradwell, T. & Schomacker, A. 2017: The configuration, sensitivity and rapid retreat of the Late Weichselian Icelandic ice sheet. *Earth-Science Reviews 166*, 223–245.

Philipps, W., Briner, J. P., Gislefoss, L., Linge, H., Koffman, T., Fabel, D., Xu, S. & Hormes, A. 2017: Late Holocene glacier activity at inner Hornsund and Scottbreen, southern Svalbard. *Journal of Quaternary Science 32*, 501–515.

Reimer, P. J., Bard, E., Bayliss, A., Beck, J. W., Blackwell, P. G., Bronk Ramsey, C., Buck, C. E., Cheng, H., Edwards, R. L., Friedrich, M., Grootes, P. M., Guilderson, T. P., Haflidason, H., Hajdas, I., Hatté, C., Heaton, T. J., Hoffmann, D. L., Hogg, A. G., Hughen, K. A., Kaiser, K. F., Kromer, B., Manning, S. W., Niu, M., Reimer, R. W., Richards, D. A., Scott, E. M., Southon, J. R., Staff, R. A., Turney, C. S. M. & van der Plicht, J. 2013: IntCal13 and Marine13 radiocarbon age calibration curves 0–50,000 years cal BP. *Radiocarbon 55*, 1869–1887.

Reusche, M., Winsor, K., Carlson, A. E., Marcott, S. A., Rood, D. H., Novak, A., Roof, S., Retelle, M., Werner, A., Caffee, M. & Clark, P. U. 2014: ^{10}Be surface exposure ages on the late-Pleistocene and Holocene history of Linnébreen on Svalbard. *Quaternary Science Reviews 89*, 5–12.

Rogers, J. C., Yang, L. & Li, L. 2005: The role of Fram Strait winter cyclones on sea ice flux and on Spitsbergen air temperatures. *Geophysical Research Letters 32*, L06709, https://doi.org/10.1029/2004gl022262.

Ronnert, L. & Landvik, J. Y. 1993: Holocene glacial advances and moraine formation at Albrechtbreen, Edgeøya, Svalbard. *Polar Research 12*, 57–63.

Røthe, T. O., Bakke, J., Vasskog, K., Gjerde, M., D'Andrea, W. J. & Bradley, R. S. 2015: Arctic Holocene glacier fluctuations reconstructed from lake sediments at Mitrahalvøya, Spitsbergen. *Quaternary Science Reviews 109*, 111–125.

Salvigsen, O. 2002: Radiocarbon-dated *Mytilus edulis* and *Modiolus modiolus* from northern Svalbard: climatic implications. *Norsk Geografisk Tidsskrift 56*, 56–61.

Salvigsen, O., Elgersma, A., Hjort, C., Lagerlund, E., Liestøl, O. & Svensson, N.-O. 1990: Glacial history and shoreline displacement on Erdmannflya and Bohemanflya, Spitsbergen, Svalbard. *Polar Research 8*, 261–273.

Sevestre, H. & Benn, D. I. 2015: Climatic and geometric controls on the global distribution of surge-type glaciers: implications for a unifying model of surging. *Journal of Glaciology 61*, 646–662.

Sigfúsdóttir, T., Benediktsson, Í. Ö. & Phillips, E. 2018: Active retreat of a Late Weichselian marine-terminating glacier: an example from Melasveit, western Iceland. *Boreas*, https://doi.org/10.1111/bor.12306.

Snyder, J. A., Werner, A. & Miller, G. H. 2000: Holocene cirque glacier activity in western Spitsbergen, Svalbard: sediment records from proglacial Linnévatnet. *The Holocene 10*, 555–563.

Solomina, O. N., Bradley, R. S., Hodgson, D. A., Ivy-Ochs, S., Jomelli, V., Mackintosh, A. N., Nesje, A., Owen, L. A., Wanner, H., Wiles, G. C. & Young, N. E. 2015: Holocene glacier fluctuations. *Quaternary Science Reviews 111*, 9–34.

Stokes, C. R., Clark, C. D. & Storrar, R. 2009: Major changes in ice stream dynamics during deglaciation of the north-western margin of the Laurentide Ice Sheet. *Quaternary Science Reviews 28*, 721–738.

Svendsen, J. I. & Mangerud, J. 1992: Paleoclimatic inferences from glacial fluctuations on Svalbard during the last 20 000 years. *Climate Dynamics 6*, 213–220.

Svendsen, J. I. & Mangerud, J. 1997: Holocene glacial and climatic variations on Spitsbergen, Svalbard. *The Holocene 7*, 45–57.

Werner, A. 1988: *Holocene glaciation and climatic change, Spitsbergen, Svalbard*. Ph.D. thesis, University of Colorado, 296 pp.

Werner, A. 1993: Holocene moraine chronology, Svalbard: lichenometric evidence for multiple neoglacial advances in the Arctic. *The Holocene 3*, 128–137.

Supporting Information

Additional Supporting Information may be found in the online version of this article at http://www.boreas.dk.

Fig. S1. TopoSvalbard maps of Lateglacial–early Holocene sites.

Fig. S2. Enlarged imagery of Lateglacial–early Holocene sites.

Table S1. Glacier length data.

Table S2. Lateglacial–early Holocene studies.

Chapter II

Lateglacial and Holocene glacier activity in the Van Mijenfjorden area, western Svalbard

Larsen, E., Lyså, A., Rubensdotter, L., Farnsworth, W.R., Jensen, M., Nadeau, M., Ottesen, D. (2018): Lateglacial and Holocene glacier activity in the Van Mijenfjorden area, western Svalbard. *arktos*. DOI: 10.1007/s41063-018-0042-2.

Oblique aerial image of the mouth of Gustavdalen, northern Van Mijenfjorden, Spitsbergen.

Chapter III

Dynamic Holocene glacial history of St. Jonsfjorden, Svalbard

Farnsworth, W.R., Ingólfsson, Ó., Noormets, R., Allaart, L., Alexanderson, H., Henriksen, M., Schomacker, A. (2017): Dynamic Holocene glacial history of St. Jonsfjorden, Svalbard. *Boreas 46,* 585-603. DOI: 10.1111/bor.12269.

Modiolus modiolus sampled at Piriepynten, inner St. Jonsfjorden, Spitsbergen, July 2015.

BOREAS An international journal of Quaternary research

Dynamic Holocene glacial history of St. Jonsfjorden, Svalbard

WESLEY R. FARNSWORTH, ÓLAFUR INGÓLFSSON, RIKO NOORMETS, LIS ALLAART, HELENA ALEXANDERSON, MONA HENRIKSEN AND ANDERS SCHOMACKER

BOREAS

Farnsworth, W. R., Ingólfsson, Ó., Noormets, R., Allaart, L., Alexanderson, H., Henriksen, M. & Schomacker, A. 2017 (July): Dynamic Holocene glacial history of St. Jonsfjorden, Svalbard. *Boreas*, Vol. 46, pp. 585–603. https://doi.org/10.1111/bor.12269. ISSN 0300-9483.

Evidence of a dynamic Holocene glacial history is preserved in the terrestrial and marine archives of St. Jonsfjorden, a small fjord-system on the west coast of Spitsbergen, Svalbard. High-resolution, remotely sensed imagery from marine and terrestrial environments was used to construct geomorphological maps that highlight an intricate glacial history of the entire fjord-system. The geomorphology and stratigraphy indicate an early Holocene local glacier advance constrained to the Lateglacial–early Holocene transition. Identification and ^{14}C dating of the thermophilous bivalve mollusc *Modiolus modiolus* to 10.0±0.12 cal. ka BP suggest a rapid northward migration of the species shortly after deglaciation. Further evidence enhances the understanding of the onset and subsequent climax of the Neoglacial-Little Ice Age in inner St. Jonsfjorden. The present-day terminus of Osbornebreen, the dominating glacier system in St. Jonsfjorden, is located over 8.5 km up-fjord from its Neoglacial maximum extent. Cross-cutting relationships suggest subsequent advances of all the smaller glaciers in the area following the break-up of Osbornebreen. Glacial deposits, landforms and their cross-cutting relationships observed in both terrestrial and marine settings imply a complex and highly dynamic environment through the later part of the Holocene.

Wesley R. Farnsworth (WesleyF@unis.no), Ólafur Ingólfsson and Riko Noormets, University Centre in Svalbard (UNIS), Longyearbyen N-9171, Norway; Wesley R. Farnsworth, Lis Allaart and Anders Schomacker, UiT The Arctic University of Norway, Tromsø N-9037, Norway; Ólafur Ingólfsson, University of Iceland, Askja, Sturlugata 7, Reykjavík IS-101, Iceland; Helena Alexanderson, Lund University, Sölvegatan 12, Lund 223 62, Sweden; Mona Henriksen, Norwegian University of Life Sciences, P.O. Box 5003, Ås N-1432, Norway; *received 3rd February 2017, accepted 19th May 2017.*

The climate during the Holocene (the last 11.7 ka) has traditionally been regarded as relatively stable, compared to the preceding Late Pleistocene (Dansgaard *et al.* 1993; Steffensen *et al.* 2008; Rockström *et al.* 2009), but this paradigm of a relatively uneventful Holocene is being increasingly challenged (Bond *et al.* 2001; Mayewski *et al.* 2004; Wanner *et al.* 2011). We are beginning to see that shifts in climate occur more rapidly than previously understood, particularly in Arctic regions at present and during the early Holocene due to Arctic amplification (Bond *et al.* 2001; Hald *et al.* 2007; Wanner *et al.* 2011; Masson-Delmotte *et al.* 2013; Briner 2016). By studying the rate and magnitude of past changes in climate we are able to better understand current climate dynamics, as well as more effectively predict antecedent climate scenarios (McKay & Kaufman 2014). Arctic glaciers can be valuable indicators for past climate variations given their sensitivity to winter precipitation and summertime temperatures (Oerlemans 2005). Not all glaciers respond uniformly to shifts in climate (Røthe *et al.* 2015), and in some cases ice-front fluctuations can be influenced by internal dynamics (surge behaviour), making the interpretation of their climatic relationships challenging (Yde & Paasche 2010; Farnsworth *et al.* 2016). Additionally, marine terminating glaciers are subject to more complex glaciodynamic conditions compared to terrestrial systems, as ice-front fluctuations are influenced by oceanic temperatures, currents, sea ice and relative sea level as well as air temperature and precipitation (Forwick & Vorren 2009; Nick *et al.* 2010).

The position of Svalbard between the northern extent of the North Atlantic Drift and the seasonal sea ice makes it an ideal setting to study the climate sensitivity of the Arctic (Rogers *et al.* 2005). In addition, Svalbard's proximity to the former margin of the Svalbard-Barents Sea Ice Sheet (SBIS) has made it a valuable locality to study the configuration, behaviour and dynamics of the ice sheet (Landvik *et al.* 1998, 2005, 2014; Mangerud *et al.* 1998; Hormes *et al.* 2013; Ingólfsson & Landvik 2013; Gjermundsen *et al.* 2015). The Holocene development of climate and glaciers in Svalbard is not well understood, partly due to the lack of case studies and, consequently, the scarceness of well-constrained (pre-Little Ice Age) chronologies for glacial events. The few detailed studies have predominantly focused on the west coast and have been somewhat biased towards younger events (Landvik *et al.* 2014), such as the Neoglacial and Little Ice Age (LIA) (e.g. Snyder *et al.* 2000; Humlum *et al.* 2005; Mangerud & Landvik 2007; Holmgren *et al.* 2010; Miller *et al.* 2017). As many Svalbard outlet glaciers terminate in fjords it is important to combine data from terrestrial and marine archives to holistically understand Holocene glacier oscillations and to make inferences about causal links in the climate-glacier system.

The aim of this study is to reconstruct a dynamic and complex series of glacial events during the Holocene that are preserved in sedimentary and morphological

DOI 10.1111/bor.12269

archives in a fjord system on the west coast of Spitsbergen. We present this through detailed Quaternary geological maps of terrestrial and marine environments from inner St. Jonsfjorden. The Holocene history is chronologically constrained by ^{14}C ages from stratigraphy, and cross-cutting relationships between glacial and marine landforms.

Holocene history of Svalbard

The Lateglacial–early Holocene on Svalbard is characterized by a rapid transition from a glacial to interglacial environment (Ingólfsson 2011; Hormes *et al.* 2013; Landvik *et al.* 2014). Between 15–12 ka BP extensive regions of the marine-based sectors of the SBIS collapsed, which resulted in a retreat of the NW margin from the shelf area into the modern coastline of the Svalbard archipelago (Jessen *et al.* 2010; Hormes *et al.* 2013; Hughes *et al.* 2016). Deglaciation on Svalbard was time transgressive and occurred initially in major troughs and fjords and subsequently in the inter-trough and terrestrial realms (Hormes *et al.* 2013; Ingólfsson & Landvik 2013; Landvik *et al.* 2014).

The Holocene Thermal Optimum (HTO) on Svalbard is recorded first in the marine environment and subsequently on land. The HTO is fingerprinted by the migration and presence of thermophilous molluscs and warm water foraminifera to waters around Svalbard between 11.2–5.5 ka BP (Salvigsen *et al.* 1992; Salvigsen 2002; Sarnthein *et al.* 2003; Hald *et al.* 2004; Blake 2006). This phase of warm stable conditions has also been interpreted from low sediment input and high productivity within lake basins between 8.5–5 ka BP (Birks 1991; Svendsen & Mangerud 1997; Holmgren *et al.* 2010; van der Bilt *et al.* 2015, 2017; Alsos *et al.* 2016). In response to the warmer conditions, some of the marine terminating glaciers retreated onto land, while some terrestrial cirque glaciers may have melted away completely (Svendsen & Mangerud 1997; Snyder *et al.* 2000; Forwick *et al.* 2010; van der Bilt *et al.* 2015).

Similar to the HTO, evidence from terrestrial and lacustrine environments related to Neoglacial climatic deterioration generally lags oceanic cooling. The decrease in abundance and number of species of thermophilous molluscs and foraminifera suggests that the marine cooling may have initiated as early as 8 ka BP (Salvigsen *et al.* 1992; Hald *et al.* 2004). Terrestrial and lacustrine studies highlight glacier advances that occur in sporadic pulses between the period ~4.5–3 ka BP (Svendsen & Mangerud 1997; Reusche *et al.* 2014; van der Bilt *et al.* 2015; Røthe *et al.* 2015). The final pulse of the Neoglacial expansion of the glacial system is synchronous with the culmination of the LIA on Svalbard (~1920 CE), and is in general suggested to be the largest and most significant glacial phase of the Holocene (Werner 1993; Humlum *et al.* 2005). The culmination of the LIA is visible in historical 1936 Norwegian Polar Institute oblique aerial photographs that display most ice margins up against or just proximal to their LIA moraine systems (Boulton *et al.* 1999; Lyså & Lønne 2001; Sletten *et al.* 2001; Paasche & Bakke 2010; Midgley & Tonkin 2017).

Widespread retreat and thinning of Svalbard glaciers have occurred since the end of the LIA, and extensive areas of recently glaciated landscape have been revealed (Nuth *et al.* 2013). In some cases, tidewater glaciers have responded similarly to the warmer conditions during the HTO and retreated back onto topographical heights and terrestrial environments (Forwick *et al.* 2010). Although the majority of glaciers have thinned and retreated in response to the 20th century climate, some glacier systems have exhibited rapid advances or speed-ups during this time, simulating the behaviour of a potential surge-type glacier (Sund *et al.* 2009; Lønne 2014; Dunse *et al.* 2015; Lovell *et al.* 2015a; Sevestre 2015; Farnsworth *et al.* 2016). These glaciers have subsequently thinned and retreated back at a considerably higher rate following their advances.

Regional setting and climate

Svalbard is an archipelago located along the dominant corridor of atmospheric moisture between the Atlantic and the Arctic Basin, spanning from 74° to 81°N (Vikhamar-Schuler *et al.* 2016; Fig. 1A). The islands are positioned at the northern extent of the Gulf Stream (North Atlantic Drift) and the southern border of the Arctic sea-ice front (Rogers *et al.* 2005). Despite the archipelago's northern location, western Spitsbergen experiences a mild climate for its latitude where the warm ocean current influences weather and sea ice (Førland *et al.* 1997, 2011). The climate is characterized by the interactions between the Icelandic Low and Siberian High pressure systems, and as a result, relatively high temperatures are driven north over Svalbard by the main North Atlantic cyclone track (Hanssen-Bauer *et al.* 1990). Svalbard precipitation is closely coupled to the mode of the North Atlantic Oscillation (NAO; Dickson *et al.* 2000) and falls predominantly in solid form.

St. Jonsfjorden is located in western Spitsbergen and opens into Forlandsundet, the sound that separates Spitsbergen from Prins Karls Forland (Fig. 1B, C). St. Jonsfjorden is 23 km long and ranges from 2 to 5 km in width (Fig. 1C). Nineteen glaciers drain into the fjord and at present three of them have marine termini, while in 1936 a total of five were marine terminating. The largest of the glaciers found at the head of the fjord is Osbornebreen with an ice front that is >2 km wide (Fig. 1C). Mountain peaks in the region range between 500–600 m a.s.l. in the outer fjord and up to 700–900 m a.s.l. in the inner fjord. The depth of the fjord basin is generally <100 m but exceeds 130 m in some areas in the outer part of the basin. The bedrock is diverse and ranges from Precambrian–Neoproterozoic marble, phyllite, quartzite and carbon-

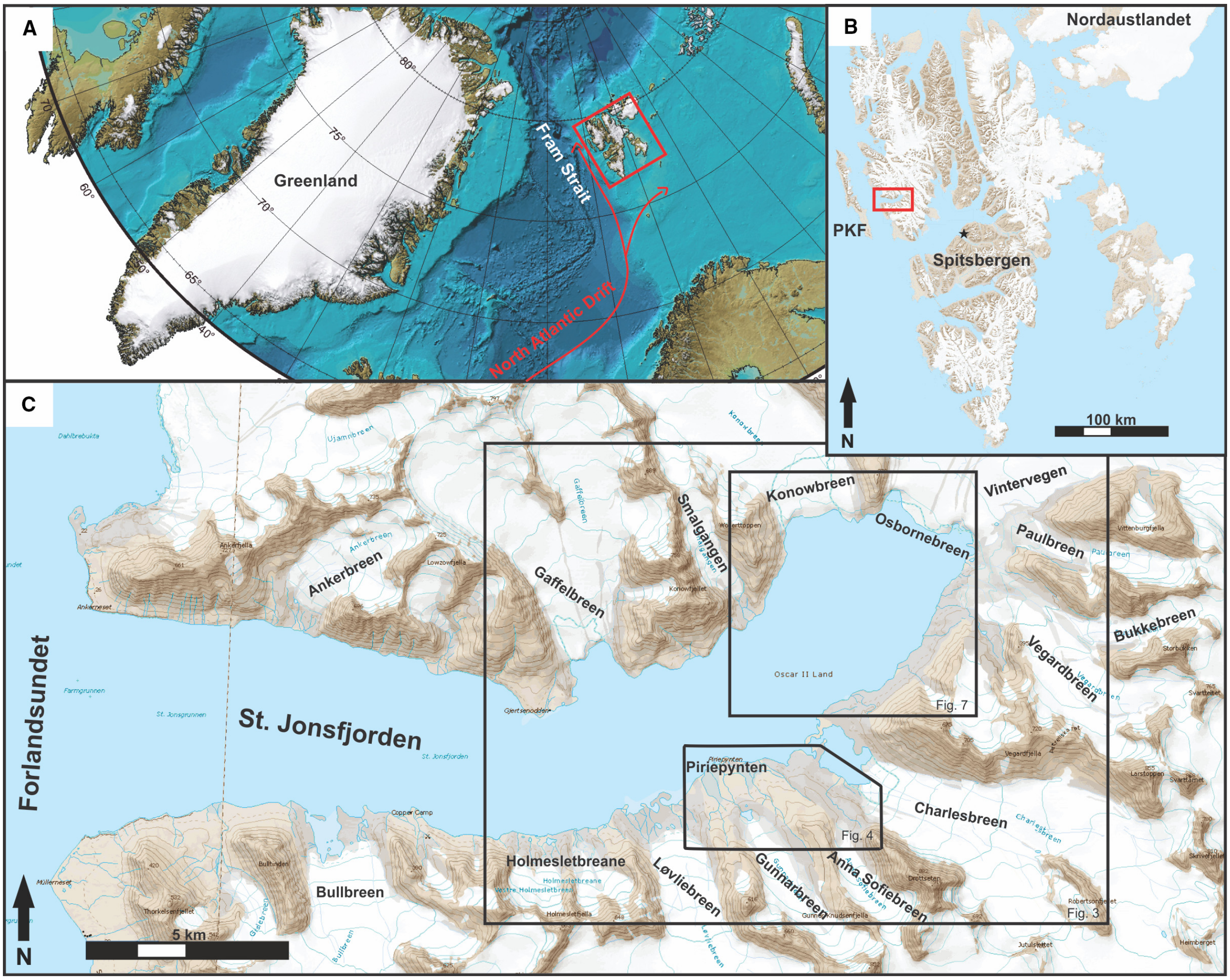

Fig. 1. A. Map of North Atlantic with Svalbard boxed in red (base map modified from www.ngdc.noaa). B. Regional topographical map of Svalbard with St. Jonsfjorden boxed in red. Longyearbyen is marked by a star and major islands Prins Karls Forland (PKF), Spitsbergen and Nordaustlandet are identified. C. Topographical map of St. Jonsfjorden, with overview frames indicating mapped regions presented in this study. Major tributary glaciers are marked. Topographical maps modified from TopoSvalbard (2017) provided by the Norwegian Polar Institute (2017). [Colour figure can be viewed at www.boreas.dk]

ates, to Ordovician–Silurian sandstones and shales (Dallmann & Elvevold 2015).

St. Jonsfjorden has been visited by whalers and sealers since the early 17th century, and the first scientific exploration of the area was carried out by the Isachsen Spitsbergen Expedition of 1909–10, where the bedrock geology was surveyed and the terminal position of Osbornebreen, the main tidewater terminus, was recorded (Hoel *et al.* 1915–1917; Hoel 1929). Over the past century, a number of studies of raised marine sediments and glacial deposits in St. Jonsfjorden have highlighted past relative sea levels and the glacial history of the area (Feyling-Hanssen & Jørstad 1950; Dinely 1953; Forman 1989; Evans & Rea 2005).

Two sets of shorelines have been identified, with an older set occurring at around 60 m a.s.l. close to where the fjord opens into Forlandsundet and dating to the pre-Late Weichselian (Forman 1989). The younger set consists of Holocene shorelines, where the highest are located ~45 m a.s.l. in agreement with the Late Weichselian–early Holocene upper marine limit of the area (Forman 1989; Evans & Rea 2005). Minimum ages of the deglaciation of the outer (fjord mouth) and inner (Piriepynten) parts of St. Jonsfjorden correspond to ~12.8 and 8.6 cal. ka BP, respectively (Forman 1989; Bunin 2015). Additionally, a Neoglacial maximum advance has been constrained by a shell-rich, coast-parallel, moraine with a maximum constraining age of 0.52±0.07 cal. BP (Evans & Rea 2005; Fig. 2).

Methods and data acquisition

Fieldwork and mollusc shell sampling were conducted in July 2013, 2014, and 2015, with focus on geomorpho-

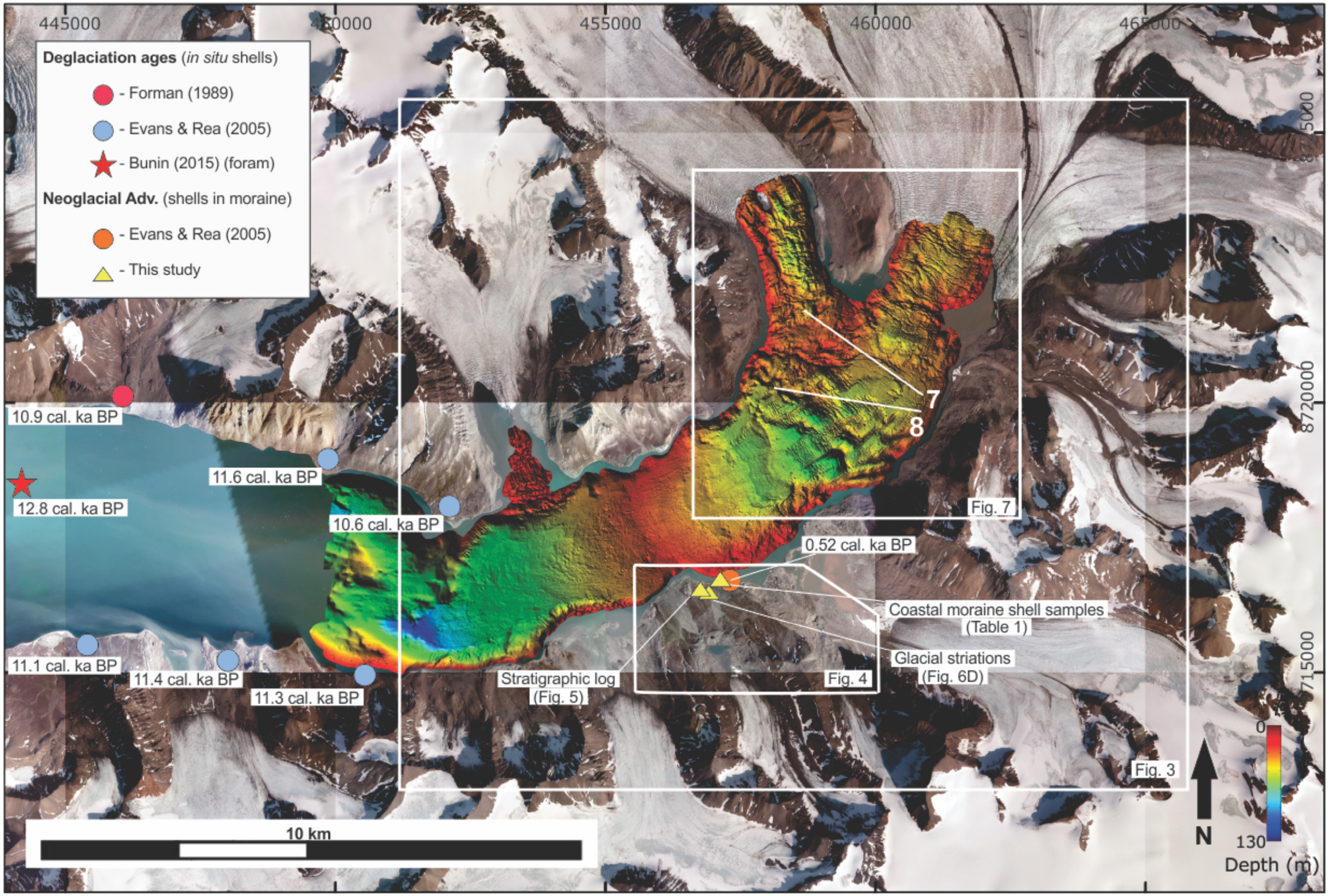

Fig. 2. Overview aerial orthophotograph mosaic and fjord bathymetric data used to map inner St. Jonsfjorden. The 2009 aerial images have a 0.5-m resolution while the marine bathymetry data were gridded with isometric grid cell size of 2 m. Locations of referenced dates from previous studies have been recalibrated and indicated. Subbottom profiles are indicated by white lines 7 and 8 in the inner fjord, and are presented in Fig. 7. Coordinates are shown in metres, UTM zone 33N, WGS84. [Colour figure can be viewed at www.boreas.dk]

Table 1. List of radiocarbon dates from this study and others cited herein (all dates corrected for reservoir age −440 years).

Lab no.	Age (^{14}C a BP)	Material	Sediments	Location	Elevation (m a.s.l.)	Lat./Long.	δ^{13}C corr. (‰)	Age (cal. a BP; median)	Age (cal. a BP; 1σ)	Source (sample date)
LuS 10790	1800±50	*M. calcarea*	Thrusted silts	Piriepynten	10	78'30"55N/13'04"13E		1286±46	1355–1181	This study (2013)
LuS 10791	1285±45	*A. montagui*	Thrusted silts	Piriepynten	8.5	78'30"57N/13'04"17E		758±57	831–680	This study (2013)
LuS 10792	5230±50	*Lithothamnion*	Thrusted silts	Piriepynten	8	78'30"55N/13'04"18E		5517±68	5608–5449	This study (2013)
LuS 10793	1615±60	*M. calcarea*	Thrusted silts	Piriepynten	10	78'30"56N/13'04"13E		1103±76	1190–964	This study (2013)
LuS 10794	4690±50	*C. islandica*	Thrusted silts	Piriepynten	10	78'30"54N/13'04"54E		4820±82	4892–4784	This study (2013)
LuS 10795	9320±60	*M. modiolus*	Sand + gravel	Piriepynten	6	78'30"41N/13'03"30E		10 004±122	10 109–9761	This study (2013)
LuS 10796	9070±55	*M. truncata*	Sand + gravel	Piriepynten	6	78'30"41N/13'03"30E		9596±60	9736–9518	This study (2013)
Ua-52524	9241±31	*M. modiolus*	Sand + gravel	Piriepynten	5.5	78'30"48N/13'03"07E	0.1	9824±92	9928–9688	This study (2015)
Ua-52525	9189±38	*M. truncata*	Sand + gravel	Piriepynten	5.25	78'30"48N/13'03"07E	1.2	9730±89	9900–9595	This study (2015)
DIC 3056	8690±85	*M. truncata*	Sub-lit. Sand	Løvliebreen	3.5		0	9231±117	9437–9021	Forman (1989)
DIC 3055	9960±90	*M. truncata*	Sub-lit. Sand	Ankerbreen	13.5		0	10 859±160	11 149–10 581	Forman (1989)
GU 8069	920±60	*M. truncata*	Thrusted silts	Piriepynten	21		1.6	518±65	567–428	Evans & Rea (2005)
GU 8070	9840±70	*M. truncata*	Gravel bench	Gjertsenodden	19.5		2.2	10 632±123	10 794–10 413	Evans & Rea (2005)
GU 8072	10 130±90	*M. truncata*	Foreset sands	Bullbreen	15.5		1.6	11 052±147	11 243–10 760	Evans & Rea (2005)
GU 8073	10 480±90	*M. truncata*	Marine silts	Gjertsenodden	13		2	11 570±185	11 841–11 256	Evans & Rea (2005)
GU 8074	10 350±80	*M. truncata*	Diamict	Bullbreen	12		2.2	11 360±139	11 643–11 197	Evans & Rea (2005)
GU 8075	10 270±80	*M. truncata*	Diamict surface	Copper camp (E)	19		2	11 251±121	11 502–11 094	Evans & Rea (2005)
HH12.956	11 345±102	*N. labradorica*	Marine muds	Outer Fjord	−111	78'31"79N/12'27"08E		12 805±95	13 029–12 678	Bunin (2015)

logical and sedimentological mapping, as well as lithostratigraphical logging in the Piriepynten area (Figs 1, 2). Sea-floor data were collected in June 2013 (Fig. 2). Bathymetric data were collected on board UNIS R/V 'Viking Explorer' with a Kongsberg EM2040 multibeam echosounder. Sea-floor sediment surface and subbottom acoustic sediment structures were studied with the Edgetech 2000 CSS combined side-scan sonar and subbottom profiler systems. The bathymetric data cover the entire St. Jonsfjorden up to the Osbornebreen and Konowbreen ice fronts.

Nine samples of subfossil marine shells were selected from the southern flank of the inner fjord near Piriepynten for radiocarbon dating, to constrain ages of glacial and marine events (Table 1). The samples were cleaned, weighed, photographed and subsequently sent for dating at the Radiocarbon Dating Laboratory at Lund University and to the Ångström Laboratory at Uppsala University. Ages are presented in calibrated kiloyears before present (OxCal v4.2; Reimer *et al.* 2013). Samples were corrected for the marine reservoir age with −440 years (according to Mangerud & Gulliksen 1975; Mangerud *et al.* 2006). Metadata are presented in accordance with Hughes *et al.* (2016). The Quaternary geological maps were created in ArcMap 10.3 and the QPS Fledermaus Software package based on aerial orthoimagery from 2009 (Norwegian Polar Institute) and high-resolution sea-floor data from 2013 (UNIS; Fig. 2). Previous studies and radiocarbon dates from the area presented by Forman (1989), Evans & Rea (2005) and Bunin (2015) are referenced to best constrain the glacial history of the fjord (Fig. 2).

Results

Terrestrial deposits, landforms and features

We present a Quaternary geological map where the terrestrial landscape and sea floor of inner St. Jonsfjorden have been portrayed (Fig. 3). The map highlights the dominant components of the terrestrial landscape in the region: glacial, fluvial and periglacial deposits and landforms (Fig. 3). Glaciers cover approximately one-third of the mapped region and their catchments are controlled by topography. Ridgelines of *in situ* weathered bedrock and alpine terrain with shallow slope deposits divide the glacier systems. This terrain characterizes most of the higher elevations. The lower elevations are predominantly glacial deposits and glacifluvial fan sediments (where glaciers are land-terminating), and the flat-lying inter-catchment areas are dominated by solifluction material.

Glacial sediments. – The most prominent deposits present in inner St. Jonsfjorden are Neoglacial glacial sediments. The glacial deposits are often confined to cirques, valleys and embayments, separated by ridges

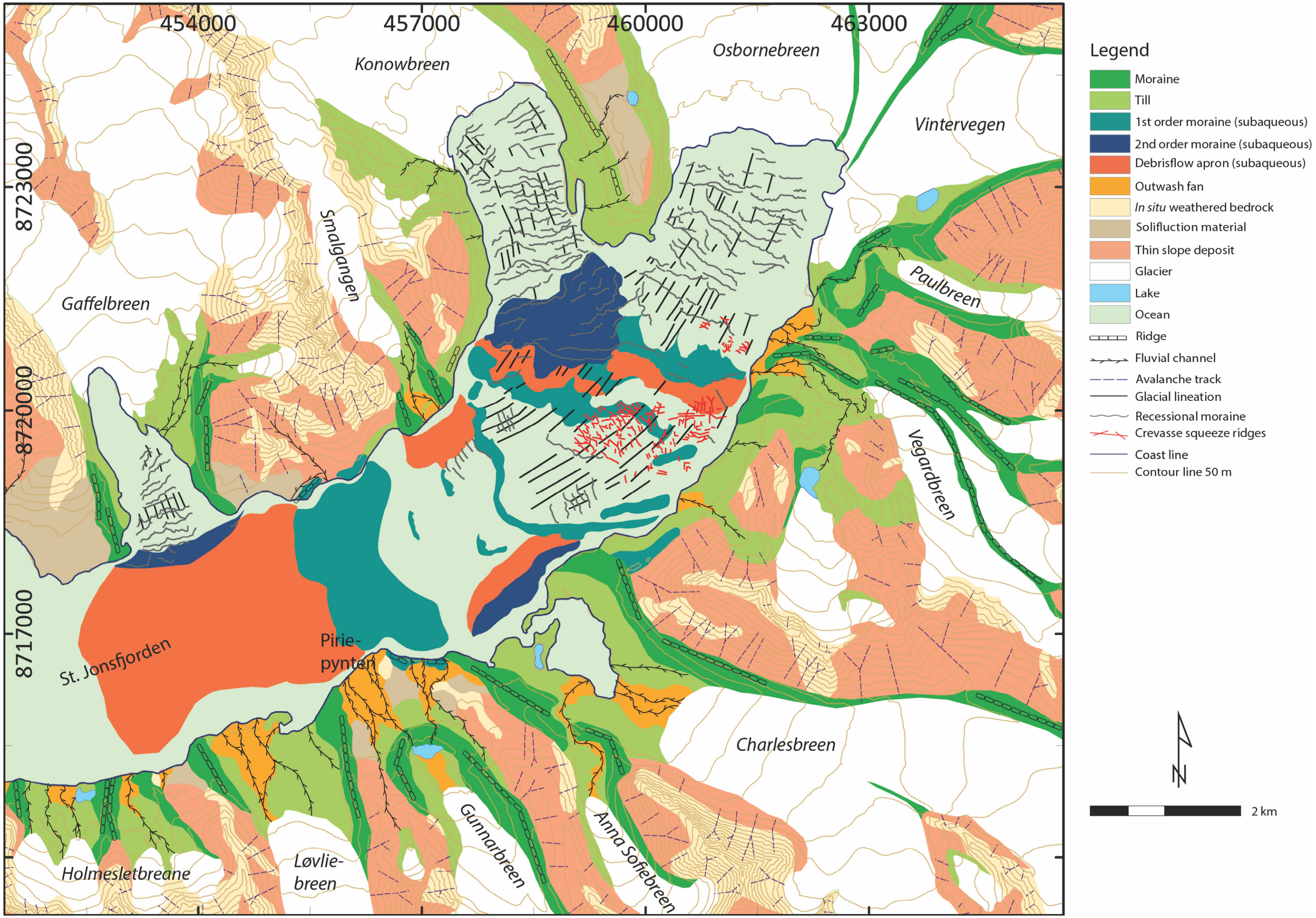

Fig. 3. Overview Quaternary geological map of inner St. Jonsfjorden. Cross-cutting glacial deposits record a complex and dynamic history. Coordinates are shown in metres, UTM zone 33N, WGS84. [Colour figure can be viewed at www.boreas.dk]

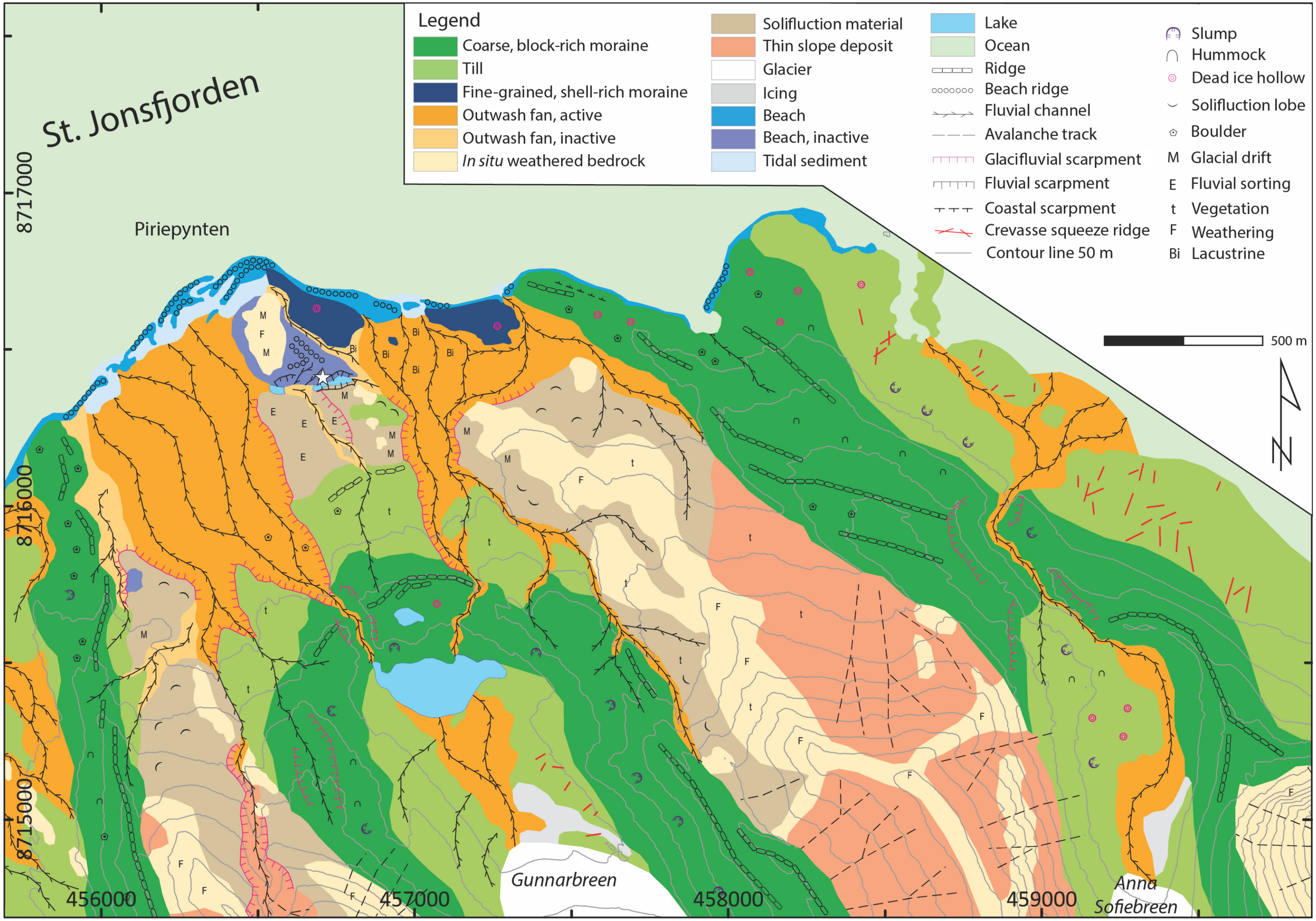

Fig. 4. Detailed Quaternary geological map of Piriepynten, inner St. Jonsfjorden. Thermophilous molluscs identified in early Holocene beach sediments just to the south of Piriepynten (white star). Coordinates are shown in metres, UTM zone 33N, WGS84. [Colour figure can be viewed at www.boreas.dk]

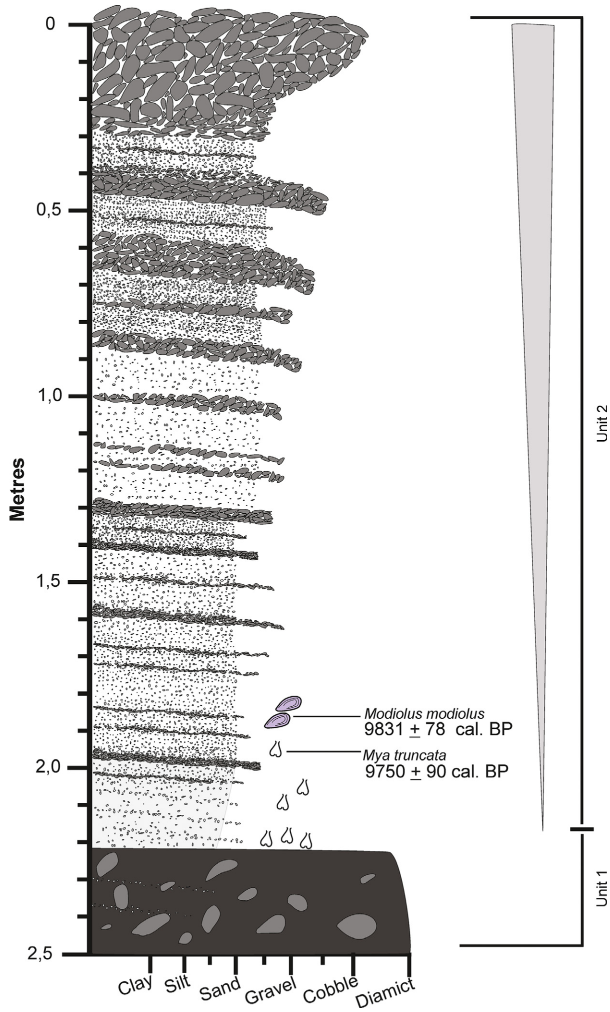

Fig. 5. Lithostratigraphical log of early Holocene sediments exposed near Piriepynten, St. Jonsfjorden. Coarsening upwards sequence overlying silty matrix-supported diamict. Calibrated radiocarbon dated samples indicated with ages given in years BP. [Colour figure can be viewed at www.boreas.dk]

and alpine terrain. An extensive but subtler glacial deposit is visible along the flanks of the inner fjord starting at Piriepynten and tracing back to the modern-day ice fronts of Konowbreen and Osbornbreen. Here, we introduce and describe this deposit, but the composition and age will be presented in the section *Coastal moraine*. The glacial deposit is situated along the coast at the northernmost point of Piriepynten and a submarine ridge can be traced on the bathymetrical data set across the fjord linking to similar sediments on the northern side of the fjord. This is a deposit of low-crested glacial sediments that flanks the coast. The sediments outline a glacial system composed of the considerably expanded marine terminating glaciers Konowbreen and Osbornebreen (Fig. 3).

The fjord-parallel till drape of the expanded Konowbreen and Osbornebreen has been cross-cut by the smaller tributary valley and cirque glaciers inside of Piriepynten. The subsequent advance of a tributary glacier is perceptible at the snout of Smalgangen on the northern side of St. Jonsfjorden where local glacial deposits cross the low-elevation, fjord-parallel till drape (Fig. 3). The subsequent advance of a tributary glacier is also visible where the ice-marginal deposits of Charlesbreen cut through coast-parallel glacial deposits (Fig. 3). The western contact can also be seen in detail as the cross-cutting relationship between an extended Osbornebreen and a subsequent extension of Charlesbreen (Fig. 4). A glacier advance subsequent to the maximum extension of Charlesbreen is indicated, where the cirque glacier Anna Sofiabreen seems to have advanced into and deformed Charlesbreen lateral moraine.

The glacial sediments and their characteristics can be better visualized in the detailed Quaternary geological map from the Piriepynten area where glacial deposits originate from five different glaciers (Løvliebreen, Gunnarbreen, Anna Sofiebreen, Charlesbreen and Osbornebreen; Fig. 4). Some glacial deposits are sparsely vegetated and appear relatively stable, while other deposits exhibit widespread slumping, fluvial-erosional cutting and dead-ice melt-out, making them unfavourable for vegetation growth (Fig. 4).

Lake sediments. – Lake sediments have been identified and mapped on the eastern glacifluvial fan system flowing from Gunnarbreen (Fig. 4). These silty lake deposits are partially preserved between fluvial channels on the western flank of the fan system where the braided river system is less active today. The lacustrine sediments are located on the south side of the glacial deposits flanking the coast. Deposits are estimated to reach decimetre thickness and are not widespread.

Raised marine sediments. – Raised marine deposits are highlighted in the detailed map of Piriepynten (Fig. 4). These sediments are not common in the inner St. Jonsfjorden area and the highest marine deposits found in the area are located just to the west of the Løvliebreen marginal moraine at ~20 m a.s.l. (Fig. 4). The upper Holocene marine limit is believed to be ~45 m a.s.l. in the outer fjord and as low as 30 m near Løvilebreen (Forman 1989; Evans & Rea 2005). No marine deposits or features above 20 m elevation were identified in the Piriepynten area. The most prominent deposit of marine sediments is preserved south of the bedrock knob at Piriepynten. The raised beach deposits have minor vegetation cover and consist of sandy gravels and cobbles predominantly disc or plate formed with subrounded to subangular morphology. Several sets of raised beach ridges are preserved on the surface of the marine sediments. The uppermost beach ridges are vegetated and display polygonal structures with sorted and unsorted patterned ground caused by periglacial sorting at the surface. The upper terrace of

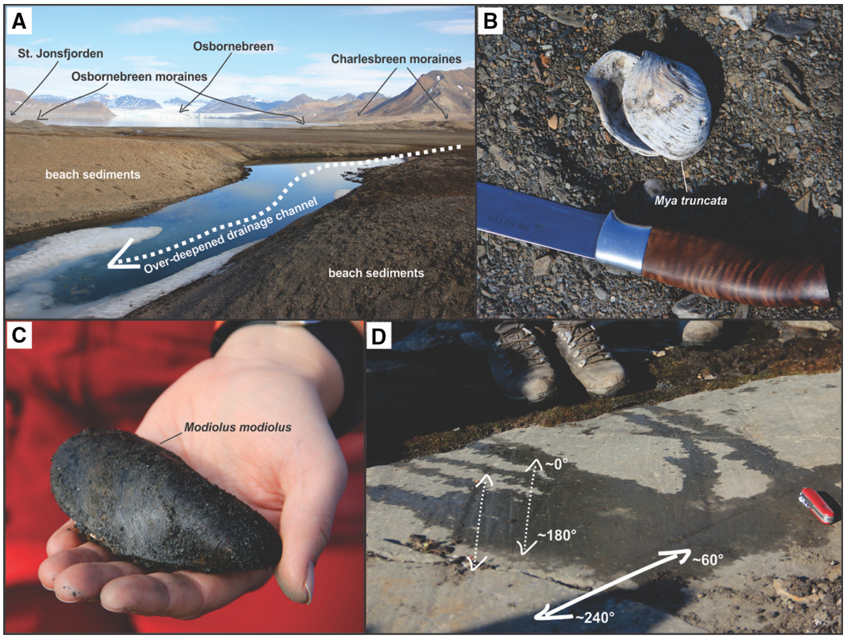

Fig. 6. A. Beach sediments at Piriepynten with view towards Osbornebreen to the NE. The over-deepened drainage channel cuts the early Holocene beach sediments with the spillway to the bottom-left of the image. Moraine systems marked in background. B, C. Mollusc shells picked from the stratigraphical section in the beach sediments, paired *in situ Mya truncata* and *Modiolus modiolus*, respectively. D. Bedrock exposure with cross-cutting striae. Finer, widespread striae with near north–south orientation, characterized as local flow. Larger, less prevalent striae with east–northeast to west–southwest orientation, regarded as regional, fjord-parallel flow. [Colour figure can be viewed at www.boreas.dk]

this deposit is ~8 m a.s.l. and forms the natural exposure on the southern half of the sediments, which are estimated to be at least 5 m thick. The upper 2.5 m of the section is characterized as a coarsening upward sequence that has been divided into two main units (Fig. 5).

- Unit 1: in the lowermost part there is more than 30 cm of massive, silty-sandy, matrix-supported diamict with outsized pebbles and cobbles frequent in its lower part. Based on the sediment composition we interpret this as a morainal bank sediment (Powell & Domack 1995), deposited at shallow depth in front of a retreating ice front.
- Unit 2: bove Unit 1 is 2.2 m of stratified sorted sediments that coarsen upwards. In the lower part the unit consists of a silty sand sequence with crude beds of sand and *in situ Mya truncata* shells (Fig. 5), which conforms to planar-bedded (cm scale) silty to gravelly sands. Several half bivalve *Modiolus modiolus* shells and fragments of blue shell (*Mytilus edulis*) were identified (Fig. 5). These shells were not in living position but do not show signs of long transport. The unit coarsens upwards to cobbles and gravels. In some beds there is silt and sand, while in other coarser beds, fine-grained sediments are scarce. The top 0.25 m is clast-supported coarse sand, gravel, and cobble with imbrication structures. The clasts are plate formed with subrounded to subangular morphology. Based on the sediment composition we interpret this as a regressional sublittoral sequence, capped by beach sediments.

Numerous shells were sampled and identified in the section, and two shells have been dated (Fig. 5). The lowermost *M. modiolus* shell and the paired *in situ M. truncata* are dated to 9.82±0.09 and 9.73±0.09 cal. ka BP, respectively (Fig. 5; Table 1). Although the lower shell (*M. truncata*) gives a slightly older age, the dates overlap and the *M. truncata* could have burrowed beneath the *M. modiolus*. These ages correspond well with a *Modiolus modiolus*, which was sampled at the foot of the natural section in 2013, dating to 10.0±0.12 cal. ka BP (Table 1). This provides the earliest shell age effectively constraining the minimum age of deglaciation of inner St. Jonsfjorden (Table 1; Sample LuS-10795) as well as constraining the timing of relative sea level at ~8 m a.s.l.

Coastal moraine. – To the east of Piriepynten, a low-crested moraine was identified (Fig. 4). The landform has little to no vegetation or lichens and generally lacks cobbles and larger clasts on its surface. The surface is dominated by dark clayey-silt with abundant mollusc shells. A light coloured precipitate was visible on some of the desiccated mud-cracked surfaces. In a natural coastal section, the silty sediments overlie crudely stratified sorted sands and gravels with occasional cobbles intermixed. A compact matrix-supported silty diamict with stratified sands and gravels overlies the sorted sands and gravels. The sediments fine upwards into a shell-rich silty clay that is visible on the surface. We interpret this as

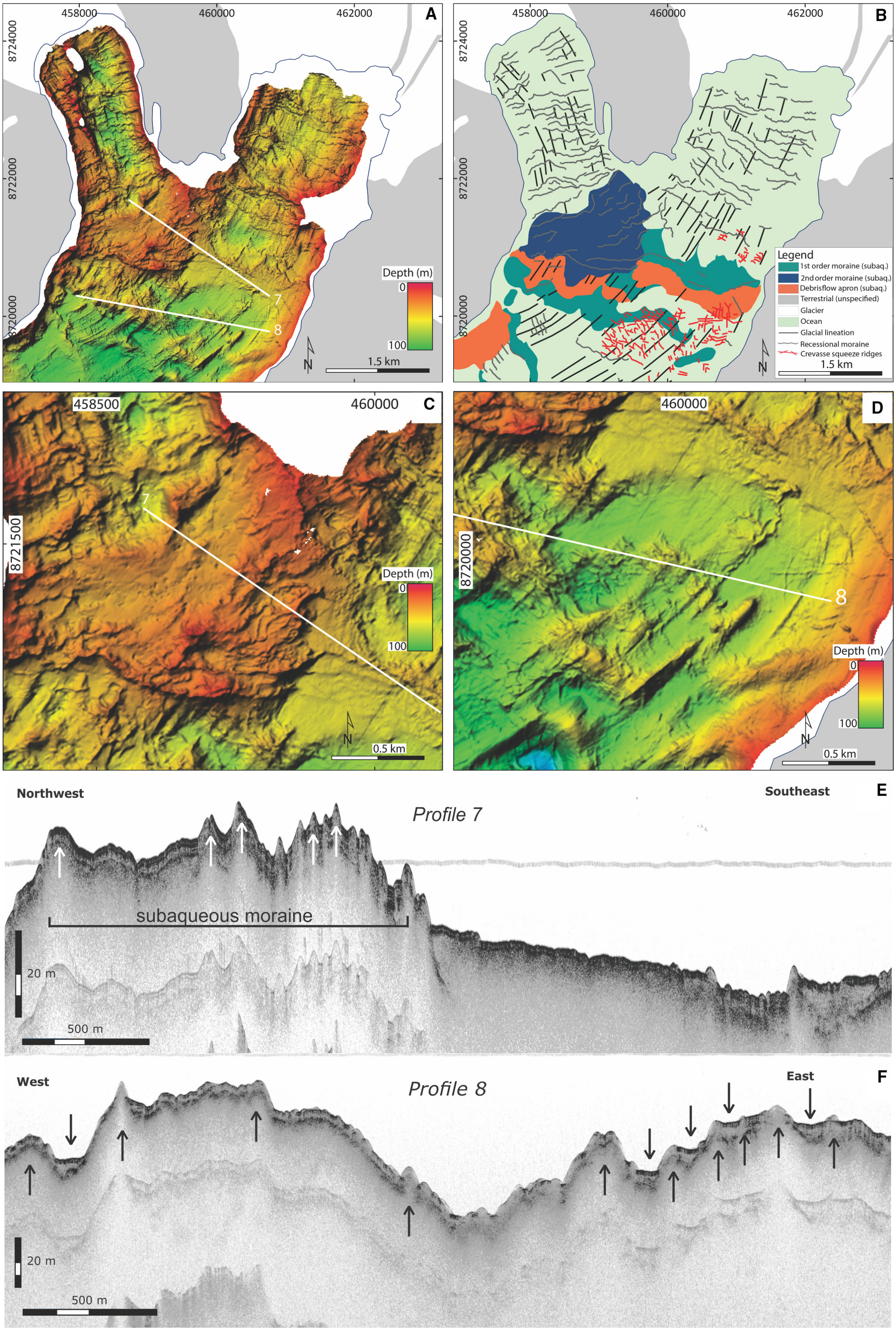
A
458000
460000
462000
8724000
8722000
8720000
7
8
Depth (m)
0
100
1.5 km
B
Legend
1st order moraine (subaq.)
2nd order moraine (subaq.)
Debrisflow apron (subaq.)
Terrestrial (unspecified)
Glacier
Ocean
Glacial lineation
Recessional moraine
Crevasse squeeze ridges
1.5 km
C
458500
460000
8721500
0.5 km
D
8720000
E
Northwest
Southeast
Profile 7
subaqueous moraine
20 m
500 m
F
West
East
Profile 8

Fig. 7. Bathymetry data and subbottom profiles (SBFs) of inner St. Jonsfjorden. A. Bathymetry data of inner St. Jonsfjorden with SBFs 7 and 8 indicated by white lines. B. Detailed Quaternary geological map of the sea floor in inner St. Jonsfjorden. C, D. Zoom in on the bathymetry of the inner fjord, with clear examples of cross-cutting glacial landforms and deposits. E. A modified SBF across the 2nd order moraine (blue colour, Fig. 7B), oblique to the streamlined features and recessional moraines (upward, white arrows). F. A SBF distal to the 2nd order moraine, showing streamlined landforms and crevasse squeeze ridges (both marked by upward, black arrows) with infill and drape of/by acoustically stratified sediment (marked by downward, black arrows). Coordinates are shown in metres, UTM zone 33N, WGS84. [Colour figure can be viewed at www.boreas.dk]

marine sediments that have been pushed up onto the beach by an advancing glacier.

Shells of numerous species were sampled and identified from the silty sediments including *Macoma calcarea*, *Astarte montagui*, *Lithothamnion* sp., *Chlamys islandica* and *Mya truncata*. Six samples were dated to constrain the age of the moraine. The youngest age from the moraine is 0.76±0.06 cal. ka BP, suggesting that the feature was deposited sometime after 1200 CE (Table 1; Sample LuS-10791). The five other shell dates from the coastal moraine range from 9.6±0.06 to 1.1±0.08 cal. ka BP suggesting conditions in the inner fjord must have been sufficiently free of ice to allow these molluscs to exist (Table 1).

Crevasse-squeeze ridges. – Fragmented networks of crevasse-squeeze ridges (CSRs) have been identified and mapped in the foreland of Gunnarbreen and Charlesbreen (Fig. 4). The CSRs are only present proximal to the wide marginal moraines (Fig. 4). The landforms have low preservation potential and are often reworked by meltwater and dead-ice melt (Lovell *et al.* 2015b). The ridges consist of matrix-supported diamict sediments and are often preserved in geometric networks located on raised till plains protected from meltwater erosion (Schomacker *et al.* 2014). The landforms are also present in front of Løvliebreen and numerous other glaciers located in St. Jonsfjorden although not shown in Fig. 3 (Farnsworth *et al.* 2016).

Drainage channels. – Several small drainage channels cut through the southern part of the raised marine sediments. The channels run to the southwest and initiate at the crest of the beach ridges around 8 m a.s.l. (Figs 4, 6A). The channels cut down nearly 2 m and at the floor of the channels, outsized, striated clasts along with shells (*Mya truncata*) have accumulated. We refer to these features as the initiation drainage channels (Fig. 6B).

The small channels are cut by a large relict drainage channel that runs approximately east to west. This channel is presently comprised of two small elongated ponds that have been divided by subsequent glacifluvial sedimentation from Gunnarbreen (Figs 4, 6A). This east–west trending channel has cut through the marine sediments and has over-deepened and formed the present-day basins. The channel is roughly 250 m long from east to west, up to 7 m deep and nearly 10 m wide. The surface level of the water in the basins was calculated to be ~3 m a.s.l. and the water is up to ~2 m deep in the large pool (Fig. 6A). Striated boulders of 50–100 cm in size are also present in the over-deepened channel. The natural section on the northern flank of this channel is

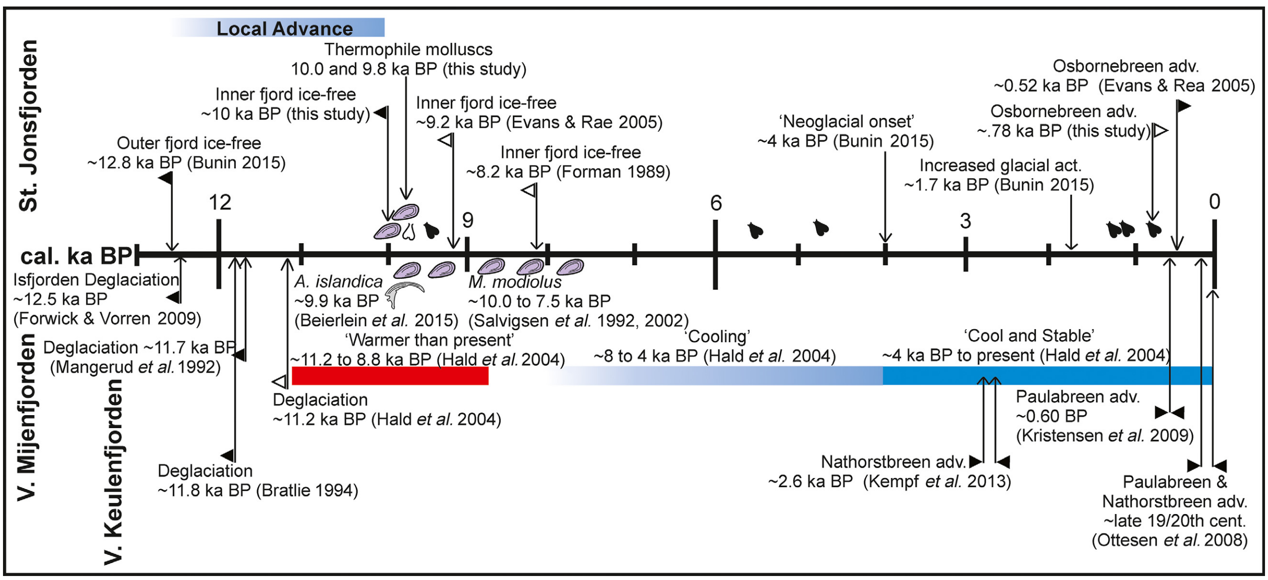

Fig. 8. Timeline of the Holocene glacial histories from fjords on the west coast of Spitsbergen. Ages are presented in calibrated kiloyears (ka) BP and corrected for marine reservoir age. St. Jonsfjorden ^{14}C ages and results are presented above the timeline, while Isfjorden, Van Mijenfjorden and Van Keulenfjorden are presented below. Dark arrowheads constrain events, while hollowed arrowheads present ages that once were constraining. Shaded *Modiolus modiolus* and white bivalve symbols represent dated samples from the St. Jonsfjorden section (Fig. 5B, C). Black bivalve symbols indicate dated shells, sampled from the coastal moraine ridge.[Colour figure can be viewed at www.boreas.dk]

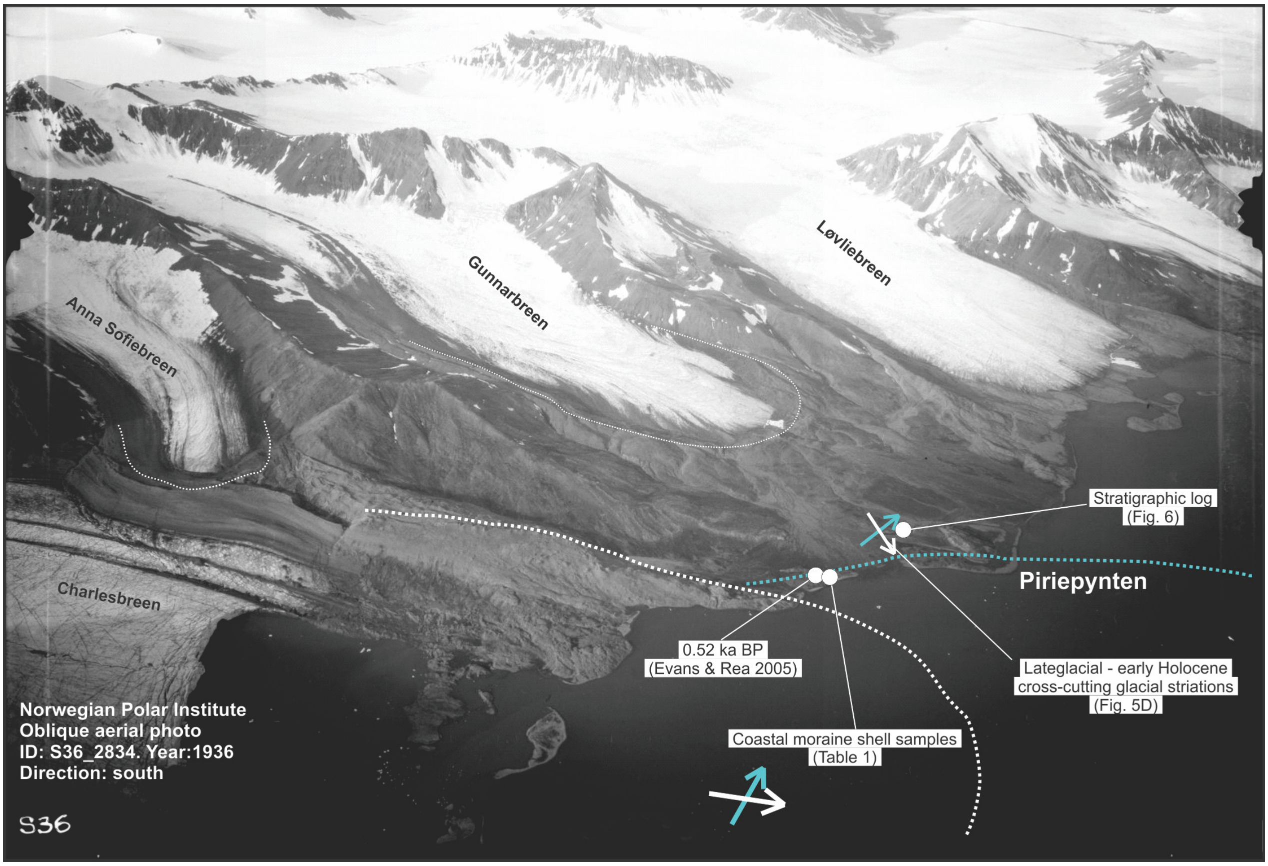

Fig. 9. Oblique aerial photograph modified from the Norwegian Polar Institute looking south onto Piriepynten taken in 1936. Site locations identified as well as rough outlines of LIA maximum positions for Gunnarbreen, Anna Sofiabreen and Charlesbreen marked by white dotted lines. Green dotted line marks the extent of the Piriepynten moraine (coastal moraine) sometime in the last 500 years. Arrows represent cross-cutting relationships between Charlesbreen and Konowbreen-Osbornbreen sometime during the last 500 years as well as Gunnarbreen and the main fjord outlet glacier during the early Holocene. Note that Gunnarbreen was at least 750 m more extended during the early Holocene and terminated into the fjord system. [Colour figure can be viewed at www.boreas.dk]

where the *M. modiolus* molluscs were sampled (Fig. 6C). We refer to this as the over-deepened drainage channel or main spillway.

A final northern, significantly smaller drainage channel is also present. This drainage channel flows to the northwest and runs between the Piriepynten bedrock knob and the coast-parallel moraines just north of the raised marine terraces. Although similar in length, this drainage incision is ~2–3 m deep (Fig. 4). We refer to this as the second spillway.

Glacial striations. – A bedrock exposure to the south of the over-deepened channel displays cross-cutting glacial striations (Fig. 6D). One set of striae is orientated approximately east-northeast to west-southwest (~60–240°). The striations are coarse and weathered. The other set of striae runs nearly north to south (~0–180°). These striae are more widespread, rough and thinner than the first set. They are present on bedrock convexities and prominences, while the fjord-parallel striations are present in the concavities (Fig. 6D).

Fjord bathymetry and submarine geomorphology

The bathymetric data of St. Jonsfjorden reveal bedrock structures and sediment basins as well as glacial landforms (Figs 2, 3). In the overview map of the inner fjord, the most prominent feature is a 3-km-wide north–south trending shallow sill initiating from Piriepynten. We focus mainly on the glacial landforms preserved in the inner fjord to the northeast of this sill. Parts of the inner basin reach nearly 150 m below sea level.

Moraines. – From the bathymetric data set, numerous large lobate ridges have been identified on the sea floor. The landforms are arcuate ridges spanning 1 to 2 km in length and 0.5 to 1.5 km in width with prominence ~25 m. This type of ridge occurs distal to the present front of Gaffelbreen, Konowbreen and Charlesbreen and the shape and orientation reflect the present-day glacier fronts (mapped as 2nd order moraines; Fig. 3). A significantly larger lobate ridge occurs in the middle of fjord, trending north–south corresponding with the location of the prominent sill north of Piriepynten (1st order moraine). The ridge is over 2 km long and roughly 1.5 km wide. The crest of the ridge is prominent and rises up from basins >70 m to roughly 30 m below sea surface. The smaller ridges (2nd order moraines), based on their proximity to the glaciers, shape and relief, are interpreted as terminal moraines that originate from Gaffelbreen, Konowbreen and Charlesbreen. The largest lobate ridge is interpreted as a terminal moraine deposited from a larger confluent Konowbreen-Osbornebreen. We refer to this ridge as the Piriepynten (1st order) moraine. Based on the spatial occurrence of these landforms, we suggest the Charlesbreen and Konowbreen (2nd order) moraines formed subsequent to the larger Piriepynten moraine. We are unable to constrain the age of the Gaffelbreen moraine relative to the constrained Piriepynten moraine.

Debrisflow aprons. – Aprons of debrisflow deposits are observed on the sea floor distal to the large moraines. The largest apron is located on the distal side of the large Piriepynten moraine extending ~3 km from the moraine crest and filling the width of the fjord basin (>2 km).The surfaces of the aprons are non-uniform, which is probably caused by the irregular distribution of iceberg scours, slumps and slides on the surface. The shape and irregular surface leads to an interpretation of the deposit as an accumulation of debrisflow lobes forming an apron of sediments. Similar submarine massflow deposits have been described from surge-type glaciers in Svalbard (Ottesen *et al.* 2008; Flink *et al.* 2015).

Streamlined features. – Widespread streamlined features have been mapped in inner St. Jonsfjorden and are interpreted as glacial lineations (Ely *et al.* 2016). They appear in subparallel swarms and are most prominent between the Piriepynten moraine and the present-day ice front of the marine terminating glaciers Konowbreen and Osbornebreen (Fig. 3). The streamlined feature orientations vary from north–south to nearly east–west, depending on the alignment of the fjord basin (Figs 3, 7A, B). Mapped lineations in some places extend over a kilometre in length and mostly exceed 5 m relief, ranging 1–15 m in height (Fig. 7). The features are roughly 10 m wide and spacing between crests ranges from 50 to 500 m (averaging ~200 m). Some of the streamlined features are overlain by minor moraines located at the western branch of the inner fjord (Fig. 7B–D).

Transverse ridges. – Ridge segments transverse to glacier flow are present throughout inner St. Jonsfjorden (Fig. 7A, B, C, E). The ridges are up to 1.5 km in length and of relatively low relief (~5 m). The ridges are located sporadically throughout the inner fjord and are common and frequently spaced in the inner-most embayments corresponding to Osbornebreen and Konowbreen. Inter-ridge spacing ranges from 50 to 400 m with typical distances from crest to crest of ~150 m (Fig. 7A, B). The ridges are less linear than the glacial lineations and other streamlined features and can be found overprinting these features. Ridges of similar appearance, morphology and spacing have been identified in other Svalbard fjords and have been interpreted as retreat moraines (Flink *et al.* 2015, 2017).

Crevasse-squeeze ridges. – A geometric ridge network has been mapped and interpreted as crevasse-squeeze ridges in inner St. Jonsfjorden (Lovell *et al.* 2015b; Figs 3, 7). The rhombohedral structures are present on a flat basin along with streamlined glacial features (Fig. 7D). This ridge network is predominantly oblique to the streamlined features. The crevasse-squeeze ridges are low-relief features (<5 m). The eastern part of subbottom profile eight crosses over the network of ridges (Fig. 7D, F). The profile shows numerous parabolas interpreted to be ridges orientated obliquely or perpendicular to the profile. In some inter-ridge areas several metres of sediment seem to have accumulated based on the flat-lying, horizontal strata between topographical features (parabolas; Fig. 7). This suggests that the landforms have been draped by and in some cases masked completely by marine sediments subsequent to their formation.

Discussion

St. Jonsfjorden deglaciation, Atlantic water and late Holocene glacial history

The outer parts of the major fjords on the central west coast of Spitsbergen were deglaciated at a similar period in time between 12.5 and 11.7 cal. ka BP (Fig. 8; Mangerud *et al.* 1992; Forwick & Vorren 2009; Kempf *et al.* 2013; Bunin 2015). Although the exact age of deglaciation is unknown, the minimum constraining deglaciation age for the outer St. Jonsfjorden is 12.8±0.10 cal. ka BP (Bunin 2015). This compares well with the range of the earliest dates of foraminifera and shells collected from the mouths of Isfjorden, Northern Bellsund, Van Mijenfjorden and Van Keulenfjorden dating to ~12.5, 12.7, 11.7 and 11.8 cal. ka BP, respectively (Landvik & Salvigsen 1987; Mangerud *et al.* 1992; Bratlie 1994; Forwick & Vorren 2009). Prominent bedrock thresholds at the western extent of Van Mijenfjorden and Van Keulenfjorden may have contributed to a later deglaciation of these fjords (Kempf *et al.* 2013). Kongsfjorden north of St. Jonsfjorden, a large trough system without a prominent bedrock threshold at the mouth, is believed to have deglaciated between 16.6 and 14.4 cal. ka BP (Lehman & Forman 1992; Henriksen *et al.* 2014).

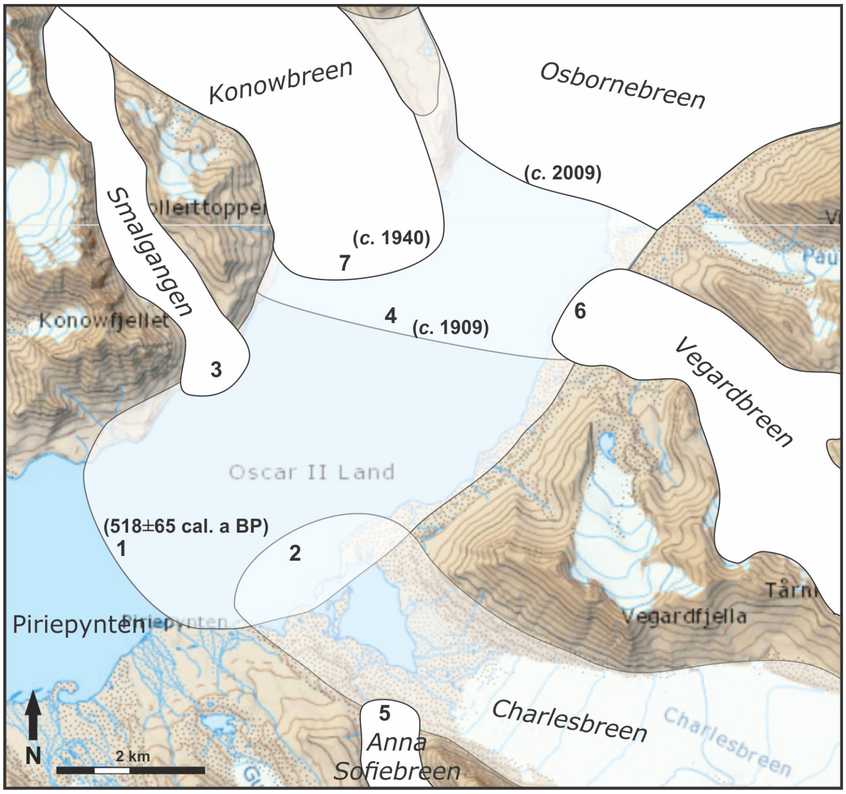

Fig. 10. Generalized map highlighting a simplified sequence of glacier front positions (1–6) in inner St. Jonsfjorden since ~500 years BP (0.52±0.07 cal. ka BP; GU 8069). Stage 7 is constrained by submarine morphology and a historical oblique aerial image from 1936 indicates a heavily crevassed Konowbreen in the early phase of a surge event (TopoSvalbard 2017). [Colour figure can be viewed at www.boreas.dk]

Cross-cutting striations on bedrock suggest a north–south orientated ice flow subsequent to fjord-parallel ice flow in St. Jonsfjorden. Stratigraphical evidence proximal to the striated bedrock suggests the north–south ice-flow phase must pre-date 9.8 cal. ka BP (Fig. 6). At some point between the deglaciation of outer St. Jonsfjorden (12.8±0.10 cal. ka BP) and before the first molluscs migrate into the inner fjord system (~10.0 cal. ka BP), Gunnarbreen advanced to a more extensive position. Although the full glacier extent is unknown, the snout extended at least 750 m further than it did in 1936 (Figs 3, 6D, 8, 9).

The HTO is fingerprinted by the migration and presence of thermophilous molluscs, and warm water foraminifera to waters around Svalbard between 11.2 and 7.7 cal. ka BP (Salvigsen 2002; Hald *et al.* 2004). Many of these species only lived in the waters around Svalbard during this short-term warm period in the early Holocene (Fig. 8). At present, many of these species can be found along the coast of mainland Norway and to the east along the coast of Russia (Salvigsen 2002; Denisenko *et al.* 2007). Few *M. modiolus* shells have been identified on Svalbard and even fewer have been radiocarbon dated. In a review of thermophilous molluscs from Svalbard, Salvigsen *et al.* (1992) highlights several dated individuals from Isfjorden (Fig. 8). There is also a reference to identification of a *M. modiolus* in St. Jonsfjorden, but dating was performed on a *Mya truncata* (DIC 3056; Table 1) in the same stratigraphical position (Forman 1989; Salvigsen *et al.* 1992). These dates suggest the species inhabited the waters around Svalbard from ~10.0 to 7.4 cal. ka BP. The two new ages of *M. modiolus* from Piriepynten presented in this study corroborate well with the earlier range of ages accumulated from previous Svalbard studies (Fig. 8; Salvigsen *et al.* 1992; Hald *et al.* 2004; Beierlein *et al.* 2015).

Not only is this mollusc age interesting with regards to the early migration of the *M. modiolus* species to Svalbard, the sample also provides the constraining age for the deglaciation of the inner part of St. Jonsfjorden (Fig. 8). This suggests that relatively warm North Atlantic waters were present at or immediately after the deglaciation of the inner fjord. Studies on mollusc shell growth bands and shell microstructures suggest strong seasonality with short favourable summers and long cold winters on Svalbard (Salvigsen *et al.* 1992; Beierlein *et al.* 2015). Studies of modern processes and glacier response to increased ocean temperatures on Svalbard (Bartholomaus *et al.* 2013) indicate high sensitivity where a minor change in subsurface water temperatures

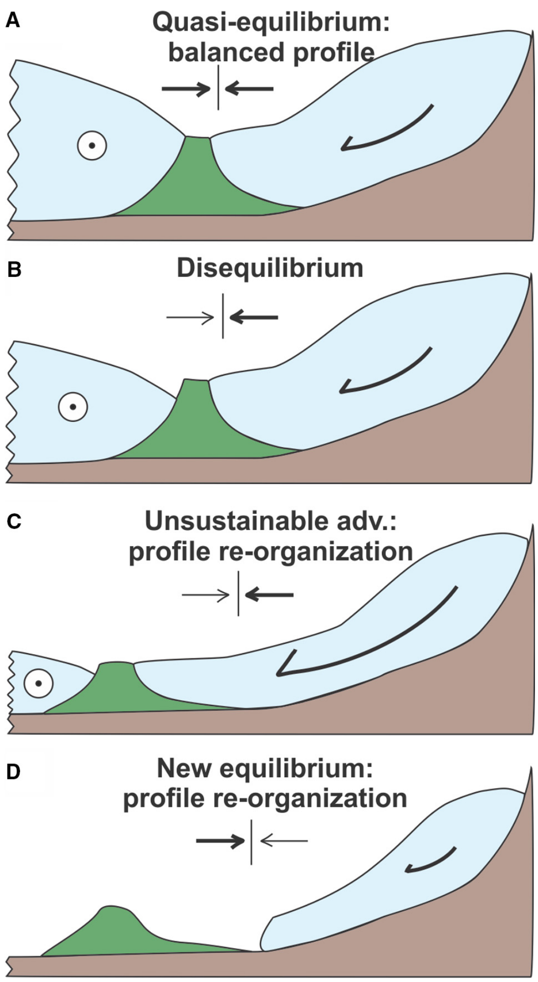

Fig. 11. Conceptual model introducing a dynamic advance resulting from unbalanced equilibrium leading to profile re-organization. A. Trunk glacier is in balance, and tributary glacier profile is in equilibrium with the back-stress of the trunk. B. The retreat of the trunk glacier creates an unbalanced system. C. Tributary glacier re-organizes its surface profile in response to the release of back-stress which results in an unsustainable advance of the ice-front (Scambos *et al.* 2004; Wuite *et al.* 2015). D. Tributary glacier retreats back to a new equilibrium state given the new conditions. Tributary pursues a new balanced profile. We choose to exclude a sea-level component from our conceptual model, yet identify the importance of further addressing this aspect. [Colour figure can be viewed at www.boreas.dk]

can have a large impact on glacier conditions (Luckman *et al.* 2015). The contemporary understanding of the modern processes and the constraining deglaciation ages provided by the *M. modiolus* shells in St. Jonsfjorden favour warm Atlantic waters as a driving factor for the deglaciation of the area.

The mid to late Holocene on Svalbard is characterized by decreasing temperatures in regional waters, which is also seen in St. Jonsfjorden (Hald *et al.* 2004; Bunin 2015). Bunin (2015) interprets cooling conditions from distal glaciomarine sediments dating ~4.0 cal. ka BP, and highlights an increase in glacial activity interpreted from the fjord sediments at ~1.7 cal. ka BP. Based on our shell dates from the coastal moraine, we suggest the inner fjord was ice-free enough to allow molluscs to exist between 10.0 and 0.76 cal. ka BP (Table 1; Fig. 8). The youngest shell date we present (0.76±0.06 cal. ka BP) corroborates with previous work that constrained the Piriepynten moraine to a late Holocene glacial advance (0.52±0.07 cal. ka BP; Evans & Rea 2005). Based on the ages of subfossil shells we suggest the Osbornbreen coastal moraine was deposited sometime in the last 500 years (Figs 8, 9; Evans & Rea 2005). In the late Holocene, numerous advances have been recorded or dated from other large glacier systems in both Van Mijenfjorden and Van Keulenfjorden (Hald *et al.* 2004; Kristensen *et al.* 2009). These events have been suggested to be related to surge-type behaviour (Ottesen *et al.* 2008; Kristensen & Benn 2012). Based on the network of crevasse-squeeze ridges identified at the sea floor in front of the Konowbreen-Osbornebreen glacier system (corresponding to the Piriepynten moraine), we suggest this advance may also be related to surge-type behaviour (Fig. 7A, B). However, we note that climatic conditions around the time of the glacier advance were also favourable for a positive glacier mass balance (Fig. 8).

A conceptual model for Neoglacial glacier dynamics in St. Jonsfjorden

By mapping the outermost extents of the larger glaciers in the inner fjord, numerous cross-cutting relationships appear (Figs 3, 9, 10). The outermost extent of Osbornebreen at Piriepynten is constrained to 0.52±0.07 cal. ka BP (GU 8069; Stage 1 in Fig. 10; Evans & Rea 2005). Subsequent advances are numbered 2–7 (Fig. 10). Stages 4 and 7 do not correspond to advances, but rather ice-front positions interpreted from the Isachsen Spitsbergen Expedition (Hoel *et al.* 1915–1917) and from bathymetry data combined with the oblique 1936 aerial imagery provided by the Norwegian Polar Institute. The innermost position of Osbornebreen indicates the glacier front position in 2009.

A conceptual model has been developed on the basis of the series of glacial advances in the inner St. Jonsfjorden (Fig. 11). The concept is that the local glaciers exhibit small advances due to unbalanced glaciodynamic conditions, and not in direct response to climate. If a tributary glacier is at equilibrium and has a stable profile given the back-stress caused by the primary trunk glacier, retreat of the trunk glacier will perturb the balance of the tributary. This leads to a re-organization of the over-steepened glacier profile, which is glaciodynamically expressed as an advance. The tributary then advances until it reaches a new dynamic equilibrium state that is marked by a new quasi-stable marginal position due to the lack of back-stress (Fig. 11; Wuite *et al.* 2015).

The re-organization of a glacier profile related to a decrease in back-stress can be a combination of the switching of thermal regime, or merely the shedding of accumulated mass that has been gained over an extended period of time. Furthermore, this behaviour is applicable at a wide range of glacier scales – from the small cirque of Anna Sofiebreen that advances into the Charlesbreen basin (Figs 4, 9), up to the size of the collapse of the Larsen B ice shelf in Antarctica and the subsequent advances of the numerous tributaries (Scambos *et al.* 2004; Wuite *et al.* 2015). Although the degree to which glaciodynamics vary between marine and terrestrial terminating glaciers with regards to back-stress is not well understood, we assume the response to be amplified in the marine environment (Nick *et al.* 2010). We choose to exclude a sea-level component from our conceptual model, yet identify the importance of further addressing this aspect.

This conceptual model provides a potential answer to the numerous descriptions of glacier advances on Svalbard that correspond to the periods of unfavourable climate conditions for glacier growth in both terrestrial and marine environments (Lønne 2005; van der Bilt *et al.* 2015). The model could as well be extended to the early Holocene advance of Gunnarbreen into a shallow marine environment subsequent to the retreat of the dominant tidewater glacier in the fjord (Fig. 9). The model also highlights how different glaciers may respond uniquely to an external force. Thus, the model steps away from the paradigm that glacier advances fit either to a phase of increased winter precipitation or reduced summer temperatures (Solomina *et al.* 2015).

It is reasonable to expect increased precipitation due to warmer sea-surface temperatures and reduced fjord cover (by sea ice or glacier), but this is not likely to drive glacier advances of that order of magnitude (Bintanja & Selten 2014). Thus, warm fjord-waters resulting in an increase in precipitation may well have occurred, but are not necessarily the sole driver of the glacier advances. Fewer assumptions are made interpreting these small advances to be dynamically driven. Additionally, the time-transgressive nature of the events suggests that the local advances are responses to glacier-specific conditions (i.e. profile re-organization) and not a regional amplification of precipitation. The principle of parsimony suggests fewer assumptions are taken for a dynamic advance as opposed to numerous climate-driven advances for each of the tributary glaciers, both marine and terrestrial, located in inner St. Jonsfjorden. The Svalbard region today is a hotspot for dynamic glacier behaviour that may not be directly in phase with atmospheric or oceanic climatic forcings (Jiskoot *et al.* 2000; Sevestre & Benn 2015). We suggest that this may be a key to the past, and the same processes were occurring at other periods during the Holocene.

Piriepynten landscape development through the Holocene

The onshore landscape and the sea-floor bathymetry of St. Jonsfjorden are dominantly fingerprinted by glaciers during the later half of the Holocene, driven by the Neoglacial – LIA glacier expansion. The widespread and prominent Neoglacial glacial deposits and the subsequent fluvial runoff greatly mask, deform and rework previous sediments, landforms and features (Landvik *et al.* 2014). In some locations early Holocene deposits and features are visible, although subtle (Lønne 2005). The older deposits are mostly visible where younger events have cut, cleared or reworked them, exposing a 'window' into the past environment. The main drainage channel that scoured from east towards west just south of the Piriepynten bedrock knob has opened the window into the early Holocene (Fig. 4).

We suggest that the glacier advance of the confluent Osbornebreen-Konowbreen that formed the Piriepynten moraine (sometime in the last 500 years) made identification of the early Holocene strata possible. Based on our interpretation of the landscape, we suggest an ice-dammed lake formed as a result of the meltwater from Gunnarbreen not being able to enter the fjord. The coastal moraine and the extended Osbornebreen, which pushed the sediments from the basin on the coast, trapped the meltwater from Gunnarbreen, which subsequently rose up to the raised marine terraces to the southeast of Piriepynten. After several small initiation drainages, the main drainage burst and drained the lake to the west around Piriepynten. Although this event has not been directly documented, an ice-marginal lake serves as a plausible explanation for the formation of the drainages through the raised marine sediments.

This channel washed the sediments from the striated bedrock as well as cut through the raised marine sediments where the two *M. modiolus* molluscs were identified (Fig. 6C, D). Without this exposed stratigraphy and glacial striae, the early Holocene glacier advance from Gunnarbreen would be impossible to detect, despite the fact that the glacier extended further than during the LIA maximum (Fig. 9). This confirms the concept of Landvik *et al.* (2014), which warns that our reconstructions are biased towards the younger events. It also highlights the challenge of identifying the often subtle signatures of early Holocene glacier events.

Conclusions

We present combined terrestrial and marine data from a small fjord on the west coast of Spitsbergen that exhibits an array of varying climatic conditions and glacier fluctuations throughout what was previously believed to be an uneventful Holocene. These data provide a holistic view of the complexity and the dynamics of these environments.

- An early Holocene advance of the St. Jonsfjorden glacier, Gunnarbreen, is constrained between 12.8±0.10 and 10.0±0.12 cal. ka BP corresponding to the Holocene maximum glacier extent.

- Identification and ^{14}C dating of the thermophilous bivalve mollusc *Modiolus modiolus* to 10.0±0.12 cal. ka BP suggests a rapid northward migration of the species shortly after deglaciation, suggesting an early Holocene invasion of warm water as a potential driving factor of ice retreat.
- We present insight into the onset, climax and breakdown of the Neoglacial-Little Ice Age maximum in St. Jonsfjorden. The Osbornebreen terminus is currently located over 8.5 km up-fjord from its Neoglacial maximum extent and cross-cutting relations suggest numerous subsequent advances of smaller tributary glaciers following the retreat of Osbornebreen.
- We suggest that late Holocene glaciodynamic behaviour of tributary glaciers in St. Jonsfjorden, following the retreat of the trunk glacier, may be related to a dynamic re-organization of their profiles.

Acknowledgements. – The authors acknowledge financial support from the University Centre in Svalbard Research Fund, which aided in costs of fieldwork and radiocarbon dating. Lena Rubensdotter kindly advised us in map preparation. Graduate students participating in the UNIS courses AG-332 and AG-832 in 2013–2015 are thanked for field assistance. The authors acknowledge Astrid Lyså and Tom Bradwell for their constructive reviews as well as Jan A. Piotrowski for editorial support.

References

Alsos, I. G., Sjögren, P., Edwards, M. E., Landvik, J. Y., Gielly, L., Forwick, M., Coissac, E., Brown, A. G., Jakobsen, L. V., Føreid, M. K. & Pedersen, M. W. 2016: Sedimentary ancient DNA from Lake Skartjørna, Svalbard: assessing the resilience of arctic flora to Holocene climate change. *The Holocene 26*, 627–642.

Bartholomaus, T. C., Larsen, C. F. & O'Neel, S. 2013: Does calving matter? Evidence for significant submarine melt. *Earth and Planetary Science Letters 380*, 21–30.

Beierlein, L., Salvigsen, O., Schöne, B. R., Mackensen, A. & Brey, T. 2015: The seasonal water temperature cycle in the Arctic Dicksonfjord (Svalbard) during the Holocene Climate Optimum derived from subfossil Arctica islandica shells. *The Holocene 25*, 1197–1207.

van der Bilt, W. G. M., Bakke, J., Vasskog, K., D'Andrea, W. J., Bradley, R. S. & Ólafsdóttir, S. 2015: Reconstruction of glacier variability from lake sediments reveals dynamic Holocene climate in Svalbard. *Quaternary Science Reviews 126*, 201–218.

van der Bilt, W. G. M., D'Andrea, W. J., Bakke, J., Balascio, N. L., Werner, J. P., Gjerde, M. & Bradley, R. S. 2017: Alkenone-based reconstructions reveal four-phase Holocene temperature evolution for High Arctic Svalbard. *Quaternary Science Reviews* 1–10, doi: 10.1016/j.quascirev.2016.10.006.

Bintanja, R. & Selten, F. M. 2014: Future increases in Arctic precipitation linked to local evaporation and sea-ice retreat. *Nature 509*, 479–482.

Birks, H. H. 1991: Holocene vegetational history and climatic change in west Spitsbergen - plant macrofossils from Skardtjørna, an Arctic lake. *The Holocene 1*, 209–218.

Blake, W. 2006: Occurrence of the Mytilus edulis complex on Nordaustlandet, Svalbard: radiocarbon ages and climatic implications. *Polar Research 25*, 123–137.

Bond, G., Kromer, B., Beer, J., Muscheler, R., Evans, M. N., Showers, W., Hoffmann, S., Lotti-Bond, R., Hajdas, I. & Bonani, G. 2001: Persistent solar influence on north Atlantic climate during the Holocene. *Science 294*, 2130–2136.

Boulton, G. S., van der Meer, J. J. M., Beets, D. J., Hart, J. K. & Ruegg, G. H. J. 1999: The sedimentary and structural evolution of a recent push moraine complex: Holmströmbreen. *Spitsbergen Quaternary Science Reviews 18*, 339–371.

Bratlie, B. 1994: *Senkvartære Sedimenter og Glasialhistorie i Van Keulenfjorden, Svalbard*. MSc. Thesis, Institutt for Geologi, Universitetet i Oslo, 124 pp.

Briner, J. P. 2016: Climate science: ice streams waned as ice sheets shrank. *Nature 530*, 287–288.

Bunin, E. 2015: *Sedimentary Processes and Paleoenvironments in St. Jonsfjorden, Western Spitsbergen*. MSc. Thesis, Department of Geology, University of Troms , The Arctic University of Norway, 167 pp.

Dallmann, W. K. & Elvevold, S. 2015: Geoscience atlas of Svalbard. *In* Dallmann, W. K. (ed.): *Geoscience Atlas of Svalbard*, 133–174. *Norsk Polarinstitutt Rapportserie 148*. Oslo.

Dansgaard, W., Johnsen, S. J., Clausen, H. B., Dahl-Jensen, D., Gundestrup, N. S., Hammer, C. U., Hvidberg, C. S., Steffensen, J. P., Sveinbjornsdottir, A. E., Jouzel, J. & Bond, G. 1993: Evidence for general instability of past climate from a 250-kyr ice-core record. *Nature 364*, 218–220.

Denisenko, N. V., Denisenko, S. G., Lehtonen, K. K., Andersin, A.-B. & Sandler, H. R. 2007: Zoobenthos of the Cheshskaya Bay (southeastern Barents Sea): spatial distribution and community structure in relation to environmental factors. *Polar Biology 30*, 735–746.

Dickson, R. R., Osborn, T. J., Hurrell, J. W., Meincke, J., Blindheim, J., Adlandsvik, B., Vinje, T., Alekseev, G. & Maslowski, W. 2000: The Arctic Ocean response to the North Atlantic Oscillation. *Journal of Climate 13*, 2671–2696.

Dinely, D. L. 1953: Quaternary faunas in the St. Jonsfjord – Eidembukta region, Vestspitsbergen. *Norsk Geologisk Tidsskrift 34*, 1–14.

Dunse, T., Schellenberger, T., Hagen, J., Kääb, A., Schuler, T. & Reijmer, C. 2015: Glacier-surge mechanisms promoted by a hydro-thermodynamic feedback to summer melt. *The Cryosphere 9*, 197–215.

Ely, J. C., Clark, C. D., Spagnolo, M., Stokes, C. R., Greenwood, S. L., Hughes, A. L. C., Dunlop, P. & Hess, D. 2016: Do subglacial bedforms comprise a size and shape continuum? *Geomorphology 257*, 108–119.

Evans, D. J. A. & Rea, B. R. 2005: Late Weichselian deglaciation and sea level history of St Jonsfjorden, Spitsbergen: a contribution to ice sheet reconstruction. *Scottish Geographical Journal 121*, 175–201.

Farnsworth, W. R., Ingólfsson, Ó., Retelle, M. & Schomacker, A. 2016: Over 400 previously undocumented Svalbard surge-type glaciers identified. *Geomorphology 264*, 52–60.

Feyling-Hanssen, R. W. & Jørstad, F. A. 1950: Quaternary fossils from the Sassen-area in Isfjorden, West Spitsbergen: (the marine mollusc fauna). *Norsk Polarinstitutt Skrifter 94, 85 pp.*

Flink, A. E., Noormets, R., Fransner, O., Hogan, K. A., Ó'Regan, M. & Jakobsson, M. 2017: Past ice flow in Wahlenbergfjorden and its implications for late Quaternary ice sheet dynamics in northeastern Svalbard. *Quaternary Science Reviews 163*, 162–179.

Flink, A. E., Noormets, R., Kirchner, N., Benn, D. I., Luckman, A. & Lovell, H. 2015: The evolution of a submarine landform record following recent and multiple surges of Tunabreen glacier, Svalbard. *Quaternary Science Reviews 108*, 37–50.

Førland, E. J., Benestad, R., Hanssen-Bauer, I., Haugen, J. E. & Skaugen, T. E. 2011: Temperature and Precipitation Development at Svalbard 1900-2100. *Advances in Meteorology 2011*, 14 pp.

Førland, E. J., Hanssen-Bauer, I. & Nordli, P. Ø. 1997: Climate statistics and longterm series of temperature and precipitation at Svalbard and Jan Mayen. *DNMI rapport 21/97 Klima*, 73 pp.

Forman, S. L. 1989: Late Weichselian glaciation and deglaciation of Forlandsundet area, western Spitsbergen, Svalbard. *Boreas 18*, 51–60.

Forwick, M. & Vorren, T. O. 2009: Late Weichselian and Holocene sedimentary environments and ice rafting in Isfjorden, Spitsbergen. *Palaeogeography, Palaeoclimatology, Palaeoecology 280*, 258–274.

Forwick, M., Vorren, T. O., Hald, M., Korsun, S., Roh, Y., Vogt, C. & Yoo, K.-C. 2010: Spatial and temporal influence of glaciers and rivers on the sedimentary environment in Sassenfjorden and Tempelfjorden, Spitsbergen. *Geological Society, London, Special Publications 344*, 163–193.

Gjermundsen, E. F., Briner, J. P., Akcar, N., Foros, J., Kubik, P. W., Salvigsen, O. & Hormes, A. 2015: Minimal erosion of Arctic alpine topography during late Quaternary glaciation. *Nature Geoscience 8*, 789–792.

Hald, M., Andersson, C., Ebbesen, H., Jansen, E., Klitgaard-Kristensen, D., Risebrobakken, B., Salomonsen, G. R., Sarnthein, M., Sejrup, H. P. & Telford, R. J. 2007: Variations in temperature and extent of Atlantic Water in the northern North Atlantic during the Holocene. *Quaternary Science Reviews 26*, 3423–3440.

Hald, M., Ebbesen, H., Forwick, M., Godtliebsen, F., Khomenko, L., Korsun, S., Ringstad Olsen, L. & Vorren, T. O. 2004: Holocene paleoceanography and glacial history of the West Spitsbergen area, Euro-Arctic margin. *Quaternary Science Reviews 23*, 2075–2088.

Hanssen-Bauer, I., Solås, M. K. & Steffensen, E. L. 1990: *The Climate of Spitsbergen*. 40 pp. Klima. Norwegian Meteorological Institute, Oslo.

Henriksen, M., Alexanderson, H., Landvik, J. Y., Linge, H. & Peterson, G. 2014: Dynamics and retreat of the Late Weichselian Kongsfjorden ice stream, NW Svalbard. *Quaternary Science Reviews 92*, 235–245.

Hoel, A. 1929: Resultater av de norske statsunderstøttede spitsbergenekspeditioner. (Skrifter om Svalbard og Ishavet) Bind 1 Nr 1: The Norwegian Svalbard Expeditions 1906–1926. Oslo. *Den Norske Stats Bekostning ved Spitsbergenkomitéen*.

Hoel, A., Kregnes, A. & Parmann, B. 1915–1917 (unpublished): Katalog over Fotografisk Materiale fra Isachsens Norske Spitsbergenekspedition 1909–1910.

Holmgren, S. U., Bigler, C., Ingólfsson, Ó. & Wolfe, A. P. 2010: The Holocene-Anthropocene transition in lakes of western Spitsbergen, Svalbard (Norwegian High Arctic): climate change and nitrogen deposition. *Journal of Paleolimnology 43*, 393–412.

Hormes, A., Gjermundsen, E. F. & Rasmussen, T. L. 2013: From mountain top to the deep sea – deglaciation in 4D of the northwestern Barents Sea ice sheet. *Quaternary Science Reviews 75*, 78–99.

Hughes, A. L. C., Gyllencreutz, R., Lohne, Ø. S., Mangerud, J. & Svendsen, J. I. 2016: The last Eurasian ice sheets – a chronological database and time-slice reconstruction, DATED-1. *Boreas 45*, 1–45.

Humlum, O., Elberling, B., Hormes, A., Fjordheim, K., Hansen, O. H. & Heinemeier, J. 2005: Late-Holocene glacier growth in Svalbard, documented by subglacial relict vegetation and living soil microbes. *The Holocene 15*, 396–407.

Ingólfsson, Ó. 2011: Fingerprints of Quaternary glaciations on Svalbard. *Geological Society, London, Special Publications 354*, 15–31.

Ingólfsson, Ó. & Landvik, J. Y. 2013: The Svalbard-Barents Sea ice-sheet – Historical, current and future perspectives. *Quaternary Science Reviews 64*, 33–60.

Jessen, S. P., Rasmussen, T. L., Nielsen, T. & Solheim, A. 2010: A new Late Weichselian and Holocene marine chronology for the western Svalbard slope 30,000–0 cal. years BP. *Quaternary Science Reviews 29*, 1301–1312.

Jiskoot, H., Murray, T. & Boyle, P. 2000: Controls on the distribution of surge-type glaciers in Svalbard. *Journal of Glaciology 46*, 412–422.

Kempf, P., Forwick, M., Laberg, J. S. & Vorren, T. O. 2013: Late Weichselian and Holocene sedimentary palaeoenvironment and glacial activity in the high-arctic van Keulenfjorden, Spitsbergen. *The Holocene 23*, 1607–1618.

Kristensen, L. & Benn, D. I. 2012: A surge of the glaciers Skobreen-Paulabreen, Svalbard, observed by time-lapse photographs and remote sensing data. *Polar Research 31*, 1751–8369.

Kristensen, L., Benn, D. I., Hormes, A. & Ottesen, D. 2009: Mud aprons in front of Svalbard surge moraines: evidence of subglacial deforming layers or proglacial glaciotectonics? *Geomorphology 111*, 206–221.

Landvik, J. Y. & Salvigsen, O. 1987: The Late Weichselian and Holocene shoreline displacement on the west-central coast of Svalbard. *Polar Research 5*, 29–44.

Landvik, J. Y., Alexanderson, H., Henriksen, M. & Ingólfsson, Ó. 2014: Landscape imprints of changing glacial regimes during ice-sheet build-up and decay: a conceptual model from Svalbard. *Quaternary Science Reviews 92*, 258–268.

Landvik, J. Y., Bondevik, S., Elverhøi, A., Fjeldskaar, W., Mangerud, J., Salvigsen, O., Siegert, M. J., Svendsen, J. I. & Vorren, T. O. 1998: The last glacial maximum of Svalbard and the Barents Sea area: ice sheet extent and configuration. *Quaternary Science Reviews 17*, 43–75.

Landvik, J. Y., Ingólfsson, Ó., Mienert, J., Lehman, S. J., Solheim, A., Elverhøi, A. & Ottesen, D. 2005: Rethinking Late Weichselian ice-sheet dynamics in coastal NW Svalbard. *Boreas 34*, 7–24.

Lehman, S. J. & Forman, S. L. 1992: Late Weichselian glacier retreat in Kongsfjorden, West Spitsbergen, Svalbard. *Quaternary Research 37*, 139–154.

Lønne, I. 2005: Faint traces of high Arctic glaciations: an early Holocene ice-front fluctuation in Bolterdalen, Svalbard. *Boreas 34*, 308–323.

Lønne, I. 2014: The influence of climate during and after a glacial surge — a comparison of the last two surges of Fridtjovbreen, Svalbard. *Geomorphology 207*, 190–202.

Lovell, H., Fleming, E. J., Benn, D. I., Hubbard, B., Lukas, S. & Naegeli, K. 2015a: Former dynamic behaviour of a cold-based valley glacier on Svalbard revealed by basal ice and structural glaciology investigations. *Journal of Glaciology 61*, 309–328.

Lovell, H., Fleming, E. J., Benn, D. I., Hubbard, B., Lukas, S., Rea, B. R., Noormets, R. & Flink, A. E. 2015b: Debris entrainment and landform genesis during tidewater glacier surges. *Journal of Geophysical Research: Earth Surface 120*, 1574–1595.

Luckman, A., Benn, D. I., Cottier, F., Bevan, S., Nilsen, F. & Inall, M. 2015: Calving rates at tidewater glaciers vary strongly with ocean temperature. *Nature Communications 6*, 8566, doi: 10.1038/ncomms9566

Lyså, A. & Lønne, I. 2001: Moraine development at a small High-Arctic valley glacier: Rieperbreen, Svalbard. *Journal of Quaternary Science 16*, 519–529.

Mangerud, J. & Gulliksen, S. 1975: Apparent radiocarbon ages of recent marine shells from Norway, Spitsbergen, and Arctic Canada. *Quaternary Research 5*, 263–273.

Mangerud, J. & Landvik, J. Y. 2007: Younger Dryas cirque glaciers in western Spitsbergen: smaller than during the Little Ice Age. *Boreas 36*, 278–285.

Mangerud, J., Bolstad, M., Elgersma, A., Helliksen, D., Landvik, J. Y., Lønne, I., Lycke, A. K., Salvigsen, O., Sandahl, T. & Svendsen, J. I. 1992: The last glacial maximum on Spitsbergen, Svalbard. *Quaternary Research 38*, 1–31.

Mangerud, J., Bondevik, S., Gulliksen, S., Hufthammer, A. K. & Høisæter, T. 2006: Marine ^{14}C reservoir ages for 19th century whales and molluscs from the North Atlantic. *Quaternary Science Reviews 25*, 3228–3245.

Mangerud, J., Dokken, T., Hebbeln, D., Heggen, B., Ingólfsson, Ó., Landvik, J. Y., Mejdahl, V., Svendsen, J. I. & Vorren, T. O. 1998: Fluctuations of the Svalbard Barents Sea Ice Sheet during the last 150 000 years. *Quaternary Science Reviews 17*, 11–42.

Masson-Delmotte, V., Schulz, M., Abe-Ouchi, A., Beer, J., Ganopolski, A., González Rouco, J. F., Jansen, E., Lambeck, K., Luterbacher, J., Naish, T., Osborn, T., Otto-Bliesner, B., Quinn, T., Ramesh, R., Rojas, M., Shao, X. & Timmermann, A. 2013: Information from paleoclimate archives. Climate Change 2013: The Physical Science Basis. *In Contribution of Working Group I to the Fifth Assessment Report of the Intergovernmental Panel on Climate Change*, 383–464. Cambridge University Press, Cambridge, UK and New York, NY, USA.

Mayewski, P. A., Rohling, E. E., Curt Stager, J., Karlén, W., Maasch, K. A., David Meeker, L., Meyerson, E. A., Gasse, F., van Kreveld, S., Holmgren, K., Lee-Thorp, J., Rosqvist, G., Rack, F., Staubwasser, M., Schneider, R. R. & Steig, E. J. 2004: Holocene climate variability. *Quaternary Research 62*, 243–255.

McKay, N. P. & Kaufman, D. S. 2014: An extended Arctic proxy temperature database for the past 2,000 years. *Scientific Data 1*, 140026, doi: 10.1038/sdata/2014.26.

Midgley, N. G. & Tonkin, T. N. 2017: Reconstruction of former glacier surface topography from archive oblique aerial images. *Geomorphology 282*, 18–26.

Miller, G. H., Landvik, J. Y., Lehman, S. J. & Southon, J. R. 2017: Episodic Neoglacial snowline descent and glacier expansion on Svalbard reconstructed from the ^{14}C ages of ice-entombed plants. *Quaternary Science Reviews 155*, 67–78.

Nick, F. M., van der Veen, C. J., Vieli, A. & Benn, D. I. 2010: A physically based calving model applied to marine outlet glaciers and implications for the glacier dynamics. *Journal of Glaciology 56*, 781–794.

Norwegian Polar Institute 2017: *TopoSvalbard*. Norwegian Polar Institute, http://toposvalbard.npolar.no/.

Nuth, C., Kohler, J., König, M., von Deschwanden, A., Hagen, J. O., Kääb, A., Moholdt, G. & Pettersson, R. 2013: Decadal changes from a multi-temporal glacier inventory of Svalbard. *The Cryosphere 7*, 1603–1621.

Oerlemans, J. 2005: Atmospheric science: extracting a climate signal from 169 glacier records. *Science 308*, 675–677.

Ottesen, D., Dowdeswell, J. A., Benn, D. I., Kristensen, L., Christiansen, H. H., Christensen, O., Hansen, L., Lebesbye, E., Forwick, M. & Vorren, T. O. 2008: Submarine landforms characteristic of glacier surges in two Spitsbergen fjords. *Quaternary Science Reviews 27*, 1583–1599.

Paasche, Ø. & Bakke, J. 2010: Defining the Little Ice Age. *Climate of the Past Discussions 6*, 2159–2175.

Powell, R. D. & Domack, E. 1995: Modern glaciomarine environments. *In* Menzies, J. (ed.): *Glacial Environments. Volume 1: Modern Glacial Environments: Processes, Dynamics and Sediments*, 445–486. Butterworth-Heinemann, Oxford.

Reimer, P. J., Bard, E., Bayliss, A., Beck, J. W., Blackwell, P. G., Bronk Ramsey, C., Buck, C. E., Cheng, H., Edwards, R. L., Friedrich, M., Grootes, P. M., Guilderson, T. P., Haflidason, H., Hajdas, I., Hatté, C., Heaton, T. J., Hoffmann, D. L., Hogg, A. G., Hughen, K. A., Kaiser, K. F., Kromer, B., Manning, S. W., Niu, M., Reimer, R. W., Richards, D. A., Scott, E. M., Southon, J. R., Staff, R. A., Turney, C. S. M. & van der Plicht, J. 2013: IntCal13 and Marine13 Radiocarbon Age Calibration Curves 0–50,000 Years cal BP. *Radiocarbon 55*, 1869–1887.

Reusche, M., Winsor, K., Carlson, A. E., Marcott, S. A., Rood, D. H., Novak, A., Roof, S., Retelle, M., Werner, A., Caffee, M. & Clark, P. U. 2014: ^{10}Be surface exposure ages on the late-Pleistocene and Holocene history of Linnébreen on Svalbard. *Quaternary Science Reviews 89*, 5–12.

Rockström, J., Steffen, W., Noone, K., Persson, A., Chapin, F. S., Lambin, E. F., Lenton, T. M., Scheffer, M., Folke, C., Schellnhuber, H. J., Nykvist, B., de Wit, C. A., Hughes, T., van der Leeuw, S., Rodhe, H., Sorlin, S., Snyder, P. K., Costanza, R., Svedin, U., Falkenmark, M., Karlberg, L., Corell, R. W., Fabry, V. J., Hansen, J., Walker, B., Liverman, D., Richardson, K., Crutzen, P. & Foley, J. A. 2009: A safe operating space for humanity. *Nature 461*, 472–475.

Rogers, J. C., Yang, L. & Li, L. 2005: The role of Fram Strait winter cyclones on sea ice flux and on Spitsbergen air temperatures. *Geophysical Research Letters 32*, L06709, doi: 10.1029/2004GL02226.

Røthe, T. O., Bakke, J., Vasskog, K., Gjerde, M., D'Andrea, W. J. & Bradley, R. S. 2015: Arctic Holocene glacier fluctuations reconstructed from lake sediments at Mitrahalvøya, Spitsbergen. *Quaternary Science Reviews 109*, 111–125.

Salvigsen, O. 2002: Radiocarbon-dated *Mytilus edulis* and *Modiolus modiolus* from northern Svalbard: climatic implications. *Norsk Geografisk Tidsskrift 56*, 56–61.

Salvigsen, O., Forman, S. L. & Miller, G. H. 1992: Thermophilous molluscs on Svalbard during the Holocene and their paleoclimatic implications. *Polar Research 11*, 1–10.

Sarnthein, M., Van Kreveld, S., Erlenkeuser, H., Grootes, P. M., Kucera, M., Pflauman, U. & Schulz, M. 2003: Centennial-to-millennial-scale periodicities of Holocene climate and sediment injections off the western Barents shelf, 75°N. *Boreas 32*, 447–461.

Scambos, T. A., Bohlander, J. A., Shuman, C. A. & Skvarca, P. 2004: Glacier acceleration and thinning after ice shelf collapse in the Larsen B embayment, Antarctica. *Geophysical Research Letters 31*, L18402, doi: 10.1029/2004GL020670.

Schomacker, A., Benediktsson, Í. Ö. & Ingólfsson, Ó. 2014: The Eyjabakkajökull glacial landsystem, Iceland: geomorphic impact of multiple surges. *Geomorphology 218*, 98–107.

Sevestre, H. 2015: *Surge-type Glaciers: Controls, Processes and Distribution*. Ph.D. thesis, University of Oslo, 68 pp.

Sevestre, H. & Benn, D. I. 2015: Climatic and geometric controls on the global distribution of surge-type glaciers: implications for a unifying model of surging. *Journal of Glaciology 61*, 646–662.

Sletten, K., Lyså, A. & Lønne, I. 2001: Formation and disintegration of a high-arctic ice-cored moraine complex, Scott Turnerbreen, Svalbard. *Boreas 30*, 272–284.

Snyder, J. A., Werner, A. & Miller, G. H. 2000: Holocene cirque glacier activity in western Spitsbergen, Svalbard: sediment records from proglacial Linnévatnet. *The Holocene 10*, 555–563.

Solomina, O. N., Bradley, R. S., Hodgson, D. A., Ivy-Ochs, S., Jomelli, V., Mackintosh, A. N., Nesje, A., Owen, L. A., Wanner, H., Wiles, G. C. & Young, N. E. 2015: Holocene glacier fluctuations. *Quaternary Science Reviews 111*, 9–34.

Steffensen, J. P., Andersen, K. K., Bigler, M., Clausen, H. B., Dahl-Jensen, D., Fischer, H., Goto-Azuma, K., Hansson, M., Johnsen, S. J., Jouzel, J., Masson-Delmotte, V., Popp, T., Rasmussen, S. O., Röthlisberger, R., Ruth, U., Stauffer, B., Siggaard-Andersen, M.-L., Sveinbjörnsdóttir, Á. E., Svensson, A. & White, J. W. C. 2008: High-resolution Greenland ice core data show abrupt climate change happens in few years. *Science 321*, 680–684.

Sund, M., Eiken, T., Hagen, J. O. & Kääb, A. 2009: Svalbard surge dynamics derived from geometric changes. *Annals of Glaciology 50*, 50–60.

Svendsen, J. I. & Mangerud, J. 1997: Holocene glacial and climatic variations on Spitsbergen, Svalbard. *The Holocene 7*, 45–57.

Vikhamar-Schuler, D., Isaksen, K., Haugen, J. E., Tømmervik, H., Luks, B., Schuler, T. V. & Bjerke, J. W. 2016: Changes in winter warming events in the Nordic Arctic region. *Journal of Climate 29*, 6223–6244.

Wanner, H., Solomina, O., Grosjean, M., Ritz, S. P. & Jetel, M. 2011: Structure and origin of Holocene cold events. *Quaternary Science Reviews 30*, 3109–3123.

Werner, A. 1993: Holocene moraine chronology, Spitsbergen, Svalbard: lichenometric evidence for multiple Neoglacial advances in the Arctic. *The Holocene 3*, 128–137.

Wuite, J., Rott, H., Hetzenecker, M., Floricioiu, D., De Rydt, J., Gudmundsson, G. H., Nagler, T. & Kern, M. 2015: Evolution of surface velocities and ice discharge of Larsen B outlet glaciers from 1995 to 2013. *The Cryosphere 9*, 957–969.

Yde, J. C. & Paasche, Ø. 2010: Reconstructing climate change: not all glaciers suitable. *Eos, Transactions American Geophysical Union 91*, 189–190.

Chapter IV

Over 400 previously undocumented Svalbard surge-type glaciers identified

Farnsworth, W.R., Ingólfsson, Ó., Schomacker, A., Retelle, M. (2016): Over 400 previously undocumented Svalbard surge-type glaciers identified. *Geomorphology 264*, 52-60. DOI: 10.1016/j.geomorph.2016.03.025.

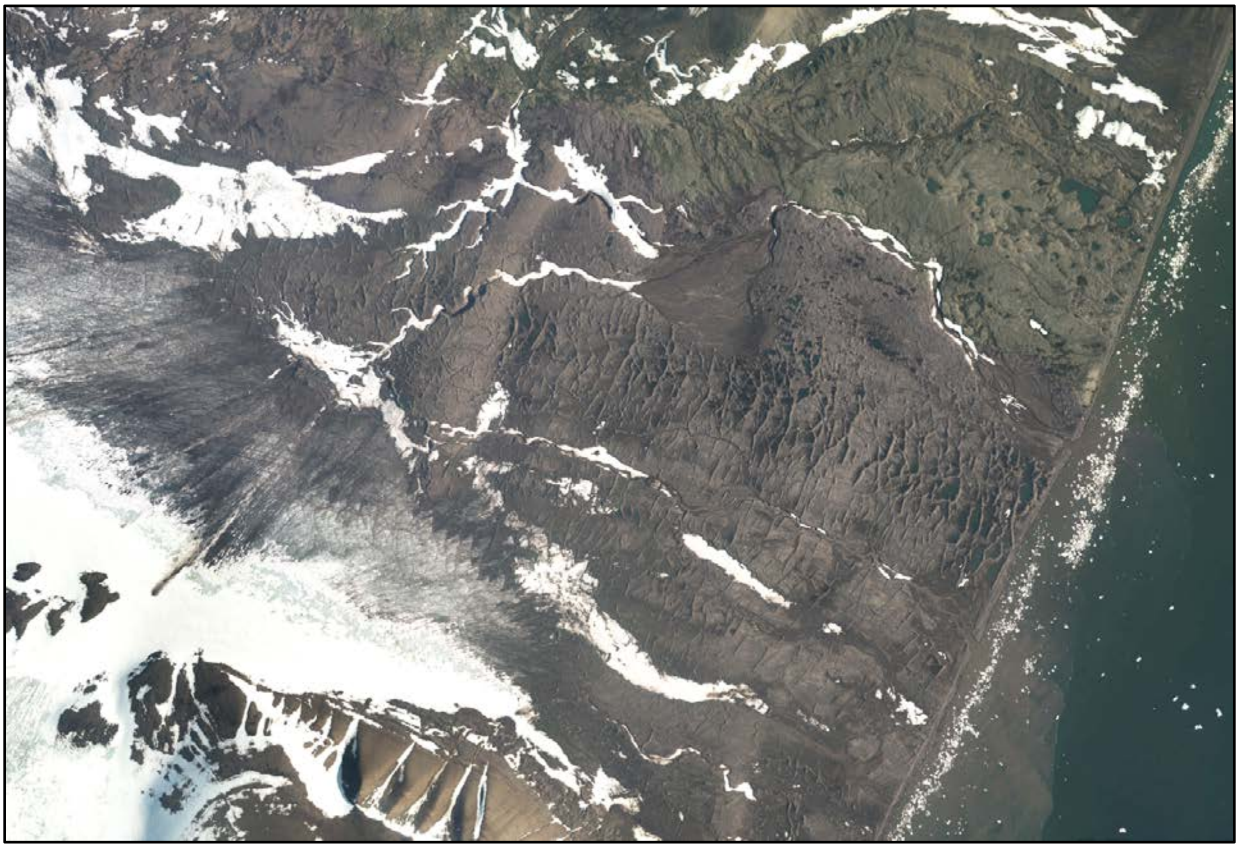

Aerial image of Pettersenbreen foreland, southeastern Edgøya (Norwegian Polar Institute).

Geomorphology 264 (2016) 52–60

Contents lists available at ScienceDirect

Geomorphology

journal homepage: www.elsevier.com/locate/geomorph

Over 400 previously undocumented Svalbard surge-type glaciers identified

Wesley R. Farnsworth [a,b,*], Ólafur Ingólfsson [a,c], Michael Retelle [a,d], Anders Schomacker [b]

[a] Department of Arctic Geology, University Centre in Svalbard (UNIS), N-9171 Longyearbyen, Norway
[b] Department of Geology, UiT The Arctic University of Norway, N-9037 Tromsø, Norway
[c] Faculty of Earth Sciences, University of Iceland, Sturlugata 7, IS-101 Reykjavík, Iceland
[d] Department of Geology, Bates College, Lewiston, ME 04240, USA

ARTICLE INFO

Article history:
Received 1 December 2015
Received in revised form 21 March 2016
Accepted 22 March 2016
Available online 13 April 2016

Keywords:
Crevasse squeeze ridges
Svalbard
Glacier surge
Aerial imagery

ABSTRACT

Identifying glaciers that exhibit surge-type behavior is important when using evidence of ice front fluctuations as a proxy for reconstructing past climate oscillations. This study identifies previously undocumented surge-type glaciers in Svalbard, based on the presence of crevasse squeeze ridges in glacier forelands. Crevasse squeeze ridges are landforms suggested to be unique to surging glacier land systems. Estimates vary greatly as to the actual percentage of surge-type glaciers in Svalbard, and consequently their distribution pattern is poorly understood. A detailed survey of recent (2008–2012), high-resolution aerial imagery from *TopoSvalbard*, provided by the Norwegian Polar Institute, allowed for a survey of all the glacier forelands in Svalbard. Before our study, 277 individual glaciers in Svalbard have been documented to exhibit surge behavior. By using crevasse squeeze ridges as indicators of surge behavior, we have identified 431 additional glaciers that have surged. We suggest that this is a modest value as the unique surge landforms were not visible in approximately one-third of the forelands with documented surge histories. Limits to the crevasse squeeze ridge technique are presented and potential controlling factors for crevasse squeeze ridge formation/preservation are discussed.

1. Introduction

Holocene climate has fluctuated between warmer and cooler periods as well as relatively humid and dry conditions on decadal to centennial timescales (Wanner et al., 2011). 'Polar amplification' refers to the sensitivity of Arctic regions to these climatic fluctuations and how the Arctic areas are affected by relatively small shifts in temperature and precipitation (Masson-Delmotte et al., 2013). Arctic glaciers and ice caps respond to even small changes in winter precipitation and summer temperatures (Masson-Delmotte et al., 2013), making them valuable indicators of changes in climate (Oerlemans, 2005). Consequently, the reconstruction of Arctic glacial oscillations and chronologies through the Holocene provides valuable insight into antecedent climate scenarios. Understanding that individual glaciers may respond uniquely to shifts in climate is vital (Røthe et al., 2015). Furthermore, surge behavior complicates the matter as glacier fluctuations sometimes are driven by internal ice dynamics (surges) that some have been suggested to be unrelated to climate (Meier and Post, 1969; Yde and Paasche, 2010). It is therefore important to establish if ice-front oscillations for individual glaciers reflect mass-balance shifts controlled by climate, variations in internal dynamics (surge activity), or a combination of the two.

The aim of this study is to identify previously undocumented surge-type glaciers on Svalbard based on the presence of crevasse squeeze ridges (CSRs; also termed crevasse fill ridges; Sharp, 1985a) visible in glacier forelands. We strive to (i) identify which glaciers are surge-type glaciers and subsequently not optimal for traditional climate reconstructions and (ii) better understand the dynamics of Svalbard glaciers.

Crevasse squeeze ridges (Sharp, 1985a; Benn and Evans, 2010; Rea and Evans, 2011) have been identified as a landform characteristic of surge-type glaciers and constitute an important component of the surging glacier land system model (Evans and Rea, 1999, 2003; Brynjólfsson et al., 2012; Schomacker et al., 2014). A detailed analysis of recent (2008–2012), high-resolution imagery from *TopoSvalbard*, provided by the Norwegian Polar Institute, allowed for an efficient survey of CSRs throughout Svalbard forelands.

1.1. Surge-type glaciers, landforms, and CSRs

A surge-type glacier cyclically exhibits major fluctuations in velocity and length over timescales that range from a few years to several decades or centuries (Benn and Evans, 2010). Initially this

* Corresponding author at: P.O. Box 156, Department of Arctic Geology, University Centre in Svalbard, UNIS, N-9171 Longyearbyen, Norway.
E-mail addresses: wesleyf@unis.no (W.R. Farnsworth), olafur.ingolfsson@unis.no (Ó. Ingólfsson), mretelle@bates.edu (M. Retelle), anders.schomacker@uit.no (A. Schomacker).

http://dx.doi.org/10.1016/j.geomorph.2016.03.025
0169-555X/

behavior was believed to be caused by oscillations in basal conditions rather than external forcing by climate (Meier and Post, 1969; Sharp, 1988). Potential triggers for surges have been suggested, including reorganization of the basal hydrological system (Kamb et al., 1985), switching of thermal regime (Fowler et al., 2001; Sevestre et al., 2015), as well as sediment deformation at the glacier bed (Clarke et al., 1984; Björnsson, 1998). These different controlling factors have since been placed under one unifying theory relating to the enthalpy balance of a glacier (Aschwanden et al., 2012; Sevestre and Benn, 2015). Enthalpy balance ties together the hydrologic, thermal regime and bed deformation themes by highlighting a simple budget of energy exchange at the surface and base of a glacier as well as the frictional heat related to ice flow.

Observations of surge events are relatively rare in Svalbard because of the remoteness of many glaciers and the extended surge cycles characteristic of the cold, dry region (Dowdeswell et al., 1991; Lønne, 2016). Commonly, surge-type glaciers are identified by the presence of specific landforms characteristic of a surge (Benn and Evans, 2010). The most frequently used landform accepted as an indicative fingerprint of surge activity is a looped medial moraine (Copland et al., 2011; Paul, 2015). Additionally, other features have also been used to indicate surge behavior, but are only unique to surge activity within a specific context. For example, trimlines above the ice surface are formed by surge-type and nonsurge-type glaciers but they have been used as surge indicators where the bulge of mass transferred from the accumulation zone to the ablation area formed a trimline of ice and debris (Sund et al., 2009; Kristensen and Benn, 2012). A surge trimline has a much lower preservation potential compared to a traditional trimline owing to the relatively high ice content. Extensive crevassing, high and widespread across the glacier that is not normally present, is indicative of a surge-type glacier during or shortly after a surge event (Hagen et al., 1993). Although these specific features are unique to surge events, their preservation potential after the surge is poor, as the crevasses disappear, the trimlines deteriorate and the looped moraines get reworked and distorted. Given the ‘switch on/switch off’ behavior of surge-type glaciers (Dowdeswell et al., 1995; Hansen, 2003), we feel these diagnostic landforms are sufficient evidence to identify surge-type behavior.

Another landform unique to surge behavior that has not yet been widely used diagnostically for identifying a surge-type glacier is a crevasse squeeze ridge (CSR; Fig. 1). The CSRs were described in Iceland as elongated ridges ca. 1 to 2 m in height and up to several hundred meters long (Sharp, 1985a,b) and were suggested to correspond with surge-type glaciers. The ridges, like looped moraines and trimlines, form during surge events but become exposed in surge-type glacier forelands during the quiescent phase. This delayed exposure allows for CSRs to potentially suggest surge behavior of a glacier decades to over a century after a single surge event (Fig. 1A). The ridges consist of matrix-supported diamict sediments and often form in networks on fluted till plains in forelands and can form oblique, transverse, or normal to ice flow (Sharp, 1985a,b; Kjær et al., 2008; Schomacker et al., 2014).

The formation of CSRs is still not well understood (Rea and Evans, 2011; Ingólfsson et al., 2016). The relationship between the CSR and

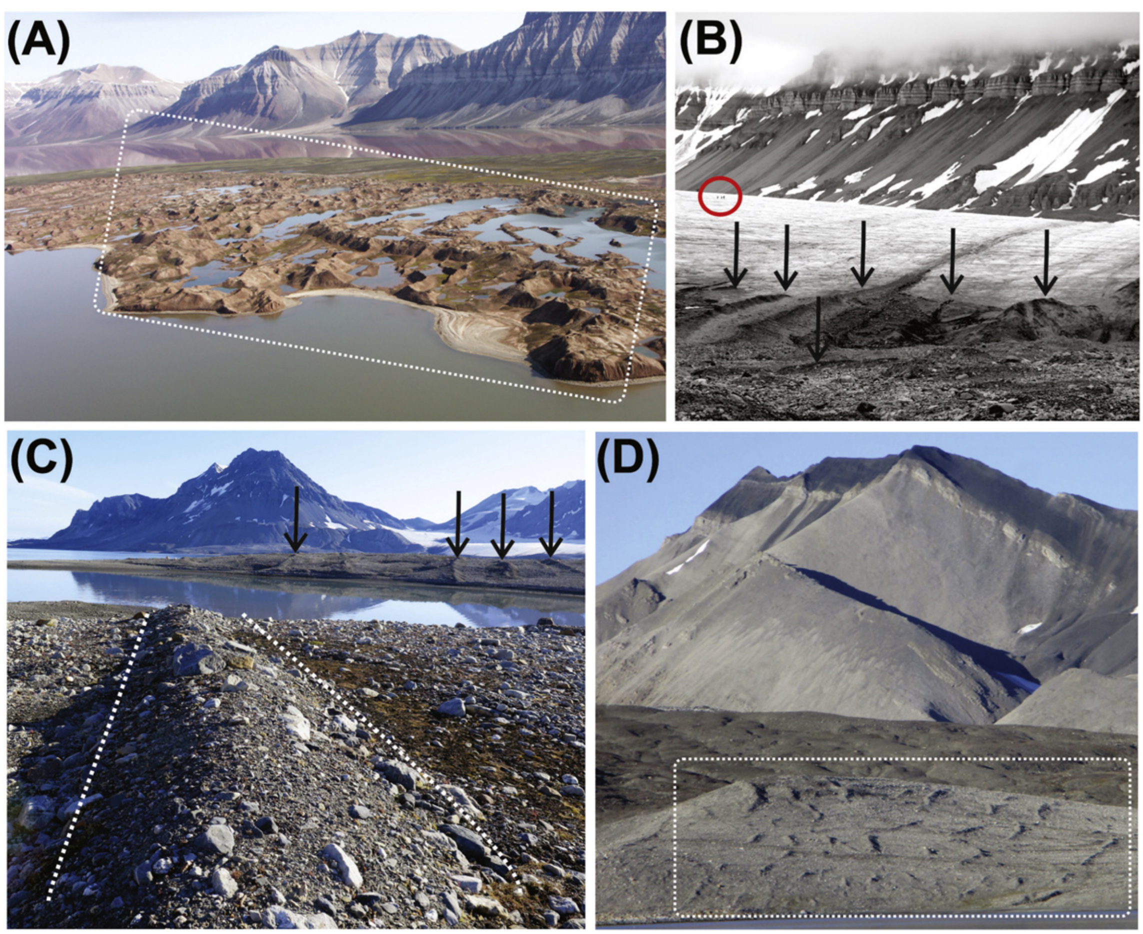

Fig. 1. (A) Oblique aerial image of Coraholmen, taken in July 2004, view to NE. Crevasse squeeze ridge network preserved subaerially on Coraholmen Island delimiting the maximum extent of the last Sefströmbreen surge ca. 1890 (Liestøl, 1993). For scale: Coastal cliffs are 8 to 10 m high. Box highlights prominent CSR network. Photograph: K.H. Kjær. (B) Image of CSRs (marked by arrows) melting out of the quiescent Von Postbreen, view to SE oblique to ice-flow, taken August 2012, by W.R. Farnsworth. Note three persons on the glacier in the background for scale, circled in red. (C) CSR preserved in the foreland of Kjerulfbreen marked with dotted lines, network visible in the background indicated with arrows, ridge in foreground roughly 0.5 m prominent composed of a matrix-supported diamict, view to the SE. Photograph: N. Aradóttir, August 2015. (D) Overview of CSR network (white box) preserved in the foreland of Kjerulfbreen, view to NE. Photograph: D. Ben-Yehoshua, August 2015.

fluted till plain suggests several possible modes of formation (Sharp, 1985b; Bjarnadóttir, 2007; Ferguson et al., 2009). Similar morphological structures can form from subaerial infill of moraine sediments (Morawski, 2005) or debris-rich thrust-faults (Glasser et al., 1998) but are not usually arranged in interconnected rhombohedral networks (Lovell et al., 2015b). Generally CSRs are believed to form by local saturated sediment infilling, from the bed upward, into basal crevasses during the latter part of a surge and subsequently meltout. In a detailed investigation of internal ice deformation structures, cross-cutting relationships between compressional and extensional phases suggested a downglacier passage of a kinematic wave consistent with a surge (Lovell et al., 2015a). Rea and Evans (2011) concluded that high basal water pressure drives the infilling of basal crevasses from the bottom up. In theory high pore-water buildup corresponds with a fine sediment fractionation. In a detailed sedimentological study of the Elisebreen surge foreland where CSRs were identified, Christoffersen et al. (2005), describe a coarse till with a silt/clay composition ca. 35% compared to 65% sand and gravel.

2. Study area, climate, and glaciers

Svalbard is an archipelago located along the dominant corridor of atmospheric moisture between the Atlantic and the Arctic Basin, spanning from 74° to 81° N (Fig. 2A; D'Andrea et al., 2012). The islands are positioned at the northern extent of the Gulf Stream (North Atlantic Drift) and the southern border of the Arctic sea ice front (Rogers et al., 2005). Presently, glaciers cover roughly 60% of the archipelago (Hagen et al., 2003), and Svalbard is categorized as having a dry High Arctic climate with periglacial conditions, low winter temperatures, and warm continuous permafrost (French, 2007; Christiansen et al., 2010). Despite the archipelago's northern location, western Spitsbergen experiences a mild climate for its latitude where the relatively warm Norwegian Current controls weather and sea ice (Førland et al., 1997). Climate is characterized by the interactions between the Icelandic Low and Siberian High pressure systems, and as a result relatively high temperatures are driven north over Svalbard by the main North Atlantic cyclone track (Hanssen-Bauer et al., 1990). Svalbard precipitation is closely coupled to the mode of the North Atlantic Oscillation (NAO; Dickson et al., 2000) and falls predominantly in solid form. Longyearbyen, the main settlement (central Spitsbergen; Fig. 2) has a mean annual air temperature ca. −5 °C, and the annual sum of precipitation averages around 195 mm w.e. (Norwegian Meteorological Institute; http://www.eklima.no, n.d).

Svalbard has over 2100 glaciers (Liestøl, 1993). These glaciers range in size from small cirque glaciers to large ice caps and exhibit a range of thermal properties (polythermal/cold/warm-based) as well as terrestrial and tidewater termini (Fig. 2B). The maximum Holocene extent of Svalbard glaciers and ice caps is generally considered to have occurred toward the end of the Little Ice Age (LIA; Werner, 1993; Humlum et al., 2003). The actual timing of the end of the LIA is dependent on whether it is defined by a warming trend in temperatures or the retreat of glacier fronts. The LIA on Svalbard culminated later (ca. 1930 CE) in comparison to Scandinavia, central Europe, and other parts of the world (Paasche and Bakke, 2010). The late culmination is visible in historic 1936 Norwegian Polar Institute oblique aerial photographs displaying most ice margins up against or proximal to their LIA moraine systems (Lyså and Lønne, 2001; Sletten et al., 2001). Since the end of the LIA retreat and thinning of Svalbard glaciers have been extensive through the twentieth century exposing an extensive recently glaciated landscape (Nuth et al., 2007).

Surge-type glaciers exist regionally in dense clusters (Jiskoot et al., 2000; Grant et al., 2009), and Svalbard is one of these regions (Benn and Evans, 2010). Despite Svalbard clearly being recognized as a 'surge hot spot', how many of the glaciers on the archipelago actually exhibit surge behavior is not clear. Published estimates of the frequency of surge-type glaciers in Svalbard range from 90% (Lefauconnier and Hagen, 1991) to as low as 13% of all glaciers (Jiskoot et al., 1998).

In our study we highlight 277 documented surge-type glaciers based on previous inventories (Fig. 2B; Dowdeswell et al., 1991; Lefauconnier and Hagen, 1991; Hamilton, 1992; Hagen et al., 1993; Liestøl, 1993; Dowdeswell et al., 1999; Jiskoot et al., 2000; Dowdeswell and Benham, 2003; Błaszczyk et al., 2009; Sund et al., 2009). In contrast to previous studies, we choose not to address the percentages of surge-type glaciers in Svalbard or the subregions as we believe the values should correspond with a temporal constraint. Given the dynamic 'switch on/switch off' of surge-type glaciers, we strictly present raw values of the number of glaciers where we have identified surge-diagnostic landforms.

We have divided Spitsbergen, Nordaustlandet, and Barentsøya-Edgeøya into six regions, based on general location and climate (Fig. 2B). The distribution of documented surge glaciers is displayed in a pie chart in Fig. 2. A clear dominance of surge-type glaciers is visible in the southern part of Spitsbergen with about 45% of the documented surge-type glaciers located in this area. The other five regions account for the remaining ~55%. This apparent distribution could be the result of (i) relatively a higher frequency of observations of glacier front fluctuations over the last ~150 years through the southern region, or (ii) the climate/enthalpy balance in these areas might be more or less conducive to surge behavior (Sevestre and Benn, 2015). Northeast Spitsbergen, NW Spitsbergen, central Spitsbergen, Nordaustlandet, and the combination of Barentsøya/Edgeøya all have a similar number of documented surges despite these regions having a large range in the actual number of glaciers (Fig. 2B).

3. Methods

Analysis of aerial imagery was carried out using *TopoSvalbard* (TopoSvalbard, 2016; http://toposvalbard.npolar.no/) provided by the Norwegian Polar Institute. The most recent aerial images available for Svalbard glacier forelands exist for years 2008, 2009, 2010, 2011, and 2012 depending on site and region. Aerial images allow detection of details with up to 0.5-m resolution. The CSRs were interpreted based on relief, morphology, location, and cross-cutting relations within the glacier foreland system (Sharp, 1985b; Evans and Rea, 1999, 2003). These interpretations were in some cases compared to structures and the presence of CSR at known glacier forelands where the landforms have been studied in the field. The CSR networks were recorded and tabularized for glaciers on Svalbard for previously undocumented surge-type glaciers and for glaciers with documented surge histories (Dowdeswell et al., 1991; Lefauconnier and Hagen, 1991; Hamilton, 1992; Hagen et al., 1993; Liestøl, 1993; Dowdeswell et al., 1999; Jiskoot et al., 2000; Dowdeswell and Benham, 2003; Błaszczyk et al., 2009; Sund et al., 2009). Images from *TopoSvalbard* were analyzed for each foreland (Fig. 3). In the case where a glacier foreland had CSR but was unnamed, the glacier was coded by the region and a number (Fig. 3B). The unnamed glaciers were systematically

Fig. 2. **(A)** Overview map of Svalbard located between the Arctic and Atlantic basins, base map modified from www.maps-world.net. **(B)** The main islands of Svalbard divided into six general geographic regions. Black dots indicate glaciers where surge behavior has been documented (Dowdeswell et al., 1991; Lefauconnier and Hagen, 1991; Hamilton, 1992; Hagen et al., 1993; Liestøl, 1993; Dowdeswell et al., 1999; Jiskoot et al., 2000; Dowdeswell and Benham, 2003; Błaszczyk et al., 2009; Sund et al., 2009). Inset pie chart displays the distribution of documented surge behavior by region. Base map modified from TopoSvalbard provided by the Norwegian Polar Institute. The three upper black dots on Vestfonna, Nordaustlandet are slightly offset on the map and correspond to glaciers to the north of map view: Søre Franklinbreen, Nordre Franklinbreen and Rijpbreen (from west to east).

numbered with the first glacier of each region being located farthest north while the final number corresponding to an unnamed glacier located furthest south in each region. For example, NWS-1 corresponds to an unnamed glacier with CSR in Northwestern Spitsbergen that is located in the upper part of the region. These glaciers are presented in the supplementary data (Table 2).

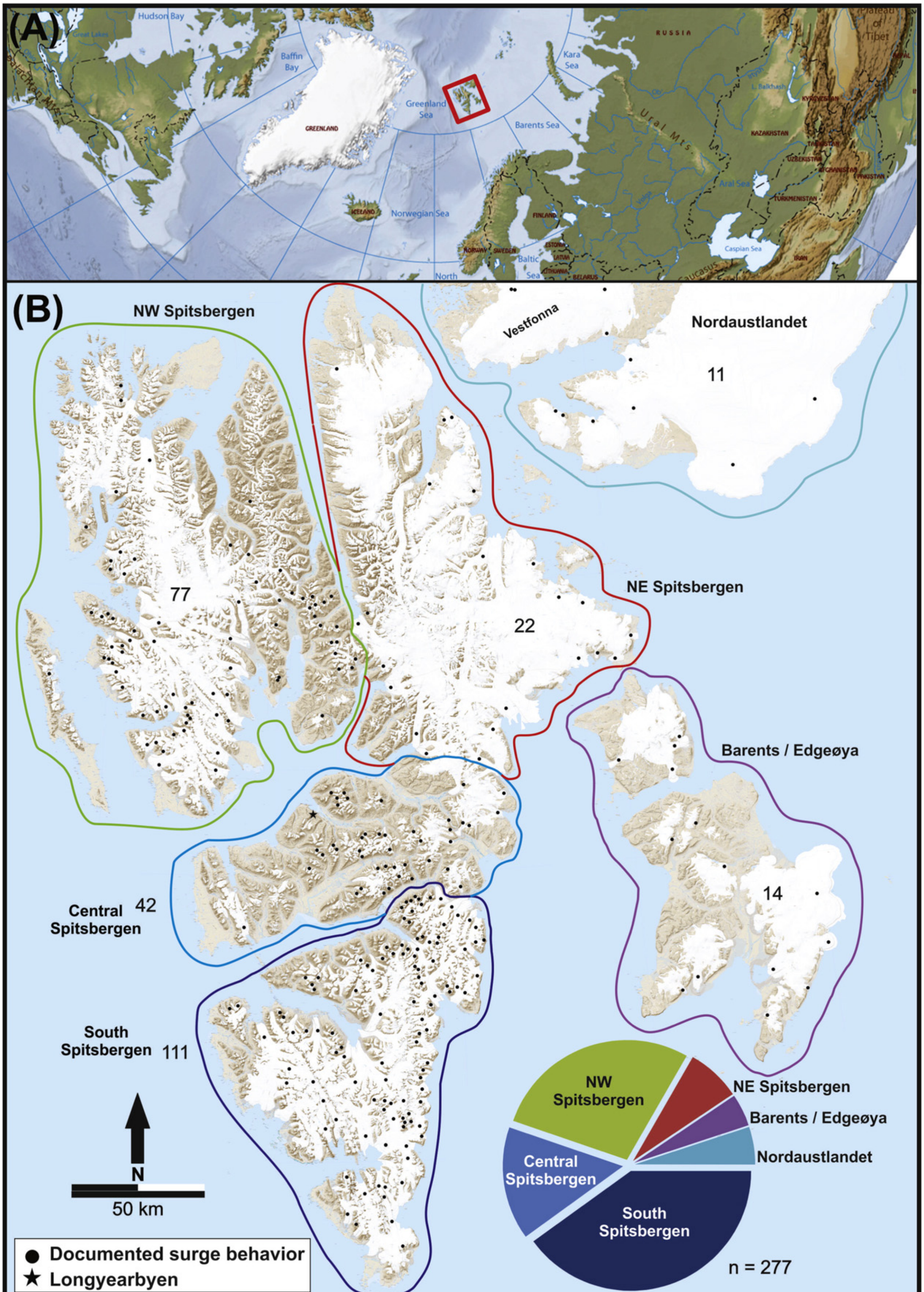

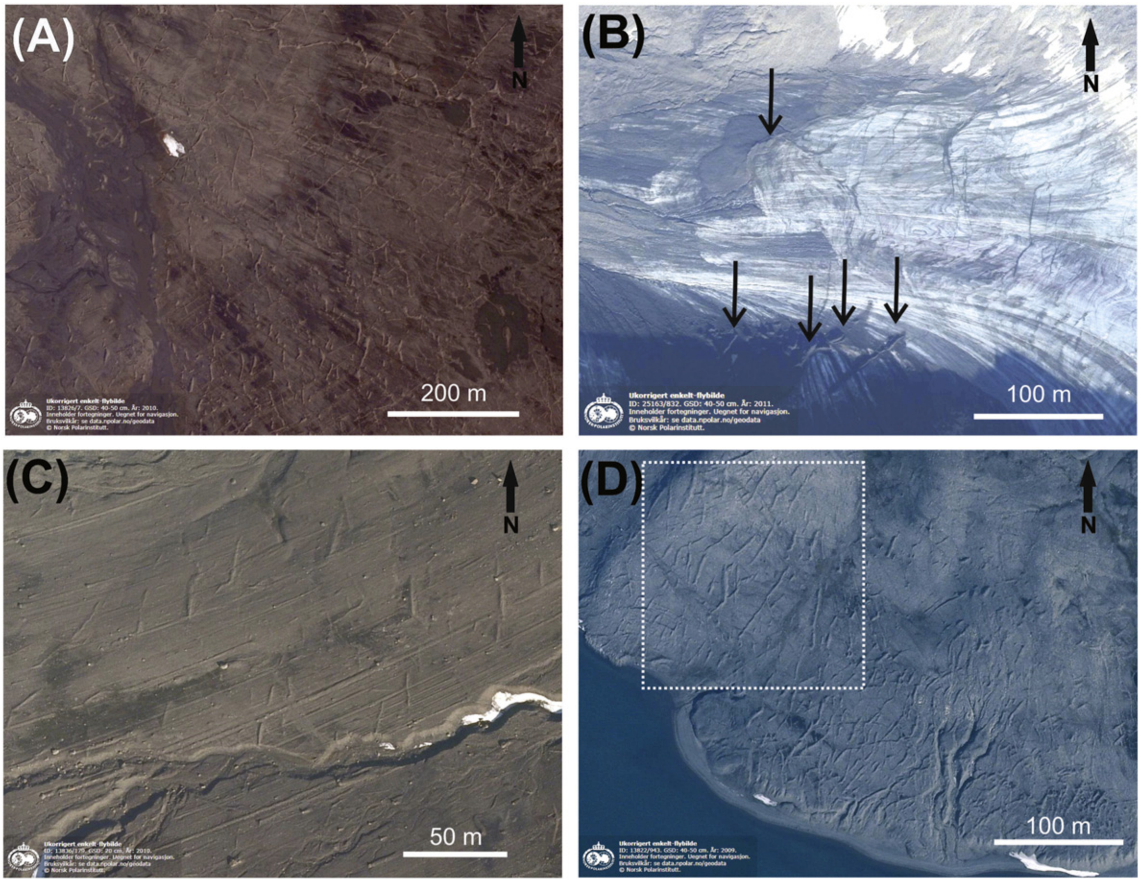

Fig. 3. Examples of CSR identified during the survey. (A) CSR network exposed in front of Keilhaubreen, South Spitsbergen. (B) CSR melting out of a small cirque in Firkantdalen, glacier coded *SS*-10. (C) Foreland of Kolfjellbreen, Central Spitsbergen, with CSR oblique to streamlined flow direction. (D) CSR network in the foreland of Kjerulfbreen, NW Spitsbergen. Field images of the same CSR network are presented in (Fig. 1D), marked by white box. Aerial images of glacier forelands modified from TopoSvalbard provided by the Norwegian Polar Institute.

4. Results

Using aerial images from 2008 to 2012, CSRs have been identified in the forelands of 431 glaciers that have previously not been documented to exhibit surge behavior. The CSRs have been identified in the front of undocumented surge-type glaciers in each of the six subregions of Svalbard: 164 in NW Spitsbergen, 55 in NE Spitsbergen, 2 in Nordaustlandet, 40 in central Spitsbergen, 42 in the Barentsøya/Edgeøya region, and 128 in south Spitsbergen. Of these six regions the range in the number of glaciers with CSR is wide. This variability is likely caused by numerous factors including not only the amount of glaciated terrain but also the number of active ice margins.

The crevasse squeeze ridges that have been identified in each of the 431 glacier forelands often are present in networks and commonly align transverse to ice flow but can in some cases form longitudinally as well (Fig. 3). The CSRs most often occur on basal till plains accompanied by, but perpendicular to, streamlined features like flutes, crag and tails, as well as the occasional eskers and drumlins (Fig. 3). Most of the CSR identified are located in the inner zone with some potentially transitioning into the intermediate zone of the surge-type glacier land system (Schomacker et al., 2014). At some glacier forelands the ridges were infrequent, melting out of the ice front or poorly preserved, making interpretation more difficult (Fig. 3B).

The CSR are predominantly distributed around outlet glaciers where forelands have been exposed during the twentieth century ice retreat. This is in slight contrast to the documented (black dots) surge glaciers that in some cases are located at higher elevations, up on ice caps or terminating in fjords, without exposed forelands (Fig. 4). This variation in distribution is a result of the different methods used for identifying surge behavior. Crevasse squeeze ridges have been interpreted from fjord bathymetry (Flink et al., 2015; Lovell et al., 2015b), and many tidewater glaciers have relatively long observation histories (Liestøl, 1993). Surging tributary glaciers at higher elevations have been mainly identified by geodetic changes (Sund et al., 2009). In theory CSR can form and preserve at higher elevations, but the limiting factor seems to be the sediments at the glacier bed. Lønne (2016) discusses how variations in available sediment and deformable beds can aid or hinder the preservation of sediment morphology. Lønne (2016) describes 'Type B′ glaciers as land-terminating basins with poorly deformable substrate and low probability of proglacial moraine formation because of the coarse-grained debris. She notes that in these types of basins, the glacier debris rapidly transforms to alluvial or colluvial facies (Lønne, 2016). This type of glacier seems to correspond to higher alpine basins that do not form CSRs despite documented surge advances.

The lowest value of forelands with CSR was identified in the Nordaustlandet region. Despite Nordaustlandet having the most extensive ice cover, it has relatively few active ice margins, especially compared to regions like NW and south Spitsbergen. A significant portion of the land-terminating ice caps on Nordaustlandet appear to have cold, passive margins owing to the cold dry climate and relatively low topography. Passive, cold-based margins are visible in aerial imagery of the region where widespread patterned ground and beach ridges are melting out from the nonerosive ice margins. The CSRs are present in front of active glacier margins, but under modern conditions very few land-terminating margins appear to be active. The exposure of preserved beach ridges from the retreating ice margins may suggest that these terrestrial margins are not only passive today but may have been throughout the Holocene. Where the number of glaciers with CSR in most regions greatly exceeded the number of documented

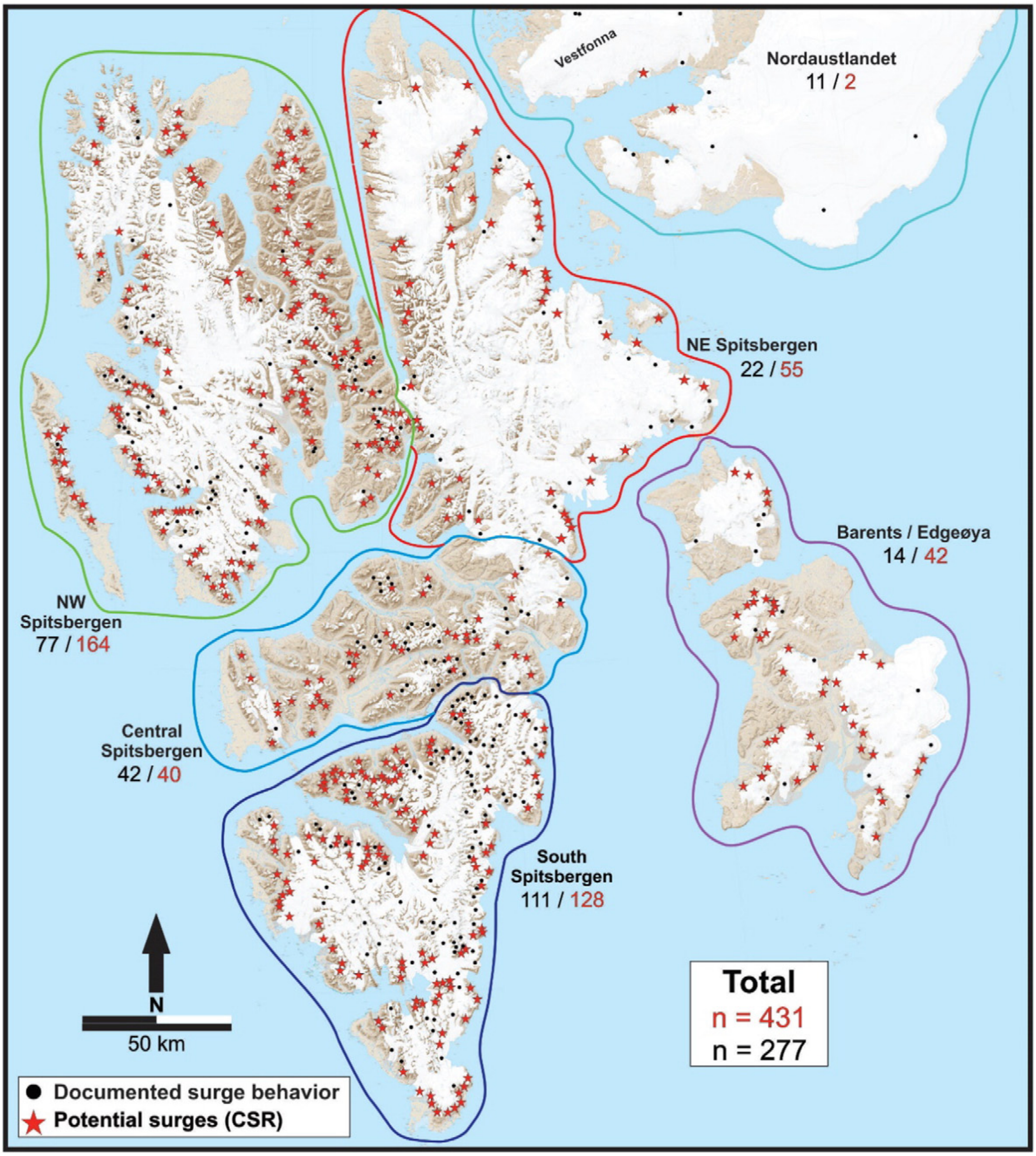

Fig. 4. Map of Svalbard divided into six subregions. Black dots indicate documented surge-type glaciers introduced in Fig. 2B. Red stars mark surge-type glaciers identified by the presence of CSRs in their forelands. Base map modified from TopoSvalbard provided by the Norwegian Polar Institute. The three upper black dots on Vestfonna are slightly offset on the map and correspond to glaciers to the north of map view; Søre Franklinbreen, Nordre Franklinbreen, and Rijpbreen (from west to east).

surge-type glaciers, central Spitsbergen (like Nordaustlandet) displayed a relatively low number of forelands with CSR, compared to the number of documented surge glaciers (Fig. 4; Table 1). This relatively low number is most likely a result of glacier front observations being much more common around the settlements of Spitsbergen and if a glacier front were to advance rapidly it would be less likely to go unnoticed.

Table 1
Distribution of CSR by region compared to documented surge events.

Regions	NW Spits.	NE Spits.	Nordaust.	Cent. Spits.	B/E-øya	S. Spits.	Total
Doc. surges	77	22	11	42	14	111	277
CSR	164	55	2	40	42	128	431
Total surges	241	77	13	82	56	239	708

A great number of forelands with CSR were identified in NW Spitsbergen and in south Spitsbergen with 164 and 128, respectively (Table 1). These high values may relate to the obvious abundance of active ice margins and retreating glacier fronts exposing fresh forelands. The high concentration could also suggest optimal conditions for CSR formation or preservation, like deformable substrate.

The CSRs were identified in the forelands of roughly two-thirds of the previously documented surge-type glaciers. The remaining one-third of the documented surge glacier forelands may lack CSR owing to a number of factors. Although a glacier has been documented to surge, the glacier (i) could be a tributary to a larger glacier, (ii) may terminate subaqueously, (iii) may not have preserved the CSR, or (iv) the landforms may not have formed because of other controls. In two forelands where CSRs were not identified, poor visibility or lack of aerial imagery made analysis impossible (Andrinebreen and Elfenbeinbreen, respectively).

5. Discussion

The CSRs and concertina eskers are thought to be unique signatures of surge-type glaciers (Sharp, 1985b; Benn and Evans, 2010; Rea and Evans, 2011). However, Evans et al. (2012) suggested that CSRs and concertina eskers identified in the foreland of Hørbyebreen, Svalbard, could have formed from meltwater pulses in a nonsurging polythermal glacier, driven by the buildup and release meltwater reservoirs. They conclude that the mapped Hørbyebreen land system does not agree with a surge-type glacier land system (Evans and Rea, 2003) and consequently provides an alternative explanation for the observed CSR and concertina eskers. We do not agree with this interpretation of Evans et al. (2012). A looped medial moraine is visible in the Norwegian Polar Institute 1936 oblique aerial image of Hørbyebreen, suggesting that the glacier has exhibited surge-type behavior. Consequently, our interpretation of the CSR and concertina eskers as landforms derived from a surge event is a simpler explanation for their origin than the interpretations of Evans et al. (2012).

The distribution of surveyed CSR reflects the formation and preservation of the landforms as well as indirectly the limits of the method. The remote sensing method only allows for the analysis of the exposed terrestrial landscape. Thus subaqueous forelands and tributary glacier systems are not effectively evaluated in this method as CSR could potentially exist but are not visible in aerial imagery. Some glaciers may have documented surge behavior yet do not exhibit CSRs that are exposed terrestrially. In Nordaustlandet, 9 of the 11 documented surge-type glaciers (82%) do not have CSR (Table 2). These glacier systems predominantly exhibit marine termini. The south Spitsbergen region also exhibits a large amount of marine-terminating glaciers, but the relatively high percentage of documented glaciers without CSRs (36%) is also a function of the minimal foreland exposure as many of the glaciers are tributary systems (Table 2).

Another region with a high percentage of documented surge glaciers without CSR is in central Spitsbergen, where nearly 50% of the glaciers lack CSR (Table 2). Unlike Nordaustlandet and the south Spitsbergen regions, which are predominantly tributaries or marine terminating systems, these glaciers are small cirques that suggest that glacier size is a critical control in the formation of CSR. Brynjólfsson et al. (2012), suggested that CSRs are only identified on rare occasions in front of small cirque glaciers in alpine settings in Iceland. In the survey of glacier forelands in central Spitsbergen, numerous small glaciers exhibited relatively massive and extensive ice-cored moraines that currently correspond to small, near-empty cirques, consistent with the land system model of small surge-type cirque glaciers (Brynjólfsson et al., 2012).

Despite glaciers needing to be of a minimum critical mass to form CSRs, the method is most effective with glaciers up to a certain size. The limiting factor of this method is exposed foreland which can be controlled by the size of a glacier, the length of a surge cycle, and the general sensitivity/response of the glacier system. For example, this method has been optimal for Svalbard because of the extended surge cycles characteristic of the region and the twentieth century warming driving significant retreat throughout the Arctic region (Dowdeswell et al., 1991; Nuth et al., 2007). The CSR method may not be as successful in the Karakoram, where glaciers are significantly larger, surge cycles are shorter, and the debris-covered snouts are less sensitive to ablation (i.e. slow response time; Copland et al., 2011; Paul, 2015). Crevasse squeeze ridges are indirectly constrained by elevation as it seems deformable substrate (Lønne, 2016) and glacier sensitivity are limiting factors. Although it would be interesting to see if CSRs can be identified in regions like the Karakoram (given the importance of size, cyclicity, and sensitivity of surge-type glaciers), the CSR method would most likely be more effective in other surge hotspot regions like Iceland, Alaska-Yukon, and Novaya Zemlya (Sevestre and Benn, 2015).

The constraints and limiting factors on CSR formation still remain poorly understood. Numerous factors could influence the formation of CSRs, such as till grain-size distribution and effective pore-water pressures. Future studies should focus on whether the lack of CSR in the surge forelands is a function of preservation or CSR simply not forming because of topographic or basal sediment conditions. Focusing on potential characteristics that govern the distribution of CSRs (geology, bed conditions, and glacier size) would develop a better understanding of landform distribution and formation. Self-organizing maps (Kohonen, 2001) have been highlighted as a valuable technique for analyzing subtle relationships between disparate data sets (Fraser and Dickson, 2007). Although traditionally developed for finance, an increasing number of geoscience studies are using self-organizing maps, for example, to explore the relationship between streamlined glacial bedforms and the geological setting of the features (Dowling, 2016).

Once the CSRs are formed, their preservation potential is relatively poor. The foreland of a retreating glacier (especially one that has surged) is a chaotic and unstable environment, where ice-cored terrain, glaciofluvial outwash, and high pore-water pressure in saturated sediments result in an environment that is susceptible to reworking and degradation (Schomacker and Kjaer, 2007, Schomacker and Kjær, 2008). The formation and origins of CSR make them susceptible to degradation, and as a landform they have a relatively low preservation potential. The landforms need to survive the initial deglaciation phase, when the ridges are exposed and highly susceptible to meltwater. They are subsequently exposed to periglacial processes where glacial terrain become reworked by frost weathering, slope processes, and degrading dead-ice bodies (Humlum et al., 2003; French, 2007; Schomacker and Kjaer, 2007, Schomacker and Kjær, 2008; Brynjólfsson et al., 2012).

Thus, like other surge landforms, CSRs have a low preservation potential, but the window of time they can be used as surge indicators is notably later in the surge cycle than looped moraines or timelines. Of all the CSR surveyed, the majority formed around or within the last century and the landforms mostly have been exposed within the last 50 years or less depending on the size and sensitivity of the glacier systems. Accordingly, Ingólfsson et al. (2016) pointed out that absence of a surge-type glacier land system does not unconditionally mean that a given glacier has not surged in the past.

6. Conclusions

- This study concludes that the CSR survey is a simple, yet effective method for remotely identifying probable surge behavior. The CSRs have been identified in the forelands of 431 glaciers on Svalbard that have not previously been identified as surge-type.
- This contribution is suggested to be a minimum estimate of glaciers that exhibit surge behavior on Svalbard because the presence of the CSR suggests surge behavior, but the lack of CSR in a foreland does not mean nonsurge behavior. Additionally, of the documented surge-type glaciers, CSRs are only visible in ca. 60% of their forelands.
- The study utilizes open access data and remote sensing techniques to further knowledge of the presence and distribution of surge behavior in Svalbard.
- Results confirm a high density, but still unknown quantity of glaciers that exhibit surge behavior on Svalbard, at least through the late Holocene.
- Sedimentological studies of CSRs (including grain-size properties and fabric analysis) are necessary to highlight the detailed processes of their formation. Additional focus could be placed on cross-cutting relationships of landforms in forelands to decipher their genesis in the subglacial environment.

Acknowledgements

We would like to recognize three anonymous reviewers and the editing staff for providing constructive comments and improving the manuscript. The authors additionally thank Kurt H. Kjær, Markus

Table 2
Distribution of documented surges by region without CSR.

Regions	NW Spits.	NE Spits.	Nordaust.	Cent. Spits.	B/E-øya	S. Spits.	Total/Avg.
Doc. surges	77	22	11	42	14	111	277
Doc. w/o CSR	14	4	9	20	1	40	88
Percent w/o CSR	18	18	82	48	7	36	32

Eckerstorfer, Harold Lovell, Heïdi Sevestre, and Lena Håkansson for feedback and constructive discussions.

Appendix A. Supplementary data

Refer to supplementary Table 1 for documented surge-type glaciers and supplementary data Table 2 for previously undocumented glaciers presented in this study. Supplementary data associated with this article can be found in the online version, at http://dx.doi.org/10.1016/j.geomorph.2016.03.025.

References

Aschwanden, A., Bueler, E., Khroulev, C., Blatter, H., 2012. An enthalpy formulation for glaciers and ice sheets. J. Glaciol. 58 (209), 441–457.
Benn, D.I., Evans, D.J.A., 2010. Glaciers and Glaciations. Hodder Education, London.
Bjarnadóttir, L.R., 2007. Ice-marginal Environments of Surging Glacier: Distribution, Formation and Morphological Evolution of Flutes and Crevasses Cast Ridges at Brúarjökull, Iceland M.S. Thesis University of Iceland, Reykjavik.
Björnsson, H., 1998. Hydrological characteristics of the drainage system beneath a surging glacier. Nature 395 (6704), 771–774.
Błaszczyk, M., Jania, J.A., Hagen, J.O., 2009. Tidewater glaciers of Svalbard: recent changes and estimates of calving fluxes. Polish Polar Research 30 (2), 85–142.
Brynjólfsson, S., Ingólfsson, Ó., Schomacker, A., 2012. Surge fingerprinting of cirque glaciers at the Trollaskagi peninsula, North Iceland. Jökull 62, 151–166.
Christiansen, H.H., Etzelmuller, B., Isaksen, K., Juliussen, H., Farbrot, H., Humlum, O., Johansson, M., Ingeman-Nielsen, T., Kristensen, L., Hjort, J., Holmlund, P., Sannel, A.B.K., Sigsgaard, C., Akerman, H.J., Foged, N.N., Blikra, L.H., Pernosky, M.A., Odegard, R.S., 2010. The thermal state of permafrost in the Nordic area during the International Polar year 2007–2009. Permafr. Periglac. Process. 21 (2), 156–181.
Christoffersen, P., Piotrowski, J.A., Larsen, N.K., 2005. Basal processes beneath an Arctic glacier and their geomorphic imprint after a surge, Elisebreen, Svalbard. Quat. Res. 64 (2), 125–137.
Clarke, G.K.C., Collins, S.G., Thompson, D.E., 1984. Flow, thermal structure, and subglacial conditions of a surge-type glacier. Can. J. Earth Sci. 21 (2), 232–240.
Copland, L., Sylvestre, T., Bishop, M., Shroder, J., Seong, Y., Owen, L., Bush, A., Kamp, U., 2011. Expanded and recently increased glacier surging in the karakoram. Arct. Antarct. Alp. Res. 43 (4), 503–516.
D'Andrea, W.J., Vaillencourt, D.A., Balascio, N.L., Werner, A., Roof, S.R., Retelle, M., Bradley, R.S., 2012. Mild Little Ice Age and unprecedented recent warmth in an 1800 year lake sediment record from Svalbard. Geology 40 (11), 1007–1010.
Dickson, R.R., Osborn, T.J., Hurrell, J.W., Meincke, J., Blindheim, J., Adlandsvik, B., Vinje, T., Alekseev, G., Maslowski, W., 2000. The Arctic Ocean response to the North Atlantic Oscillation. J. Clim. 13 (15), 2671–2696.
Dowdeswell, J.A., Hamilton, G.S., Hagen, J.O., 1991. The duration of the active phase on surge-type glaciers: contrasts between Svalbard and other regions. J. Glaciol. 37 (127), 388–400.
Dowdeswell, J.A., Hodgkins, R., Nuttall, A.M., Hagen, J.O., Hamilton, G.S., 1995. Mass balance change as a control on the frequency and occurrence of glacier surges in Svalbard, Norwegian High Arctic. Geophys. Res. Lett. 22 (21), 2909–2912.
Dowdeswell, J.A., Unwin, B., Nuttall, A.M., Wingham, D.J., 1999. Velocity structure, flow instability and mass flux on a large Arctic ice cap from satellite radar interferometry. Earth Planet. Sci. Lett. 167 (3–4), 131–140.
Dowdeswell, J.A., Benham, T.J., 2003. A surge of Perseibreen, Svalbard, examined using aerial photography and ASTER high resolution satellite imagery. Polar Res. 22 (2), 373–383.
Dowling, T.P.F., 2016. The Drumlin Problem — Stream-lined Bedforms in Southern Sweden Ph.D. Thesis University of Lund, Lund.
Evans, D.J.A., Rea, B.R., 1999. Geomorphology and sedimentology of surging glaciers: a land-systems approach. Ann. Glaciol. 28 (1), 75–82.
Evans, D.J.A., Rea, B.R., 2003. Surging glacier landsystems, in glacial landsystems. In: Evans, D.J.A. (Ed.), Glacial Landsystems. Arnold, London, pp. 259–284.
Evans, D.J.A., Strzelecki, M., Milledge, D.G., Orton, C., 2012. Hørbyebreen polythermal glacial landsystem, Svalbard. J. Maps 8 (2), 146–156.
Ferguson, A., Ferguson, J.J.M., van der Meer, J.J.M., Benediktsson, Í.Ö., Schomacker, A., Andersson, T., 2009. The sedimentological and glaciological relationships between tills, flutes and crevasse-fill ridges during a surge, Eyjabakkajökull, Iceland. European Geoscience Union General Assembly, 2009, Vienna Austria.
Flink, A.E., Noormets, R., Kirchner, N., Benn, D.I., Luckman, A., Lovell, H., 2015. The evolution of a submarine landform record following recent and multiple surges of Tunabreen glacier, Svalbard. Quat. Sci. Rev. 108, 37–50.
Fowler, A.C., Murray, T., Ng, F.S.L., 2001. Thermally controlled glacier surging. J. Glaciol. 47 (159), 527–538.
Fraser, S., Dickson, B., 2007. A new method for data integration and intergrated data interpretation: self-organizing maps. In: Milkereit, B. (Ed.), Fifth Decennial International Conference of Mineral Exploration, pp. 907–910.
French, H.M., 2007. Periglacial Climates, The Periglacial Environment. John Wiley & Sons Ltd, Chichester, pp. 31–46.
Førland, E.J., Hanssen-Bauer, I., Nordli, P.Ø., 1997. Climate statistics and longterm series of temperature and precipitation at Svalbard and Jan Mayen. DNMI rapport 21/97 Klima.
Glasser, N.F., Huddart, D., Bennett, M.R., 1998. Ice-marginal characteristics of Fridtjovbreen (Svalbard) during its recent surge. Polar Res. 17 (1), 93–100.
Grant, K.L., Stokes, C.R., Evans, I.S., 2009. Identification and characteristics of surge-type glaciers on Novaya Zemlya, Russian Arctic. J. Glaciol. 55 (194), 960–972.
Hagen, J.O., Liestol, O., Roland, E., Jørgensen, T., 1993. Glacier Atlas of Svalbard and Jan Mayen. Norsk Polarinstitutt Meddelelser 129, 1–141.
Hagen, J.O., Kohler, J., Melvold, K., Winther, J.-G., 2003. Glaciers in Svalbard: mass balance, runoff and freshwater flux. Polar Res. 22 (2), 145–159.
Hamilton, G.S., 1992. Investigations of Surge-type Glaciers in Svalbard Ph.D. Thesis University of Cambridge, Cambridge.
Hansen, S., 2003. From surge-type to non-surge-type glacier behaviour: Midre Lovénbreen, Svalbard. Ann. Glaciol. 36, 97–102.
Hanssen-Bauer, I., Solås, M.K., Steffensen, E.L., 1990. The climate of Spitsbergen., Klima. The Norwegian Meteorological Institute, Oslo. 39 (90), 40.
Humlum, O., Instanes, A., Sollid, J.L., 2003. Permafrost in Svalbard: a review of research history, climatic background and engineering challenges. Polar Res. 22 (2), 25.
Ingólfsson, Ó., Benediktsson, Í.Ö., Schomacker, A., Kjær, K.H., Brynjólfsson, S., Jónsson, S.A., Korsgaard, N.J., Johnson, M.D., 2016. Glacial geological studies of surge-type glaciers in Iceland — research status and future challenges. Earth Sci. Rev. 152, 37–69.
Jiskoot, H., Boyle, P., Murray, T., 1998. The incidence of glacier surging in Svalbard: evidence from multivariate statistics. Comput. Geosci. 24 (4), 387–399.
Jiskoot, H., Murray, T., Boyle, P., 2000. Controls on the distribution of surge-type glaciers in Svalbard. J. Glaciol. 46 (154), 412–422.
Kamb, B., Raymond, C.F., Harrison, W.D., Engelhardt, H., Echelmeyer, K.A., Humphrey, N., Brugman, M.M., Pfeffer, T., 1985. Glacier surge mechanism: 1982–1983 surge of variegated glacier, Alaska. Science 227 (4686), 469–479.
Kjær, K.H., Korsgaard, N.J., Schomacker, A., 2008. Impact of multiple glacier surges—a geomorphological map from Brúarjökull, East Iceland. J. Maps 4 (1), 5–20.
Kohonen, T., 2001. Self-organizing Maps. Springer Series in Information Sciences, Berlin, p. 30.
Kristensen, L., Benn, D.I., 2012. A surge of the glaciers Skobreen-Paulabreen, Svalbard, observed by time-lapse photographs and remote sensing data. Polar Res. 31, 11106.
Lefauconnier, B., Hagen, J.O., 1991. Surging and Calving Glaciers in Eastern Svalbard. Norsk Polarinstitutt, Meddeleler, p. 116.
Liestøl, Ø., 1993. Glaciers of Svalbard, Norway. In: Williams, R.S., Ferrigno, J.C. (Eds.), Glacier of Europe in Satellite Image Atlas of Glaciers of the World. U.S. Geological Survey Professional Paper, 1386-*E*-5, pp. 127–151.
Lovell, H., Fleming, E.J., Benn, D.I., Hubbard, B., Lukas, S., Naegeli, K., 2015a. Former dynamic behaviour of a cold-based valley glacier on Svalbard revealed by basal ice and structural glaciology investigations. J. Glaciol. 61 (226), 309–328.
Lovell, H., Fleming, E.J., Benn, D.I., Hubbard, B., Lukas, S., Rea, B.R., Noormets, R., Flink, A.E., 2015b. Debris entrainment and landform genesis during tidewater glacier surges. J. Geophys. Res. Earth Surf. 120 (8), 1574–1595.
Lyså, A., Lønne, I., 2001. Moraine development at a small high-Arctic valley glacier: Rieperbreen, Svalbard. J. Quat. Sci. 16 (6), 519–529.
Lønne, I., 2016. A new concept for glacial geological investigations of surges, based on high-Arctic examples (Svalbard). Quat. Sci. Rev. 132, 74–100.
Masson-Delmotte, V., Schulz, M., Abe-Ouchi, A., Beer, J., Ganopolski, A., González Rouco, J.F., Jansen, E., Lambeck, K., Luterbacher, J., Naish, T., Osborn, T., Otto-Bliesner, B., Quinn, T., Ramesh, R., Rojas, M., Shao, X., Timmermann, A., 2013. Information from paleoclimate archives. Climate change 2013: The Physical science Basis. Contribution of Working Group I to the Fifth Assessment Report of the Intergovernmental Panel on Climate Change, pp. 383–464.
Meier, M.F., Post, A., 1969. What are glacier surges? Can. J. Earth Sci. 6 (4), 807–817.
Met.no, 2015d. In: Institute, N.M. (Ed.), eKlima. Norwegian Meteorological Institute http://www.eklima.no.
Morawski, W., 2005. Reconstruction of ice sheet movement from the orientation of glacial morpholineaments (crevasse landforms): an example from Northeastern Poland. Geol. Q. 49 (4), 403–416.
Nuth, C., Kohler, J., Aas, H.F., Brandt, O., Hagen, J.O., 2007. Glacier geometry and elevation changes on Svalbard (1936–90): a baseline dataset. Ann. Glaciol. 46 (1), 106–116.
Oerlemans, J., 2005. Atmospheric science: extracting a climate signal from 169 glacier records. Science 308 (5722), 675–677.
Paasche, Ø., Bakke, J., 2010. Defining the Little Ice Age. Clim. Past Discuss. 6 (5), 2159–2175.

Paul, F., 2015. Revealing glacier flow and surge dynamics from animated satellite image sequences: examples from the Karakoram. Cryosphere 9 (6), 2201–2214.
Rea, B.R., Evans, D.J.A., 2011. An assessment of surge-induced crevassing and the formation of crevasse squeeze ridges. J. Geophys. Res. Earth Surf. 116 (F4).
Rogers, J.C., Yang, L., Li, L., 2005. The role of Fram Strait winter cyclones on sea ice flux and on Spitsbergen air temperatures. Geophys. Res. Lett. 32 (6).
Røthe, T.O., Bakke, J., Vasskog, K., Gjerde, M., D'Andrea, W.J., Bradley, R.S., 2015. Arctic Holocene glacier fluctuations reconstructed from lake sediments at Mitrahalvøya, Spitsbergen. Quat. Sci. Rev. 109, 111–125.
Schomacker, A., Kjaer, K.H., 2007. Origin and de-icing of multiple generations of ice-cored moraines at Brúarjökull, Iceland. Boreas 36 (4), 411–425.
Schomacker, A., Kjær, K.H., 2008. Quantification of dead-ice melting in ice-cored moraines at the high-Arctic glacier Holmströmbreen, Svalbard. Boreas 37 (2), 211–225.
Schomacker, A., Benediktsson, Í.Ö., Ingólfsson, Ó., 2014. The Eyjabakkajökull glacial landsystem, Iceland: geomorphic impact of multiple surges. Geomorphology 218, 98–107.
Sevestre, H., Benn, D.I., 2015. Climatic and geometric controls on the global distribution of surge-type glaciers: implications for a unifying model of surging. J. Glaciol. 61 (228), 646–662.
Sevestre, H., Benn, D.I., Hulton, N.R.J., Bælum, K., 2015. Thermal structure of Svalbard glaciers and implications for thermal switch models of glacier surging. J. Geophys. Res. Earth Surf. 120 (10), 2220–2236.
Sharp, M., 1985a. "Crevasse-fill" ridges: a landform type characteristic of surging glaciers? Geografiska Annaler. Series A. Phys. Geogr. 67 (3/4), 213–220.
Sharp, M., 1985b. Sedimentation and stratigraphy at Eyjabakkajökull—an Icelandic surging glacier. Quat. Res. 24 (3), 268–284.
Sharp, M., 1988. Surging glaciers: behaviour and mechanisms. Prog. Phys. Geogr. 12 (3), 349–370.
Sletten, K., Lyså, A., Lønne, I., 2001. Formation and disintegration of a high-arctic ice-cored moraine complex, Scott Turnerbreen, Svalbard. Boreas 30 (4), 272–284.
Sund, M., Eiken, T., Hagen, J.O., Kääb, A., 2009. Svalbard surge dynamics derived from geometric changes. Ann. Glaciol. 50 (52), 50–60.
TopoSvalbard, 2016. In: Institute, N.P. (Ed.), TopoSvalbard. Norwegian Polar Institute (http://toposvalbard.npolar.no/).
Wanner, H., Solomina, O., Grosjean, M., Ritz, S.P., Jetel, M., 2011. Structure and origin of Holocene cold events. Quat. Sci. Rev. 30 (21–22), 3109–3123.
Werner, A., 1993. Holocene moraine chronology, Spitsbergen, Svalbard: lichenometric evidence for multiple Neoglacial advances in the Arctic. The Holocene 3 (2), 128–137.
Yde, J.C., Paasche, Ø., 2010. Reconstructing climate change: not all glaciers suitable. EOS Trans. Am. Geophys. Union 91 (21), 189–190.

Chapter V

Holocene glacial and climate history of Svalbard - status, perspectives and challenges

Farnsworth, W.R., Ingólfsson, Ó., Alexanderson, H., Forwick, M., Noormets, R., Retelle, M., Schomacker, A. (*in prep.*): Holocene glacial and climate history of Svalbard - status, perspectives and challenges.

The cold-based, alpine ice cap, Bassen, northern Adventdalen, central Spitsbergen.

Holocene glacial and climate history of Svalbard - status, perspectives and challenges

Wesley R. Farnsworth [1, 2*] Ólafur Ingólfsson [1, 3] Helena Alexanderson [4], Matthias Forwick [2] Riko Noormets [1], Michael Retelle [5] Anders Schomacker [2]

[1]*Department of Arctic Geology, University Centre in Svalbard, UNIS Longyearbyen Norway* [2]*Department of Geoscience, UiT, The Arctic University of Norway, Tromsø Norway*
[3]*Institute of Earth Sciences, University of Iceland, Askja, Sturlugata 7, IS-101 Reykjavík, Iceland*
[4]*Department of Geology, Lund University, Sölvegatan 12, Lund 223 62, Sweden*
[5]*Department of Geology, Bates College, Lewiston Maine USA*

*Corresponding Author:
Wesley R. Farnsworth
WesleyF<a>unis.no

KEYWORDS:
Holocene, Spitsbergen, Neoglacial, Little Ice Age, glaciers, climate.

Manuscript remains in preparation until database is finalized and ArcGIS supplement is completed.

ABSTRACT:
This study is a review of published literature of Holocene glacier and climate history from Svalbard and its surrounding waters. A database of (radiocarbon, terrestrial cosmogenic nuclide and optically stimulated luminescence) ages has been constructed, quality assessed and categorized by marine, terrestrial and lacustrine archive. Our review summarizes our understanding of glaciers and climate on Svalbard from the end of the Late Pleistocene (12.0 ka BP) to roughly the end of the Little Ice Age (LIA) as well as addresses gaps in our current knowledge. We (1) present a brief summary of major shifts in climate and ice cover across the Svalbard region throughout the Holocene; (2) introduce a quality assessed database of published ages that constrain glacier fluctuations (deglaciation, ice free, re-advance and marginal position) and climatic characteristics (warming ocean and ice cover expansion); (3) discuss challenges in methodology as well as potentials regarding sedimentary archives and finally (4) address the complexities of glacier systems and their dynamics in response to changes in climate. Furthermore, we identify some of current unknowns and propose possible prospects in order to approach these challenges in future studies.

INTRODUCTION

Syntheses of accumulated field and geochronology data are prerequisite for putting new observations in context as well as re-assessing existing interpretations (Hughes *et al.* 2016). Empirical constraints are critical for developing and calibrating models that simulate palaeoclimate as well as past glacier dynamics and processes (Patton *et al.* 2017). Within this context, we synthesize published literature of Holocene glacier and climate history from the Svalbard archipelago and its surrounding waters. We introduce a database of empirical data specific to the Svalbard region as well as summarize the prominent climatic shifts and glacier fluctuations through the last 12,000 years (Fig. 1).

The onset of the Holocene period (at 11.7 ka BP) marks a rapid transition from the end of the Pleistocene, characterized by a relatively cold period known as the Younger Dryas (YD), to the subsequent warmer interglacial conditions (Dansgaard *et al.*, 1989; Wanner *et al.*, 2008 Cohen *et al.* 2018). The global climate during the Holocene has traditionally been regarded as relatively stable, compared to the preceding Late Pleistocene (Dansgaard *et al.* 1993; Steffensen *et al.* 2008; Rockström *et al.* 2009), but this paradigm of a relatively uneventful Holocene is being increasingly challenged (Bond *et al.* 2001; Mayewski *et al.* 2004; Wanner *et al.* 2011). Reviews of Holocene climate and glacier oscillations have been synthesized globally (e.g. Solomina *et al.* 2015) as well as compiled for numerous Arctic and Alpine regions including the European Alps, Iceland, Arctic Canada and Greenland (Ivy-Ochs *et al.* 2009; Guðmundsson 1997; Geirsdóttir *et al.* 2009; Briner *et al.* 2016).

In the north Atlantic, the Holocene climate has displayed a range of variability and fluctuations between warm and cold as well as humid and dry conditions on the multidecadal to multicentennial timescale (Mayewski *et al.* 2004; Wanner *et al.* 2011). A phrase coined ‘polar amplification’ refers to the sensitivity of Arctic regions to these climatic fluctuations and how these areas are greatly affected by small shifts in temperature and precipitation (Masso-Delmotte *et al.* 2013). By studying the rate and magnitude of past changes in climate we are able to better understand current climate dynamics, as well as more effectively predict antecedent climate scenarios (McKay & Kaufman 2014).

This review summarizes the state of the art of glaciers and climate on Svalbard from the end of the Pleistocene to shortly after the end of the Little Ice Age (LIA) as well as addresses gaps in our current knowledge. While the end of the end of the Pleistocene and the Holocene with its three sub-divisions are defined (Greenlandian = Early, Northgrippian = Mid and Meghalayan = Late), the review targets the time interval up until the early 20th century when a temperature record began in central Spitsbergen (Cohen et al. 2013; updated; Christiansen et al. 2013).

Fig. 1 Location maps with A) inset map of the North Atlantic region with the Svalbard archipelago framed in black box. B) Overview map of Svalbard identifying key islands and regions. The warm West Spitsbergen Current (wsc) runs up along Svalbard's western margin while the cool East

Spitsbergen Current (esc) traces down and around from the east. Figure maps modified from IBCAO and TopoSvalbard, respectively.

We reconstruct Svalbard glacier and climate history by synthesizing geochronological data presented in published manuscripts detailing Holocene sedimentary archives (marine, terrestrial and lacustrine) and landforms. Our synthesis leads us up to the earliest historical ice front observations from Svalbard, and puts this accumulated Holocene data and observations in context with the ever-developing understanding of ice dynamics and the Arctic climate system. Thus, we strive to not only distinguish spatial trends in ice expansion of Svalbard glaciers and ice caps through the Holocene, but to correlate phases of ice-expansion with climatic periods, internal glacial processes, sea-level fluctuations, or some form of combination. Understanding how Arctic climate has fluctuated through the Holocene can provide insight as to how future changes may influence glaciers, sea level and potential environmental conditions.

Svalbard has a long and rich history of scientific observations. The first field observations of Svalbard coincide with the earliest undisputed discovery of "Spitsbergen" by Willem Barentsz in 1596 (Clasezoon 1598; Hacquebord 1995; Arlov 2005). Although early settlers were initially drawn north to the coasts of Svalbard for hunting, whaling and trapping, by the mid-1800s scientific expeditions began accumulating detailed observations of the landscape, climate and ice-cover around the archipelago (Lottin *et al.* 1842; Bertrand 1852). In the mid-19th century numerous international scientific expeditions visited Svalbard eventually culminating in the first International Polar Year in 1882-1883 (Ekholm *et al.* 1887; Fig. 2). Through the last c. 150 years, the Svalbard archipelago has become a natural laboratory for observing the landforms, processes and dynamics of glaciers as well as the terrain which ice masses have shaped through the Quaternary (Holmström 1865; Ingólfsson 2011; Ingólfsson & Landvik 2013). The bulk of this work has focused on constraining the growth and break-up of the marine-based Svalbard-Barents Sea ice sheet in time and place (SBSIS; Boulton 1979; Blake 1962; Österholm 1990; Landvik *et al.* 1998; Mangerud *et al.* 1998; Hormes *et al.* 2013; Ingólfsson & Landvik 2013; Hughes *et al.* 2016). These reviews have predominantly focused on the Last Glacial Maximum (LGM) ice configuration, timing and disintegration and for clarity have often excluded data younger than the last termination. In several cases, studies of postglacial sea level and subsequent isostatic uplift have been used to better understand LGM ice cover and previous centers of mass, which indirectly has summarized chronological shoreline development through the Holocene (e.g. Salvigsen *et al.* 1981; Forman *et al.* 1990; Bondevik *et al.* 1995; Forman *et al.* 2004).

Holocene studies have long targeted unknowns of the glacier and climate history of Svalbard. Our synthesis addresses the following outstanding research questions: (1) is there evidence of Younger Dryas cooling and glacier re-advances on Svalbard? (2) Did meltwater from the collapsing Laurentide Ice Sheet (LIS) influence climate on Svalbard during the 8.2 ka BP event? (3) When was the Holocene (glacial) minimum and how extensive was the ice-cover during this period? (4) When was ice-cover the most extensive during the Holocene period and was the Little Ice Age the climax of the Neoglacial during the Late Holocene? (5) Which sedimentary archives provide the best detail of Holocene glaciers and climate? (6) To what extent has ice dynamics and surge-type behavior influenced Holocene glacier fluctuations on Svalbard?

Setting

Located along the dominant corridor of atmospheric moisture between the Atlantic and the Arctic Basin, Svalbard spans from 74° – 81° N (Fig. 1; Drange *et al.* 2005). At present, glaciers and ice caps cover roughly 57 % of the archipelago (Nuth *et al.* 2013). The region has a sensitive climate due to its position at the northern extent of the North Atlantic Drift (West Spitsbergen Current; Fig. 1) and the southern border of the Arctic sea ice front (Rogers *et al.* 2005). Svalbard is categorized as having a dry High Arctic climate with periglacial conditions, extreme winter temperatures and warm continuous permafrost (French 2007; Christiansen *et al.* 2010).

Fig. 2. Photograph taken in Trygghamna in 1908 by Oscar Halldin. Glaciers Protektorbreen and Harrietbreen with ice-margins calving into the bay beyond Swedish Expedition Ships. From (De Geer 1908).

Despite its high northern latitude, Spitsbergen currently experiences a relatively mild climate where the warm West Spitsbergen Current travels off the western extent of Svalbard and influences weather and sea ice (Førland *et al.* 1997). Regional climate is directed by the interactions between the Icelandic Low and Siberian High pressure systems and as a result high temperatures are driven north over Svalbard by the main North Atlantic cyclone track (Hanssen-Bauer *et al.* 1990). Svalbard precipitation is closely coupled to the mode of the North Atlantic Oscillation (NAO; Dickson *et al.* 2000) and falls predominantly in solid form. The interactions of these air masses along the western flank of the archipelago now commonly drive winter conditions with warmer and wetter climate than normally expected as such latitudes (Førland *et al.* 1997; Eckerstorfer & Christiansen 2011).

Sedimentary archives, landforms and geological reconstructions

Holocene reconstructions of glaciers and climate represent a mosaic of data developed through a suite of sedimentary archives and landforms present in both marine and terrestrial environments. The different stratigraphic archives used to reconstruct glacier and climate history include terrestrial geological sections, marine sediment cores and threshold-lake records (Fig. 3). Geophysical data such as ground penetrating radar or chirp sub-bottom acoustic records can be paired with sediment cores and terrestrial stratigraphy, to extrapolate across larger areas. Additionally, the relative (and absolute) age of landforms and their cross-cutting relationships identified in submarine and subaerial data (marine bathymetry and aerial imagery) are used to reconstruct past glacier extent and other environmental conditions like relative sea level (Fig. 3). Despite over ten studies from 12 different ice-cores taken across Svalbard, ice core stratigraphy is discussed, but is not the focus of this review given the relatively short and young cryostratigraphic record (less than 1 ka BP; Isaksson *et al.* 2005; Grinsted *et al.* 2006; Divine *et al.* 2011).

Methods

Compilation of Ages

Holocene geochronology from Svalbard and the surrounding waters that provide chronological evidence constraining glacier cover and marginal fluctuations or insight into climatic conditions over the last 12.0 ka were compiled into the SVALHOLA database (Table S1). Given the past variations in correction and calibration for the geochronological methods, we extent the databased to include ages in which mid-points of the 68th percentile fall below 12.0 ka BP as well as mid-points that fall above 12.0 ka yet error margins indicate the potential the ages is younger than 12.0 ka BP. Compiled ages and their meta-data were mined from scientific manuscripts, books, doctoral theses, geological reports (NP and Årsrapport / annual report from Oslo) and maps (Table 1). Dates obtained from compilations are cited as well as original source. To assure quality and consistency, ages from MSc. theses were excluded unless subsequently referenced in a peer-reviewed manuscript.

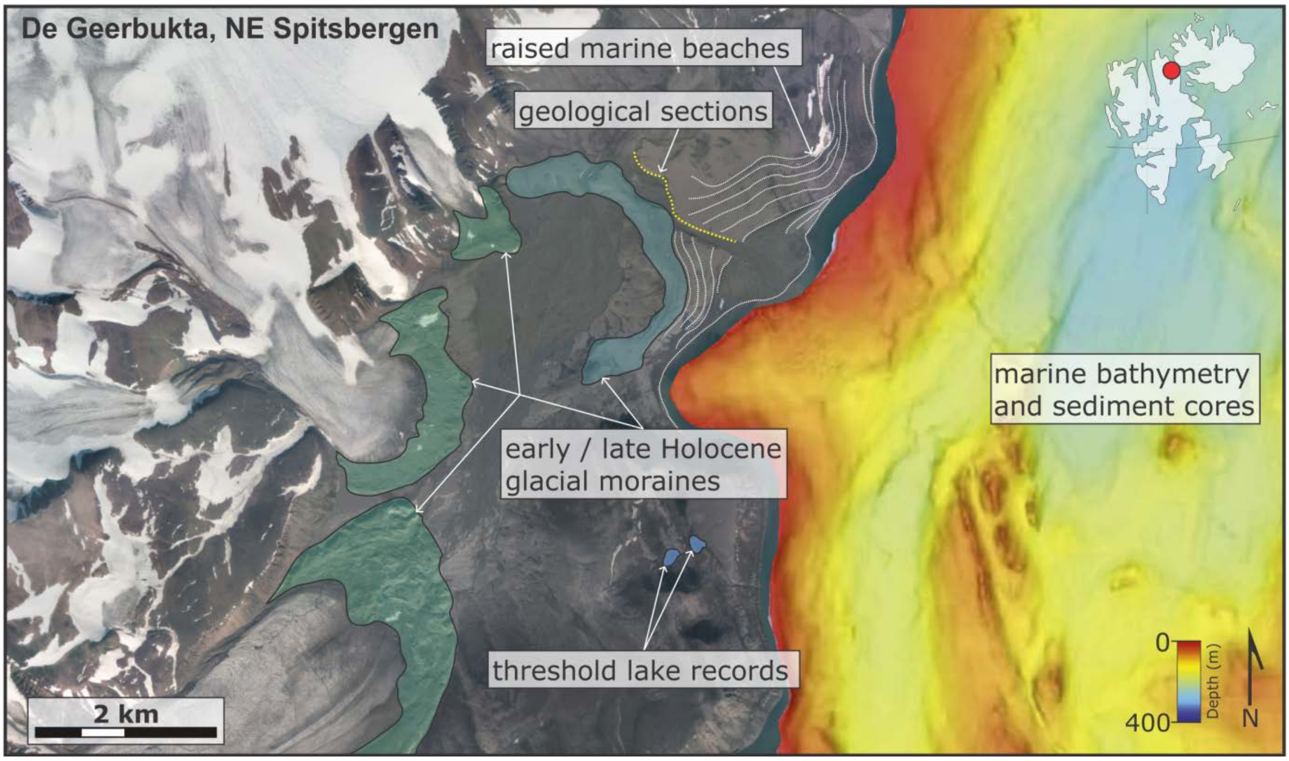

Fig. 3. Examples of Holocene landforms and sedimentary archives from De Geerbukta, NE Spitsbergen which provide insight into the glacial and climate history of Svalbard. Archives include marine, terrestrial and lacustrine records. Moraines formed on land or at the margin of a tidewater glacier have been identified and correspond to glacier re-advances. Raised marine sediments fingerprint post-glacial coastlines around Svalbard in some cases contain datable drift material (i.e. molluscs, whalebones and driftwood). Aerial images from TopoSvalbard and fjord bathymetry modified from Streuff et al. (2017).

The SVALHOLA database compiles previously published ages of radiocarbon (^{14}C, ^{14}C AMS, ^{14}C Conv.), luminescence (optically and infrared stimulated, OSL and IRSL) and terrestrial cosmogenic nuclide (TCN^{10}Be, TCN^{26}Al, TCN^{36}Cl). Given the scope of the review and the Holocene focus, dating methods like thermo-luminescence (TL), electron spin resonance (ESR), U series and ^{210}Pb have been omitted from the database. The database attempts to have a census date of 1 July 2018. We expect some published dates have been overlooked and hope any missing information can be updated and included in future versions of the SVALHOLA database.

Table 1. Presented metadata recorded for each date, included in the database (Table S1). Metadata from the database form the core of the criteria for quality assessment and palaeoglaciological classifications of each date as defined by the DATED1 database (Modified from Hughes *et al.* 2016).

SVALHOLA ID	-Unique database identification number
Location	-Country/sea, region, site name, SVALHOLA site number -Latitude and longitude co-ordinates: °N, °E (WGS84) -Comment on precision of location if not reported from original source.
Sample characteristics	-Site type: marine core, lake core, section, surface -Elevation (m a.s.l.) -Sample depth (m), if applicable
Dated material	-Sample field number and/or Laboratory ID number -Class of dated material: TPM (terrestrial plant macrofossils, including wood), organic (peat, detritus, bulk, mixed, aquatic macrofossils), bone (whalebone, tusks), shell (molluscs and mollusc fragments), foram (single species and mixed), sand, boulder, bedrock -Detailed description of dated material: free text -Organic material type: terrestrial (T), marine (M)
Stratigraphic context	-Detailed notes on stratigraphic setting: free text -Glacial context class: advance, margin, deglacial, ice free, exposure time (cumulative)
Dating method	-Radiocarbon (^{14}C, ^{14}C AMS, ^{14}C Conv.), optically stimulated luminescence (OSL), infrared stimulated luminescence (IRSL), terrestrial cosmogenic nuclide (TCN^{10}Be, TCN^{26}Al, TCN^{36}Cl) -Thermo-luminescence (TL), electron spin resonance (ESR), U series and Pb210 often fell out of the age range and scope of this review
Quality control	-Reliability of the age: 1 = reliable; 2 = possibly reliable; 3 = unlikely to be reliable (see Table 2 for criteria)
Ages	-Uncalibrated radiocarbon age / error (as reported, without correction for marine reservoir effect) -TCN age and error (as reported in source) -Calibrated/calendar age and error (reported to 1 SD). Radiocarbon ages calibrated to INTCAL13 or MARINE13 (Reimer *et al.* 2013) as appropriate (on basis of type of organic material: T/M). ^{10}Be and ^{26} Al TCN ages recalculated using 'Arctic' production rate (Young *et al.* 2013) and Lal/Stone scaling (Lal 1991; Stone 2000). Necessary information to recalculate ^{10}Be and ^{26}Al TCN ages using different production rates additionally collated and recorded in Table S3 -Comments on calibration (e.g. beyond calibration curve limit)
Comments	-Any additional pertinent comments (e.g. reliability of date)
Citation information	-Source reference (author, year) -Compilation reference (author, year) -Database reference (for ages also included in other datasets, e.g. (Hormes *et al.* 2013; Mangerud and Svendsen 2017))

Calibration of radiocarbon ages

To present and evaluate the SVALHOLA dataset consistently, all radiocarbon dates were recalibrated with INTCAL13 and MARINE13 calibration curves using the Calib Rev. 7.0.4 program (Reimer *et al.* 2013). Calibrated age ranges are included for both the 68 and 95% probability in the database. In accordance with the DATED1 database we use the mid-point ± half of the total range at 68% probability to represent the calendar age and uncertainty for each age in our review (Hughes *et al.* 2016). The ages presented in text and figures are calibrated median ages in kilo-years before present (cal. ka BP) unless otherwise clarified.

A marine reservoir age has been implemented for all marine samples by selecting 'MARINE13' and inputting a "Delta R" of 70 ± 30 (Table 1, S1; Mangerud & Svendsen 2017). Our chosen ΔR of 70±30 is specific for the Svalbard region (Mangerud *et al.* 2006; Mangerud & Svendsen 2017) and deviates from the DATED1 compilation, which for simplicity utilized a ΔR value of 0 for all marine samples from their reconstruction of the last Eurasian ice sheets (Hughes *et al.* 2016). Both radiocarbon ages and corrected ages are presented in the SVALHOLA data base (Table S1).

Recalculation of terrestrial cosmogenic exposure ages

Terrestrial cosmogenic exposure ages were (re-) calculated using the CRONUS-EARTH online calculator v3 (Balco *et al.* 2008; https://hess.ess.washington.edu) with the Arctic production rate calibration datasets (Young *et al.* 2013, 2014). An 'Lm' scaling (Lal 1991; Stone 2000) has been used in accordance with Youn *et al.* (2018). As argued by Hughes *et al.* and Young *et al.* (2016; 2018), no corrections have been made for post exposure uplift, erosion, or snow cover.

Calculation of luminescence ages

A luminescence age is calculated by determining the dose recorded by the grains and dividing it with the amount of dose received by the grains per unit of time (dose rate). The precision and accuracy of a luminescence age is dependent on a number of factors that affect these components and the largest uncertainties are typically related to geological factors rather than technical ones. For example, the dose rate is dependent on the amount of radioactive elements in the surrounding sediments, the water or ice content in the sediment as well as the depth below the ground surface (Rhodes 2011) and these factors must be measured and their changes through time estimated to arrive at an accurate age. The dose, on the other hand, can only be assumed to be correct if the resetting at the time of deposition was effective. If it was not, the grains are 'incompletely bleached' and some luminescence signal from a prior event remains, making the measured dose and resulting age appear too high (old). This is not uncommon in depositional environments where sediment transport is short, deposition occurs rapidly or in turbid water or other setting where light is limited (Fuchs & Owen 2008).

Experiments have shown that the TL signal bleaches more slowly than the IRSL signal which in turn is slower than the OSL signal (Godfrey-Smith *et al.* 1988; Alexanderson & Murray 2012a). In settings with limited light, it can therefore be argued that it is more likely that an OSL age gives a correct age than an IRSL or TL age. TL is nowadays considered less suitable for sediment dating and is not used much (Fuchs & Owen 2008; Wintle 2008); TL ages have therefore not been included in this compilation. For quality assessment criteria of OSL and IRSL ages, see Table 2. In the SVALHOLA database, ages are listed as presented in original publications (Table S2).

Consistency and quality assessment of dates

The SVALHOLA database consists of accumulated information acquired over the last 50 years. Dating techniques have developed over this period of time and the standard of what is considered "reliable" has risen (Hughes *et al.* 2016). We utilize the structure of the quality assessment criteria introduced in the DATED1 database (Table 2) to characterize the reliability of each age in the SVALHOLA database (Hughes *et al.* 2016). We have rated all ages depending on the dating technique on a 3-point system (quality 1-3) to rule-out potentially misleading ages. According to Hughes *et al.* (2016) a quality mark of; 1 = all criteria is met (likely reliable), 2 = some of the criteria are met but not all (probably reliable), 3 = no criteria are met (likely unreliable). Dates suggested being unreliable by original authors or other subsequent databases / compilations are rated quality 3. Dates of quality 1 and 2 standard have been used to reconstruct glacial and climate history while ages deemed quality 3 are presented in Table S1, but have been excluded from the developed reconstruction. We deviate from the DATED1 standard in one key aspect; sediment feeding marine molluscs (i.e. *Portlandia arctica*) are considered likely unreliable. Instead of receiving a lower rating, we strictly rate them as quality 3, thus excluding them from the reconstruction due to the high probability of an exaggerated age (England *et al.* 2013; Hughes *et al.* 2016).

Table 2. Age quality control criteria (based on Duller 2006, 2008; Thrasher *et al.* 2009; Wohlfarth 2009; Heyman *et al.* 2011; Alexanderson & Murray 2012b; England *et al.* 2013; Reimer *et al.* 2013). Ages within SVALHOLA are given a quality control (QC) rating based on the criteria specific to the dating method used. QC = 1, all criteria are satisfied; QC = 2, most of the criteria are satisfied; QC = 3 no (or few) criteria are satisfied (standard modified from Hughes *et al.* 2016).

Dating technique	Quality control criteria
Radiocarbon 14C Conv (Conventional), 14C AMS	-Known and uncontaminated sample material; sediment-feeding marine mollusc (e.g. Portlandia arctica) receives the lowest rating -Organic content >5% LOI -Sample composition: Conv - bulk samples not acceptable; AMS - bulk sample acceptable if age <20 ka -Within calibration range of INTCAL/MARINE13 -Uncalibrated 14C age determination provided with errors to enable recalibration using the latest calibration curves -Multiple and/or stratigraphically consistent ages
Terrestrial cosmogenic nuclide TCN 10Be, 26Al, 36Cl	-Multiple (ideally three or more, but at least two) samples from the same feature/site -Ages are internally consistent and clustered (reduced Chi-square value ~1) -Observed spread in ages is similar to expected measurement uncertainty -Geomorphological setting is accounted for: erosion, submergence, uplift -Data necessary to recalculate ages (10Be, 26Al) using different production rates (Balco *et al.* 2008) -No indication of isotopic inheritance, or if present expected/stated
Luminescence OSL, IRSL	-Quartz have a higher rating than feldspar-derived ages -Single-grain or small aliquot -Homogenous sample; preferably aeolian, fluvial, glacifluvial sediments that are likely to have received sufficient exposure. -Sample setting considered and accounted for; e.g. water-content history -Dose rate information and equivalent dose including errors described in source -Multiple and/or stratigraphically consistent ages
All dating methods	-Sample considered in situ, i.e. no post-depositional disturbance or reworking -Specified error margins -Precise ages: errors <10% of age -Details of geological and stratigraphical setting given -Considered by original authors to be reliable

Palaeoglaciological interpretation and climatic association of dates

We have simplified the palaeo-glaciolocical/climatological significance for a portion of the ages compiled in the SVALHOLA database based on metadata from the manuscripts or the author's suggestions presented in the different studies. We assume all radiocarbon ages are sampled from ice free conditions. In some cases, additional classifications are placed on the ages. We choose not to classify palaeo-glaciological / climatological significance of individual ages taken from marine or lacustrine cores, but address their chronologies as a whole in both the results and discussion.

Re-advance

Radiocarbon ages of dateable material (i.e. vegetation, shell or bone) that has been reworked or overridden by an advancing glacier are classified as maximum constraining ages for a glacier re-advance (Baranowski & Karlén 1976; Ronnert & Landvik 1995; Kristensen *et al.* 2009). In a study where numerous samples have been dated to constrain one glacier re-advance all ages are classified as a "re-advance" in the SVALHOLA database, but only the best constraining age (i.e. the youngest) is referred to in text and figures (Humlum *et al.* 2004; Table S1). Few Holocene glacier advances have been constrained in time by both maximum and minimum limiting ages (Lønne 2005; Farnsworth *et al.* 2018). Based on consideration by original authors ages classified as a "re-advance" are interpreted to correspond to a glacier fluctuation at or shortly following the mid-point of the youngest age (within the error margin).

Deglacial

Unlike previous reviews (Landvik *et al.* 1998; Ingólfsson & Landvik 2013; Hughes *et al.* 2016; Hogan *et al.* 2017) we choose not focus on the deglaciation in this paper. Furthermore, it is believed that most of the modern western and northern coastline of Spitsbergen had deglaciated by the onset of the Holocene (Hormes *et al.* 2013; Fig. 2a). In select locations we classify ages as "deglacial" where the site possesses stratigraphic information suggesting ice-free conditions shortly following ice-cover. Such dates include basal organic material from lake cores, the lowermost shells in marine cores from fjords and raised glacial marine sediments from fjord-heads (Alsos *et al.* 2015; Hald *et al.* 2004; Bartels *et al.* 2018; Farnsworth *et al.* 2018; Larsen *et al.* 2018). Additionally, the classification is used for radiocarbon ages of dateable material that has been sampled up-ice of modern margin (Blake 1989; Oerlemans *et al.* 2011) suggesting reduced ice-cover.

Margin

Although exposure age of erratic boulders is often used as an indication of the age of deglaciation (e.g. Hormes *et al.* 2011; 2013; Gjermundsen *et al.* 2013; Young *et al.* 2018), erratic boulder ages in the SVALHOLA database almost strictly target moraines and relate to an ice marginal position. Unlike ages association with a re-advance, where the youngest age is considered the best constraint, exposure ages corresponding to an ice margin often are presented in cumulative probability or in a histogram. The margin classification could also be used for a radiocarbon ages relating to an ice-contact delta.

Climatic associations

We assign associated climatic conditions to two types of radiocarbon samples, thermophile marine molluscs and terrestrial plants that have been entombed by (passive) ice (Mangerud and Svendsen 2017; Miller *et al.* 2017). We associate warm regional waters to thermophile marine molluscs

(TMM; *Arctica islandica, Mytilus edulis, Modiolus modiolus and Zirfaea crispata*) that have been sampled around Svalbard and radiocarbon date to different periods in the Holocene. The occurrence of these shallow marine molluscs, which are "effectively" extinct today, suggest warmer then present conditions and are indicators of the (marine) Holocene Thermal Maximum on Svalbard (Feyling-Hanssen 1955; Salvigsen *et al.* 1992; Hjort *et al.* 1995; Salvigsen 2002; Hansen *et al.* 2011; Farnsworth *et al.* 2017; Mangerud & Svendsen 2017).

We classify radiocarbon ages of terrestrial plants that have been entombed by (passive) ice as indicators of ice-cover expansion (ICE; Miller *et al.* 2017). These samples contrary to ages associated to a "re-advance" do not correspond to unique/specific glacier systems. Large populations of these ages sampled over a vertical range have been associated with regional snow-line lowering, however a sole age does not indicate a conclusive driving factor of ice-cover expansion (summer temperature, winter precipitation, wind direction or some combination).

Results

The SVALHOLA database

SVALHOLA contains 1707 individual dates from over 1200 discrete locations compiled from over 230 published sources (Fig. 5, Table S1–3). The spatial distribution is uneven and ages are dominantly from the western coast and fjords of Spitsbergen. The lacustrine archive has the lowest density of ages (~10 %) followed by marine cores (~29 %). Samples dated from terrestrial archives make up the final population of (~61 %). Over 90% of the dates in the SVALHOLA database are from radiocarbon analysis and roughly 50% of those samples are marine organisms. In the database, there are a total of 99 ages from Luminenscence dating (~6 %) while there is a total of 50 ages (~3 %) from TCN dating.

Holocene dates from Svalbard are skewed in age toward the earlier half of the interglacial period. Roughly 60% of the SVALHOLA database dates between 12.0 – 6.0 ka BP with nearly half of the ages falling between 11.5 – 9.5 ka BP. Roughly 20% of the ages date to within the last 2 ka BP. Although the Mid Holocene has comparatively fewer dates per 500-year period, there is a relatively consistent distribution of ages, with a gentle decline from 9 – 2 ka BP. There is a lower percentage of "likely reliable" (quality 1) verse less reliable ages in the Early Holocene (12.0 – 8.0 ka BP).

Holocene climate and glaciers

Late Pleistocene – Early Holocene

Reworked dateable material of Late Pleistocene and Early Holocene age has been identified within and sampled from glacial deposits across Svalbard. Most often, this material is shell fragments re-sedimented in glacial (marine) diamict suggesting glacier override and in some cases glaciotectonism (Lønne 2005; Farnsworth *et al.* 2018). Several of the radiocarbon ages fall within the latter half of the Younger Dryas while the majority of ages date between 12.0 - 9.5 ka BP. The youngest age dates 9.1 ka BP. No clear clustering or synchronicity is visible in the age distribution of these reworked shells (Fig. 6). The oldest re-advances have been identified near the mouths of the fjords while younger Early Holocene re-advances are found in the inner tributaries and heads of fjords (Larsen *et al.* 2018).

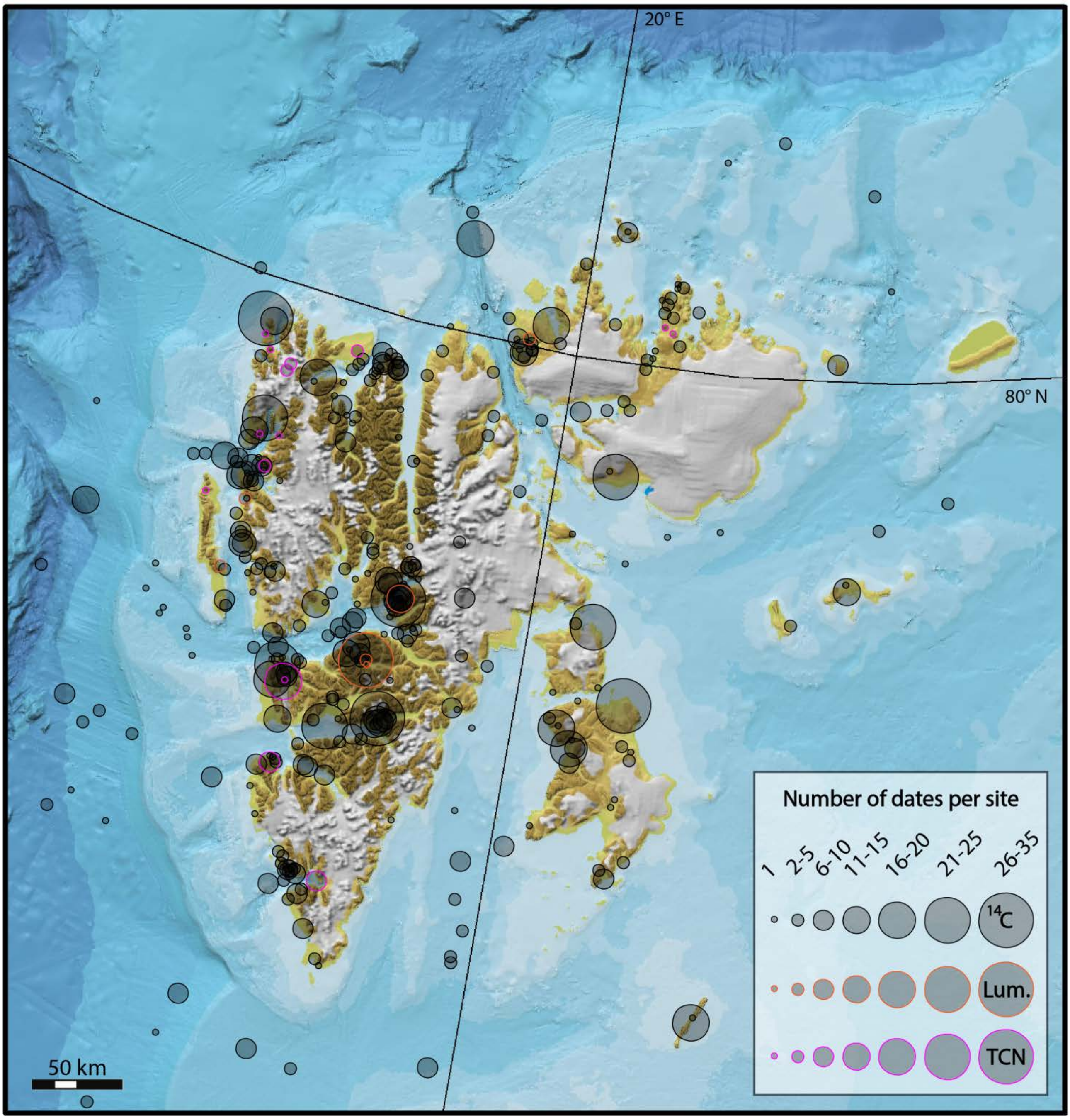

Fig. 4. Spatial distribution of ages compiled in the SVALHOLA database. Colored circles are

proportional to the number of dates of each method per site. Note the low density of chronological data from the eastern Svalbard and the east coast of Spitsbergen. The bulk of the ages are radiocarbon dates from low elevation coastal regions and in shallow waters to the west of Spitsbergen. Dates were compiled from citations present in Table S1 and at the end of this manuscript (full references are included in the supporting information; Data S4).

Thermophilous marine molluscs that once inhabited Svalbard can be found preserved in raised marine sediments of Early Holocene age (Fig. 6; Feyling-Hanssen 1955; Salvigsen *et al.* 1992; Hjort *et al.* 1995; Salvigsen 2002; Blake *et al.* 2006; Hansen *et al.* 2011; Farnsworth *et al.* 2017; Mangerud & Svendsen 2017).

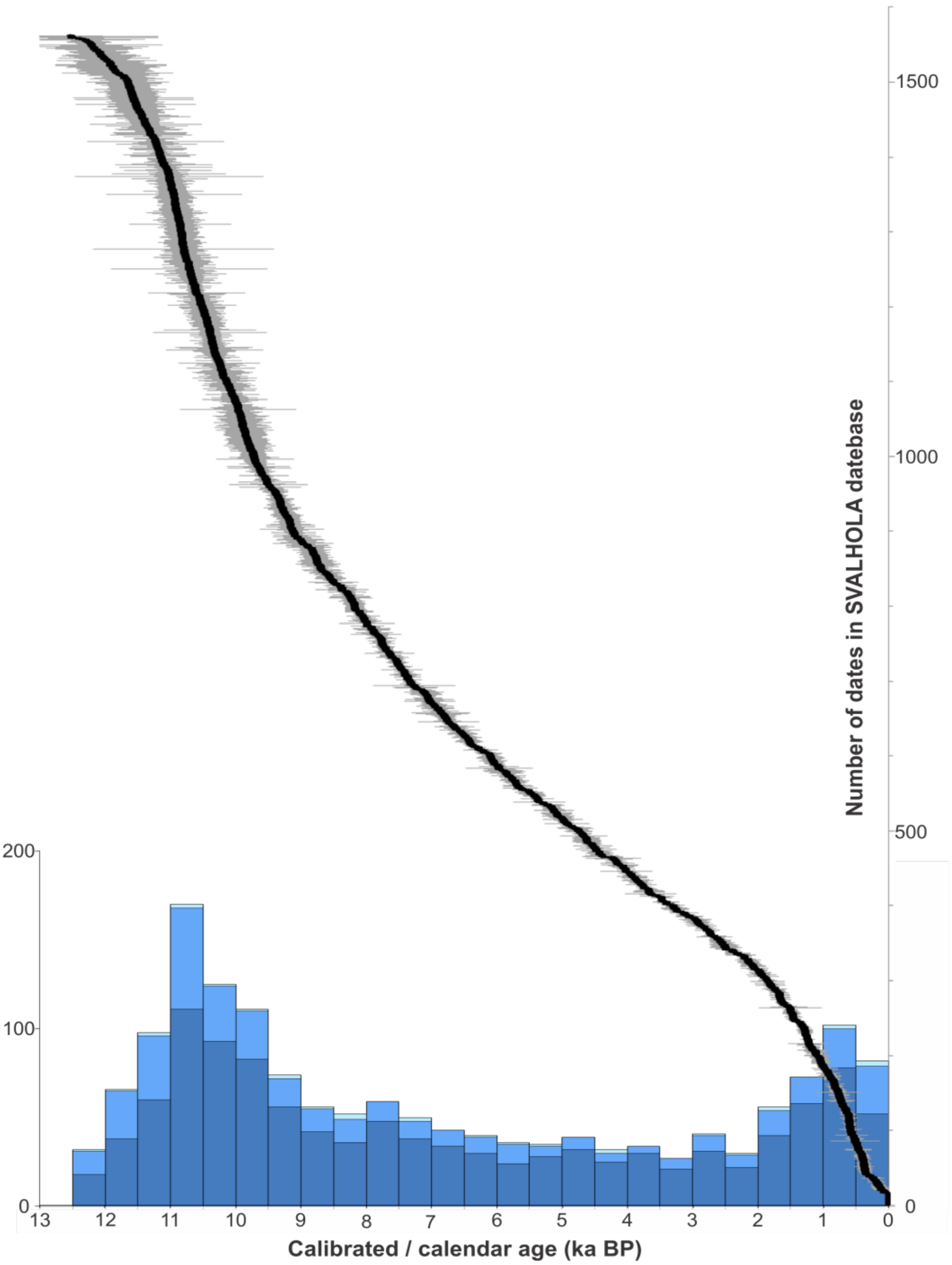

Fig. 5. Histogram of radiocarbon ages contained within the SVALHOLA database with dates presented with a 500-year bin size modified from 1000-year bin size presented by Hughes et al. (2016). Dates colored according to quality rating 1 (dark blue), 2 (light blue) and 3 (pale blue). Plot displays the same 1554 SVALHOLA dates with the mid-points stacked chronologically (black diamonds) and associated error bars (grey). Mid point ages extent over 12.0 ka BP as the database includes all ages in which error margins fall within the Holocene.

The earliest radiocarbon ages of the warm water shell, *Mytilus edulis* date slightly before 11.0 ka BP and suggest the sea temperatures around Svalbard were roughly 2° C warmer than present (Fig. 6; Mangerud & Svendsen 2017). The occurrence of the *Zirfaea crispata* and *Arctica islandica* around Svalbard was used to compare modern conditions to the Holocene and suggests ocean temperatures peak between 10.0 – 9.2 ka BP and were at least 6° C warmer then present (Mangerud & Svendsen 2017).

The Early Holocene terrestrial record is characterized by flights of raised marine beach sediments. These raised beaches indicate previous shorelines that have subsequently been uplifted relative to local sea level as a result of isostatic rebound (Forman *et al.* 1987; Bondevik *et al.* 1995). Early Holocene uplift rates have been derived from radiocarbon dated whalebones; drift wood and shells found on raised beaches (Salvigsen 1981; Häggblom 1982; Forman *et al.* 2004). Minimum rates derived from raised marine shorelines suggest 10 – 25 meters of uplift per 1.0 ka during the Early Holocene on Svalbard (Salvigsen 1981; Salvigsen & Österholm 1982; Forman *et al.* 2004). The occurrence of radiocarbon dated driftwood on the raised marine shorelines of Svalbard indicates an increasing rate of arrival between 12.0 – 10.5 ka BP which is followed by a stepped and variable decline in occurrence to 9.0 ka (Fig. 6). Peak driftwood arrival occurs between 10.5 – 11.0 ka BP (Fig. 6).

Mid Holocene

No (constraining) radiocarbon ages of re-sedimented material found within glacial deposits date to the Mid Holocene (Fig. 6). However, many thermophilous molluscs date to within the Mid Holocene. A slight decline in the occurrence of thermophilous marine molluscs suggests a short lived cooling following the marine Holocene thermal Optium (HTO) between 9 and 8.2 ka BP, however ocean temperatures still remained roughly 2° C warmer than present (Mangerud & Svendsen 2017). The persistence of the *Mytilus edulis* and the *Modiolus modiolus* in the Mid Holocene suggests Atlantic water continued to reach Svalbard and ocean temperatures were c. 4° C warmer than present between 8.0 – 6.5 ka BP (Salvigsen *et al.* 1992; Salvigsen 2002; Blake *et al.*

2006; Mangerud & Svendsen 2017). This period of stable warm ocean conditions is followed by a gradual decrease in temperatures until the end of the Mid Holocene where values reach those comparable to modern (Mangerud & Svendsen 2017).

The presence of driftwood on raised Mid Holocene shorelines remains lower than the peak in occurrence from the Early Holocene, yet suggests consistent arrival of material from roughly 9.0 – 6.5 ka BP. This interval is followed by a decline in the arrival of driftwood at 6.5 ka BP and continuing through the end of the Mid Holocene (Fig. 6).

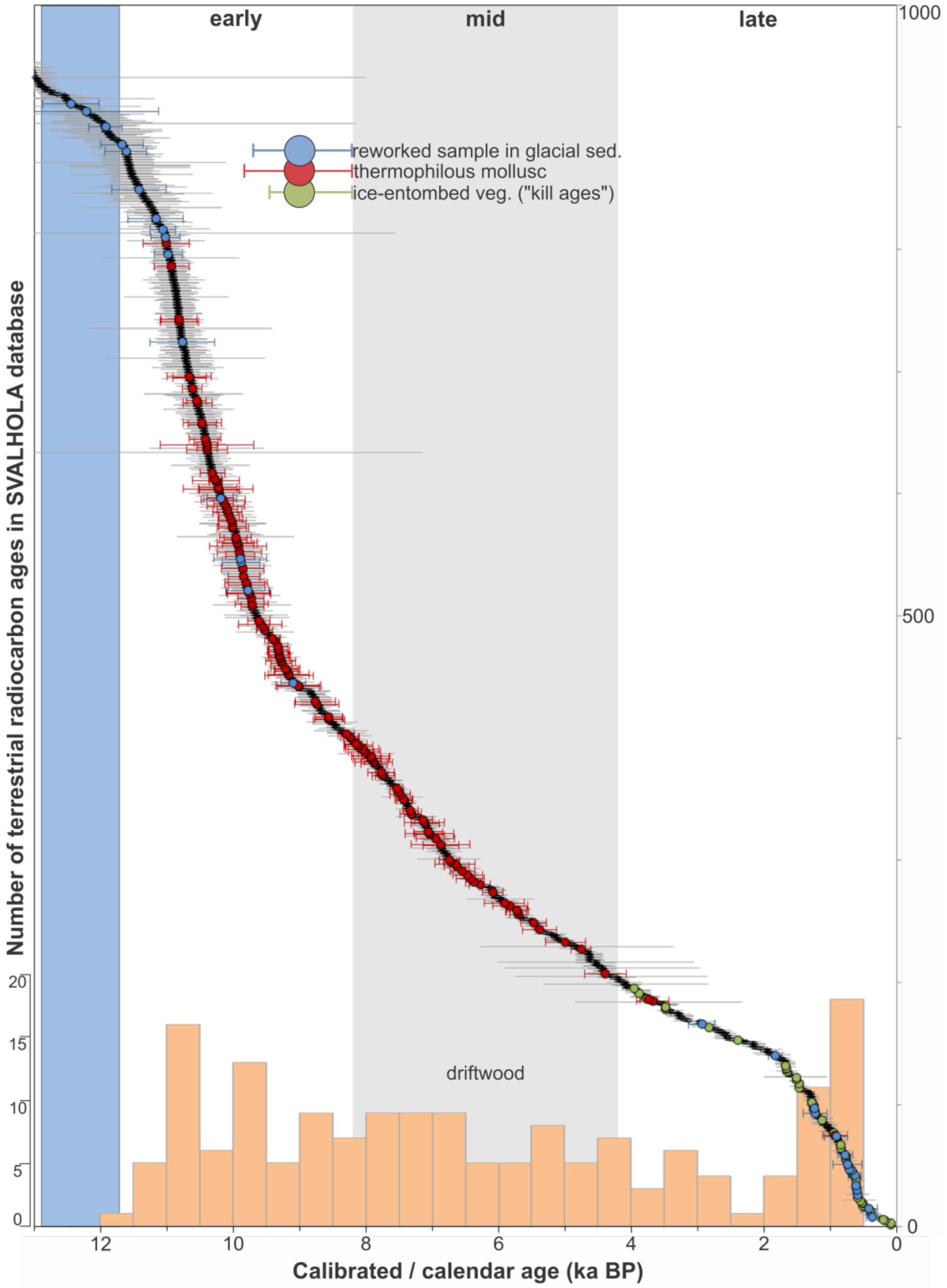

Fig. 6. Plot of the 930 radiocarbon ages from terrestrial archvies (including raised marine) from the SVALHOLA database with the mid-points stacked chronologically (black diamonds) and

associated error bars (grey) modified from Fig. 5. The Younger Dryas period is marked with a blue column while the Early and Late Holocene is divided by a grey column delimiting the Mid Holocene. Specific radiocarbon ages from the database have been highlighted based on palaeo-glaciological / climatological associations. Dateable material reworked in glacial sediments (blue); thermophilous marine molluscs (red) and ice-entombed moss (green) are represented by enlarged colored circles with error whiskers. Histogram plot at base indicates the number (n=168) of radiocarbon dated driftwood samples from Svalbard presented within a 500 year bin size (modified from Dyke et al. 1997). The youngest bin (modern – 0.5 ka BP) has been excluded due to lack of studies focusing on driftwood from modern shorelines.

Late Holocene

There are an increasing number of radiocarbon dates from material re-sedimented in or overlain by glacial deposits throughout the Late Holocene (Fig. 6). Although some Late Holocene samples are of re-worked shells (Punning *et al.* 1976; Sharin *et al.* 2014; Farnsworth *et al.* 2017), roughly half of the samples are from over-ridden (*in situ*) vegetation (Baranowski & Karlén 1976; Dzierzek *et al.* 1990; Furrer 1991; Humlum *et al.* 2005). These samples have been collected across Svalbard and ages become more frequent in the last 2 millennia (Fig. 6). Over half of the ages date to between 1.0 – 0.5 ka BP (Fig. 6).

In addition to material that has been reworked or overridden by glacier, plants that have been entombed in passive ice (cold, perennial snow patches and fonna / thin ice-caps) have also been sampled and dated (Fig. 6). Over 40 samples of moss and vegetation preserved under cold-based ice have been collected from retreating modern ice margins in central Spitsbergen (Miller *et al.* 2017). While the oldest ages range back to nearly 4 ka BP, c. 80% of the samples are younger than 2.0 ka BP (Fig. 6).

The occurrence of thermophilous molluscs decreases through the Mid Holocene and tapers off entirely at the start of the Late Holocene (Fig. 6). In addition to the final two *Mytilus edulis* dating c. 3.7 ka BP, it appears the species may have returned to inner Isfjorden based on a single young sample dating 0.9 ka BP (Fig. 10; Samtleben 1985; Mangerud & Svendsen 2017).

During the first half of the Late Holocene driftwood occurrence remains low (Fig. 6). The period between 2.5 - 2.0 ka BP marks the Holocene minimum in driftwood arrival and matches the occurrence rate seen during the end of the Younger Dryas (Fig. 6). A sharp increase in driftwood arrival is exhibited during the final two millennia. The driftwood count from the most recent 500-years (bin 0.5 ka BP to modern) has been excluded given the general lack of studies targeting radiocarbon dating driftage from the modern shorelines.

Holocene sediment chronologies from lakes and fjords

On Svalbard, the resolution of lake and fjord core chronology ranges widely owing to core length and datable material (Fig. 7). Based on a collection of the highest resolution lake and fjord chronologies from published Svalbard Holocene studies, lake cores generally tend to be shorter in length (avg. 2.4 m) than fjord cores (avg. 4.9 m) and average a greater amount of dates (Fig. 7; 4.6 verse 1.8 dates per meter, respectively).

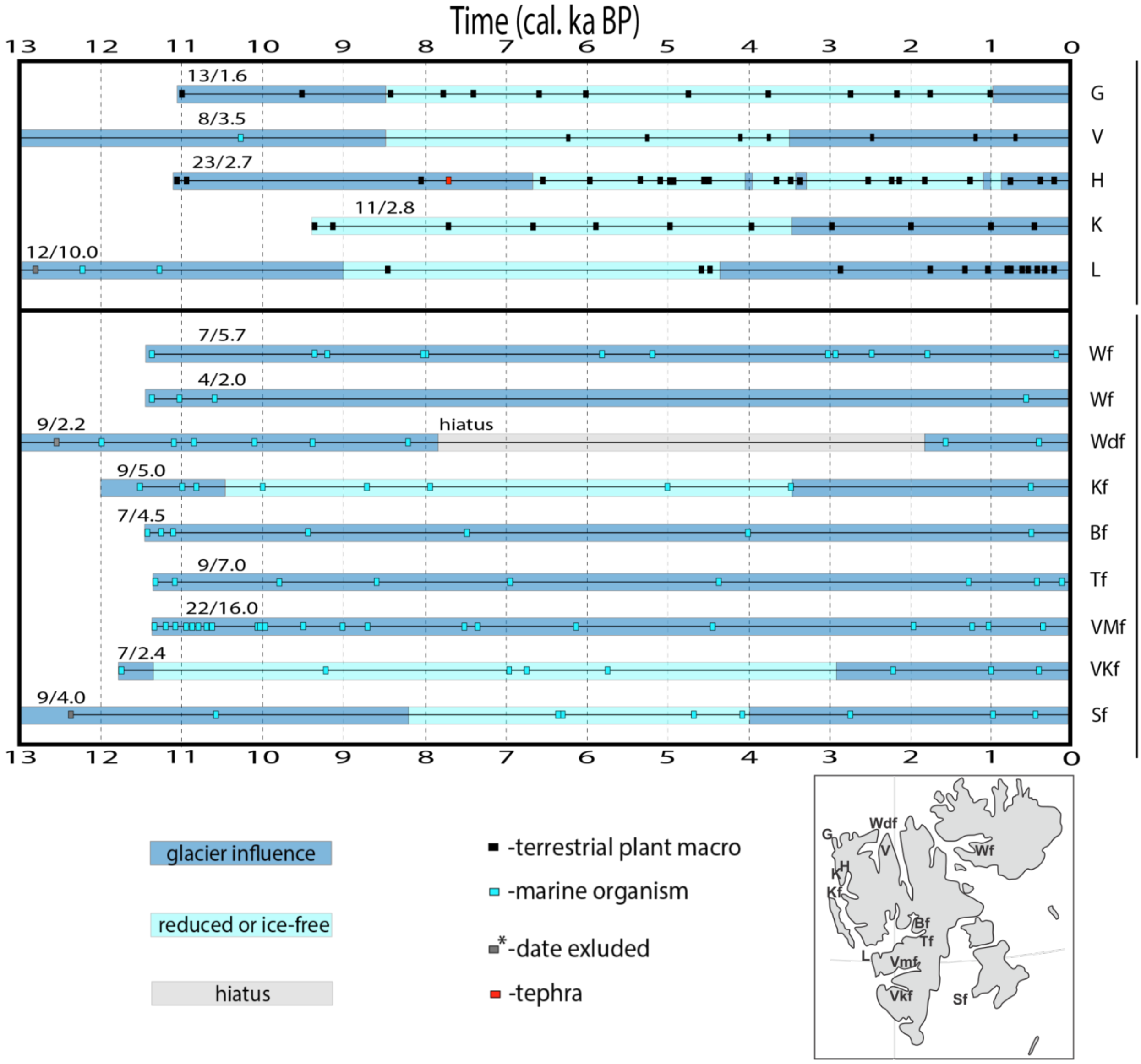

Fig. 7. Diagram highlighting the age and distribution of dates used to constrain the highest resolution lake (n=11) and fjord (n=8) sediment cores used for Holocene environmental reconstructions around Svalbard. Bulk sediment (white boxes), terrestrial plant macrofossils (black boxes), crypto-tephra (green boxes), marine molluscs and foraminifera (blue boxes) are used to constrain core chronologies. Values beneath chronologies indicate the number of dates per core length of each study.

Holocene environmental reconstructions from marine sediments often use mollusc shells or foraminifera for radiocarbon dating and constraining core chronologies. In lake sediment cores, a mixture of material has been used to constrain chronologies (Fig. 7). Early studies relied on radiocarbon dating bulk sediment (e.g. Hyvärienen 1970), while modern studies target terrestrial plant macrofossils (de Wet *et al.* 2017) and occasional mollusc shells sampled just below the lacustrine-marine boundary in isolation basins (Svendsen & Mangerud 1997). Recent studies have used tephra and crypto-tephra to constrain lake chronologies where terrestrial macrofossils have been sparse (Fig. 7; D`Andrea *et al.* 2012; van der Bilt *et al.* 2017).

DISCUSSION

The three Holocene sub-divisions; Early, Mid and Late Holocene, presented in this review correspond to the Greenlandian, Northgrippian and Meghalayan respectively (Cohen *et al.* 2013; updated). For each Holocene stage, we discuss findings from the marine, terrestrial and lacustrine archives respectively. The stage intervals are from 11.7 – 8.2 ka BP, 8.2 – 4.2 ka BP and 4.2 ka BP to present. We introduce these three sections by briefly discussing the conditions at the transition, from the end of the Pleistocene into the Early Holocene. We close this summary describing the transition from the end of the Little Ice Age into the 20th century as this marks the start of the rich observational record of Svalbard climate, ice cover and landscape. Despite certain micro-climatic variability, we choose not to sub-group data, but generally discuss ages for the entire Svalbard region. In some cases, we refer to locations at the mouth of a fjord relative to the tributary of head of the fjord-system.

Late Pleistocene - Holocene transition

Maximum ice cover during the last 12 ka was likely around 12 ka BP, as residual SBSIS still covered a large portion of Svalbard (Fig. 8). The exact ice extent is not well understood given the sparse ice marginal positions known from this period. Additionally, it is unknown how tightly the deglaciation ages from marine sediment cores and raised marine sediments constrain the actual deglaciation as these ages are minimum constraining values and could potentially reflect conditions centuries after the actual deglaciation (Larsen *et al.* 2018). Several recent studies present new radiocarbon ages that suggest less extensive ice cover at 12.0 ka BP (Farnsworth *et al.* 2018; Larsen *et al.* 2018) than the DATED-1 time slice suggests (Fig. 8; Hughes *et al.* 2016).

Furthermore, the resolution of these ice extent reconstructions does not effectively depict the detail of residual ice-cover during the transition from Pleistocene to Holocene. For example, no terrestrial evidence from the Seven Islands, northern Svalbard, suggests ice free conditions prior to the Early Holocene (polygon with dashed line; Fig. 7). The earliest deglaciation ages are from raised beaches dating to c. 11.0 ka BP and at present the Seven Islands are not glaciated (Forman & Ingólfsson 2000).

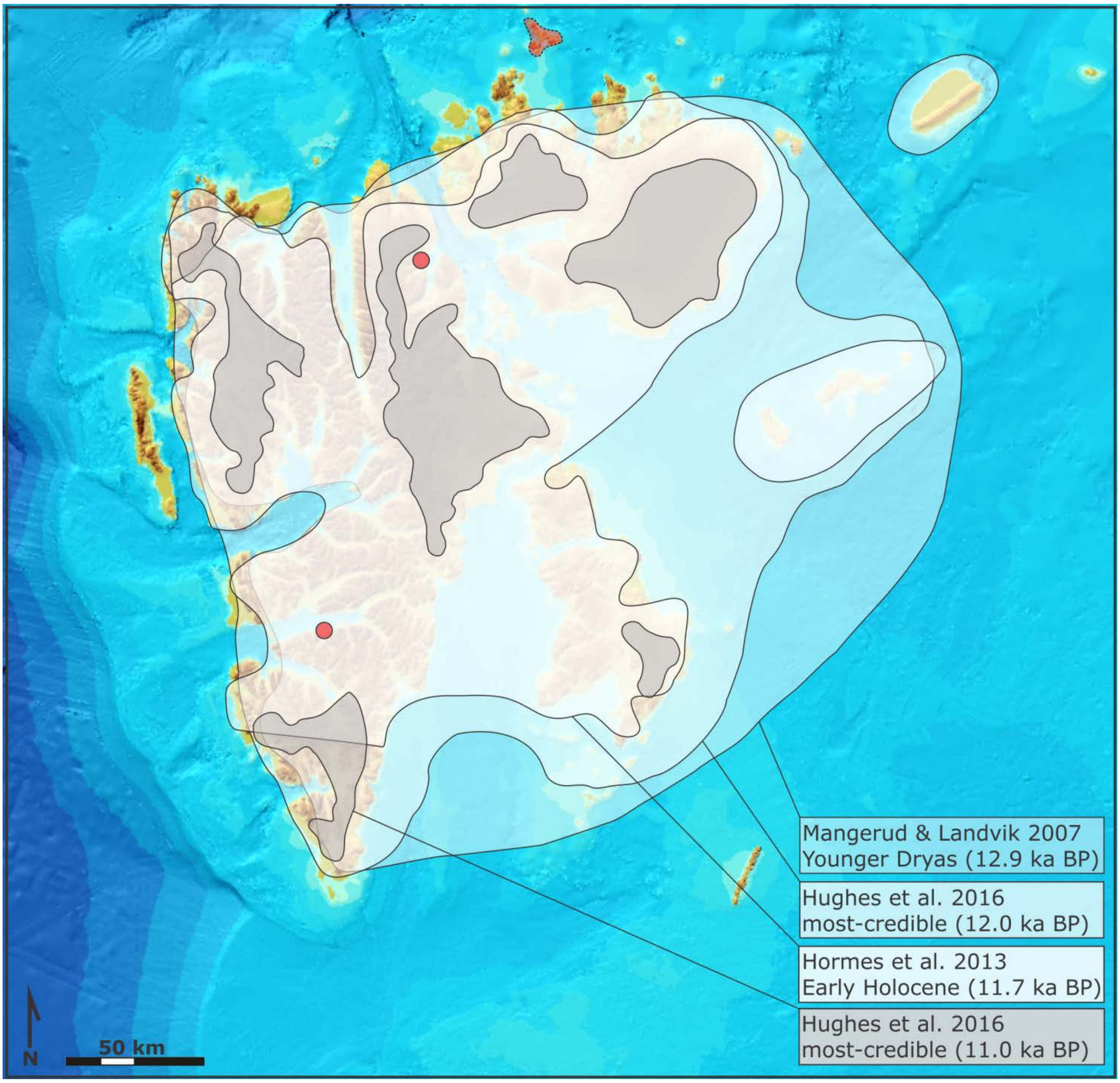

Fig. 8. IBCAO map of Svalbard with polygons reflecting ice cover at different time-slice reconstructions during the Lateglacial and Early Holocene. The most-credible time-slice reconstructions from Hughes et al. (2016) are from the DATED-1 database of Eurasian ice sheets, while the marginal positions from Mangerud & Landvik (2007) and Hormes et al. (2013) are modified from studies. Red circles mark sample locations where recent radiocarbon ages suggest ice free conditions prior to 12.0 ka BP (Farnsworth et al. 2018; Larsen et al. 2018). Red shaded polygon over the Seven Islands highlights reconstructed ice cover that existed until the onset of the Holocene (but lacks from other reconstructions due to resolution).

Younger Dryas-The period between 12.9 and 11.7 ka BP is believed to have been a phase of pronounced cooling interpreted from a marked boundary in Scandinavian pollen records, indicating the return of the *Dryas octopetala*, a cold-tolerant plant (Andersson 1896; Rasmussen *et al.* 2006) Interpretations of $\boldsymbol{\delta}^{18}$O from Greenland ice core records suggest a rapid ~10°C deviation in atmospheric temperature during this time interval (Carlsen 2013). Data suggest that this period was not only characterized by pronounced cooling, but the event was a rapid climate shift and may have had implications for larger regions than just the North Atlantic (Dansgaard *et al.* 1993; Isarin & Renssen 1999). Studies have gone on to search for signatures of the Younger Dryas globally, suggesting contemporaneous (and synchronous) glacier re-advances in the European Alps, the North American Rockies as well as shifts in lake chemistry records from Chile to lake Baikal are believed to evidence a global response to this rapid climate event (Bennet *et al.* 2000; Ivy-Ochs *et al.* 2009; Davies *et al.* 2009).

Although the North Atlantic is interpreted to have been the epicenter of this rapid climate event and despite the far-reaching fingerprints of the Younger Dryas cooling suggested by some studies, no conclusive evidence of any such event has been identified on Svalbard (Hormes *et al.* 2013). Similarly, our review finds no conclusive evidence for a Younger Dryas cooling driving synchronous glacier re-advances during any period between 12.9 – 11.7 ka BP. Radiocarbon ages from this time interval predominantly correspond to shells found in raised marine sediments suggesting ice-free conditions and active beach formation (Landvik *et al.* 1987; Forman *et al.* 1990; Eitel *et al.* 2002; Bruckner *et al.* 2003; Landvik & Mangerud 2007). Recent studies have also suggested substantial ice loss constrained to the Younger Dryas time interval thus, instead of glaciers re-advances or marked standstills, evidence in some locations suggests the contrary (Fig. 8; Hogan *et al.* 2017; Farnsworth *et al.* 2018; Larsen *et al.* 2018). Several radiocarbon ages, often of shell fragments re-sedimented in glacial (marine) sediments suggest that glacier re-advances occurred during the latter half of the Younger Dryas period (Fig. 6). These glacier re-advances are generally not well constrained in time (lacking both maximum and/or minimum age constraints) and exhibit no clear synchronicity (Fig. 6; Mangerud *et al.* 1992; Rasmussen & Thomsen 2014; Farnsworth *et al.* 2017, 2018; Larsen *et al.* 2018).

Early Holocene (11.7 - 8.2 ka BP)

By the beginning of the Holocene, the majority of the marine based sectors of the SBIS had already collapsed, and ice margins had retreated back inside the modern coastline of Svalbard (Mangerud *et al.* 1992; Hormes *et al.* 2013; Hughes *et al.* 2016). Deglaciation continued in a time transgressive manner, characterized by initial retreat through the fjords and subsequently in the fjord-valleys and terrestrial realms (Ingólfsson & Landvik 2013; Gilbert *et al.* 2018). Additionally, during this period, summer insolation approaches its Holocene maximum in the northern hemisphere (Laskar *et al.* 2004).

Marine- Data from the marine archives suggest early and marked warm regional conditions driven by the incursion of Atlantic waters around Svalbard (Hald *et al.* 2004; Mangerud & Svendsen 2017). Evidence from marine microfossils suggests warm regional condition prior to the onset and throughout the Early Holocene (Hald *et al.* 2004, 2007; Ślubowska-Woldengen *et al.* 2007; Skirbekk *et al.* 2010; Jernas *et al.* 2013; Łącka *et al.* 2015). Marine sediment core chronology from fjords in western and northern Svalbard suggest high sedimentation rates with regular outsized particles interpreted as ice rafted debris (IRD; Hald *et al.* 2004; Flink *et al.* 2017; Bartels *et al.* 2017; 2018). Reconstructions of sea ice cover during the onset of the Early Holocene are characterized by an abrupt decrease in sea ice proxy IP25 suggesting a decline in sea ice extent (Müller & Stein 2014; Bartels *et al.* 2018).

Terrestrial- The Early Holocene exhibits the greatest rates of isostatic uplift recorded in the last 11.7 ka BP. Minimum rates derived from dated raised marine shorelines suggest 10 – 25 meters of uplift per 1.0 ka during the Early Holocene on Svalbard (Salvigsen 1981; Salvigsen & Österholm 1982; Forman *et al.* 2004).

The occurrence of driftwood found on Arctic shorelines has been used as a proxy for semi-permanent sea ice concentrations (Häggblom 1982; Funder *et al.* 2011; Hole & Macias-Fauria 2017). Where sea ice cover is too low no driftwood arrives, while with multiyear sea ice, driftwood is shielded from the shorelines (Funder *et al.* 2011). The initial growth in driftwood arrival could be related to sea ice concentrations transitioning from permanent to semi-permanent cover at the onset of the Holocene as well as the increased availability of deglaciated shorelines as catchment for driftwood (Fig. 6; Häggblom 1982):

The records of raised marine organisms identified in Early Holocene sediments across the coastal regions of Svalbard also corroborates with the marine data. Reviews of thermophilous marine molluscs found around Svalbard also indicate early and exceptionally warm regional waters (Salvigsen *et al.* 1992; Salvigsen 2002; Blake *et al.* 2006; Mangerud & Svendsen 2017). The occurrence of the *Zirfaea crispata* and *Arctica islandica* only existing in the Svalbard raised marine record between 10.0 - 9.2 ka BP suggests that the maximum ocean temperatures experienced in the

Holocene occurred in the beginning, slightly prior to peak summer insolation (Lasker *et al.* 2004; Mangerud & Svendsen 2017).

Lacustrine- Few lacustrine chronologies on Svalbard begin prior to the onset of the Holocene (Fig. 6). Alkenone and hydrogen isotope reconstructions have been used as proxy records from lake sediments collected in northwestern Spitsbergen and suggest warm, moist conditions as early as 12.8 cal. ka BP (Balascio *et al.* 2018; van der Bilt *et al.* 2018; Gjerde *et al.* 2018). Most of the investigated lakes became ice-free (Holmgren *et al.* 2010; Alsos *et al.* 2015; Røthe *et al.* 2015; van der Bilt *et al.* 2016; de Wet *et al.* 2018) or isolated from the marine environment during the Early Holocene (Snyder *et al.* 1994; Svendsen & Mangerud 1997; Røthe *et al.* 2018). Lacustrine records from Svalbard often exhibit high mineragentic fractionation and sedimentation rates that taper off through the Early Holocene (Snyder *et al.* 1994; Svendsen and Mangerud 1997; Røthe *et al.* 2015; van der Bilt *et al.* 2016; de Wet *et al.* 2018; Røthe *et al.* 2018).

Holocene marine thermal optimum and re-advancing glaciers

Although the majority of the terrestrial landscape is still evacuating SBSIS-ice, the marine seas around Svalbard undergo an Early Holocene Thermal Optimum roughly between 10.0 and 9.2 ka BP (Hormes *et al.* 2013; Mangerud & Svendsen 2017). As the landscape is dominantly engulfed by ice, it is safe to say the marine and terrestrial environments are climatically out of phase at this period in the Holocene.

Glacier response to Early Holocene conditions appears complex. In general, marine terminating glaciers responded to the warming by retreating back to land while cirque glaciers greatly diminish in size and in some cases disappeared completely (Svendsen & Mangerud 1997; Snyder *et al.* 2000; Forwick & Vorren 2009; de Wet *et al.* 2018). On Nordaustlandet, mollusc shell samples from within a thrusted debris band located 6 km inside of the Søre Franklinbreen ice margin date 10.3 ka BP and suggest that the NE outlet of Vestfonna had retreated to at least this position early in the Holocene (Blake 1989).

Despite the progressive deglaciation and imminent retreat characterizing the Early Holocene, evidence from glaciers of varying size found across Svalbard, suggests asynchronous ice margin re-advance (Fig. 8; Salvigsen *et al.* 1990; Mangerud *et al.* 1992; Ronnert & Landvik 1993; Brückner *et al.* 2002; Eitel *et al.* 2002; Lønne 2005; Farnsworth *et al.* 2017, 2018; Larsen *et al.* 2018). Although the exact magnitudes of the re-advances are unknown, ice margin extent is often several kilometers outside of Late Holocene glacier maxima (Lønne 2005; Farnsworth *et al.* 2018). Similar to the late Younger Dryas, glacier re-advances are most often interpreted from shell fragments re-sedimented in glacial (marine) sediments suggesting glacier override, reworking and in some cases glaciotectonism (Lønne 2005; Farnsworth *et al.* 2018). The oldest re-advances have been identified near the mouths of the fjords while younger Early Holocene re-advances are found in the inner tributaries and heads of fjords (Larsen *et al.* 2018). Generally, the timing of the re-advances seems to follow the time transgressive deglaciation (Landvik *et al.* 2014; Farnsworth *et al.* 2018). The final glacier re-advance identified in the first half of the Holocene deposited shells 180 m a.s.l. in inner Wijdefjorden (c. 6.5 km inside of the present margin; Klysz *et al.* 1988). Although the extent of the re-advance interpreted from these deposits is unknown, the data suggests not only had the palaeo-outlet glacier undergone significant Early Holocene retreat, it re-advanced to a marginal position un-matched at any point in the Late Holocene. Still today, there are numerous pre-Mid Holocene moraines that have been identified in marine and terrestrial environments, yet still are undated (Salvigsen & Österholm 1982; Forwick & Vorren 2010; Henriksen *et al.* 2014; Røthe *et al.* 2015 Flink *et al.* 2018; Farnsworth *et al.* 2018).

Mid Holocene (8.2 – 4.2 ka BP)

After summer insolation peaked during the Early Holocene, northern hemisphere insolation values begin a decreasing trend that progresses throughout the rest of the Holocene (Laskar *et al.* 2004).

Marine- Data from the marine archive suggests a general decline in ocean temperatures during the Mid Holocene. Evidence from marine microfossils suggests cooling of regional waters during this period (Hald *et al.* 2004; 2007; Ślubowska-Woldengen *et al.* 2007; Skirbekk *et al.* 2010; Jernas *et al.* 2013; Łącka *et al.* 2015). Marine sediment cores exhibit a decline in sedimentation rate and IRD dissipates in most fjords (Forwick & Vorren 2009; Skirbekk *et al.* 2010; Kempf *et al.* 2013; Nielsen & Rasmussen 2018). Reconstructions of sea ice cover derived from IP25 records spanning the Mid Holocene suggest a progressive increase in ice-cover starting around 8.0 ka BP (Müller & Stein 2012).

Terrestrial- Similar to the Early Holocene, most of our understanding of the Mid Holocene environment on Svalbard is from raised marine sediments and driftage. Mid Holocene raised marine shorelines suggest glacio-isostatic uplift rates decline throughout the Mid Holocene on the order of 5 m per 1 ka (Bondevik *et al.* 1995; Forman *et al.* 2004). In several locations on the northern and western coasts of Svalbard, Mid Holocene transgressions have been interpreted through a combination of shoreline morphology and chronology (Forman 1990; Forman & Ingólfsson 2000).

The presence of driftwood on raised Mid Holocene shorelines remains lower than the peak in occurrence from the Early Holocene (Fig. 6), yet suggests consistent arrival of material from roughly 9.0 – 6.5 ka BP. This interval is followed by a gentle decline in the arrival of driftwood towards the end of the Mid Holocene (Fig. 8). The pattern of driftwood occurrence through the Mid Holocene seems to loosely follow trend with declining ocean temperatures reconstructed from marine microfossils as well as inversely correlated with sea ice reconstructions derived from IP25 (Hald *et al.* 2004, 2007; Ślubowska-Woldengen *et al.* 2007; Skirbekk *et al.* 2010; Müller &Stein 2012).

A slight decline the occurrence of thermophilous marine molluscs suggests a short lived cooling following the marine HTO between 9 and 8.2 ka BP, however ocean temperatures still remained roughly 2° C warmer than present (Mangerud & Svendsen 2017). The persistence of the *Mytilus edulis* and the *Modiolus modiolus* in the Mid Holocene suggests Atlantic water continued to reach Svalbard and ocean temperatures were c. 4° C warmer than present between 8.0 – 6.5 ka BP (Salvigsen *et al.* 1992; Salvigsen 2002; Blake *et al.* 2006; Mangerud & Svendsen 2017). This period of stable warm ocean conditions is followed by a gradual decrease in temperatures until the end of the Mid Holocene where values reach those comparable to modern (Mangerud & Svendsen 2017).

Lacustrine- Lake sediment records spanning the Mid Holocene suggest high productivity and low sedimentation rates (Birks 1991; van der Bilt *et al.* 2015; Alsos *et al.* 2015; Gjerde *et al.* 2018). Chronologies from modern glacial lakes suggest greatly reduced or ice-free catchments during the Mid Holocene characterized by organic rich strata with minimal mineragenic accumulation (Svendsen & Mangerud 1997; Snyder *et al.* 2000; Røthe *et al.* 2015, 2018; de Wet *et al.* 2018).

Glaciers retreat (entirely?) to the Holocene Glacial Minimum while waters cooled

Based on glacial lake records and the summer insolation curve, we presume that Svalbard glaciers retreated back to their Holocene minimum during the early-Mid Holocene (Fig 7; Laskar *et al.* 2014). However, we have no exact spatial constraint on any Svalbard ice margins during the Mid Holocene. We assume if glaciers existed in the Mid Holocene, they were more reduced then any Late Holocene glacier extent on Svalbard. We therefore have no morphological evidence (frontal/marginal moraines) identifying any glacier re-advances during this period (Fig. 6). Two marine stratigraphy studies have suggested Mid Holocene glacier activity at the mouth of Isfjorden and western Nordaustlandet based on fluctuating rates of mineragenic sedimentation (Forwick & Vorren 2007; Kubischta *et al.* 2011). It is inconclusive if marine stratigraphy from these sites relates to glacier re-advances or is a result of submarine mass failures or enhanced melting from proximal glacier systems. Glacial lake studies from the west coast of Spitsbergen suggest there was no glaciogenic input from their corresponding cirque glaciers during the Mid Holocene (Fig. 9; Linnébreen, Svendsen & Mangerud 1997; Linnébreen, Snyder *et al.* 2000; Kløsa, Røthe *et al.* 2015; Hajeren, van der Bilt *et al.* 2016; Gjøavatnet, de Wet *et al.* 2018). Terrestrial vegetation thrusted up into tidewater glacier ice suggests the marine terminus had retreated back from the fjord, at the mouth of Hornsund prior to 8.0 ka BP (Oerlemans *et al.* 2011).

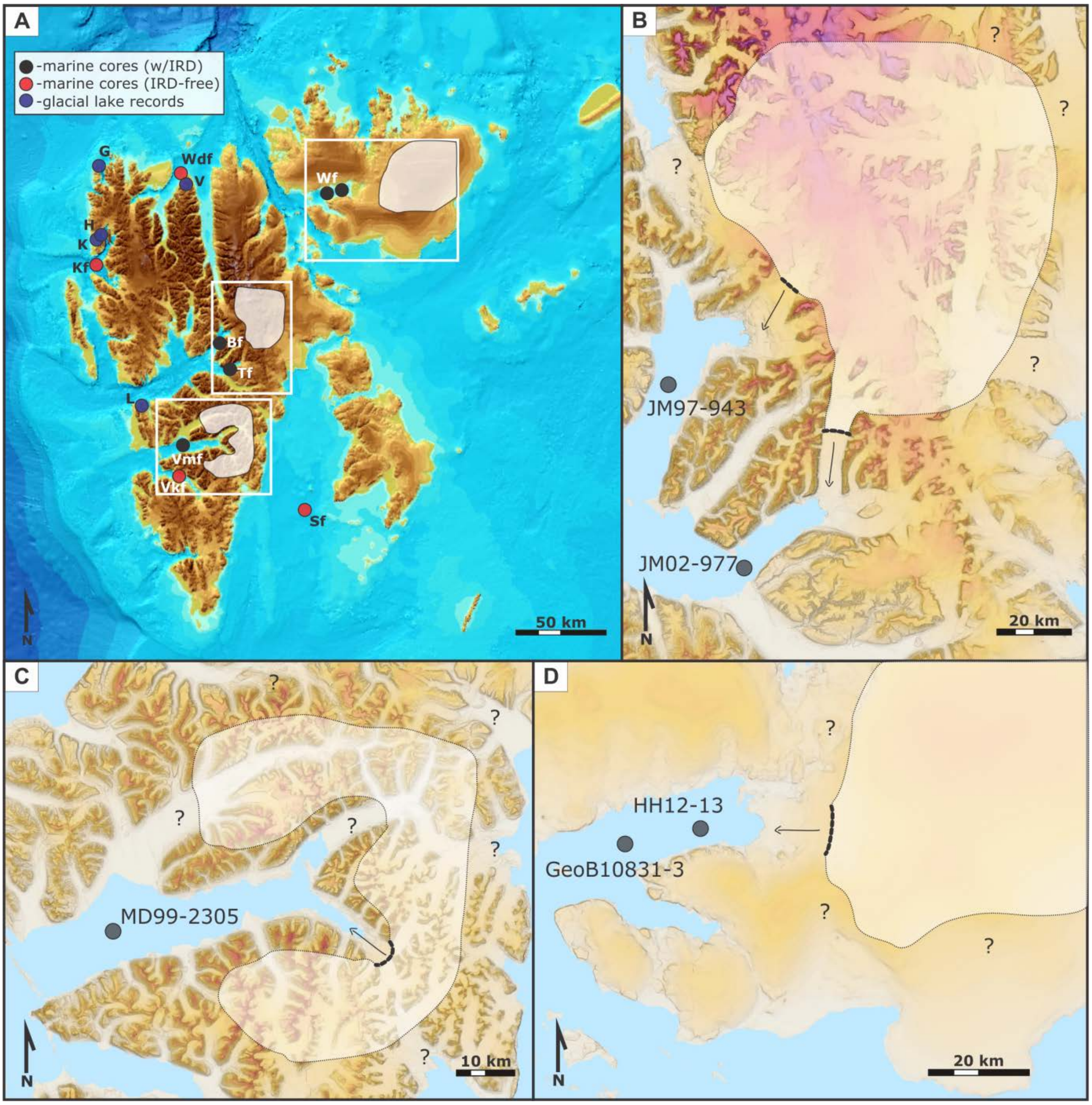

Fig. 9. Maps of Holocene minimum ice extent on Svalbard c. 8-7 ka BP. A) Glacial lakes records from Gjøavatnet (G), Hajeren (H), Kløsa (K) Vårfluesjøen (V) and Linnévatnet (L), suggest ice-free or greatly reduced glaciers in catchments during the Mid Holocene (Svendsen & Mangerud 1997; Snyder et al. 2000; Røthe et al. 2015; van der Bilt et al. 2016; Røthe et al. 2018; de Wet et al.

2018). Reduced ice rafted debris in marine sediment cores from Kongsfjorden (Kf), Van Kuelenfjorden (Vk), Woodfjorden (Wf) and Storfjorden (Sf) suggests tidewater glaciers have retreated back to terrestrial margins (Skirbekk et al. 2010; Kempf et al. 2013; Bartels et al. 2017; Nielsen & Rasmussen 2018). B) Ice rafted debris in marine sediment records suggest tidewater termini persistent in Billefjorden (JM97-943), Tempelfjorden (JM02-977), C) Van Mijenfjorden (MD99-2305) and D) Wahlenbergfjorden HH12-13 & GeoB10831-3) throughout the Holocene (Hald et al. 2004; Baetan et al. 2010; Forwick & Vorren 2010; Flink et al. 2017; Bartels et al. 2018).

There are over 850 km of marine terminating glacier margin in Svalbard today, (Blaszczyk *et al.* 2009). However, it has been speculated if any tidewater glaciers survived the Mid Holocene as most marine sediment records from Svalbard glacial-fjords exhibit reduced or zero Mid Holocene IRD (Fig. 9; Isfjorden, Forwick & Vorren 2009; Kongsfjorden, Skirbekk *et al.* 2010; Van Kuelenfjorden, Kempf *et al.* 2013; Woodfjorden, Bartels *et al.* 2017; Storfjorden, Nielsen & Rasmussen 2018).

However, ice rafted debris has been observed through the entire Holocene in sediment cores from several Svalbard fjords including Van Mijenfjorden, Billefjorden, Templefjorden and Wahlenbergfjorden (Hald *et al.* 2004; Forwick and Vorren 2009, 2010; Baeten *et al.* 2010; Flink *et al.* 2017; Bartels *et al.* 2018). Ice rafted debris is a strong indicator of marine terminating glaciers within a fjord-system but has also been associated with sea ice both as a raft for beach sediments, as well as a (semi-) permanent restraint limiting ice rafting (Forwick & Vorren 2009). If we assume this IRD relates to tidewater glacier systems, the IRD records indicate, Svalbard glaciers not only survive the entire Holocene interglacial, but several Svalbard glaciers never entirely retreated from their fjord-heads. A new modeling study based on Holocene relative sea level concludes that Svalbard glaciers survived the HTO and suggests Nordaustlandet and eastern Spitsbergen were the main regions that hosted this Mid Holocene ice (Fjeldskaar *et al.* 2018). These regions are characterized by cooler climate based on elevation and distance from the West Spitsbergen Current (Fig. 1; Førland *et al.* 2011). Although the Van Mijenfjorden region has summits reaching over 1000 m a.s.l. it generally does not reflect these same cool characteristics. While Paulabreen in southeastern Van Mijenfjorden is the primary source of IRD in the fjord at present; it was not necessarily the dominant or only source of IRD during the Early and Mid Holocene (Fig. 9). Based on the size of the Reindalen and Kjellströmdalen valleys, they seem to have held larger glacier systems in their catchments and may have more efficiently their residual SBSIS ice.

8.2 ka event

The largest cold excursion seen in the Holocene stable oxygen isotope record from the NGRIP ice core occurs at 8.2 ka BP marking the transition from Early to Mid Holocene (Young *et al.* 2012). The 8.2 ka BP event is believed to be a product of one of the catastrophic drainages from the collapsing Laurentide Ice Sheet which released a meltwater pulse from Hudson Bay into the Labrador Sea (Barber *et al.* 1999). These meltwater pulses or Heinrich Events are characterized by peaks in detrital carbonate seen in marine records through the North Atlantic (Heinrich 1988; Bond *et al.* 1993; Jennings *et al.* 2015). Studies have discussed the implication of meltwater pulses from the collapsing LIS influencing Svalbard glacier and climate during the Holocene (Hald & Korsun 2008; Hormes *et al.* 2013; van der Bilt *et al.* 2016). Despite the apparent climatic influence and subsequent glacial response seen on both sides of Baffin Bay to some of the peaks in detrital carbonate associated with the meltwater pulses (Young *et al.* 2012, 2013; Lesnek & Briner 2018), there is no terrestrial evidence yet identified that suggests similar glacier response in Svalbard.

A high resolution marine sediment core from Van Mijenfjorden suggests reduction in $\delta^{18}O$ of the benthic foraminifera *C. reniforme* as well as an increase in microfossil foraminifera implying a freshening and cooling of the fjord water around 8.2 ka BP. Although the catastrophic meltwater pulses may have influenced the oceanic conditions for a short time on Svalbard, the magnitude of ice margin retreat already experienced during the Early Holocene may have put the 8.2 ka BP ice fronts within the preceding Late Holocene glacier extent. Where glacial lake records have been used to reconstruct Holocene ice fluctuations for cirque glaciers, records suggest no peaks in mineragenic sedimentation suggesting glacial invigoration around 8.2 ka BP (Svendsen & Mangerud 1997; van der Bilt *et al.* 2016; de Wet *et al.* 2018; Røthe *et al.* 2018). We can cautiously interpret this lack of glacial evidence on Svalbard during the 8.2 event as a result of the magnitude of the Early Holocene ice-loss as well as the degree of Neoglacial-LIA re-advance. Whatever glacial response may have transpired as a result of this climatic event, it apparently occurred within the extent of the Late Holocene glacial maximum. Additionally, the high occurrence and wide diversity of thermosphilous molluscs during this transition from Early to Mid Holocene suggests the warm water species were seemingly unaffected by a mark cooling in fjord waters and Atlantic waters persisted widespread throughout Svalbard.

Late Holocene (4.2 ka BP – present)

The combination of decreasing summer insolation (Laskar *et al.* 2004) and the progressive cooling of regional waters around Svalbard draws the Late Holocene into the Neoglacial period (Fig. 10 & 11).

Marine- Trends in marine microfossil fauna assemblages indicate ocean cooling around Svalbard (Werner *et al.* 2013). Regional waters exhibit an increasing flux of IRD suggesting a growing glacial influence (Ślubowska-Woldengen *et al.* 2007; Rasmussen *et al.* 2014). Sedimentation rates in Svalbard fjords increases through the Late Holocene (Hald *et al.* 2004; Baeten *et al.* 2010; Kempf *et al.* 2013; Łącka *et al.* 2015; Streuff *et al.* 2017; Flink *et al.* 2017; Bartels *et al.* 2018). Reconstructions of sea ice cover derived from IP25 records spanning the Mid Holocene suggest a continued increase in ice-cover starting through the Late Holocene (Müller & Stein 2012; Bartels *et al.* 2018). In inner fjords, a decrease in IRD has been related to persistent sea ice suppressing iceberg rafting (Forwick and Vorren 2010).

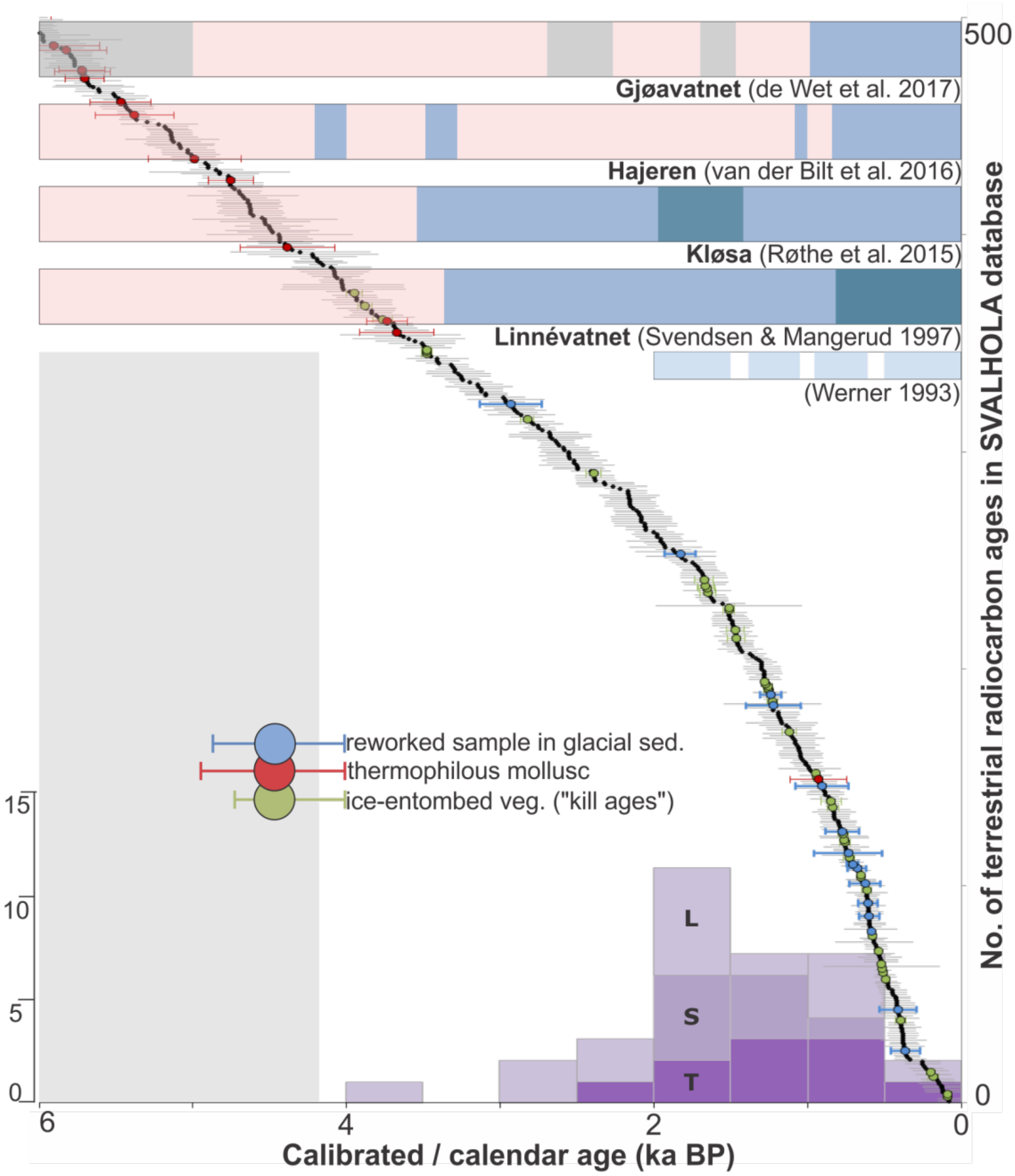

Fig. 10. Plot of 492 terrestrial SVALHOLA dates from the last 6 ka BP. Grey column delimits the end of the Mid Holocene. Specific radiocarbon ages from the database have been highlighted based on palaeo-glaciological and climatological associations. Dateable material reworked or over-

ridden by a glacier re-advance (blue), thermophilous marine molluscs (red) and ice cover expansion (green) are represented by enlarged colored circles with error bars. Histogram at base indicates TCN exposure age distribution within 500 year bins for moraine ridge boulders for three sites, L = Linnébreen, S = Scottbreen and T = Treskelen (Reusche et al. 2014; Philipps et al. 2017) Shaded bars at top represent a schematic view of Late Holocene glacial activity reconstructed with lake sediments of four glacial lakes from western Spitsbergen (Gjøavatnet, Hajeren, Kløsa and Linnévatnet). Blue boxes represent periods of glacial activity (dark blue suggest enhanced glacial activity), red boxes suggest no glacier was present in the catchment or glacial activity was greatly reduced; gray boxes indicate periods of reduced organic matter accumulation (Gjøavatnet; modified from de Wet et al. 2017). Narrow light blue boxes indicate periods of glacier growth interrupted by moraine stabilization (white boxes) reconstructed with lichenometry (Werner 1993).

Terrestrial- Through the Late Holocene the ages of raised marine shorelines indicate a further decrease in relative uplift rates (Forman *et al.* 2004). Despite Mid Holocene transgression, it is believed that relative sea level was regressive throughout the Late Holocene. Currently, in several locations across northern and western Svalbard, uplift rates are surpassed by eustatic sea level and a transgression is being observed (Fjeldskaar *et al.* 2018). Although it is unclear when this modern transgression initiated, it is believed to be a relatively recent phenomenon, as coast line erosion proximal to pre-1900 cultural heritage and trapper huts have been some of the key indicators of active transgression (Andersson *et al.* 2000; Sessford *et al.* 2015).

The period between 2.5 – 2.0 ka BP marks the Holocene minimum in driftwood arrival and matches the occurrence rate seen during the end of the Younger Dryas (Fig. 6). We assume the Holocene minimum in driftwood arrival relates to persistent or semi-permanent land-fast ice, minimizing the transport and catchment for driftwood accumulation (Funder *et al.* 2011). The increase in driftwood arrival exhibited through the last 2 ka of the Holocene record resembles the increase seen in the first half of the Early-Holocene (Fig. 6). Sea ice reconstructions derived from IP25 proxy records suggest variability in sea ice cover during the Late Holocene associated with sporadic warm sea surface temperatures (Müller *et al.* 2012; Sarnthein *et al.* 2003). Brine formation is believed to reflect sea ice cover above basins and a Late Holocene record from Storfjorden suggests episodic periods of intense production separated by periods of reduced brine formation (Rasmussen & Thomsen 2014). It is unclear if this trend-reversal in Holocene driftwood arrival is a result of decreasing sea ice cover around Svalbard (Fig. 6). The occurrence of Holocene driftwood on raised marine shorelines is influenced by preservation, and therefore may as well be influenced by Mid and Late Holocene shoreline transgressions.

The occurrence of thermophilous molluscs decreases through the latter half of the Holocene and tapers off entirely at the start of the Late Holocene (Fig. 10). In addition to the final two *Mytilus edulis* dating c. 3.7 ka BP, it appears the species may have returned to inner Isfjorden based on a single young sample dating 0.9 ka BP (Fig. 10; Samtleben 1985; Mangerud & Svendsen 2017). The lower occurrence of warm water molluscs through the Holocene suggests waters around Svalbard are cooling and the islands are transitioning into the Neoglacial in phase with declining summer insolation. The re-occurrence of the Mytilus at 0.9ka BP overlaps with the Medieval Warm Period and may suggest warm Atlantic waters were arriving to Svalbard. The mapped distribution of these warm water molluscs within fjords suggests the species thrive in the inner shallow branches of fjord-systems with minimal glacial influence (Dicksonfjorden and Billefjorden; Salvigsen *et al.* 1992; Salvigsen 2002; Blake *et al.* 2006; Mangerud & Svendsen 2017).

An increasing number of glacier re-advances are constrained by radiocarbon dates of material re-sedimented in or overlain by glacial deposits throughout the Late Holocene (Fig. 10). These samples have been collected across Svalbard and become more frequent in the last 2 millennia (Fig. 6). The majority of the ages date to between 1.0 – 0.5 ka BP (Fig. 10). These sample dates constrain the maximum age of glacier re-advance during the Neoglacial or early LIA where they subsequently went on to reach their Late Holocene maximum extent (Baranowski & Karlén 1976; Dzierzek *et al.* 1990; Furrer 1991; Humlum *et al.* 2005). Several additional studies indicate Late Holocene glacier maxima occurred even earlier in the Neoglacial (Punning *et al.* 1976; Werner 1993; Sharin *et al.* 2014). Despite recent criticism, simplistic lichenometry studies suggest glaciers across Svalbard have experienced numerous phases of glacier advance, followed by moraine stabilization during the last 2.0 ka BP (Fig. 10; Werner 1993; Osborn *et al.* 2015). Exposure dating of moraine ridges has been conducted on several Late Holocene glacier forelands as a means of testing whether the LIA was the greatest glacial event of the Late Holocene (Fig. 10; Reusche *et al.* 2014; Philipps *et al.* 2017). The TCN studies have effectively supported earlier works, endorsing there have been numerous phases of glacial re-advance during the Late Holocene and concluding LIA is not the largest glacial event (at least in some locations; Werner 1993).

Another technique suggesting an episodic phase of cooling during the Neoglacial is radiocarbon dating ice-entombed plants over a range of elevations to reconstruct snow-line-lowering or ice cover expansion throughout a region (Miller *et al.* 2017). Results from a study presenting over 40 radiocarbon ages from central Spitsbergen suggest that there were at least four phases of widespread ice cover expansion resulting in a general snow line lowering between 2.0 ka BP and 0.5 ka BP prior to the LIA-ice expansion (Miller *et al.* 2017). They further demonstrate that ice expansion occurred as early as 4.0 ka BP (Fig. 10; Miller *et al.* 2017).

Lacustrine- Late Holocene glacial lake records all suggest increasing glacial influence, characterized by increasing rates of sedimentation and transitions from organic-rich to mineragentic strata (Fig. 10). Other less maritime glacial lake records suggest episodic increases in glacial activity within catchments starting as early as c. 4 ka BP (Hajeren; van der Bilt *et al.* 2016) and prior to 3.0 ka BP (Kløsa and Linnévatnet; Røthe *et al.* 2015; Svendsen & Mangerud 1997). In Gjøavatnet (1 m a.s.l.), located in Northwestern Svalbard, the transition from organic-rich to glacial sedimentation does not occur until c. 1 ka BP. All glacial lake records show enhanced glacial influence during the last millennium (Fig. 10). Lacustrine records from non-glacial lakes (Hakluytvatnet and Skardsjøen) suggest decreasing productivity, declining plant species diversity as well as increased Late Holocene mineragenic input due to increased runoff (Alsos *et al.* 2015; Gjerde *et al.* 2018). Additionally, a 1.8 ka alkenone record from Kongressvatnet, located in central western Spitsbergen suggests the LIA was relatively mild in the region implying precipitation may be the key driver behind Late Holocene glacier expansion (D'Andrea *et al.* 2013).

Neoglacial – Little Ice Age re-advances

The classical perspective of the (Late) Holocene glacial maximum occurring during the culmination of the LIA is increasingly being challenged (Svendsen & Mangerud 1997; Snyder *et al.* 2000). Svalbard glaciers re-advanced throughout the Neoglacial period (Werner 1993; Reusche *et al.* 2014; Røthe *et al.* 2015; van der Bilt *et al.* 2016; Philipps *et al.* 2017) and during the LIA (Svendsen & Mangerud 1997; Snyder *et al.* 2000; Humlum *et al.* 2005; de Wet *et al.* 2018). Early observations of glaciers during the 1900s describe Svalbard glaciers near to their Late Holocene maximum extents. However this does not suggest anything about the timing of glacier re-advance, but rather that the glaciers were slowly starting to retreat. The majority of Late Holocene glacier re-advances (dated by overridden vegetation or mollusc shells) date to the early (between 1.0 - 0.5 ka BP), not the late LIA (Fig. 10).

Several glacier re-advances constrained to the Neoglacial – LIA have been characterized as surges based on size, extent of glacial deposits and preservation of landforms (related to rapid ice advances) corresponding to associated ice-margins (Ottesen *et al.* 2008; Kristensen *et al.* 2009; Kempf *et al.* 2013; Farnsworth *et al.* 2016, 2017; Lovell & Boston 2017; Lyså *et al.* 2018; Flink *et al.* 2017). While the most extensive Late Holocene glacier deposits have been associated with surge-type behavior during, or at, the culmination of the LIA (Kristensen *et al.* 2009; Kempf *et al.* 2013; Flink *et al.* 2015; Lyså *et al.* 2018) an increasing number of studies have identified both complete and fragmented moraine ridges outboard of the LIA maxima (Werner 1993; Sletten *et al.* 2001; Reusche *et al.* 2014; Philipps *et al.* 2017; Larsen *et al.* 2018).

Little is known about patterns of Late Holocene precipitation across Svalbard. One alkenone-based (summer) temperature reconstruction from western Spitsbergen lake sediments suggests the Little Ice Age was "mild" and that precipitation played a larger contribution to regional glacier re-advances than previously acknowledged (D'Andrea *et al.* 2013). While it is important to highlight our limited knowledge of past precipitation, there is ample evidence suggesting that air and ocean temperatures were relatively cool and favored glaciers during the late Neoglacial and LIA (Divine *et al.* 2011; Bartels *et al.* 2017; Røthe *et al.* 2018; van der Bilt *et al.* 2018; Balascio *et al.* 2018; Luoto *et al.* 2018).

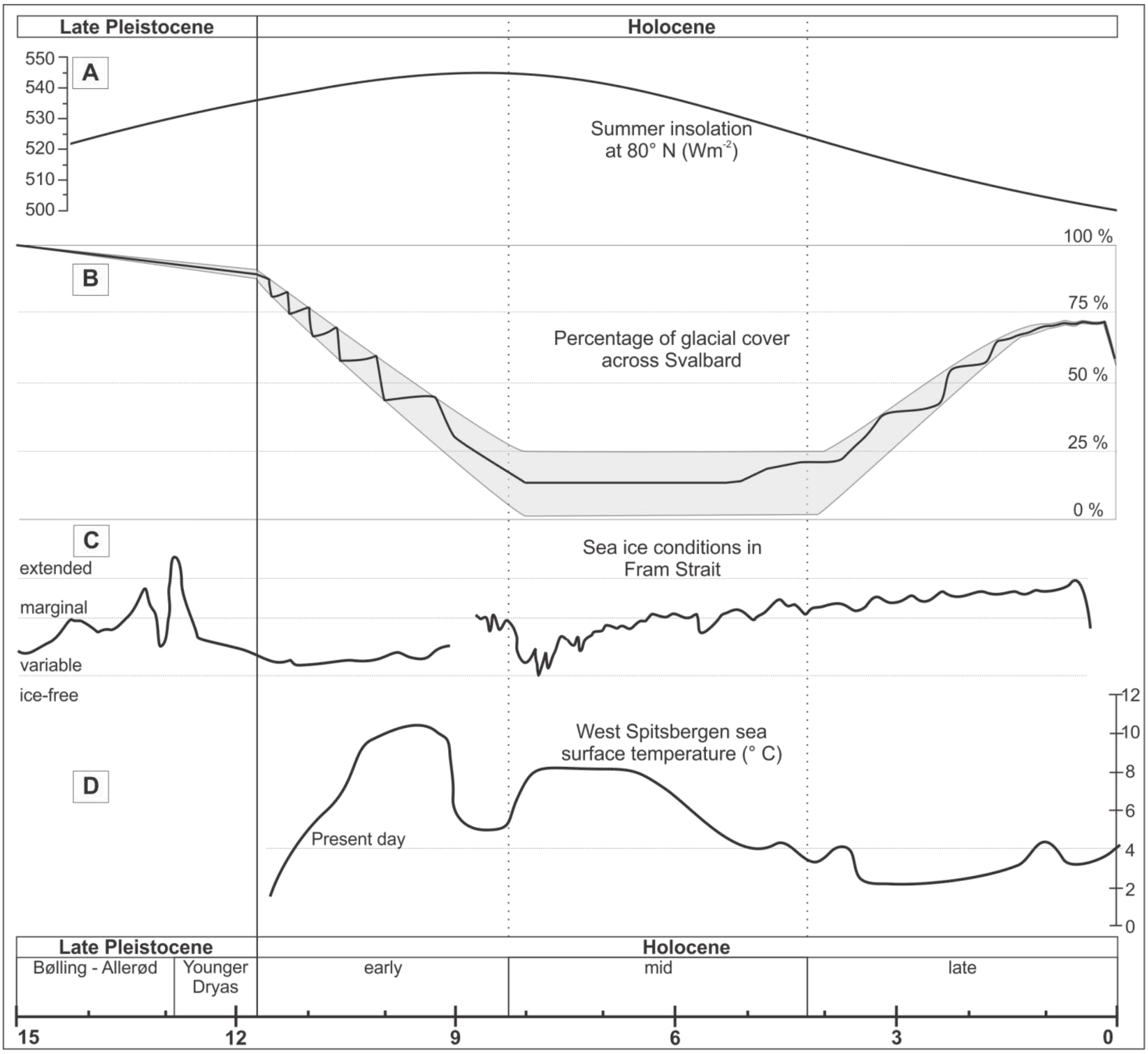

Fig. 11 Timeline of Late Pleistocene and Holocene with divisions of the Holocene indicated (Cohen et al. 2013; updated). Curves of A) summer insolation at 80 °N (Wm^{-2}; Laskar et al. 2004) B) the percentage of project glacier cover across Svalbard. Grey shade reflects uncertainty; low-end

estimates relate to evidence of the extent of small cirque and valley glaciers, while upper-end estimates correspond to high elevation ice caps. C) Reconstructed sea ice cover from Fram Strait derived from sea ice proxy IP25 (Müller et al. 2012; Müller & Stein 2014) and D) sea surface temperatures from western Spitsbergen derived from presence of warm water molluscs (Mangerud & Svendsen 2017) are presented.

Sea ice conditions during the Neoglacial and LIA are characterized by increasing but variable ice extent around Svalbard (Fig. 11; Müller & Stein 2012; Müller et al. 2014 Bartels et al. 2017). Although increasing sea ice cover reconstructed through most of the Late Holocene is presumed to favor glacier growth (suppressing summer temperatures, minimizing the number of positive degree days and decreasing frontal ablation) it is unclear how much this restricts precipitation.

A summary timeline of reconstructed conditons from Svalbard indicates the relationship of estimated glacier cover over Svalbard compared reconstructed sea ice conditions and sea surface temperature as well as summer insolation (Fig. 11; Laskar *et al.* 2004). Glaciers were most likely at their maximum Holocene extent during the onset of the Holocene. The Mid Holocene is characterized by a low percentage ice cover. Glaciers re-advance during the Early and Late Holocene. The marine Holocene thermal optimum occurred in the Early Holocene while the terrestrial thermal optium likely occurred during the Mid Holocene (Mangerud & Svendsen 2017). Glaciers located in small, low elevation valleys and cirques likely degalciated completely during the Mid Holocene (de Wet *et al.* 2018). Marine terminating outlet glaciers seem to remain throughout the Mid Holocene in some locations. However, these outlet glaciers likely corresponded to high elevation catchments. Glaciers re-advanced through the Late Holocene and predominantly reach Neoglacial maximums some time in the last millennium. Widespread glacier retreat has been exhibited across Svalbard through the last century.

SUMMARY

(1) Is there evidence of Younger Dryas cooling and glacier re-advances on Svalbard?

No evidence of a synchronous glacial event is observed during the Younger Dryas on Svalbard. There is mounting evidence suggesting glacier re-advances during the end of the Younger Dryas into the Early Holocene. These deposits are not well dated, but re-advances appear to span the transition from Late Pleistocene to Early Holocene. This phase of glacier activity may relate to glacio-dynamic behavior resulting from a transition into a period with less extensive sea ice cover leading to increased precipitation as well as warming oceans and atmosphere. These factors all have the potential to influence glacier hydrological systems and thermal, which could result in a dynamic, unsustainable advance or surge-type behavior (Dunse *et al.* 2015; Østby *et al.* 2017; Farnsworth *et al.* 2018; Sevestre *et al.* 2015, 2018).

(2) Did meltwater from the collapsing Laurentide Ice Sheet influence climate on Svalbard (8.2 ka BP)?

It is possible, but data remains inconclusive. In select locations, marine stratigraphic studies suggest cooling and freshening of waters around 8.2 ka BP. We are unable to know if these shifts in ocean conditions were great enough to impact the Svalbard glaciers systems. The absence of a Svalbard glacier event relating to the 8.2 ka BP meltwater pulse may reflect both the severity of Early Holocene retreat and the magnitude of Late Holocene re-advances during the Neoglacial and Little Ice Age. As of yet, there has been no 8.2 ka BP glacial event identified on Svalbard. Less is known about the influence of earlier melt water pulses from the LIS.

(3) When was the Holocene glacial minimum and what was the ice cover during this period?

We do not (yet) know when glaciers on Svalbard reached a Holocene minimum, nor how reduced ice cover became. While lake sediment studies targeting cirque glaciers suggest that catchments were ice-free through the Mid Holocene, lake studies have yet to target larger glacier systems. Marine IRD studies suggest that tidewater glaciers in some fjords retreated back to unknown terrestrial positions, while other fjords probably hosted a calving ice front throughout the entire Holocene. The Holocene glacial minimum probably occurred in the Mid Holocene sometime between 8.0 - 6.5 ka BP. The glacial minimum certainly occurred after the marine thermal optimum (10.0 – 9.2 ka BP), potentially lagging the peak in ocean temperatures and summer insolation on a millennium time scale.

(4) *When was the most extensive ice cover during the Holocene period and was the Little Ice Age the climax of the Neoglacial?*

Ice cover was probably most extensive at the onset of the Holocene based on the presumed amount of residual SBSIS-ice. Glacier re-advances have been identified, both in the Early and Late Holocene, but it is unknown which phase of glacier re-advance was the greatest. The LIA is generally believed to be the biggest Holocene glacial event on Svalbard. However, increasing numbers of moraines outboard of the LIA extent of both Neoglacial and Early Holocene age suggest ice margins extended further at different periods during the Holocene. As we do not yet know how reduced glaciers were prior to the advance, it is difficult to reconcile which event was of the greatest magnitude. Furthermore the lack of knowledge regarding the rate of advance limits our understanding of how rapidly Svalbard glaciers have responded to shifts in Holocene climate.

(5) Which sedimentary archives provide the best detail of Holocene glaciers and climate?

This depends on which questions one is targeting. But studies should have a holistic approach to systems and processes; taking into account a mixture of methods, archives and disciplines.

(6) To what extend has ice dynamics and surge-type behavior influenced Holocene glacier fluctuations on Svalbard?

Ice dynamics play an important role in glacier fluctuations today. The extent is unknown, but ice dynamics are believed to have also played a role in ice marginal fluctuations during the Early and the Late Holocene.

- Throughout the Holocene, Svalbard glaciers have responded to a varying combination of climatic, environmental and dynamic driving factors which influence both the extent and behavior of ice margins.
- Glaciers during the Late Pleistocene and Early Holocene were dynamic, exhibited re-advances and extended well beyond Late Holocene glacier maxima in many locations across Svalbard.
- The marine Holocene thermal optimum on Svalbard marked by the early arrival of warm water species to the coasts of Svalbard during the onset of the Holocene, pre-dates the peak in northern hemisphere summer insolation and the terrestrial thermal optimum.
- Glaciers covered a small, but unknown percentage of Svalbard, in some locations terminated at sea level, during the Holocene glacial minimum.
- Evidence of episodic Neoglacial glacier re-advances is being identified more commonly across Svalbard, suggesting an irregular phase of glacier favorable conditions during the Late Holocene.
- The Little Ice Age maximum does not reflect the glacial maximum extent across Svalbard; since the deglaciation, the onset of the Holocene or even during the Late Holocene, in most locations.

REFERENCES for SVALHOLA Database

Aagaard-Sørensen *et al.* (2014), Adrielsson *et al.* (1992), Alsos *et al.* (2015), Andersen *et al.* (1996), Andersson *et al.* (1999, 2000), Baeten *et al.* (2010), Bakke *et al.* (2017), Balascio *et al.* (2018), Baranowski & Karlén (1976), Bartels *et al.* (2017, 2018), Beierlein *et al.* (2015), Berben *et al.* (2014) Bernardová & Kosnar (2012), Berge *et al.* (2005), van der Bilt *et al.* (2015, 2017a, 2017b), Birkenmajer & Olsson (1970), Birks (1991), Blake (1961a, 1961b, 1962, 1989, 2006), Blake *et al.* (1965), Bondevik *et al.* (1995), Boulton (1979), Boulton *et al.* (1999), Bratlie, B. (1994), Brooks & Birks (2001, 2004), Brückner & Halfar (1994), Brückner (1996), Brückner *et al.* (2002), Brückner & Schellmann (2003), Bunin (2015), Bøyum & Kjensmo (1980), Cameron *et al.* (1999), Chauhan *et al.* (2014, 2016), Corbel (1966), Cyposa *et al.* (1982), D'Andrea *et al.* (2012), Divine *et al.* (2011), Dinely (1953), Dokken (1995), Dokken & Hald (1996), Dylmer *et al.* (2013), Dzieriek *et al.* (1990), Ebbesen *et al.* (2007), Eitel *et al.* (2002), Elgersma & Helliksen(1986), Elverhøi & Solheim (1983), Elverhøi *et al.* (1995a, 1995b, 1998), Evans & Rea (2005), Farnsworth *et al.* (2017, 2018) Feyling-Hanssen (1955), Feyling-Hanssen & Jørstad (1950), Feyling-Hanssen & Olsson (1960), Fjeldskaar *et al.* (2018), Flink *et al.* (2017a, 2017b), Flink & Noormets (2018), Forman (1989, 1990a,1990b), Forman *et al.* (1987, 2004), Forman & Miller (1984), Forman & Ingólfsson (2000), Forwick & Vorren (2007, 2009), Forwick *et al.* (2010), Fransner *et al.* (2017, 2018), Furrer *et al.* (1991), Gilbert *et al.* (2018), Gjerde *et al.* (2017), Gjermundsen *et al.* (2015), Goslar & Pazdur (1985), Guilizzoni *et al.* (2006), Gottlich & Hornburg (1982), Haga (1978), Hald & Korsum (2008), Hald *et al.* (2001a, 2001b, 2004, 2007), Hansen & Knudsen (1995), Hansen *et al.* (2011), Hebbeln & Wefer (1997), Heiri *et al.* (2011), Henriksen *et al.* (2014), Hjort *et al.* (1995), Hogan *et al.* (2010a, 2010b, 2017), Hole & Macias-Fauria (2017), Holm *et al.* (2011), Holmgren *et al.* (2010), Hoppe (1972), Hoppe *et al.* (1969), Hormes *et al.* (2011, 2013), Houmark-Nielsen & Funder (1999), Humlum *et al.* (2005), Hughes *et al.* (2016), Hyvärinen (1970), Haggblom (1982), Isakssonv *et al.* (2005), Jankovská (1994), Jernas *et al.* (2013), Jessen *et al.* (2010), Jonsson (1983), Kaakinen *et al.* (2009), Karlén (1987), Kjellström (1901), Kempf *et al.* (2013), Klysz *et al.* (1988), van der Knaap, W.O. (1985, 1988a, 1988b, 1989), Knape (1971), Koç *et al.* (2002), Kristensen *et al.* (2009, 2013), Kubishcta *et al.* (2011), Łącka *et al.* (2015), Landvik *et al.* (1987, 1992a, 1992b, 1995, 1998, 2003, 2005, 2013, 2014), Larsen *et al.* (2018), Lehman (1989), Lehman & Forman (1992,1987), Lindner *et al.* (1991), Lloyd *et al.* (1996), Long *et al.* (2012), Lucchi *et al.* (2013, 2015), Luoto *et al.* (2011, 2018), Lyså *et al.* (2018), Lønne & Fuglei (1997), Lønne & Mangerud (1991), Lønne & Nemec (2004), Lønne (2005), Majewski *et al.* (2009), Mangerud & Gulliksen (1975), Mangerud & Landvik (2007), Mangerud & Svendsen (1990a, 1990b, 1992, 2017), Mangerud *et al.* (1992, 1998, 2006), Mäusbucher *et al.* (2002), Miller (1982), Miller *et al.* (2017), Möller *et al.* (1995), Müller *et al.* (2012), Müller & Stein (2014), Nagy (1984), Nevalainen *et al.* (2012), Nielsen & Rasmussen (2018), Oerlemans *et al.* (2011), Ojala *et al.* (2014, 2016), Olsson (1960, 1969), Olsson & Piyanui (1965), Ottesen *et al.* (2007, 2008), Paasche & Bakke (2015), Panieri *et al.* (2014), Péwé *et al.* (1982), Philipps *et al.* (2017), Plassen *et al.* (2004), Pike (1898), Punning *et al.* (1976, 1978, 1980, 1982), Rasmussen & Thomsen (2009, 2014, 2015), Rasmussen *et al.* (2007, 2014a, 2014b), Reusche *et al.* (2014), Ronnert & Landvik (1993), Rowanm *et al.* (1982), Rozema *et al.* (2006), Rüther *et al.* (2012), Røthe *et al.* (2015, 2018), Salvigsen, O. (1977, 1978, 1979, 1981, 1984, 2002), Salvigsen & Elgersma (1993), Salvigsen & Høgvard (2005), Salvigsen & Mangerud (1991), Salvigsen & Nydal (1981), Salvigsen & Österholm (1982), Salvigsen & Winsnes (1987), Salvigsen *et al.* (1990, 1991, 1992), Samtleben (1985), Sarnthein *et al.* (2003), Schytt *et al.* (1968), Sessford *et al.* (2015), Sharin & Arslanov (2011), Sharin & Derzhavin (2012), Sharin *et al.* (2007, 2014), Singh *et al.* (2011), Skirbekk *et al.* (2010), Sletten *et al.* (2001), Ślubowska-Woldengen *et al.* (2005, 2007, 2008), Snyder *et al.* (1994, 2000), Spielhagen *et al.* (2004, 2005), Stuiver & Polach (1977), Stankowski *et al.* (1989), Sternal *et al.* (2014), Streuff *et al.* (2017a, 2017b), Sun *et al.* (2006), Svendsen & Mangerud (1997), Svendsen *et al.* (1992, 1996), Szczucinski *et al.* (2009), Troitsky *et al.* (1979), Werner (1988, 1990, 1993), Werner *et al.* (2013), de Wet, *et al.* (2018), Winkelmann & Knies (2005), Wójcik, A., Zala, W. (1993), Yang *et al.* (2018), Yuan *et al.*

(2009, 2011), Young *et al*. (2018), Zale & Brydsten (1993), Zelikson (1971), Ziaja & Salvigsen (1995), Österholm (1986, 1990).

ACKNOWLEDGEMENTS

This review has benefited from constructive disucssions and feedback from Skafti Brynjólfsson. Fianancial support has been provided by the Svalbard Environmental Protection Fund (16/35; to WRF), the Carlsberg Foundation (CF14-0756 to AS) and Arctic Research and Studies (to AS & WRF). Authors are grateful for extensive support from Berit Jakobsen and Catherine Fjeldstad at the UNIS Library.

REFERENCES

Note this list only includes citations from the manuscripts main text. Database references can be found in Table S4.

Alexanderson, H., Murray, A.S. (2012a): Luminescence signals from modern sediments in a glaciated bay, NW Svalbard. *Quaternary Geochronology 10,* 250–256.

Alexanderson, H., Murray, A.S. (2012b): Problems and potential of OSL dating Weichselian and Holocene sediments in Sweden. *Quaternary Science Reviews 44,* 37–50.

Alsos, I.G., Sjögren, P., Edwards, M.E., Landvik, J.Y., Gielly, L., Forwick, M., Coissac, E., Brown, A.G., Jakobsen, L.V., Føreid, M.K., Pedersen, M.W. (2015): Sedimentary ancient DNA from Lake Skartjørna, Svalbard: assessing the resilience of arctic flora to Holocene climate change. *The Holocene 26,* 627–642.

Andersson, G. (1896): Svenska växtvärldens historia. Stockholm: P.A. Norstedt & Söner.

Arlov, T.B. (2005) The Discovery and Early Exploitation of Svalbard. Some Historiographical Notes. *Acta Borealia 22,* 3–19.

Baeten, N.L., Forwick, M., Vogt, C., Vorren, T.O. (2010): Late Weichselian and Holocene sedimentary environments and ice rafting in Isfjorden, Spitsbergen. *Geological Society of London, Special Publications 344,* 207–223.

Balascio, N.L., D'Andrea, W.J., Gjerde, M., Bakke, J. (2018): Hydroclimate variability of High Arctic Svalbard during the Holocene inferred from hydrogen isotopes of leaf waxes. *Quaternary Science Reviews 183,* 177–187.

Baranowski, S., Karlén, W. (1976): Remnants of Viking Age tundra in Spitsbergen and northern Scandinavia: *Geografiska Annaler Series A 58,* 35–39.

Bartels, M., Titschack, J., Fahl, K., Stein, R., Seidenkrantz, M.S., Hillaire-Marcel, C., Hebbeln, D. (2017): Atlantic water advection vs. glacier dynamics in northern Spitsbergen since early deglaciation. *Climate of the Past 13,* 1717–1749.

Bartels, M., Titschack, J., Fahl, K., Stein, R., Hebbeln, D. (2018): Wahlenbergfjord, eastern Svalbard: a glacier-surrounded fjord reflecting regional hydrographic variability during the Holocene? *Boreas 48.* DOI: 10.1111/bor.12325.

Bennett, K.D., Haberle, S.G., Lumley, S.H. (2000): The Last Glacial-Holocene Transition in Southern Chile. *Science 290,* 325–328.

Bertrand, A. (1852): Voyages de la Commission scientifique du Nord en Scandinavie. 1, Danemark, Norvège, Spitzberg: Atlas historique et pittoresque, lithographié d'aprés les dessins de MM. Mayer, Lauvergne et Giraud.

van der Bilt, W.G.M., Bakke, J., Vasskog, K., D’Andrea, W.J., Bradley, R.S., Olafsdóttir, S. (2016): Reconstructionof glacier variability from lake sediments reveals dynamic Holocene climate in Svalbard. *Quaternary Science Reviews 126,* 201–218.

van der Bilt, W.G.M., Lane, C.S., Bakke, J. (2017): Ultra-distal Kamchatkan ash on Arctic Svalbard: Towards hemispheric cryptotephra correlation. *Quaternary Science Reviews 164,* 230–235.

van der Bilt, W.G.M., D'Andrea, W.J., Bakke, J., Balascio, N.L., Werner, J.P., Gjerde, M., Bradley, R.S. (2018): Alkenone-based reconstructions reveal four-phase Holocene temperature evolution for High Arctic Svalbard. *Quaternary Science Reviews 183,* 204–213.

Birks, H. (1991): Holocene vegetational history and climatic change in west Spitsbergen – Plant macrofossils from Skardtjørna, an Arctic lake. *The Holocene 1,* 209–218.

Blake, W.J. (1962): Geomorphology and Glacial Geology in Nordaustlandet, Spitsbergen. PhD thesis, Department of Geology, Ohio State University, Columbus, 1–477.

Blake, W.J. (1989): Radiocarbon dating by accelerator mass spectrometry: A contribution to the chronology of Holocene events in Nordaustlandet, Svalbard. *Geografiska Annaler Series A 71,* 59–74.

Blake, W.J. (2006): Occurrence of the Mytilus edulis complex on Nordaustlandet, Svalbard: Radiocarbon ages and climatic implications. *Polar Research 25,* 123–137.

Blaszczyk, M., Jania, J.A., Hagen, J.O. (2009): Tidewater glaciers of Svalbard: Recent changes and estimates of calving fluxes. *Polish Polar Research 30,* 85–142.

Bond, G., Broecker, W., Johnsen, S., McManus, J., Labeyrie, L., Jouzel, J., Bonani, G. (1993) Correlations between climate records from North Atlantic sediments and Greenland ice. *Nature 365,* 143–147.

Bond, G., Kromer, B., Beer, J., Muscheler, R., Evans, M.N., Showers, W., Hoffmann, S., Lotti-Bond, R., Hajdas, I., Bonani, G. (2001): Persistent solar influence on north Atlantic climate during the Holocene. *Science 294,* 2130–2136.

Bondevik, S., Mangerud, J., Ronnert, L., Salvigsen, O. (1995): Postglacial sea-level history of Edgeoya and Barentsoya, eastern Svalbard. *Polar Research 14,* 153–180.

Boulton, G.S. (1979): Glacial history of the Spitsbergen archipelago and the problem of a Barents Shelf ice sheet. *Boreas 8,* 31–57.

Briner, J.P., McKay, N.P., Axford, Y., Bennike, O., Bradley, R.S., de Vernal, A., Fisher, D., Francus, P., Fréchette, B., Gajewski, K., Jennings, A., Kaufman, D.S., Miller, G., Rouston, C., Wagner, B. (2016): Holocene climate change in Arctic Canada and Greenland. *Quaternary Science Reviews 147,* 340–364.

Brückner, H., Schellmann, G. (2003): Late Pleistocene and Holocene Shorelines of Andreeland, Spitsbergen (Svalbard): Geomorphological Evidence and Palaeo-Oceanographic Significance. *Journal of Coastal Research 19,* 971–982.

Carlson, A.E. (2013): The Younger Dryas Climate Event. In: Elias S.A. (ed.) Amsterdam: Elsevier. *The Encyclopedia of Quaternary Science 3,* 126–134.

Christiansen, H.H., Etzelmüller, B., Isaksen, K., Juliussen, H., Farbrot, H., Humlum, O., Johansson, M., Ingeman-Nielsen, T., Kristensen, L., Hjort, J., Holmlund, P., Sannel, A.B.K., Sigsgaard, C., Åkerman, H.J., Foged, N., Blikra, L.H., Pernosky, M.A., Ødegård, R.S. (2010): The thermal state of permafrost in the nordic area during the international polar year 2007–2009. *Permafrost and Periglacial Processes 21,* 156–181.

Claesz, C. (1598): Het Nieuwe Land (Dutch for “the New Land”) Map of Arctic exploration.

Cohen, K.M., Finney, S.C., Gibbard, P.L., Fan, J.X. (2013; updated): The ICS international chronostratigraphic chart. *Episodes 36,* 199–204.

D'Andrea, W.J., Vaillencourt, D.A., Balascio, N.L., Werner, A., Roof, S.R., Retelle, M., Bradley R.S. (2012): Mild little ice age and unprecedented recent warmth in an 1800 year lake sediment record from Svalbard. *Geology 40,* 1007–1010.

Dansgaard, W., Johnsen, S.J., Clausen, H.B., Dahl-Jensen, D., Gundestrup, N.S., Hammer, C.U., Hvidberg, C.S., Steffensen, J.P., Sveinbjörnsdottir, A.E., Jouzel, J. Bond, G. (1993): Evidence for general instability of past climate from a 250-kyr ice-core record. *Nature 364,* 218–220.

Davis, P.T., Menounos, B., Osborn, G. (2009): Holocene and latest Pleistocene alpine glacier fluctuations: A global perspective. *Quaternary Science Reviews 28,* 2021–2033.

De Geer, G. (1908): The Spitsbergen expedition of 1908 and the geological excursion to Spitsbergen 1910. Exkursionen till Spetsbergen 1908 och expeditionen till Spetsbergen 1910 (Gerard De Geer). Ymer. 341–344.

Dickson, R.R., Osborn, T.J., Hurrell, J.W., Meincke, J., Blindheim, J., Adlandsvik, B., Vinje, T., Alekseev, G., Maslowski, W. (2000): The Arctic Ocean response to the North Atlantic Oscillation. *Journal of Climate 13,* 2671–2696.

Divine, D., Isaksson, E., Martma, T., Meijer, H.A.J., Moore, J., Pohjola, V., van de Wal, R.S.W., Godtliebsen, F. (2011): Thousand years of winter surface air temperature variations in Svalbard and northern Norway reconstructed from ice-core data. *Polar Research 30,* 73–79.

Drange H, Dokken T, Furevik T Gerdes, R., Berger, W., Nesje, A., Orvik, K.A., Skagseth, Ø., Skjelvan, I., Østerhus, S. (2005): The Nordic Seas: an overview. In: Drange H, Dokken T, Furevik T et al (eds) The Nordic seas: an integrated perspective. American Geophysical Union, Washington, DC, 1–10.

Dunse, T., Schellenberger, T., Hagen, J., Kääb, A., Schuler, T., Reijmer, C. (2015): Glacier-surge mechanisms promoted by a hydro-thermodynamic feedback to summer melt. *The Cryosphere 9,* 197–215.

Duller, G.A.T. (2006): Single grain optical dating of glacigenic deposits. *Quaternary Geochronology 1,* 296–304.

Duller, G.A.T. (2008): Single-grain optical dating of Quaternary sediments: why aliquot size matters in luminescence dating. *Boreas 37,* 589–612.

Dzieriek, J., Nitychoruk, J., Rzetkowska, A. (1990): Geological-geomorphological analysis and ^{14}C dating of submoraine organogenic deposits within the Renardhreen outer margin, Wedel-Jarlsherg Land, Spitsbergen. *Polar Research 8,* 215–281.

Eckerstorfer, M., Christiansen, H.H. (2011): The “High Arctic Maritime Snow Climate” in Central Svalbard. *Arctic, Antarctic, and Alpine Research 43,* 11–21.

Ekholm, N.G. (1887): Observations Faites au Cap Thorsden, Spitzberg par l’Expédition Suédoise. L'Academie Royale des Sciences de Suede, Vol. 1, 1–218, Vol. 2, 1–207.

England, J., Dyke, A. S., Coulthard, R. D., McNeely, R., Aitken, A. (2013): The exaggerated radiocarbon age of deposit-feeding molluscs in calcareous environments. *Boreas 42*, 362–373.

Eitel, B., van der Borg, K., Eberle, J., Megies, H. (2002): Late Pleistocene/Early Holocene glacial history of northern Andreeland (northern Spitsbergen/Svalbard Archipelago): evidence from glacial and fluvio-glacial deposits. *Zeitschrift Fur Geomorphologie 46,* 337–364.

Farnsworth, W.R., Ingólfsson, Ó., Retelle, M., Schomacker, A. (2016): Over 400 previously undocumented Svalbard surge-type glaciers identified. *Geomorphology 264,* 52–60.

Farnsworth, W.R., Ingólfsson, Ó., Noormets, R., Allaart, L., Alexanderson, H., Henriksen, M., Schomacker, A. (2017): Dynamic Holocene glacial history of St. Jonsfjorden, Svalbard. *Boreas 46*, 585–603.

Farnsworth, W.R., Ingólfsson, Ó., Retelle, M., Allaart, L., Håkansson, L., Schomacker, A. (2018): Svalbard glaciers re-advanced during the Pleistocene-Holocene transition. *Boreas 47*, 1022–1032.

Farnsworth, W.R., Ingólfsson, Ó., Alexandersson H., Forwick, M., Noormets, R., Retelle, M., Schomacker, A. (*in prep.)* Holocene glacial and climate history of Svalbard - status, perspectives and challenges.

Feyling-Hanssen. R.W. (1955): Stratigraphy of the marine Late- Pleistocene of Billefjorden, Vestspitsbergen. *Norsk Polarinstitutts Skrifter 107,* 1–226.

Fjeldskaar, W., Bondevik, S., Amantov, A. (2018): Glaciers on Svalbard survived the Holocene thermal optimum. *Quaternary Science Reviews 199*, 18–29.

Flink, A.E., Noormets, R., Kirchner, N., Benn, D.I., Luckman, A., Lovell, H. (2015): The evolution of a submarine landform record following recent and multiple surges of Tunabreen glacier, Svalbard. *Quaternary Science Reviews 108,* 37–50.
Flink, A.E., Noormets, R., Fransner, O., Hogan, K.A., O'Regan, M., Jakobsson, M. (2017): Past ice flow in Wahlenbergfjorden and its implications for late Quaternary ice sheet dynamics in northeastern Svalbard. *Quaternary Science Reviews 163,* 162–179.
Flink, A.E., Noormets, R. (2018): Submarine glacial landforms and sedimentary environments in Vaigattbogen, northeastern Spitsbergen. *Marine Geology 402,* 244-263.
Forman, S.L., Mann, D.H., Miller, G.H. (1987): Late Weichselian and Holocene relative sea-level history of Bröggerhalvöya, Spitsbergen. *Quaternary Research 27,* 41–50.
Forman, S.L. (1990): Post-glacial relative sea-level history of northwestern Spitsbergen, Svalbard. *Geological Society of America Bulletin 102,* 1580–1590.
Forman, S.L., Ingólfsson, Ó., (2000): Late Weichselian glacial history and postglacial emergence of Phippsøya, Sjuøyane, northern Svalbard: a comparison of modelled and empirical estimates of a glacial-rebound hinge line. *Boreas 29,* 16–25.
Forman, S.L., Lubinski, D.J., Ingólfsson, Ó., Zeeberg, J.J., Snyder, J.A., Siegert, M.J., Matishov, G.G. (2004): A review of postglacial emergence on Svalbard, Franz Josef Land and Novaya Zemlya, northern Eurasia. *Quaternary Science Reviews 23,* 1391–1434.
Forwick, M., Vorren, T. (2007): Holocene mass-transport activity and climate in outer Isfjorden, Spitsbergen: marine and subsurface evidence. *The Holocene 17,* 707–716.
Forwick, M. Vorren, T.O. (2009): Late Weichselian and Holocene sedimentary environments and ice rafting in Isfjorden, Spitsbergen. *Palaeogeography, Palaeoclimatology, Palaeoecology 280,* 258–274.
Forwick, M., Vorren, T. O., Hald, M., Korsun, S., Roh, Y., Vogt, C., Yoo, K.-C. (2010): Spatial and temporal influence of glaciers and rivers on the sedimentary environment in Sassenfjorden and Tempelfjorden, Spitsbergen. *Geological Society, London, Special Publications 344,* 163–193.
French, M.H. (2007): The Periglacial Environment. Third edition. Chichester, U.K. and Hoboken, New Jersey John Wiley & Sons, 1–458.
Fuchs, M., Owen, L.A. (2008): Luminescence dating of glacial and associated sediments: review, recommendations and future directions. *Boreas 37,* 636–659.
Funder, S., Goosse, H., Jepsen, H., Kaas, E., Kjær, K.H., Korsgaard, N.J., Larsen, N.K., Linderson, H., Lyså, A., Möller, P., Olsen, J., Willerslev, E. (2011): A 10,000-Year Record of Arctic Ocean Sea-Ice Variability—View from the Beach. *Science 333,* 747–750.
Furrer, G., Stapfer, A., Glaser, U. (1991): Zur nacheiszeitlichen Gletschergeschichte des Liefdefjords (Spitzbergen) Ergebnisse der Geowissenschaftlichen Spitzbergenexpedition 1990. *Geographica Helvetica 1991,* 147–155.
Førland, E.J., Hanssen-Bauer, I., Nordli, P.Ø. (1997): Climate statistics and longterm series of temperature and precipitation at Svalbard and Jan Mayen. Rapport 21/97 - *Report Series of the Norwegian Meteorological Institute* 1–92.
Førland, E.J., Benestad, R, Hanssen-Bauer, I. (2011): Temperature and precipitation development at Svalbard 1900–2100. *Advances in Meteorology 2011,* 1–14.
Geirsdóttir, Á., Miller, G.H., Axford, Y., Sædís, Ó. (2009): Holocene and latest Pleistocene climate and glacier fluctuations in Iceland. *Quaternary Science Reviews 28,* 2107–2118.
Gilbert, G.L., O'Neill, H.B., Nemec, W., Thiel, C., Christiansen, H.H., Buylaert, J.-P. (2018): Late Quaternary sedimentation and permafrost development in a Svalbard fjord-valley, Norwegian high Arctic. *Sedimentology 65*. DOI:10.1111/sed.12476.
Gjerde, M., Bakke, J., D'Andrea, W.J., Balascio, N.L., Bradley, R.S., Vasskog, K., Ólafsdóttir, S., Røthe, T.O., Perren, B.B., Hormes, A. (2017): Holocene multi-proxy environmental reconstruction from lake Hakluytvatnet, Amsterdamøya Island, Svalbard (79.5°N). *Quaternary Science Reviews 183,* 164–176.

Gjermundsen, E.F., Briner, J.P., Akçar, N., Salvigsen, O., Kubik, P., Gantert, N., Hormes, A. (2013): Late Weichselian local ice dome configuration and chronology in Northwestern Svalbard: early thinning, late retreat. *Quaternary Science Reviews 72,* 112–127.
Godfrey-Smith, D.I., Huntley, D.J., Chen, W.-H. (1988): Optical dating studies of quartz and feldspar sediment extracts. *Quaternary Science Reviews 7,* 373–380.
Grinsted, A., Moore, J.C., Jevrejeva S. (2009): Reconstructing sea level from paleo and projected temperatures 200 to 2100AD. *Climate Dynamics 34,* 461–472.
Guðmundsson, H.J. (1997): A review of the Holocene environmental history of Iceland. *Quaternary Science Reviews 16*, 81–92.
Hacquebord, L. (1995): In search of Het-Behouden-Huys A survey of the remains of the house of Barentsz, Willem on Novaya-Zemlya. *Arctic 48*, 248–256
Hald, M., Ebbesen, H., Forwick, M., Godtliebsen, F., Khomenko, L., Korsun, S., Ringstad Olsen, L., Vorren, T.O. (2004): Holocene paleoceanography and glacial history of the West Spitsbergen area, Euro-Arctic margin. *Quaternary Science Reviews 23*, 2075–2088.
Hald, M., Andersson, C., Ebbesen, H., Jansen, E., Klitgaard-Kristensen, D., Risebrobakken, B., Salomonsen, G.R., Sarnthein, M., Sejrup, H.P., Telford, R.J. (2007): Variations in temperature and extent of Atlantic Water in the northern North Atlantic during the Holocene. *Quaternary Science Reviews 26*, 3423–3440.
Hald, M, Korsum, S. (2008): The 8200 cal. yr. BP reflected in the Arctic fjord, Van Mijenfjorden. *The Holocene 18,* 981–990.
Hansen, J, Hanken, N-M., Nielsen, J.K., Thomsen, E. (2011): Late Pleistocene and Holocene distribution of Mytilus edulis in the Barents Sea region and its palaeoclimatic implications. *Journal of Biogeography 38,* 1197–1212.
Hanssen-Bauer, I., Kristensen Solås, M., Steffensen, E.L. (1990): The climate of Spitsbergen. *Norwegian Meteorological Institute Report 39/90*. 1–40.
Häggblom, A. (1982): Driftwood in Svalbard as an indicator of sea ice conditions. *Geografiska Annaler Series A 64,* 81–94.
Heinrich, H. (1988): Origin and consequences of cyclic ice rafting in the Northeast Atlantic Ocean during the past 130,000 years. *Quaternary Research 29,* 142–152.
Henriksen, M., Alexanderson, H., Landvik, J.Y., Linge, H., Peterson, G. (2014): Dynamics and retreat of the Late Weichselian Kongsfjorden ice stream, NW Svalbard. *Quaternary Science Reviews 92*, 235–245.
Heyman, J., Stroeven, A.P., Harbor, J.M., Caffee, M.W. (2011): Too young or too old: evaluating cosmogenic exposure dating based on an analysis of compiled boulder exposure ages. *Earth and Planetary Science Letters 302,* 71–80.
Hjort, C., Mangerud, J., Adrielsson, L., Bondevik, S., Landvik, J.Y., Salvigsen, O. (1995): Radiocarbon dated common mussels Mytilus edulis from eastern Svalbard and the Holocene marine climatic optimum. *Polar Research 14*, 239–243.
Hogan, K.A., Dowdeswell, J.A., Hillenbrand, C.-D., Ehrmann, W., Noormets, R. Wacker, L. (2017): Subglacial sediment pathways and deglacial chronology of the northern Barents Sea Ice Sheet. *Boreas 46*, 750–771.
Hole, G.M., Macias-Fauria, M. (2017): Out of the woods: Driftwood insights into Holocene pan-Arctic sea ice dynamics. *Journal of Geophysical Research: Oceans 122,* 7612–7629.
Holmgren, S.U., Bigler, C., Ingólfsson, Ó. Wolfe, A.P. (2010): The Holocene-Anthropocene transition in lakes of western Spitsbergen, Svalbard (Norwegian High Arctic): climate change and nitrogen deposition. *Journal of Paleolimnology 43,* 393–412.
Holmström, L.P. (1865): Märken efter istiden, iagttagna i Skåne. Cronholmska boktryckeriet, Malmö.
Hoppe, G., 1972. Ice sheets around the Norwegian Sea during the Würm glaciation. *Ambio Special Report 2,* 25–29.

Hormes, A., Akçar, N., Kubik, P.W. (2011): Cosmogenic radionuclide dating indicates ice-sheet configuration during MIS 2 on Nordaustlandet, Svalbard. *Boreas 40,* 636–649.

Hormes, A., Gjermundsen, E.F., Rasmussen, T.L. (2013): From mountain top to the deep sea—deglaciation in 4D of the northwestern Barents Sea ice sheet. *Quaternary Science Reviews 75,* 78–99.

Hughes, A.L.C., Gyllencreutz, R., Lohne, Ø.S., Mangerud, J., Svendsen, J.I. (2016): The last Eurasian ice sheets—a chronological database and time-slice reconstruction, DATED-1. *Boreas 45,* 1–45.

Humlum, O., Elberling, B., Hormes, A., Fjordheim, K., Hansen, O.H., Heinemeier, J. (2005): Late-Holocene glacier growth in Svalbard, documented by subglacial relict vegetation and living soil microbes. *The Holocene 15,* 396–407.

Hyvärinen, H. (1970): Flandrian pollen diagrams from Svalbard. *Geografiska Annaler Series A 52,* 213-222.

Ingólfsson, Ó. (2011): Fingerprints of Quaternary glaciations on Svalbard. *Geological Society, London, Special Publications 354,* 15–31.

Ingólfsson, Ó., Landvik, J.Y. (2013): The Svalbard-Barents Sea ice sheet– Historical, current and future perspectives. *Quaternary Science Reviews 64,* 33–60.

Isaksson, E., Divine, D., Kohler, J., Martma, T., Pohjola, V., Motoyama, H., Watanabe, O. (2005): Climate oscillations as recorded in Svalbard ice core delta^{18}O records between AD 1200 and 1997. *Geografiska Annaler Series A 87,* 203–214.

Isarin, R.F.B., Renssen, H. (1999): Reconstructing and modelling Late Weichselian climates: the Younger Dryas in Europe as a case study. *Earth-Science Reviews 48,* 1–38.

Ivy-Ochs, S., Kerschner, H., Maisch, M., Christl, M., Kubik, P.W., Schlüchter, C. (2009): Latest Pleistocene and Holocene glacier variations in the European Alps. *Quaternary Science Reviews 28,* 2137–2149.

Jennings, A., Andrews, J., Pearce, C., Wilson, L., Ólfasdótttir, S. (2015): Detrital carbonate peaks on the Labrador shelf, a 13–7ka template for freshwater forcing from the Hudson Strait outlet of the Laurentide Ice Sheet into the subpolar gyre. *Quaternary Science Reviews 107,* 62–80.

Jernas, P., Klitgaard Kristensen, D., Husum, K., Wilson, L., Koç, N. (2013): Palaeoenvironmental changes of the last two millennia on the western and northern Svalbard shelf. *Boreas 42,* 236–255.

Kempf, P., Forwick, M., Laberg, J.S., Vorren, T.O. (2013): Late Weichselian and Holocene sedimentary palaeoenvironment and glacial activity in the high-arctic van Keulenfjorden, Spitsbergen. *The Holocene 23,* 1607–1618.

Klysz, P., Lindner, L., Makowska, A., Leszek, M., Wysokinski, L. (1988): Late Quaternary glacial episodes and sea level changes in the northeastern Billefjorden region, Central Spitsbergen. *Acta Geologica Polonica 38,* 107–123.

Kristensen, L., Benn, D.I., Hormes, A., Ottesen, D. (2009): Mud aprons in front of Svalbard surge moraines: evidence of subglacial deforming layers or proglacial glaciotectonics? *Geomorphology 111,* 206–221.

Kubishcta, F., Knudsen, K.L., Ojala, A.E.K., Salonen, V.−P. (2011): Holocene benthic foraminiferal record from a high−arctic fjord, Nordaustlandet, Svalbard. *Geografiska Annaler Series A 93,* 227–242.

Łącka, M., Zajączkowski, M., Forwick, M., Szczuciński, W. (2015): Late Weichselian and Holocene palaeoceanography of Storfjordrenna, southern Svalbard. *Climate of the Past 11,* 587–603.

Landvik, J.Y., Mangerud, J., Salvigsen, O. (1987): The Late Weichselian and Holocene shoreline displacement on the west-central coast of Svalbard. *Polar Research 5,* 29–44.

Landvik, J.Y., Bondevik, S., Elverhøi, A., Fjeldskaar, W., Mangerud, J., Salvigsen, O., Siegert, M.J., Svendsen, J.I., Vorren, T.O. (1998): The last glacial maximum of Svalbard and the Barents Sea area: ice sheet extent and configuration. *Quaternary Science Reviews 17,* 43–75.

Landvik, J.Y., Alexanderson, H., Henriksen, M., Ingólfsson, Ó. (2014): Landscape imprints of changing glacial regimes during ice-sheet build-up and decay: a conceptual model from Svalbard. *Quaternary Science Reviews 92,* 258–268.

Larsen, E.A., Lyså, A., Rubensdotter, L., Farnsworth, W.R., Jensen, M., Nadeau, M.J., Ottesen, D. (2018): Late-Glacial and Holocene glacier activity in the Van Mijenfjorden area, western Svalbard. *arktos 4,* 1–9. DOI: 10.1007/s41063-018-0042-2.

Laskar, J., Correia, A.C.M., Gastineau, M., Joutel, F., Levrard, B., Robutel, P. (2004): Long term evolution and chaotic diffusion of the insolation quantities of Mars. *Icarus 170,* 343–364.

Lesnek, A.J., Briner, J.P. (2018): Response of a land-terminating sector of the western Greenland Ice Sheet to early Holocene climate change: Evidence from ^{10}Be dating in the Søndre Isortoq region. *Quaternary Science Reviews, 180,* 145–156.

Lottin, V., Bravais, A., Lilliehöök, C.B. (1842): Voyages de la commission scientifique du nord, en Scandinavie, en Laponie, au Spitzberg et aux Feröe, pendant les années 1838, 1839 et 1840, sur la corvette ‘La Recherche’. Paris: Arthus Bertrand.

Lovell, H., Boston, C.M. (2017): Glacitectonic composite ridge systems and surge-type glaciers: an updated correlation based on Svalbard, Norway. *arktos 3,* 1–16.

Luoto, T.P., Ojala, A.E.K., Arppe, L., Brooks, S.J., Kurki, E., Oksman, M., Wooller, M.J., Zajączkowski, M. (2018): Synchronized proxy-based temperature reconstructions reveal mid- to late Holocene climate oscillations in High Arctic Svalbard. *Journal of Quaternary Science 33,* 93–99.

Lyså, A., Larsen, E., Høgaas, F., Jensen, M.A., Klug, M., Rubensdotter, L., Szczucinski, W. (2018): A temporary glacier-surge ice-dammed lake, Braganzavågen, Svalbard. *Boreas 47,* 837–854.

Lønne, I. (2005): Faint traces of high Arctic glaciations: an early Holocene ice-front fluctuation in Bolterdalen, Svalbard. *Boreas 34,* 308–323.

Mangerud, J., Gulliksen, S. (1975): Apparent radiocarbon ages of recent marine shells from Norway, Spitsbergen, and Arctic Canada. *Quaternary Research 5,* 263–273.

Mangerud, J., Bolstad, M., Elgersma, A., Helliksen, D., Landvik, J.Y., Lønne, I., Lycke, A. K., Salvigsen, O., Sandahl, T., Svendsen, J.I. (1992): The last glacial maximum on Spitsbergen, Svalbard. *Quaternary Research 38,* 1–31.

Mangerud, J., Dokken, T., Hebbeln, D., Heggen, B., Ingólfsson, Ó., Landvik, J.Y., Mejdahl, V., Svendsen, J.I. Vorren, T.O. (1998): Fluctuations of the Svalbard Barents Sea Ice Sheet during the last 150 000 years. *Quaternary Science Reviews 17,* 11–42.

Mangerud, J., Bondevik, S., Gulliksen, S., Hufthammer, A., Høisæter, T. (2006): Marine ^{14}C reservoir ages for 19th century whales and molluscs from the North Atlantic. *Quaternary Science Reviews 25,* 3228–3245.

Mangerud, J., Landvik, J.Y. (2007): Younger Dryas cirque glaciers in western Spitsbergen: smaller than during the Little Ice Age. *Boreas 36,* 278–285.

Mangerud, J., Svendsen, J.I. (2017): The Holocene Thermal Maximum around Svalbard, Arctic North Atlantic; molluscs show early and exceptional warmth. *The Holocene 28,* 65–83.

Masson-Delmotte, V., Schulz, M., Abe-Ouchi, A., Beer, J., Ganopolski, A., Gonzalez Rouco, J. F., Jansen, E., Lambeck, K., Luterbacher, J., Naish, T., Osborn, T., Otto-Bliesner, B., Quinn, T., Ramesh, R., Rojas, M., Shao, X., Timmermann, A. (2013): Information from paleoclimate archives. Climate Change 2013: The Physical Science Basis. In Contribution of Working Group I to the Fifth Assessment Report of the Intergovernmental Panel on Climate Change, 383–464. Cambridge University Press, Cambridge, UK and New York, NY, USA.

Mayewski, P.A., Rohling, E.E., Curt Stager, J., Karlen, W., Maasch, K.A., David Meeker, L., Meyerson, E.A., Gasse, F., van Kreveld, S., Holmgren, K., Lee-Thorp, J., Rosqvist, G.,

Rack, F., Staubwasser, M., Schneider, R.R., Steig, E.J. (2004): Holocene climate variability. *Quaternary Research 62*, 243–255.
McKay, N.P., Kaufman, D.S. (2014): An extended Arctic proxy temperature database for the past 2,000 years. *Scientific Data 1*, 140026.
Miller, G.H., Landvik, J.Y., Lehman, S.J. Southon, J.R. (2017): Episodic Neoglacial snowline descent and glacier expansion on Svalbard reconstructed from the 14C ages of ice-entombed plants. *Quaternary Science Reviews 155*, 67–78.
Müller, J., Werner, K., Stein, R., Fahl, K., Moros, M., Jansen, E. (2012): Holocene cooling culminates in sea ice oscillations in Fram Strait. *Quaternary Science Reviews 47*, 1–14.
Müller, J., Stein, R. (2014): High-resolution record of late glacial and deglacial sea ice changes in Fram Strait corroborates ice–ocean interactions during abrupt climate shifts. *Earth and Planetary Science Letters 403*, 446–455.
Nielsen, T., Rasmussen, T.L. (2018): Reconstruction of ice sheet retreat after the Last Glacial maximum in Storfjorden, southern Svalbard. *Marine Geology 402*, 228-243.
Nuth, C., Kohler, J., König, M., von Deschwanden, A., Hagen, J.O., Kääb, A., Moholdt, G., Pettersson, R. (2013): Decadal changes from a multitemporal glacier inventory of Svalbard. *The Cryosphere 7*, 1603–1621.
Oerlemans, J., Jania, J., Kolondra, L. (2011): Application of a minimal glacier model to Hansbreen, Svalbard. *The Cryosphere 5*, 1–11.
Osborn, G., McCarthy, D., LaBrie, A., Burke, R. (2015): Lichenometric Dating: Science or Pseudo-Science? *Quaternary Research 83*, 1–12.
Ottesen, D., Dowdeswell, J.A., Benn, D.I., Kristensen, L., Christiansen, H.H., Christensen, O., Hansen, L., Lebesbye, E., Forwick, M., Vorren, T.O. (2008): Submarine landforms characteristic of glacier surges in two Spitsbergen fjords. *Quaternary Science Reviews 27*, 1583–1599.
Patton, H., Hubbard, A., Andreassen, K., Auriac, A., Whitehouse, P.L., Stroeven, A.P., Shackleton, C., Winsborrow, M.C.M., Heyman, J., Hall, A.M. (2017): Deglaciation of the Eurasian ice sheet complex. *Quaternary Science Reviews 169*, 148–172.
Philipps, W., Briner, J.P., Gislefoss, L., Linge, H., Koffman, T., Fabel, D., Xu, S., Hormes, A. (2017): Late Holocene glacier activity at inner Hornsund and Scottbreen, southern Svalbard. *Journal of Quaternary Science 32*, 501–515.
Punning, J-M., Troitsky, L., Rajamäe, R. (1976): The genesis and age of the Quaternary deposits in the eastern part of Van Mijenfjorden, West Spitsbergen. *Föreningens i Stockholm Förhandlingar 9*, 343–347.
Rasmussen, S.O., Andersen, K.K., Svensson, A.M., Steffensen, J.P., Vinther, B.M., Clausen, H.B., Siggaard-Andersen, M.L., Johnsen, S.J., Larsen, L.B., Dahl-Jensen, D., Bigler, M., Röthlisberger, R., Fischer, H., Goto-Azuma, K., Hansson, M.E., Ruth, U. (2006): A new Greenland ice core chronology for the last glacial termination. *Journal of Geophysical Research 111*, D06102.
Rasmussen, T.L., Thomsen, E. (2014): Brine formation in relation to climate changes and ice retreat during the last 15,000 years in Storfjorden, Svalbard, 76–78°N. *Paleoceanography 29*, 911–929.
Rasmussen, T.L., Thomsen, E., Skirbekk, K., Slubowska-Woldengen, M., Klitgaard Kristensen, D., Koç, N. (2014): Spatial and temporal distribution of Holocene temperature maxima in the northern Nordic seas: interplay of Atlantic, Arctic and polar water masses. *Quaternary Science Reviews 92*, 280–291.
Reusche, M., Winsor, K., Carlson, A.E., Marcott, S.A., Rood, D.H., Novak, A., Roof, S., Retelle, M., Werner, A., Caffee, M., Clark, P.U. (2014): ^{10}Be surface exposure ages on the late-Pleistocene and Holocene history of Linnébreen on Svalbard. *Quaternary Science Reviews 89*, 5–12.

Reimer, P.J., Bard, E., Bayliss, A., Beck, J.W., Blackwell, P.G., Bronk Ramsey, C., Buck, C. E., Cheng, H., Edwards, R.L., Friedrich, M., Grootes, P.M., Guilderson, T.P., Haflidason, H., Hajdas, I., Hatte, C., Heaton, T.J., Hoffmann, D.L., Hogg, A.G., Hughen, K.A., Kaiser, K.F., Kromer, B., Manning, S.W., Niu, M., Reimer, R.W., Richards, D.A., Scott, E.M., Southon, J.R., Staff, R.A., Turney, C.S.M., van der Plicht, J. (2013): IntCal13 and Marine13 Radiocarbon Age Calibration Curves 0–50,000 Years cal BP. *Radiocarbon 55,* 1869–1887.

Rhodes, E.J. (2011): Optically Stimulated Luminescence Dating of Sediments over the Past 200,000 Years. *Annual Review of Earth and Planetary Sciences 39,* 461–488.

Rockström, J., Steffen, W., Noone, K., Persson, A., Chapin, F.S., Lambin, E.F., Lenton, T.M., Scheffer, M., Folke, C., Schellnhuber, H.J., Nykvist, B., de Wit, C.A., Hughes, T., van der Leeuw, S., Rodhe, H., Sorlin, S., Snyder, P.K., Costanza, R., Svedin, U., Falkenmark, M., Karlberg, L., Corell, R.W., Fabry, V.J., Hansen, J., Walker, B. Liverman, D., Richardson, K., Crutzen, P., Foley, J.A. (2009): A safe operating space for humanity. *Nature 461,* 472–475.

Rogers, J.C., Yang, L., Li, L. (2005): The role of Fram Strait winter cyclones on sea ice flux and on Spitsbergen air temperatures. *Geophysical Research Letters 32,* L06709.

Ronnert, L., Landvik, J.Y. (1993): Holocene glacial advances and moraine formation at Albrechtbreen, Edgeøya, Svalbard. *Polar Research 12,* 57–63.

Røthe, T.O., Bakke, J., Vasskog, K., Gjerde, M., D'Andrea, W.J., Bradley, R.S. (2015): Arctic Holocene glacier fluctuations reconstructed from lake sediments at Mitrahalvøya, Spitsbergen. *Quaternary Science Reviews 109,* 111–125.

Røthe, T.O., Bakke, J., Støren, E.W.N., Bradley, R.S. (2018): Reconstructing Holocene Glacier and Climate Fluctuations from Lake Sediments in Vårfluesjøen, Northern Spitsbergen. *Frontiers in Earth Science 6,* 1–20.

Salvigsen, O. (1981): Radiocarbon dated raised beaches in Kong Karls Land, Svalbard, and their consequences for the glacial history of the Barents Sea area. *Geografiska Annaler Series A 63,* 283–291.

Salvigsen, O., Nydal, R. (1981): The Weichselian glaciation in Svalbard before 15000 BP. *Boreas 10,* 433–446.

Salvigsen, O., Österholm, H. (1982): Radiocarbon dated raised beaches and glacial history of the northern coast of Spitsbergen, Svalbard. *Polar Research 1982,* 97–115.

Salvigsen, O., Elgersma, A., Hjort, C., Lagerlund, E., Liestøl, O., Svensson, N-O. (1990): Glacial history and shoreline displacement on Erdmannflya and Bohemanflya, Spitsbergen, Svalbard. *Polar Research 8,* 261–273.

Salvigsen, O., Forman, S.L., Miller, G.H. (1992): Thermophilous molluscs on Svalbard during the Holocene and their paleoclimatic implications. *Polar Research 11,* 1–10.

Salvigsen, O. (2002): Radiocarbon-dated *Mytilus edulis* and *Modiolus modiolus* from northern Svalbard: Climatic implications. *Norsk Geografisk Tidsskrift 56,* 56–61.

Samtleben, C. (1985): Climatic influence on shell microstructure in *Mytilus edulis* from Spitsbergen. In: Paper presented at the 75. Jahrestagung der Geologischen Vereinung, Kiel.

Sarnthein, M., Van Kreveld, S., Erlenkeuser, H., Grootes, P.M., Kucera, M., Pflauman, U., Schulz, M. (2003): Centennial-to millennial-scale periodicities of Holocene climate and sediment injections off the western Barents shelf, 75°N. *Boreas 32,* 447–461.

Schytt, V., Hoppe, G., Blake, W.J., Grosswald, M.G. (1968): The extent of the Würm glaciation in the European Arctic. *International Association of Scientific Hydrology General Assembly of Bern 1967 79,* 207–216.

Sessford, E.G., Strzelecki, M.C., Hormes, A. (2015): Reconstruction of past patterns of change in a High Arctic coastal landscape, southern Sassenfjorden, Svalbard. *Geomorphology 234,* 98–107.

Sevestre, H. Benn, D.I. (2015): Climatic and geometric controls on the global distribution of surge-type glaciers: implications for a unifying model of surging. *Journal of Glaciology 61,* 646–662.

Sevestre, H., Benn, D.I., Luckman, A., Nuth, C., Kohler, J., Lindbäck, K., Pettersson, R. (2018): Tidewater Glacier Surges Initiated at the Terminus. *Journal of Geophysical Research: Earth Surface 123,* 1035–1051.

Sharin V, Kokin O, Gusev E.A., Okunev, A.S., Arslanov, Kh.A., Maksimov, F.E. (2014): New geochronological data from Quaternary sediments of the Nordenskiöld Land area (the Spitsbergen Archipelago). Vestnik St. Petersburg State University, Series 7: *Geology, Geography 1,* 159–168 (in Russian with English abstract).

Skirbekk, K., Klitgaard-Kristensen, D., Rasmussen, T.L. Koç, N., Forwick M. (2010): Holocene climate variations at the entrance to a warm Arctic fjord: evidence from Kongsfjorden trough, Svalbard. *Geological Society, London, Special Publications 344,* 289–304.

Sletten, K., Lyså, A., Lønne, I. (2001): Formation and disintegration of a high-arctic ice-cored moraine complex, Scott Turnerbreen, Svalbard. *Boreas 30,* 272–284.

Ślubowska-Woldengen, M., Rasmussen, T.L., Koç, N., Klitgaard-Kristensen, D., Nilsen, F., Solheim, A. (2007): Advection of Atlantic Water to the western and northern Svalbard shelf since 17 500 cal yr BP. *Quaternary Science Reviews 26,* 463–478.

Snyder, J.A., Miller, G.H., Werner, A., Jull, A.J.T., Stafford J.T.W. (1994): AMS-radiocarbon dating of organic-poor lake sediment, an example from Linnévatnet, Spitsbergen, Svalbard. *The Holocene 4,* 413–421.

Snyder, J.A., Werner, A., Miller, G.H. (2000): Holocene cirque glacier activity in western Spitsbergen, Svalbard: sediment records from proglacial Linnévatnet. *The Holocene 10,* 555–563.

Solomina, O.N., Bradley, R.S., Hodgson, D.A., Ivy-Ochs, S., Jomelli, V., Mackintosh, A.N., Nesje, A., Owen, L.A., Wanner, H., Wiles, G.C., Young, N.E. (2015): Holocene glacier fluctuations. *Quaternary Science Reviews 111,* 9–34.

Steffensen, J.P., Andersen, K.K., Bigler, M., Clausen, H.B., Dahl-Jensen, D., Fischer, H., Goto-Azuma, K., Hansson, M., Johnsen, S.J., Jouzel, J., Masson-Delmotte, V., Popp, T., Rasmussen, S.O., Röthlisberger, R., Ruth, U., Stauffer, B., Siggaard-Andersen, M.-L., Sveinbjörnsdóttir, A.E., Svensson, A., White, J.W.C. (2008): High resolution Greenland ice core data show abrupt climate change happens in few years. *Science 321,* 680–684.

Streuff, K., Ó Cofaigh, C., Noormets, R., Lloyd, J.M. (2017): Submarine landforms and glacimarine sedimentary processes in Lomfjorden, East Spitsbergen. *Marine Geology 390,* 51–71.

Svendsen, J.I., Mangerud, J. (1997): Holocene glacial and climatic variations on Spitsbergen, Svalbard. *The Holocene 7,* 45–57.

Thrasher, I.M., Mauz, B., Chiverrell, R.C., Lang, A., Thomas, G.S.P. (2009): Testing an approach to OSL dating of Late Devensian glaciofluvial sediments of the British Isles. *Journal of Quaternary Science 24,* 785–801.

Wanner, H., Beer, J., Bütikofer, J., Crowley, T.J., Cubasch, U., Flückiger, J., Goosse, H., Grosjean, M., Joos, F., Kaplan, J.O., Küttel, M., Müller, S.A., Prentice, I.C., Solomina, O., Stocker, T.F., Tarasov, P., Wagner, M., Widmann, M. (2008): Mid- to Late Holocene climate change: an overview. *Quaternary Science Reviews 27,* 1791-1828.

Wanner, H., Solomina, O., Grosjean, M., Ritz, S. P., Jetel, M. (2011): Structure and origin of Holocene cold events. *Quaternary Science Reviews 30,* 3109–3123.

Werner, A. (1993): Holocene moraine chronology, Spitsbergen, Svalbard: lichenometric evidence for multiple Neoglacial advances in the Arctic. *The Holocene 3,* 128–137.

de Wet, G.A., Balascio, N.L., D'Andrea, W.J., Bakke, J., Bradley, R.S., Perren, B. (2018): Holocene glacier activity reconstructed from proglacial lake Gjøavatnet on Amsterdamøya, NW Svalbard. *Quaternary Science Reviews 183,* 188–203. doi: 10.1016/j.quascirev.2017.03.018.

Wintle, A.G. (2008): Fifty years of luminescence dating. *Archaeometry 50,* 276-312.

Wohlfarth, B. (2009): *Ice-free conditions in Fennoscandia during Marine Oxygen Isotope Stage 3?* Technical Report: TR-09-12. Swedish Nuclear Fuel and Waste Management Company, Stockholm.
Young, N.E., Briner, J.P., Rood, D.H., Finkel, R.C. (2012): Glacier Extent During the Younger Dryas and 8.2-ka Event on Baffin Island, Arctic Canada. *Science 337*, 1330-1333.
Young, N.E., Briner, J.P., Rood, D.H., Finkel, R.C., Corbett, L.B., Bierman, P.R. (2013): Age of the Fjord Stade moraines in the Disko Bugt region, western Greenland, and the 9.3 and 8.2 ka cooling events. *Quaternary Science Reviews 60*, 76-90.
Young, N.E., Lamp, J., Koffman, T., Briner, J.P., Schaefer, J., Gjermundsen, E.F., Linge, H., Zimmerman, S., Guilderson, T.P., Fabel, D., Hormes, A., (2018): Deglaciation of coastal south-western Spitsbergen dated with in situ cosmogenic ^{10}Be and ^{14}C measurements. *Journal of Quaternary Science 33.* DOI: 10.1002/jqs.3058.
Østby, T.I., Schuler, T.V., Hagen, J.O., Hock, R., Kohler, J., Reijmer, C.H. (2017): Diagnosing the decline in climatic mass balance of glaciers in Svalbard over 1957–2014. *The Cryosphere 11*, 191–215.
Österholm, H. (1990): The Late Weichselian Glaciation and Holocene Shore Displacement on Prins Oscars Land, Nordaustlandet, Svalbard. *Geografiska Annaler Series A 72,* 301–317.

Appendix

Chapter I	-Fig S1 Topographic maps of Lateglacial Early Holocene ice margins -Fig S2 Aerial images of Lateglacial Early Holocene ice margins -Table S1 Glacier Length Data -Table S2 Lateglacial-early Holocene studies -References
Chapter II	-Table S1 Radiocarbon dates from Sveagruva area -Quaternary geological & geomorphological map Svea, Svalbard (link)
Chapter III	-Not applicable
Chapter IV	-Table S1 Documented surge-type glaciers -Table S2 Glaciers with crevasse squeeze ridges
Chapter V	-Table S1 Radiocarbon ages from the SVALHOLA database (link) -Table S2 Luminesence ages from the SVALHOLA database (link) -Table S3 Cosmogenic exposure ages from the SVALHOLA database (link) -Table S4 References from SVALHOLA database

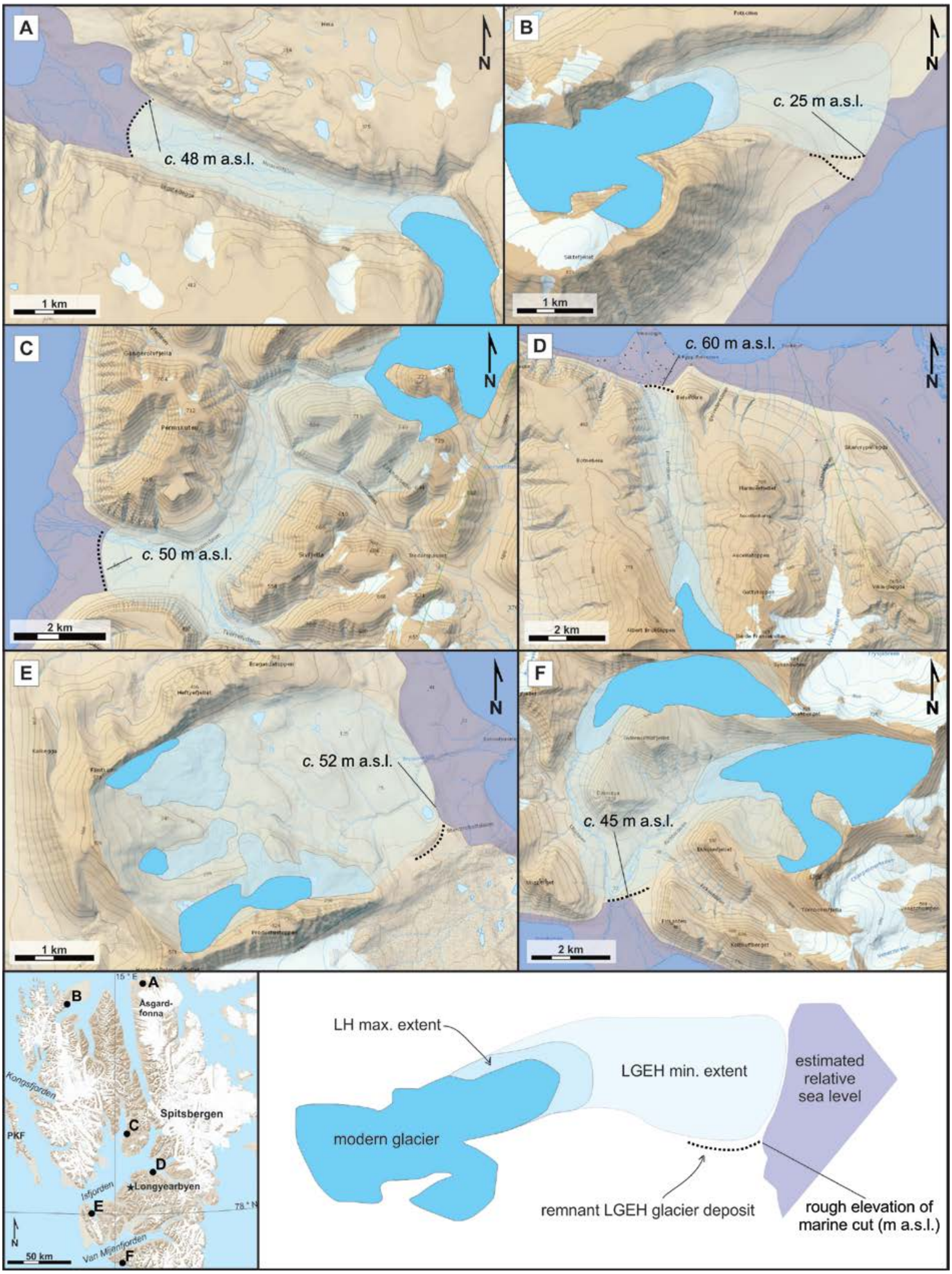

Figure S1. Topographic maps of Lateglacial-early Holocene (LGEH) glacier deposits labeled A-F corresponding to glaciers; (A) Tåbreen, (B) Albertbreen, (C) Lyckholmdalen, (D) Flowerbreen, (E) Heftybreen and (F) Richterbreen respectively. Light blue shades represent inferred modern glacier extent, Late Holocene (LH) max. extent and Lateglacial early Holocene min. extent. Remnant glacier deposits indicated with dotted lines while dark shade of blue represents high relative sea level. Inset map exhibits location of respective sites on Spitsbergen. Topographic maps modified from TopoSvalbard (http://toposvalbard.npolar.no/).

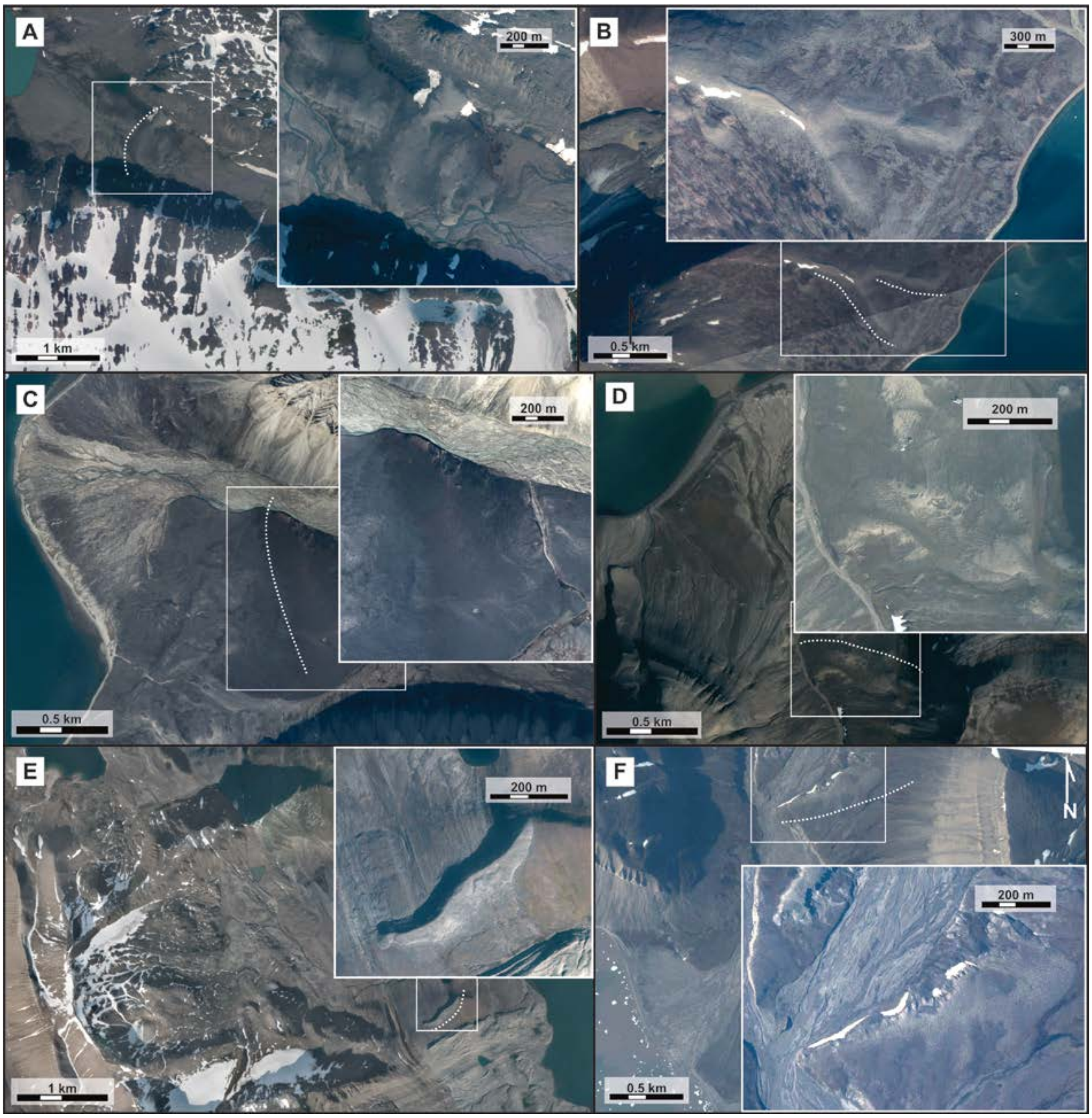

Figure S2. Enlarged high resolution aerial imagery of six selected sites presented in Fig. 4, where glacier deposits (marked by white dotted lines) are remotely constrained in age to Lateglacial-early Holocene age. Imagery freely accessible on TopoSvalbard provided by the Norwegian Polar Institute.

Table S1. Glacier Length Data

ID	Region	Location	Glacier	Length (km)*	Snout to NG (km)	NG –LGEH (km)	Snout –LGEH (km)	Glacier type
-	Lomfjorden	De Geerbukta	Gullfaksebreen	19.64	1.2	4.37	5.57	outlet (Åsgardfonna)
A	Wijdefjorden	Mosseldalen	Tåbreen	7.63	0.29	3.81	4.1	outlet (Åsgardfonna)
B	Liefdefjorden	Sørdalsbukta	Albertbreen	2.61	0.47	2.30	2.77	cirque glacier
C	Dicksonfjorden	Lyckholmdalen	Lyckholmbreen*	1.90	0.61	8.10	8.71	outlet (Friggkåpa)
D	Sassenfjorden	Vindodden	Flowerbreen	2.76	1.01	4.09	5.1	valley glacier
E	Grønfjorden	Sandefjorden	Heftybreen	1.34	1.02	2.65	3.67	cirque glacier
F	Van Keulenfjorden	Richter/Ulladalen	Richterbreen	5.04	1.32	4.15	5.47	valley glacier

Note: Distance measurements made in TopoSvalbard (2017).
*Unofficial glacier names based valley or site name.
Abbreviations are as follows; NG = Neoglacial; LGEH = Lateglacial-early Holcoene

TABLE S2. Lateglacial-early Holocene studies

Ref. ID	Reference	Location	Glacier / Site	Focus	Sample	^{14}C age BP	Cal. a BP Median	Description
1	Eitel *et al.* (2002)	Andreeland	Gråhukdalen	Morphology				LGEH advance
2	Eitel *et al.* (2002)	Andreeland	Vogtdalen	Stratigraphy / Map	Shell frag.	10096±77	11022	Max. constraining age
3	Eitel *et al.* (2002)	Andreeland	Vatnedalen	Morphology				LGEH advance
4	Eitel *et al.* (2002)	Andreeland	Cirrusdalen	Morphology				LGEH advance
5	Eitel *et al.* (2002)	Andreeland	Torrelldalen	Stratigraphy / Map	Shell frag.	10340±120	11310	Max. constraining age
6	Eitel *et al.* (2002)	Andreeland	Jakobsenbukta	Stratigraphy / Map	Shell frag.	10580±60	11722	Max. constraining age
7	Brückner *et al.* (2002)	Andreeland	Verdalspynten	Stratigraphy	Shell	9311±57	10074	Min. constraining age (Hd 20997)
8	Eitel *et al.* (2002)	Andreeland	Wigdehlpynten	Morphology				LGEH advance
9	Salvigsen & Österholm (1982)	Reinsdyrflya	Sørdalsflya	Morphology				Lateglacial ice margin suggested
10	van der Bilt *et al.* (2015)	Mitrahalvøya	Hajeren	Lake sediments	Terrestrial Macro	Age-depth model	-	Early Holocene glacial maxima
11	Røthe *et al.* (2015)	Mitrahalvøya	Kløsa / Karlbreen	Lake sediments	Terrestrial Macro	Age-depth model	-	Pre 6.7 ka BP
12	Henriksen *et al.* (2014)	Kongsfjorden	Kongsfjordhallet	Stratigraphy / Map	Moraine Boulder	9200	-	Cosmogenic nuclide
12	Henriksen *et al.* (2014)	Kongsfjorden	Kongsfjordhallet	Stratigraphy / Map	Moraine Boulder	12100	-	Cosmogenic nuclide
13	Andersson *et al.* (1999)	Prins Karls Forland	McVitiepynten	Stratigraphy / Map	Shell	12590±70	14002	Max. constraining age (T-2096)
14	Andersson *et al.* (2000)	Prins Karls Forland	Poolepynten	Stratigraphy / Map	Whalebone	11650±180	13054	Max. constraining age (1-13795)
14	Farnsworth *et al.* (2017)	St. Jonsfjorden	Gunnarbreen	Stratigraphy / Map	*N.labradorica* (Foram)	11345±102	12750	Max. constraining age (HH12.956)
15	Farnsworth *et al.* (2017)	St. Jonsfjorden	Gunnarbreen	Stratigraphy / Map	*M. modiolous*	9320±60	10081	Min. constraining age (LuS 10795)

16	Salvigsen *et al.* 1990)	Isfjorden	Ymerbukta	Stratigraphy / Map	*M. truncata*	9500±100	10290	Max. constraining age (T-6286)
17	Lønne 2005)	Bolterdalen	Scott Turnerbreen	Stratigraphy / Map	*M. truncata*	9775±125	10595	Max. constraining age (T-13883)
17	Lønne 2005)	Bolterdalen	Scott Turnerbreen	Stratigraphy / Map	*M. truncata*	9625±95	10408	Min. constraining age (T-13884)
18	Landvik & Salvigsen 1985)	Reindalen	Gangdalen	Stratigraphy	-	-	-	Post deglaciation advance
19	Lønne 2005) (Salvigsen)	Grønfjorden	Aldegondabreen	Stratigraphy	Shell frag.	9980±120	10871	Max. constraining age (T-6290)
20	Larson *et al.* (in press)	Van Mijenfjorden	Gustravdalen	Stratigraphy / Map		10340±110	11392	Max. constraining age (Tln-146 3,6)
20	Larson *et al.* (in press)	Van Mijenfjorden	Gustravdalen	Shoreline	Shell	9510±90	10367	Min. constraining age (Tln-145 3,6)
21	Mangerud *et al.* (1992)	Van Mijenfjorden	Bromelldalen	Stratigraphy / Map	Shell	10940±200	12319	Max. constraining age (T-5368)
21	Mangerud *et al.* (1992)	Van Mijenfjorden	Bromelldalen	Stratigraphy / Map	Shell	10570±150	11659	Min. constraining age (T-5369)
22	Landvik *et al.* (1992)	Bellsund	Skilvika	Stratigraphy	Shell			Pre LGM tributary advance
23	Ronnert & Landvik (1993)	Edgeøya	Albrechtbreen	Stratigraphy / Map	Whalebone	8635±125	9211	Max. constraining age (T-9911)
-	van der Bilt *et al.* (2018)	Mitrahalvøya / Amsterdamøya	Hajeren / Hakluytvatnet	Lake sed. / Alkenones	Terrestrial macros	Age-depth model	-	Early warmth 12-10.5 ka BP
-	Balascio *et al.* (2018)	Amsterdamøya	Hakluytvatnet	Lake sed. / Leaf waxes	Terrestrial macros	Age-depth model	-	Early warmth 12.8-9.5 ka BP
-	Mangerud & Svendsen (2018)	Spitsbergen	Isfjorden	Thermophiles	Molluscs	Review with 21 new ages	-	Early warm fjords 11-9 ka BP
-	Hald *et al.* (2004)	Spitsbergen	West Spitsbergen	Marine Sed. / Proxy	Forams	Age-depth model	-	Early warm regional waters 11.2-8.8 ka BP
-	Müller & Stein (2014)	Spitsbergen	West Spitsbergen	Marine Sed. / Proxy	IP_{25}	Age-depth model	-	Sea-ice reduction ~12 ka BP

Note: All dates corrected for marine reservoir age with a ΔR = 70 ± 30 (Mangerud & Svendsen 2017) and calibrated with Marine13 on Calib Rev 7.0.4

References:

Andersen, K. K., Azuma, N., Barnola, J. M., & Bigler, M. 2004: High-resolution record of Northern Hemisphere climate extending into the last interglacial period. *Nature 431*(7005), 147.

Andersson, T., Forman, S. L., Ingólfsson, Ó. & Manley, W. F. 1999: Late Quaternary environmental history of central Prins Karls Forland, western Svalbard. *Boreas. 28*, 292-307.

Andersson, T., Forman, S. L., Ingólfsson, Ó. & Manley, W. F. 2000: Stratigraphic and Morphologic Constraints on the Weichselian Glacial History of Northern Prins Karls Forland, Western Svalbard. *Geografiska Annaler A 82*, 455-470.

Balascio, N. L., D'Andrea, W. J., Gjerde, M. & Bakke, J. 2018: Hydroclimate variability of High Arctic Svalbard during the Holocene inferred from hydrogen isotopes of leaf waxes. *Quaternary Science Reviews* doi.org/10.1016/j.quascirev.2016.11.036.

van der Bilt, W. G. M., Bakke, J., Vasskog, K., D'Andrea, W. J., Bradley, R. S. & Ólafsdóttir, S. 2015: Reconstruction of glacier variability from lake sediments reveals dynamic Holocene climate in Svalbard. *Quaternary Science Reviews 126,* 201-218.

van der Bilt, W. G. M., D'Andrea, W. J., Bakke, J., Balascio, N. L., Werner, J. P., Gjerde, M. & Bradley, R. S. 2018: Alkenone-based reconstructions reveal four-phase Holocene temperature evolution for High Arctic Svalbard. *Quaternary Science Reviews,* http://dx.doi.org/10.1016/j.quascirev.2016.10.006

Brückner, H., Schellmann, G. & van der Borg, K. 2002: Uplifted beach ridges in Northern Spitsbergen as indicators for glacio-isostasy and palaeo-oceanography: *Zeitschrift für Geomorphologie 46,* 309-336.

Eitel, B., van der Borg, K., Eberle, J. & Megies, H. 2002: Late Pleistocene/Early Holocene glacial history of northern Andreeland (northern Spitsbergen/Svalbard Archipelago): evidence from glacial and fluvio-glacial deposits. *Zeitschrift für Geomorphologie 46,* 337-364.

Farnsworth, W. R., Ingólfsson, Ó., Noormets, R., Allaart, L., Alexanderson, H., Henriksen, M. & Schomacker, A. 2017: Dynamic Holocene glacial history of St. Jonsfjorden, Svalbard. *Boreas. 46*, 585-603.

Hald, M., Ebbesen, H., Forwick, M., Godtliebsen, F., Khomenko, L., Korsun, S., Ringstad Olsen, L. & Vorren, T. O. 2004: Holocene paleoceanography and glacial history of the West Spitsbergen area, Euro-Arctic margin. *Quaternary Science Reviews 23,* 2075-2088.

Hald, M., Andersson, C., Ebbesen, H., Jansen, E., Klitgaard-Kristensen, D., Risebrobakken, B., Salomonsen, G. R., Sarnthein, M., Sejrup, H. P. & Telford, R. J. 2007: Variations in temperature and extent of Atlantic Water in the northern North Atlantic during the Holocene. *Quaternary Science Reviews 26,* 3423-3440.

Henriksen, M., Alexanderson, H., Landvik, J. Y., Linge, H. & Peterson, G. 2014: Dynamics and retreat of the Late Weichselian Kongsfjorden ice stream, NW Svalbard. *Quaternary Science Reviews 92,* 235-245.

König, M., Nuth, C., Kohler, J., Moholdt, G. & Pettersen, R. 2014: A digital glacier database for svalbard. *in* Kargel, S. J., Leonard, J. G., Bishop, P. M., Kääb, A.,

and Raup, H. B., eds., Global Land Ice Measurements from Space: Berlin, Heidelberg, *Springer Berlin Heidelberg,* 229-239.
Landvik, J. Y. & Salvigsen, O. 1985: Glaciation development and interstadial sea-level on central Spitsbergen, Svalbard. *Polar Research 3,* 1-10.
Landvik, J. Y., Bolstad, M., Lycke, A. K., Mangerud, J. & Sejrup, H. P. 1992: Weichselian stratigraphy and palaeoenvironments at Bellsund, western Svalbard. *Boreas 21,* 335-358.
Lønne, I. 2005: Faint traces of high Arctic glaciations: an early Holocene ice-front fluctuation in Bolterdalen, Svalbard. *Boreas 34,* 308-323.
Mangerud, J., Bolstad, M., Elgersma, A., Helliksen, D., Landvik, J. Y., Lønne, I., Lycke, A. K., Salvigsen, O., Sandahl, T. & Svendsen, J. I. 1992: The last glacial maximum on Spitsbergen, Svalbard. *Quaternary Research 38,* 1-31.
Mangerud, J. & Svendsen, J. I. 2018: The Holocene Thermal Optimum around Svalbard, Arctic North Atlantic; molluscs show early and exceptional warmth. *The Holocene XX,* 1-19.
Müller, J. & Stein, R. 2014: High-resolution record of late glacial and deglacial sea ice changes in Fram Strait corroborates ice–ocean interactions during abrupt climate shifts. *Earth and Planetary Science Letters 403,* 446-455.
Reimer, P. J., Bard, E., Bayliss, A., Beck, J. W., Blackwell, P. G., Bronk Ramsey, C., Buck, C. E., Cheng, H., Edwards, R. L., Friedrich, M., Grootes, P. M., Guilderson, T. P., Haflidason, H., Hajdas, I., Hatté, C., Heaton, T. J., Hoffmann, D. L., Hogg, A. G., Hughen, K. A., Kaiser, K. F., Kromer, B., Manning, S. W., Niu, M., Reimer, R. W., Richards, D. A., Scott, E. M., Southon, J. R., Staff, R. A., Turney, C. S. M. & van der Plicht, J. 2013: IntCal13 and Marine13 Radiocarbon Age Calibration Curves 0–50,000 Years cal BP. *Radiocarbon 55,* 1869-1887
Ronnert, L. & Landvik, J. Y. 1993: Holocene glacial advances and moraine formation at Albrechtbreen, Edgeøya, Svalbard. *Polar Research 12,* 57-63.
Røthe, T. O., Bakke, J., Vasskog, K., Gjerde, M., D'Andrea, W. J. & Bradley, R. S. 2015: Arctic Holocene glacier fluctuations reconstructed from lake sediments at Mitrahalvøya, Spitsbergen. *Quaternary Science Reviews 109,* 111-125.
Salvigsen, O., Elgersma, A., Hjort, C., Lagerlund, E., Liestøl, O. & Svensson, N.-O. 1990: Glacial history and shoreline displacement on Erdmannflya and Bohemanflya, Spitsbergen, Svalbard. *Polar Research 8,* 261-273.
Salvigsen, O. & Österholm, H. 1982: Radiocarbon dated raised beaches and glacial history of the northern coast of Spitsbergen, Svalbard. *Polar Research 1,* 97-115.

Documented surge-type glaciers Supplementary Table 1

Glacier Name	Island	Region	Lat. / Long.	CSR	Photo year	Ref.
Nord Buchananisen	Prince Karls Foreland	NWS	78.6863 N, 11.0047 E	Yes	2008	J. et al. 2000
Aavatsmarkbreen	Spitsbergen	NWS	78.7000 N, 12.1467 E	Yes	2009	B. et al. 2009
Abrahamsenbreen	Spitsbergen	NWS	79.1050 N, 14.4097 E	Yes	2011	Liestøl 1993
Ankerbreen	Spitsbergen	NWS	78.5499 N, 12.6494 E	Yes	2009	Hamilton 1992
Anna Sofiebreen	Spitsbergen	NWS	78.4899 N, 13.1787 E	No	2009	Hamilton 1992
Arbobreen	Spitsbergen	NWS	78.9744 N, 15.6381 E	Yes	2011	Hamilton 1992
Austgotabreen	Spitsbergen	NWS	78.4375 N, 13.0506 E	Yes	2009	Hamilton 1992
Austre Broggerbreen	Spitsbergen	NWS	78.8889 N, 11.8537 E	Yes	2010	Hamilton 1992
Battyebreen	Spitsbergen	NWS	78.9731 N, 15.0005 E	Yes	2011	Hamilton 1992
Biksebreen	Spitsbergen	NWS	78.8769 N, 14.9838 E	Yes	2011	Hamilton 1992
Blindernbreen	Spitsbergen	NWS	78.9867 N, 15.2820 E	Yes	2011	Hamilton 1992
Blomstrandbreen	Spitsbergen	NWS	79.0652 N, 12.3765 E	Yes	2009	Liestøl 1993
Blåshaugbreen	Spitsbergen	NWS	79.1967 N, 11.4738 E	No	2009	Hamilton 1992
Borebreen	Spitsbergen	NWS	78.4422 N, 13.8830 E	Yes	2009	Hamilton 1992
Botnfjellbreen	Spitsbergen	NWS	78.8429 N, 12.4199 E	Yes	2009	Hamilton 1992
Bukkebreen	Spitsbergen	NWS	78.5449 N, 13.4647 E	Yes	2009	Hamilton 1992
Charlesbreen	Spitsbergen	NWS	78.5068 N, 13.3628 E	Yes	2009	Hamilton 1992
Chauveauxbreen	Spitsbergen	NWS	79.6424 N, 11.9868 E	No	2009	S. et al. 2009
Cissybreen	Spitsbergen	NWS	78.7479 N, 11.9397 E	Yes	2009	Hamilton 1992
Comfortlessbreen	Spitsbergen	NWS	78.7635 N, 12.1304 E	Yes	2009	S. et al. 2009
Delbreen	Spitsbergen	NWS	78.8738 N, 15.7890 E	Yes	2011	Hamilton 1992
Eidembreen	Spitsbergen	NWS	78.4065 N, 13.1986 E	Yes	2009	Hamilton 1992
Elisebreen	Spitsbergen	NWS	78.6467 N, 12.2550 E	Yes	2009	S. et al. 2009
Elnabreen	Spitsbergen	NWS	79.1596 N, 14.1118 E	Yes	2011	Liestøl 1993
Erikkabreen	Spitsbergen	NWS	78.7330 N, 12.0671 E	Yes	2009	Hamilton 1992
Fjortende Julibreen	Spitsbergen	NWS	79.1224 N, 12.1576 E	Yes	2009	M. et al., 2012
Fyrisbreen	Spitsbergen	NWS	78.9384 N, 15.5715 E	Yes	2011	Liestøl 1993
Gaffelbreen	Spitsbergen	NWS	78.5671 N, 12.8878 E	Yes	2009	Hamilton 1992
Gonvillebreen	Spitsbergen	NWS	78.7754 N, 16.0328 E	No	2011	Hamilton 1992
Gyldenbreen	Spitsbergen	NWS	78.8580 N, 16.0815 E	Yes	2011	Hamilton 1992
Haakenbreen	Spitsbergen	NWS	78.7452 N, 11.9759 E	Yes	2009	Hamilton 1992
Hansdalsbreen	Spitsbergen	NWS	78.6899 N, 15.0196 E	No	2011	Hamilton 1992
Høegdalsbreen	Spitsbergen	NWS	78.9516 N, 15.7087 E	Yes	2011	Hamilton 1992
Holmstrombreen	Spitsbergen	NWS	78.8318 N, 14.0566 E	Yes	2009	Liestøl 1993
Hørbyebreen	Spitsbergen	NWS	78.7623 N, 16.2847 E	Yes	2011	Hamilton 1992
Hydrografbreen	Spitsbergen	NWS	78.4544 N, 12.7489 E	Yes	2009	Hamilton 1992
Kappfjellbreen	Spitsbergen	NWS	79.0840 N, 11.9651 E	Yes	2009	Hamilton 1992
Kastellbreen	Spitsbergen	NWS	78.9730 N, 15.9871 E	No	2011	Hamilton 1992
Kinamurbreen	Spitsbergen	NWS	78.8152 N, 15.9694 E	Yes	2011	Hamilton 1992
Klampebreen	Spitsbergen	NWS	78.6016 N, 13.4796 E	Yes	2009	Hamilton 1992
Kongsvegen	Spitsbergen	NWS	78.8154 N, 12.7764 E	Yes	2009	Liestøl 1993
Konowbreen	Spitsbergen	NWS	78.6025 N, 12.9480 E	Yes	2009	Hamilton 1992
Konsulbreen	Spitsbergen	NWS	79.0961 N, 12.3668 E	No	2009	Hamilton 1992
Kronebreen	Spitsbergen	NWS	78.8747 N, 12.7883 E	Yes	2009	Hamilton 1992
Lisbetbreen	Spitsbergen	NWS	79.0679 N, 15.0314 E	Yes	2011	Liestøl 1993
Manchesterbreen	Spitsbergen	NWS	78.8148 N, 16.0747 E	Yes	2011	Hamilton 1992
Mannbreen	Spitsbergen	NWS	78.9506 N, 15.8503 E	Yes	2011	Hamilton 1992
Mediumbreen	Spitsbergen	NWS	78.5379 N, 14.1445 E	No	2009	Hamilton 1992
Meyerbreen	Spitsbergen	NWS	78.6969 N, 15.0265 E	Yes	2011	Hamilton 1992
Midtre Lovénbreen	Spitsbergen	NWS	78.8782 N, 12.0415 E	Yes	2009	Liestøl 1993
Monacobreen	Spitsbergen	NWS	79.3979 N, 12.6080 E	No	2009	B. et al. 2009
Muninbreen	Spitsbergen	NWS	78.7245 N, 16.0895 E	Yes	2011	Hamilton 1992
Nonsenbreen	Spitsbergen	NWS	78.3747 N, 13.8966 E	Yes	2009	Liestøl 1993
Nordenfjeldskebreen	Spitsbergen	NWS	78.7905 N, 12.2445 E	Yes	2009	Hamilton 1992
Nordre Vasskilbreen	Spitsbergen	NWS	78.9142 N, 15.6626 E	Yes	2011	Hamilton 1992
Olssonbreen	Spitsbergen	NWS	79.0600 N, 11.9472 E	No	2009	Hamilton 1992

Orsabreen	Spitsbergen	NWS	78.9688 N, 14.2764 E	Yes	2011	J. et al. 2000
Osbornebreen	Spitsbergen	NWS	78.6550 N, 13.1276 E	No	2009	D. et al. 1991
Paulbreen	Spitsbergen	NWS	78.5603 N, 13.4415 E	Yes	2009	Hamilton 1992
Roysbreen	Spitsbergen	NWS	78.9049 N, 13.4415 E	Yes	2009	Hamilton 1992
Samebreen	Spitsbergen	NWS	78.6337 N, 14.1172 E	No	2009	Hamilton 1992
Sefstrombreen	Spitsbergen	NWS	78.7468 N, 13.9464 E	Yes	2009	Liestøl 1993
Skansdalsbreen	Spitsbergen	NWS	78.5588 N, 15.7619 E	Yes	2011	Liestøl 1993
Smalfjellbreen	Spitsbergen	NWS	78.7751 N, 12.2156 E	No	2009	Hamilton 1992
Studentbreen	Spitsbergen	NWS	78.9696 N, 15.4662 E	Yes	2011	Hamilton 1992
Størmerbreen	Spitsbergen	NWS	79.0281 N, 14.5840 E	Yes	2009	S. et al. 2009
Supanbreen	Spitsbergen	NWS	79.3288 N, 11.9827 E	Yes	2009	Hamilton 1992
Sveabreen	Spitsbergen	NWS	78.6937 N, 13.6096 E	Yes	2009	Hamilton 1992
Svelgfjellet Nord*	Spitsbergen	NWS	79.2921 N, 14.5535 E	Yes	2010	Liestøl 1993
Svenbreen	Spitsbergen	NWS	78.7259 N, 16.3060 E	Yes	2011	Hamilton 1992
Tindebreen	Spitsbergen	NWS	79.6995 N, 11.9562 E	No	2009	Hamilton 1992
Uversbreen	Spitsbergen	NWS	78.8107 N, 12.3480 E	Yes	2009	Hamilton 1992
Vegardbreen	Spitsbergen	NWS	78.5319 N, 13.4192 E	Yes	2009	Hamilton 1992
Vestgotabreen	Spitsbergen	NWS	78.4611 N, 12.9015 E	Yes	2009	Hamilton 1992
Vestre Lovenbreen	Spitsbergen	NWS	78.9028 N, 11.9216 E	Yes	2010	Hamilton 1992
Vintervegen	Spitsbergen	NWS	78.5846 N, 13.4866 E	Yes	2009	S. et al. 2009
Wahlenbergbreen	Spitsbergen	NWS	78.5825 N, 13.8586 E	Yes	2009	Liestøl 1993
Allfarvegen	Spitsbergen	NES	79.0535 N, 19.7140 E	Yes	2011	L & H 1991
Backlundbreen	Spitsbergen	NES	78.6458 N, 19.9593 E	Yes	2011	L & H 1991
Ebbabreen	Spitsbergen	NES	78.7287 N, 16.8639 E	Yes	2011	Hamilton 1992
Eskolabreen	Spitsbergen	NES	78.9149 N, 16.6148 E	Yes	2011	Hamilton 1992
Ganskijbreen	Spitsbergen	NES	78.7210 N, 20.6709 E	Yes	2011	L & H 1991
Hannbreen	Spitsbergen	NES	78.7684 N, 21.2900 E	Yes	2011	L & H 1991
Hayesbreen	Spitsbergen	NES	78.3756 N, 18.5826 E	No	2011	Liestøl 1993
Hochstetterbreen	Spitsbergen	NES	78.8810 N, 20.4419 E	Yes	2011	Liestøl 1993
Kantbreen	Spitsbergen	NES	79.3508 N, 17.8594 E	Yes	2010	J. et al. 2000
Kosterbreen	Spitsbergen	NES	79.3175 N, 18.7222 E	Yes	2010	L & H 1991
Longstaffbreen	Spitsbergen	NES	79.7762 N, 16.0648 E	No	2010	Liestøl 1993
Mittag Lefflerbreen	Spitsbergen	NES	78.8768 N, 16.4652 E	Yes	2011	Hamilton 1992
Negribreen	Spitsbergen	NES	78.5929 N, 18.7927 E	Yes	2011	L & H 1991
Nordenskïoldbreen	Spitsbergen	NES	78.6580 N, 17.0094 E	Yes	2009	J. et al. 2000
Odinjøkulen	Spitsbergen	NES	79.5746 N, 18.3008 E	No	2010	L & H 1991
Oslobreen	Spitsbergen	NES	79.0905 N, 18.7590 E	No	2011	Liestøl 1993
Pedasenkobreen	Spitsbergen	NES	78.7071 N, 21.0479 E	Yes	2011	L & H 1991
Petermannbreen	Spitsbergen	NES	78.4993 N, 18.7832 E	Yes	2011	J. et al. 2000
Sonklarbreen	Spitsbergen	NES	78.7240 N, 20.3340 E	Yes	2011	L & H 1991
Tunabreen	Spitsbergen	NES	78.4739 N, 17.4255 E	Yes	2009	Liestøl 1993
Vestre Odinjokulen*	Spitsbergen	NES	79.5792 N, 18.1914 E	No	2010	Liestøl 1993
Von Postbreen	Spitsbergen	NES	78.4209 N, 17.5214 E	Yes	2009	Liestøl 1993
Andrinebreen	Spitsbergen	CS	77.9573 N, 17.0216 E	No	2011	S. et al. 2009
Ankerbreen	Spitsbergen	CS	77.9566 N, 16.3181 E	Yes	2011	Hamilton 1992
Ayerbreen	Spitsbergen	CS	78.0888 N, 16.0147 E	Yes	2009	Hamilton 1992
Bergmesterbreen	Spitsbergen	CS	78.0797 N, 16.9182 E	Yes	2009	Hamilton 1992
Blackbreen	Spitsbergen	CS	78.2859 N, 16.1383 E	No	2009	Hamilton 1992
Blekumbreen	Spitsbergen	CS	78.2478 N, 16.0051 E	No	2009	Hamilton 1992
Brandtbreen	Spitsbergen	CS	78.2868 N, 15.9483 E	No	2009	Hamilton 1992
Bødalen	Spitsbergen	CS	78.0953 N, 16.4452 E	No	2011	Hamilton 1992
Drønbreen	Spitsbergen	CS	78.1319 N, 16.8223 E	Yes	2009	Hamilton 1992
Duboisbreen	Spitsbergen	CS	78.2601 N, 16.7753 E	No	2009	Hamilton 1992
Elfenbeinbreen	Spitsbergen	CS	78.1643 N, 18.1371 E	No	No	Hamilton 1992
Fangenbreen	Spitsbergen	CS	78.2887 N, 16.2126 E	Yes	2009	Hamilton 1992
Fridtjovbreen	Spitsbergen	CS	77.7953 N, 14.5101 E	No	2008	Liestøl 1993
Glitrebreen	Spitsbergen	CS	78.0295 N, 17.1445 E	No	2009	Hamilton 1992
Gløttfjellbreen	Spitsbergen	CS	78.1391 N, 16.4566 E	No	2009	Hamilton 1992
Helsingborgbreen	Spitsbergen	CS	77.9597 N, 16.8318 E	Yes	2009	Hamilton 1992

Höganäsbreen	Spitsbergen	CS	77.9398 N, 16.7633 E	No	2009	Hamilton 1992
Innerbreen	Spitsbergen	CS	78.1057 N, 17.4057 E	No	2011	Hamilton 1992
Klauvbreen	Spitsbergen	CS	78.2997 N, 18.1949 E	No	2012	Hamilton 1992
Klunsbreen	Spitsbergen	CS	78.1563 N, 18.2662 E	No	2012	Hamilton 1992
Kokbreen	Spitsbergen	CS	78.0801 N, 16.4633 E	Yes	2009	Hamilton 1992
Livbreen	Spitsbergen	CS	77.9375 N, 16.3441 E	Yes	2009	Hamilton 1992
Lunckebreen	Spitsbergen	CS	78.0315 N, 16.7935 E	Yes	2009	Hamilton 1992
Margitbreen	Spitsbergen	CS	78.0074 N, 17.7975 E	No	2011	Hamilton 1992
Marmorbreen	Spitsbergen	CS	78.1777 N, 17.8231 E	No	2012	Hamilton 1992
Marthabreen	Spitsbergen	CS	78.0193 N, 16.6904 E	Yes	2009	Hamilton 1992
Medalsbreen	Spitsbergen	CS	78.0249 N, 15.5412 E	No	2011	Hamilton 1992
Møysalbreen	Spitsbergen	CS	78.1341 N, 16.4935 E	No	2009	Hamilton 1992
Målarbreen	Spitsbergen	CS	78.2709 N, 16.0848 E	Yes	2009	Hamilton 1992
Pålsjöbreen	Spitsbergen	CS	77.9992 N, 17.0231 E	Yes	2009	Hamilton 1992
Scott Turnerbreen	Spitsbergen	CS	78.1076 N, 15.9598 E	Yes	2009	Hamilton 1992
Skoltbreen	Spitsbergen	CS	78.1421 N, 16.7374 E	No	2009	Hamilton 1992
Skruisbreen	Spitsbergen	CS	78.1524 N, 17.8133 E	Yes	2012	Hamilton 1992
Skutbreen	Spitsbergen	CS	78.0355 N, 17.5192 E	Yes	2011	Hamilton 1992
Sveigbreen	Spitsbergen	CS	78.1093 N, 17.8000 E	Yes	2011	Hamilton 1992
Svellnosbreen	Spitsbergen	CS	78.0802 N, 16.4094 E	No	2009	Hamilton 1992
Tillbergfonna	Spitsbergen	CS	78.0717 N, 15.7960 E	Yes	2011	Hamilton 1992
Tinkarpbreen	Spitsbergen	CS	77.9876 N, 17.1855 E	No	2009	S. et al. 2009
Ulvebreen	Spitsbergen	CS	78.2096 N, 18.6497 E	Yes	2012	Hamilton 1992
Usherbreen	Spitsbergen	CS	78.2727 N, 18.6724 E	Yes	2012	Hamilton 1992
Vegbreen	Spitsbergen	CS	78.0250 N, 16.9524 E	Yes	2009	Hamilton 1992
Vendombreen	Spitsbergen	CS	78.1429 N, 17.2921 E	No	2009	Hamilton 1992
Amundsenisen	Spitsbergen	SS	77.2842 N, 15.5406 E	No	2010	S. et al. 2009
Anna Margrethebreen	Spitsbergen	SS	77.3415 N, 17.3157 E	Yes	2011	L & H 1991
Arnesenbreen	Spitsbergen	SS	77.7986 N, 18.0908 E	Yes	2012	L & H 1991
Aurkollfonna	Spitsbergen	SS	77.3983 N, 15.9905 E	No	2011	Hamilton 1992
Austjøkulen	Spitsbergen	SS	76.8761 N, 16.6199 E	Yes	2010	S. et al. 2009
Bakaninbreen	Spitsbergen	SS	77.7590 N, 17.4863 E	Yes	2011	D. et al. 1991
Barettbreen	Spitsbergen	SS	77.1845 N, 16.6386 E	No	2011	Hamilton 1992
Beinbreen	Spitsbergen	SS	77.1176 N, 16.9637 E	No	2011	Hamilton 1992
Bellingbreen	Spitsbergen	SS	77.3100 N, 17.3039 E	Yes	2011	Hamilton 1992
Bendfjellbreen	Spitsbergen	SS	77.2137 N, 16.6902 E	No	2011	Hamilton 1992
Bereznikovbreen	Spitsbergen	SS	77.7927 N, 18.2338 E	Yes	2012	L & H 1991
Billesholmbreen	Spitsbergen	SS	77.8982 N, 17.1603 E	Yes	2009	Hamilton 1992
Bjuvbreen	Spitsbergen	SS	77.9046 N, 17.2194 E	Yes	2009	Hamilton 1992
Blümckebreane	Spitsbergen	SS	77.5287 N, 15.0317 E	No	2011	Hamilton 1992
Bosarpbreen	Spitsbergen	SS	77.8814 N, 17.0558 E	Yes	2009	Hamilton 1992
Bratthengbreen	Spitsbergen	SS	77.7560 N, 18.3776 E	No	2012	Hamilton 1992
Brodtkorbfjellet	Spitsbergen	SS	77.8393 N, 17.1965 E	Yes	2011	S. et al. 2009
Bungebreen	Spitsbergen	SS	76.8153 N, 16.0941 E	Yes	2010	S. et al. 2009
Buttbreen	Spitsbergen	SS	77.6846 N, 16.4830 E	Yes	2011	Hamilton 1992
Charpentierbreen	Spitsbergen	SS	77.6163 N, 15.5409 E	Yes	2011	Liestøl 1993
Crollbreen	Spitsbergen	SS	77.2070 N, 17.2646 E	Yes	2011	L & H 1991
Davisbreen	Spitsbergen	SS	77.2463 N, 17.2500 E	Yes	2011	Liestøl 1993
Dobrowolskibreen	Spitsbergen	SS	77.3499 N, 16.6929 E	No	2011	S. et al. 2009
Doktorbreen	Spitsbergen	SS	77.5276 N, 16.6780 E	Yes	2011	Hamilton 1992
Dvergfonna	Spitsbergen	SS	77.4603 N, 15.4428 E	No	2011	Hamilton 1992
Edvardbreen	Spitsbergen	SS	77.8885 N, 17.6170 E	Yes	2011	S. et al. 2009
Filantropbreen	Spitsbergen	SS	77.7115 N, 16.7107 E	Yes	2011	Hamilton 1992
Finsterwalderbreen	Spitsbergen	SS	77.4595 N, 15.2446 E	Yes	2011	Hamilton 1992
Firmbreen	Spitsbergen	SS	77.8703 N, 17.2276 E	No	2009	S. et al. 2009
Flatbreen	Spitsbergen	SS	77.1553 N, 16.8051 E	Yes	2011	Hamilton 1992
Fredfonna	Spitsbergen	SS	76.9126 N, 16.6501 E	No	2010	S. et al. 2009
Gribnefjellbreen	Spitsbergen	SS	77.7558 N, 17.6153 E	No	2011	Hamilton 1992
Hambergbreen	Spitsbergen	SS	77.0534 N, 17.0115 E	Yes	2011	L & H 1991

Hessbreen	Spitsbergen	SS	77.5079 N, 15.1125 E	Yes	2011	Liestøl 1993
Hettebreen	Spitsbergen	SS	77.7472 N, 16.7945 E	Yes	2011	Hamilton 1992
Hornbreen	Spitsbergen	SS	77.0640 N, 16.6945 E	Yes	2011	J. et al. 2000
Hyllingebreen	Spitsbergen	SS	77.9090 N, 17.2928 E	Yes	2009	Liestøl 1993
Høgstebereen	Spitsbergen	SS	77.3334 N, 15.1421 E	Yes	2011	S. et al. 2009
Indrebøbreen	Spitsbergen	SS	77.6123 N, 17.9269 E	Yes	2012	S. et al. 2009
Ingerbreen	Spitsbergen	SS	77.7481 N, 18.2846 E	Yes	2012	S. et al. 2009
Inglefieldbreen	Spitsbergen	SS	77.8263 N, 17.9488 E	Yes	2012	L & H 1991
Isbroddbreen	Spitsbergen	SS	77.2087 N, 16.9720 E	No	2011	Hamilton 1992
Karibreen	Spitsbergen	SS	77.6089 N, 17.7828 E	Yes	2012	Hamilton 1992
Keipbreen	Spitsbergen	SS	77.7741 N, 17.6222 E	No	2011	Hamilton 1992
Søre Kjølhø*	Spitsbergen	SS	77.6375 N, 17.2950 E	No	2012	S. et al. 2009
Kjølhøbreen	Spitsbergen	SS	77.6647 N, 17.3053 E	No	2012	S. et al. 2009
Kleivbreen	Spitsbergen	SS	77.9115 N, 17.3469 E	Yes	2009	S. et al. 2009
Klubbebreen	Spitsbergen	SS	77.7225 N, 17.0614 E	Yes	2011	S. et al. 2009
Knoppbreen	Spitsbergen	SS	77.6781 N, 17.2340 E	No	2012	S. et al. 2009
Kroppbreen	Spitsbergen	SS	77.8967 N, 17.4149 E	Yes	2011	S. et al. 2009
Liten Kroppebreen*	Spitsbergen	SS	77.9154 N, 17.5779 E	No	2011	S. et al. 2009
Kvalbreen	Spitsbergen	SS	77.5822 N, 18.0621 E	Yes	2012	S. et al. 2009
Kvastbreen	Spitsbergen	SS	77.4456 N, 17.2824 E	Yes	2011	Hamilton 1992
Körberbreen	Spitsbergen	SS	76.9463 N, 16.0814 E	Yes	2010	Liestøl 1993
Langleikbreen	Spitsbergen	SS	77.2170 N, 16.5182 E	No	2011	Hamilton 1992
Langryggbreen	Spitsbergen	SS	77.3859 N, 15.9164 E	No	2011	Hamilton 1992
Lognbreen	Spitsbergen	SS	77.7793 N, 17.3864 E	No	2011	Hamilton 1992
Luntebreen	Spitsbergen	SS	77.7240 N, 16.8725 E	No	2011	Hamilton 1992
Markhambreen	Spitsbergen	SS	77.1211 N, 17.2016 E	Yes	2011	S. et al. 2009
Martinbreen	Spitsbergen	SS	77.6446 N, 15.6694 E	Yes	2011	Liestøl 1993
Mendelejevbreen	Spitsbergen	SS	76.9276 N, 16.5523 E	Yes	2010	S. et al. 2009
Mühlbacherbreen	Spitsbergen	SS	77.1461 N, 15.9167 E	No	2011	S. et al. 2009
Noglebreen	Spitsbergen	SS	77.5568 N, 17.2035 E	No	2012	S. et al. 2009
Notaschabreen	Spitsbergen	SS	77.6898 N, 17.5438 E	No	2011	S. et al. 2009
Nothorstbreen	Spitsbergen	SS	77.2833 N, 16.7208 E	Yes	2011	S. et al. 2009
Nordsysselbreen	Spitsbergen	SS	77.8493 N, 17.7867 E	No	2011	Hamilton 1992
Nornebreen	Spitsbergen	SS	77.2288 N, 15.7106 E	No	2011	S. et al. 2009
Novbreen	Spitsbergen	SS	77.2071 N, 16.7680 E	No	2011	Hamilton 1992
Oksbreen	Spitsbergen	SS	77.1311 N, 16.9866 E	No	2011	Hamilton 1992
Paierlbreen	Spitsbergen	SS	77.1229 N, 15.7230 E	No	2011	**B**. et al. 2009
Paulabreen	Spitsbergen	SS	77.7362 N, 17.3125 E	Yes	2011	S. et al. 2009
Peisbreen	Spitsbergen	SS	77.7381 N, 17.1280 E	Yes	2011	Hamilton 1992
Penckbreen	Spitsbergen	SS	77.4741 N, 15.6391 E	Yes	2011	Hamilton 1992
Persejbreen	Spitsbergen	SS	77.4575 N, 17.3803 E	Yes	2012	D. et al. 2003
Plogbreen	Spitsbergen	SS	76.7866 N, 16.1875 E	Yes	2010	Hamilton 1992
Polakkbreen	Spitsbergen	SS	77.2729 N, 16.1693 E	No	2011	S. et al. 2009
Profilbreen	Spitsbergen	SS	77.2769 N, 15.1777 E	Yes	2011	S. et al. 2009
RagNo-Mariebreen	Spitsbergen	SS	77.7942 N, 17.3597 E	Yes	2011	S. et al. 2009
Recherchebreen	Spitsbergen	SS	77.4370 N, 14.8208 E	No	2011	Liestøl 1993
Richardsbreen	Spitsbergen	SS	77.7314 N, 18.0373 E	Yes	2012	**B**. et al. 2009
Richterbreen	Spitsbergen	SS	77.6429 N, 15.5267 E	Yes	2011	Hamilton 1992
Ryggbreen	Spitsbergen	SS	77.1666 N, 17.0547 E	No	2011	Hamilton 1992
Samarinbreen	Spitsbergen	SS	76.8858 N, 16.3490 E	Yes	2010	Hamilton 1992
Scheelebreen	Spitsbergen	SS	77.6929 N, 16.9702 E	Yes	2011	S. et al. 2009
Scottbreen	Spitsbergen	SS	77.5439 N, 14.3668 E	Yes	2011	Liestøl 1993
Sergievskifjellet	Spitsbergen	SS	77.5357 N, 17.4598 E	Yes	2012	S. et al. 2009
Siegerbreen	Spitsbergen	SS	77.4513 N, 15.8743 E	Yes	2011	Liestøl 1993
Skilfonna	Spitsbergen	SS	76.9307 N, 16.9131 E	Yes	2010	S. et al. 2009
Skimebreen	Spitsbergen	SS	77.2834 N, 17.2410 E	Yes	2011	B. et al. 2009
Skobreen	Spitsbergen	SS	77.7062 N, 17.2081 E	No	2012	S. et al. 2009
Snokuvbreen	Spitsbergen	SS	77.7021 N, 16.3589 E	Yes	2011	S. et al. 2009
Spaelbreen	Spitsbergen	SS	77.4186 N, 17.2275 E	Yes	2011	Hamilton 1992

St. Olgafjellet	Spitsbergen	SS	77.5830 N, 17.7880 E	No	2012	S. et al. 2009
Stabbfonna	Spitsbergen	SS	77.1466 N, 16.9560 E	No	2011	Hamilton 1992
Staupbreen	Spitsbergen	SS	77.0813 N, 17.2518 E	Yes	2011	Liestøl 1993
Steenstrupbreen	Spitsbergen	SS	77.6053 N, 16.2919 E	Yes	2011	Hamilton 1992
Stolbreen	Spitsbergen	SS	77.1360 N, 17.1078 E	Yes	2011	Hamilton 1992
Storbreen	Spitsbergen	SS	77.1299 N, 16.3370 E	Yes	2010	Hamilton 1992
Strongbreen	Spitsbergen	SS	77.5815 N, 17.5069 E	Yes	2012	L & H 1991
Sulsbreen	Spitsbergen	SS	77.8155 N, 17.7378 E	No	2011	Hamilton 1992
Svalbreen	Spitsbergen	SS	77.6608 N, 16.5462 E	Yes	2011	Hamilton 1992
Sykorabreen	Spitsbergen	SS	77.0179 N, 17.0045 E	Yes	2011	L & H 1991
Søkkbreen	Spitsbergen	SS	77.6204 N, 17.3235 E	No	2012	S. et al. 2009
Thomsonbreen	Spitsbergen	SS	77.6380 N, 18.2098 E	Yes	2012	L & H 1991
Tjørndalsbreen	Spitsbergen	SS	77.5362 N, 14.2363 E	No	2011	Hamilton 1992
Vallåkrabreen (Bringen)	Spitsbergen	SS	77.8600 N, 17.1127 E	Yes	2009	S. et al. 2009
Vasilievbreen	Spitsbergen	SS	76.7894 N, 16.7383 E	Yes	2010	L & H 1991
Vasilievbreen (Rundtuva)	Spitsbergen	SS	76.7023 N, 16.8632 E	No	2010	L & H 1991
Venetzbreen	Spitsbergen	SS	77.6016 N, 15.5816 E	Yes	2011	Hamilton 1992
Vindeggbreen	Spitsbergen	SS	77.4932 N, 17.2880 E	Yes	2012	S. et al. 2009
Zawadskibreen	Spitsbergen	SS	77.3390 N, 15.8828 E	Yes	2011	S. et al. 2009
Bodleybreen	Nord Austlandet	NA	79.8370 N, 21.4901 E	No	2011	D. et al. 1999
Bråsvellbreen (Af B1)	Nord Austlandet	NA	79.3680 N, 23.4389 E	No	2011	D. et al. 1999
Austfonna (B3)	Nord Austlandet	NA	79.7769 N, 24.6528 E	No	2011	Liestøl 1993
Clasebreen	Nord Austlandet	NA	79.5775 N, 20.3272 E	No	2011	L & H 1991
Franklinbreen nordre	Nord Austlandet	NA	80.1050 N, 19.6123 E	No	2010	D. et al. 1999
Franklinbreen Søre	Nord Austlandet	NA	80.0629 N, 19.4651 E	No	2010	Liestøl 1993
Palanderbreen	Nord Austlandet	NA	79.5320 N, 21.0316 E	No	2011	L & H 1991
Palenderisen	Nord Austlandet	NA	79.5665 N, 21.8560 E	No	2011	L & H 1991
Rijpbreen	Nord Austlandet	NA	80.1013 N, 21.5677 E	No	2010	Liestøl 1993
Etonbreen	Nord Austlandet	NA	79.7298 N, 21.9163 E	Yes	2011	D. et al. 1999
Holtenbreen	Nord Austlandet	NA	79.5642 N, 20.4385 E	No	2011	L & H 1991
Duckwitzbreen	Barentsøya	BEØ	78.3416 N, 20.8540 E	Yes	2010	Liestøl 1993
Freemanbreen	Barentsøya	BEØ	78.2911 N, 21.7744 E	Yes	2010	Liestøl 1993
Hübnerbreen	Barentsøya	BEØ	78.3718 N, 21.9848 E	Yes	2010	Liestøl 1993
Reymondbreen	Barentsøya	BEØ	78.3943 N, 22.0054 E	Yes	2010	Liestøl 1993
Austre Kvitisen	Edgeøya	BEØ	78.0531 N, 21.6311 E	Yes	2010	Liestøl 1993
Deltabreen	Edgeøya	BEØ	77.5590 N, 23.0057 E	Yes	2010	L & H 1991
Kong Johans Bre	Edgeøya	BEØ	77.6268 N, 23.8996 E	Yes	2010	Liestøl 1993
Kuhrbreen	Edgeøya	BEØ	77.5567 N, 21.7792 E	Yes	2010	L & H 1991
Marsjøbreen	Edgeøya	BEØ	77.9367 N, 22.4144 E	Yes	2010	Liestøl 1993
Pettersenbreen	Edgeøya	BEØ	77.4809 N, 23.4976 E	Yes	2010	Liestøl 1993
Skrentbreen	Edgeøya	BEØ	77.5363 N, 21.5107 E	Yes	2010	Liestøl 1993
Stonebreen	Edgeøya	BEØ	77.8110 N, 23.9041 E	Yes	2010	L & H 1991
Suraustre Bergfonna	Edgeøya	BEØ	78.1171 N, 22.0333 E	No	2010	Liestøl 1993
Vestre Kvitkåpa	Edgeøya	BEØ	77.4043 N, 22.8036 E	Yes	2010	Liestøl 1993

B. et al. 2009	**Blaszczyk et al. 2009**
D. et al. 1991	**Dowdeswell et al. 1991**
D. et al. 1999	**Dowdeswell et al. 1999**
D. et al. 2003	**Dowdeswell et al. 2003**
Hamilton 1992	**Hamiliton 1992**
J. et al. 2000	**Jiskoot et al. 2000**
L & H 1991	**Lefauconnier and Hagen 1991**
Liestøl 1993	**Liestøl 1993**
S. et al. 2009	**Sund et al. 2009**

Glaciers with CSR Supplementary Table 2

Glacier Name	Island	Region	Lat. / Long.	CSR	Photo year	Ref.
Alfredbreen	Prince Karls Foreland	NWS	78.5753 N, 11.1083 E	Yes	2008	This study
Archibald Geikiebreen	Prince Karls Foreland	NWS	78.4532 N, 11.5596 E	Yes	2008	This study
Doddsbreen	Prince Karls Foreland	NWS	78.5188 N, 11.3129 E	Yes	2008	This study
Fallbreen	Prince Karls Foreland	NWS	78.7011 N, 10.9903 E	Yes	2008	This study
James Geikiebreen	Prince Karls Foreland	NWS	78.4955 N, 11.4219 E	Yes	2008	This study
Magdabreen	Prince Karls Foreland	NWS	78.5654 N, 11.1672 E	Yes	2008	This study
Midtre Buchananisen	Prince Karls Foreland	NWS	78.6641 N, 11.0177 E	Yes	2008	This study
Millerbreen	Prince Karls Foreland	NWS	78.7085 N, 10.8261 E	Yes	2008	This study
Murraybreen	Prince Karls Foreland	NWS	78.7292 N, 11.0023 E	Yes	2008	This study
Parnassbreen	Prince Karls Foreland	NWS	78.6275 N, 10.9316 E	Yes	2008	This study
Søre Buchananisen	Prince Karls Foreland	NWS	78.6444 N, 11.0670 E	Yes	2008	This study
Agnorbreen	Spitsbergen	NWS	78.6571 N, 12.1823 E	Yes	2009	This study
Albertbreen	Spitsbergen	NWS	79.6578 N, 12.7306 E	Yes	2011	This study
Andreasbreen	Spitsbergen	NWS	78.6123 N, 12.2633 E	Yes	2009	This study
Andreebreen	Spitsbergen	NWS	79.6692 N, 12.4784 E	Yes	2011	This study
Angelbreen	Spitsbergen	NWS	79.0704 N, 15.3702 E	Yes	2011	This study
Anne-Mariebreen	Spitsbergen	NWS	79.3924 N, 14.9266 E	Yes	2010	This study
Arthurbreen	Spitsbergen	NWS	78.7722 N, 11.9098 E	Yes	2009	This study
Aulbreen	Spitsbergen	NWS	78.3213 N, 13.2483 E	Yes	2009	This study
Austre Holmesletbreen	Spitsbergen	NWS	78.4896 N, 12.9385 E	Yes	2009	This study
Austre Lovenbreane	Spitsbergen	NWS	78.8746 N, 12.1463 E	Yes	2009	This study
Balliolbreen	Spitsbergen	NWS	78.8067 N, 16.3140 E	Yes	2011	This study
Bardebreen	Spitsbergen	NWS	78.6739 N, 14.1829 E	Yes	2009	This study
Barmfjellbreen	Spitsbergen	NWS	78.9068 N, 14.7812 E	Yes	2011	This study
Belshornbreen	Spitsbergen	NWS	79.1683 N, 15.0329 E	Yes	2011	This study
Bertilbreen	Spitsbergen	NWS	78.6912 N, 16.2658 E	Yes	2011	This study
Binnebreen	Spitsbergen	NWS	79.2771 N, 15.2119 E	Yes	2010	This study
Bitihornbreen	Spitsbergen	NWS	78.8703 N, 14.6593 E	Yes	2011	This study
Botnefjellet	Spitsbergen	NWS	78.8586 N, 12.4051 E	Yes	2009	This study
Brurskankbreen	Spitsbergen	NWS	78.9641 N, 14.8508 E	Yes	2011	This study
Bukkebreen	Spitsbergen	NWS	79.1258 N, 15.1951 E	Yes	2011	This study
Bullbreen	Spitsbergen	NWS	78.4867 N, 12.6591 E	Yes	2009	This study
Børrebreen	Spitsbergen	NWS	79.5118 N, 13.0568 E	Yes	2011	This study
Caiusbreen	Spitsbergen	NWS	78.7645 N, 16.0552 E	Yes	2011	This study
Cambridgebreen	Spitsbergen	NWS	78.8001 N, 16.3845 E	Yes	2011	This study
Conwaybreen	Spitsbergen	NWS	78.9929 N, 12.6170 E	Yes	2009	This study
Dahlbreen	Spitsbergen	NWS	78.6021 N, 12.5327 E	Yes	2009	This study
D'Arodesbreen	Spitsbergen	NWS	79.1537 N, 12.0970 E	Yes	2009	This study
Eddabreen	Spitsbergen	NWS	79.2717 N, 14.8895 E	Yes	2010	This study
Edithbreen	Spitsbergen	NWS	78.8569 N, 12.0977 E	Yes	2009	This study
Eivindbreen	Spitsbergen	NWS	78.6310 N, 12.2802 E	Yes	2009	This study
Erikbreen	Spitsbergen	NWS	79.6187 N, 12.4779 E	Yes	2011	This study
Ernstbreen	Spitsbergen	NWS	79.5849 N, 14.4412 E	Yes	2010	This study
Esmarkbreen	Spitsbergen	NWS	78.3205 N, 13.8122 E	Yes	2009	This study
Evabreen	Spitsbergen	NWS	79.6870 N, 12.6347 E	Yes	2011	This study
Feiringbreen	Spitsbergen	NWS	79.0199 N, 12.4807 E	Yes	2009	This study
Ferdinandbreen	Spitsbergen	NWS	78.7104 N, 16.3408 E	Yes	2011	This study
Flakbreen	Spitsbergen	NWS	79.1740 N, 11.9764 E	Yes	2009	This study
Førstebreen	Spitsbergen	NWS	79.2706 N, 11.1494 E	Yes	2009	This study
Garmbreen	Spitsbergen	NWS	79.7505 N, 14.5524 E	Yes	2010	This study
Gavlhaugbreen	Spitsbergen	NWS	78.8760 N, 15.5155 E	Yes	2011	This study
Geabreen	Spitsbergen	NWS	78.3295 N, 14.0666 E	Yes	2009	This study
Georgbreen	Spitsbergen	NWS	79.5662 N, 14.4422 E	Yes	2010	This study
Ginnungagapbreen	Spitsbergen	NWS	79.2136 N, 14.6479 E	Yes	2010	This study
Gislebreen	Spitsbergen	NWS	78.4758 N, 12.5535 E	Yes	2009	This study
Glopbreen	Spitsbergen	NWS	79.5284 N, 13.0110 E	Yes	2011	This study

Gufsbreen	Spitsbergen	NWS	78.8651 N, 14.8311 E	Yes	2011	This study
Gullmarbreen	Spitsbergen	NWS	79.6722 N, 11.3604 E	Yes	2011	This study
Gunnarbreen	Spitsbergen	NWS	78.4908 N, 13.1080 E	Yes	2009	This study
Gygrebreen	Spitsbergen	NWS	78.8054 N, 14.9144 E	Yes	2011	This study
Harrietbreen	Spitsbergen	NWS	78.2667 N, 13.5973 E	Yes	2009	This study
Hillbreen	Spitsbergen	NWS	79.6188 N, 11.2314 E	Yes	2011	This study
Hodsbreen	Spitsbergen	NWS	78.9883 N, 15.5275 E	Yes	2011	This study
Hoelbreen	Spitsbergen	NWS	78.7552 N, 16.2600 E	Yes	2011	This study
Holmesletbreane	Spitsbergen	NWS	78.4891 N, 12.9020 E	Yes	2009	This study
Hønnbreen	Spitsbergen	NWS	79.1612 N, 15.1796 E	Yes	2011	This study
Høvbreen	Spitsbergen	NWS	79.4369 N, 14.4308 E	Yes	2010	This study
Isrypebreen	Spitsbergen	NWS	78.7033 N, 14.0743 E	Yes	2009	This study
Johanbreen	Spitsbergen	NWS	79.1642 N, 13.9657 E	Yes	2011	This study
Kaalaasbreen	Spitsbergen	NWS	79.0198 N, 15.6983 E	Yes	2011	This study
Karlsbreen	Spitsbergen	NWS	79.3468 N, 13.4088 E	Yes	2011	This study
Keisarbreen	Spitsbergen	NWS	79.5532 N, 12.9111 E	Yes	2011	This study
Kjerulfbreen	Spitsbergen	NWS	78.2873 N, 13.6556 E	Yes	2009	This study
Kongsbreen	Spitsbergen	NWS	78.9255 N, 12.7588 E	Yes	2009	This study
Kyrkjebreen	Spitsbergen	NWS	78.8747 N, 14.0060 E	Yes	2009	This study
Landbreen	Spitsbergen	NWS	79.6815 N, 14.5829 E	Yes	2010	This study
Lappbreen	Spitsbergen	NWS	78.6412 N, 14.2767 E	Yes	2009	This study
Lexfjellbreen	Spitsbergen	NWS	78.2617 N, 13.4925 E	Yes	2009	This study
Lilliehöökbreen	Spitsbergen	NWS	79.3501 N, 11.7191 E	Yes	2009	This study
Løvliebreen	Spitsbergen	NWS	78.4846 N, 13.0154 E	Yes	2009	This study
Maribreen	Spitsbergen	NWS	78.9498 N, 15.4010 E	Yes	2011	This study
Miethebreen	Spitsbergen	NWS	79.5628 N, 11.2986 E	Yes	2011	This study
Morabreen	Spitsbergen	NWS	78.8694 N, 14.2196 E	Yes	2009	This study
Målarbreen	Spitsbergen	NWS	78.8520 N, 14.5902 E	Yes	2011	This study
Ottobreen	Spitsbergen	NWS	79.6089 N, 14.4820 E	Yes	2010	This study
Pedersenbreen	Spitsbergen	NWS	78.8682 N, 12.2868 E	Yes	2009	This study
Protektorbreen	Spitsbergen	NWS	78.2379 N, 13.6791 E	Yes	2009	This study
Purpurbreen	Spitsbergen	NWS	78.9585 N, 15.9234 E	Yes	2011	This study
Qvarnstrombreen	Spitsbergen	NWS	78.7485 N, 14.3778 E	Yes	2009	This study
Ringertzbreen	Spitsbergen	NWS	79.2047 N, 13.5174 E	Yes	2011	This study
Robertsonbreen	Spitsbergen	NWS	78.7902 N, 15.9749 E	Yes	2011	This study
Sagtindbreen	Spitsbergen	NWS	79.2802 N, 12.2090 E	Yes	2009	This study
Schjelderupbreen	Spitsbergen	NWS	79.3955 N, 13.3686 E	Yes	2011	This study
Sellströmbreen	Spitsbergen	NWS	79.6960 N, 11.3319 E	Yes	2011	This study
Serlabreen	Spitsbergen	NWS	79.7307 N, 12.6631 E	Yes	2011	This study
Skaugumbreen	Spitsbergen	NWS	79.5556 N, 14.7806 E	Yes	2010	This study
Skreifjellbreen	Spitsbergen	NWS	79.0171 N, 12.2921 E	Yes	2009	This study
Slørbreen	Spitsbergen	NWS	79.2835 N, 11.4513 E	Yes	2009	This study
Smalgangenbreen	Spitsbergen	NWS	78.5617 N, 13.0116 E	Yes	2009	This study
Smithbreen	Spitsbergen	NWS	79.7382 N, 11.8618 E	Yes	2011	This study
Southhamptonbreen	Spitsbergen	NWS	78.8082 N, 16.1549 E	Yes	2011	This study
Stabeisbreen	Spitsbergen	NWS	79.0065 N, 15.0167 E	Yes	2011	This study
Stallobreen	Spitsbergen	NWS	78.3746 N, 13.2644 E	Yes	2009	This study
Svardalsbreen	Spitsbergen	NWS	79.6774 N, 14.8455 E	Yes	2010	This study
Svelgfjellbreen Søre	Spitsbergen	NWS	79.2855 N, 14.4713 E	Yes	2010	This study
Sølvbreen	Spitsbergen	NWS	78.8482 N, 14.8794 E	Yes	2011	This study
Søre Vasskilbreen	Spitsbergen	NWS	78.8922 N, 15.6646 E	Yes	2011	This study
Tassbreen	Spitsbergen	NWS	78.7830 N, 11.8956 E	Yes	2009	This study
Torgnybreen	Spitsbergen	NWS	78.2380 N, 13.5723 E	Yes	2009	This study
Uggbreen	Spitsbergen	NWS	79.2333 N, 15.1339 E	Yes	2010	This study
Ujamnbreen	Spitsbergen	NWS	78.5781 N, 12.6174 E	Yes	2009	This study
Universitetsbreen	Spitsbergen	NWS	78.9846 N, 15.3607 E	Yes	2011	This study
Venbreen	Spitsbergen	NWS	78.9362 N, 14.7178 E	Yes	2011	This study
Venernbreen	Spitsbergen	NWS	78.3403 N, 13.2113 E	Yes	2009	This study
Veobreen	Spitsbergen	NWS	79.2257 N, 11.4782 E	Yes	2009	This study

Vestre Brøggerbreane	Spitsbergen	NWS	78.9131 N, 11.7426 E	Yes	2009	This study
Vetternbreen	Spitsbergen	NWS	78.2924 N, 13.3811 E	Yes	2009	This study
Vogtbreen	Spitsbergen	NWS	79.6590 N, 14.6250 E	Yes	2010	This study
Vonbreen	Spitsbergen	NWS	79.2006 N, 13.7021 E	Yes	2011	This study
Waldemarbreen	Spitsbergen	NWS	78.6749 N, 12.0469 E	Yes	2009	This study
Yggbreen	Spitsbergen	NWS	79.1096 N, 15.2932 E	Yes	2011	This study
*** NWS-1**	Spitsbergen	NWS	79.5936 N, 14.7008 E	Yes	2010	This study
*** NWS-2**	Spitsbergen	NWS	79.5234 N, 14.6465 E	Yes	2010	This study
*** NWS-3**	Spitsbergen	NWS	79.5028 N, 14.3789 E	Yes	2010	This study
*** NWS-4**	Spitsbergen	NWS	79.4849 N, 14.6117 E	Yes	2010	This study
*** NWS-5**	Spitsbergen	NWS	79.3715 N, 14.5618 E	Yes	2010	This study
*** NWS-6**	Spitsbergen	NWS	79.3317 N, 14.7224 E	Yes	2010	This study
*** NWS-7**	Spitsbergen	NWS	79.3044 N, 14.8876 E	Yes	2010	This study
*** NWS-8**	Spitsbergen	NWS	79.2418 N, 14.5704 E	Yes	2011	This study
*** NWS-9**	Spitsbergen	NWS	79.1827 N, 12.2420 E	Yes	2009	This study
*** NWS-10**	Spitsbergen	NWS	79.1417 N, 14.7231 E	Yes	2011	This study
*** NWS-11**	Spitsbergen	NWS	79.1245 N, 14.6855 E	Yes	2011	This study
*** NWS-12**	Spitsbergen	NWS	79.1056 N, 14.6841 E	Yes	2011	This study
*** NWS-13**	Spitsbergen	NWS	79.0271 N, 14.8898 E	Yes	2011	This study
*** NWS-14**	Spitsbergen	NWS	79.0009 N, 15.6862 E	Yes	2011	This study
*** NWS-15**	Spitsbergen	NWS	78.8666 N, 15.9476 E	Yes	2011	This study
*** NWS-16**	Spitsbergen	NWS	78.8311 N, 14.8404 E	Yes	2011	This study
*** NWS-17**	Spitsbergen	NWS	78.8005 N, 11.8869 E	Yes	2009	This study
*** NWS-18**	Spitsbergen	NWS	78.7973 N, 11.8371 E	Yes	2009	This study
*** NWS-19**	Spitsbergen	NWS	78.7752 N, 16.5404 E	Yes	2011	This study
*** NWS-20**	Spitsbergen	NWS	78.7137 N, 16.1528 E	Yes	2011	This study
*** NWS-21**	Spitsbergen	NWS	78.7117 N, 14.9811 E	Yes	2011	This study
*** NWS-22**	Spitsbergen	NWS	78.7070 N, 15.9753 E	Yes	2011	This study
*** NWS-23**	Spitsbergen	NWS	78.7034 N, 15.7074 E	Yes	2011	This study
*** NWS-24**	Spitsbergen	NWS	78.7025 N, 15.8999 E	Yes	2011	This study
*** NWS-25**	Spitsbergen	NWS	78.6914 N, 16.0344 E	Yes	2011	This study
*** NWS-26**	Spitsbergen	NWS	78.6320 N, 15.8399 E	Yes	2011	This study
*** NWS-27**	Spitsbergen	NWS	78.6169 N, 14.2329 E	Yes	2009	This study
*** NWS-28**	Spitsbergen	NWS	78.6135 N, 16.0110 E	Yes	2011	This study
*** NWS-29**	Spitsbergen	NWS	78.6034 N, 12.3576 E	Yes	2009	This study
*** NWS-30**	Spitsbergen	NWS	78.5577 N, 12.4685 E	Yes	2009	This study
*** NWS-31**	Spitsbergen	NWS	78.5374 N, 15.8909 E	Yes	2011	This study
*** NWS-32**	Spitsbergen	NWS	78.5243 N, 15.7647 E	Yes	2011	This study
*** NWS-33**	Spitsbergen	NWS	78.5240 N, 14.2120 E	Yes	2009	This study
*** NWS-34**	Spitsbergen	NWS	78.5150 N, 14.2284 E	Yes	2009	This study
*** NWS-35**	Spitsbergen	NWS	78.4665 N, 14.1794 E	Yes	2009	This study
*** NWS-36**	Spitsbergen	NWS	78.4660 N, 13.9817 E	Yes	2009	This study
*** NWS-37**	Spitsbergen	NWS	78.4625 N, 14.1963 E	Yes	2009	This study
*** NWS-38**	Spitsbergen	NWS	78.4308 N, 12.6925 E	Yes	2009	This study
*** NWS-39**	Spitsbergen	NWS	78.3853 N, 14.0697 E	Yes	2009	This study
*** NWS-40**	Spitsbergen	NWS	78.3593 N, 13.1976 E	Yes	2009	This study
*** NWS-41**	Spitsbergen	NWS	78.3414 N, 13.8878 E	Yes	2009	This study
*** NWS-42**	Spitsbergen	NWS	78.2963 N, 13.8004 E	Yes	2009	This study
*** NWS-43**	Spitsbergen	NWS	78.2908 N, 13.8159 E	Yes	2009	This study
Beckerfjelletbreen	Spitsbergen	NES	78.9795 N, 20.2595 E	Yes	2011	This study
Berglibreen	Spitsbergen	NES	79.6698 N, 16.0693 E	Yes	2010	This study
Bogebreen	Spitsbergen	NES	78.4607 N, 17.5689 E	Yes	2009	This study
Brucebreen	Spitsbergen	NES	78.4671 N, 17.2855 E	Yes	2009	This study
Buldrebreen	Spitsbergen	NES	79.8088 N, 17.6740 E	Yes	2010	This study
Burn Murdochbreen	Spitsbergen	NES	78.4590 N, 17.0617 E	Yes	2009	This study
Chydeniusbreen	Spitsbergen	NES	79.2379 N, 18.2541 E	Yes	2010	This study
Dunerbreen	Spitsbergen	NES	79.8115 N, 16.8123 E	Yes	2010	This study
Dvergbreen	Spitsbergen	NES	79.4602 N, 17.7084 E	Yes	2010	This study
Fairweatherbreen	Spitsbergen	NES	78.5796 N, 16.8609 E	Yes	2009	This study

Florabreen	Spitsbergen	NES	78.5975 N, 17.2908 E	Yes	2009	This study
Formidablebreen	Spitsbergen	NES	78.8771 N, 16.5887 E	Yes	2011	This study
Frøyabreen	Spitsbergen	NES	79.5469 N, 18.1483 E	Yes	2010	This study
Glintbreen	Spitsbergen	NES	79.3756 N, 17.9801 E	Yes	2010	This study
Glærbreen	Spitsbergen	NES	79.6187 N, 17.5781 E	Yes	2010	This study
Gullfaksebreen	Spitsbergen	NES	79.5629 N, 17.4294 E	Yes	2010	This study
Heuglinbreen	Spitsbergen	NES	78.3794 N, 18.8252 E	Yes	2012	This study
Hinlopenbreen	Spitsbergen	NES	79.0721 N, 18.9968 E	Yes	2011	This study
Hodbreen	Spitsbergen	NES	79.3616 N, 18.7956 E	Yes	2010	This study
Hønerbreen	Spitsbergen	NES	79.1259 N, 18.7711 E	Yes	2011	This study
Johansenbreen	Spitsbergen	NES	78.5244 N, 18.7531 E	Yes	2011	This study
Keiserkampen	Spitsbergen	NES	79.0486 N, 20.6421 E	Yes	2011	This study
Koristkabreen	Spitsbergen	NES	78.8191 N, 21.2386 E	Yes	2011	This study
Königsbreen	Spitsbergen	NES	78.3439 N, 18.6524 E	Yes	2012	This study
Laubefjellebreen	Spitsbergen	NES	78.8501 N, 21.0229 E	Yes	2011	This study
Loderbreen	Spitsbergen	NES	79.2031 N, 18.8506 E	Yes	2011	This study
McWhaebreen	Spitsbergen	NES	78.7792 N, 16.6587 E	Yes	2011	This study
Methuenbreen	Spitsbergen	NES	78.5249 N, 17.1335 E	Yes	2009	This study
Nordbreen	Spitsbergen	NES	79.6378 N, 15.9158 E	Yes	2010	This study
Ordonnansbreen	Spitsbergen	NES	78.6390 N, 18.9873 E	Yes	2011	This study
Planckbreen	Spitsbergen	NES	79.1834 N, 16.4026 E	Yes	2010	This study
Polarisbreen	Spitsbergen	NES	79.2260 N, 18.5248 E	Yes	2011	This study
Ragnarbreen	Spitsbergen	NES	78.7540 N, 16.7125 E	Yes	2011	This study
Reinsbukkbreen	Spitsbergen	NES	79.2025 N, 16.6432 E	Yes	2010	This study
Reliktbreen	Spitsbergen	NES	79.4365 N, 18.7668 E	Yes	2010	This study
Rimfaksebreen	Spitsbergen	NES	79.6007 N, 17.5133 E	Yes	2010	This study
Ringhornbreen	Spitsbergen	NES	79.3324 N, 16.4563 E	Yes	2010	This study
Roonbreen	Spitsbergen	NES	79.0132 N, 19.7522 E	Yes	2011	This study
Royal Societybreen	Spitsbergen	NES	79.3115 N, 16.4657 E	Yes	2010	This study
Sanderbreen	Spitsbergen	NES	79.0894 N, 16.5005 E	Yes	2011	This study
Sistebreen	Spitsbergen	NES	79.3703 N, 17.3138 E	Yes	2010	This study
Skinfaksbebreen	Spitsbergen	NES	79.5038 N, 17.3460 E	Yes	2010	This study
Stubendorffbreen	Spitsbergen	NES	78.9623 N, 16.6063 E	Yes	2011	This study
Sven Ludvigbreen	Spitsbergen	NES	79.3868 N, 18.7860 E	Yes	2010	This study
Sørbreen	Spitsbergen	NES	79.4944 N, 15.9824 E	Yes	2010	This study
Tommelbreen	Spitsbergen	NES	79.4965 N, 18.6292 E	Yes	2010	This study
Tryggvebreen	Spitsbergen	NES	79.1081 N, 16.5216 E	Yes	2011	This study
Veitebreen	Spitsbergen	NES	79.1546 N, 18.8300 E	Yes	2011	This study
Veteranbreen	Spitsbergen	NES	79.3335 N, 17.3172 E	Yes	2010	This study
Wichefjelletbreen	Spitsbergen	NES	78.4673 N, 18.9005 E	Yes	2011	This study
*** NES-1**	Spitsbergen	NES	79.6632 N, 17.8133 E	Yes	2010	This study
*** NES-2**	Spitsbergen	NES	79.2160 N, 18.8140 E	Yes	2011	This study
*** NES-3**	Spitsbergen	NES	78.6239 N, 19.3801 E	Yes	2011	This study
*** NES-4**	Spitsbergen	NES	78.4485 N, 18.9460 E	Yes	2011	This study
*** NES-5**	Spitsbergen	NES	78.4241 N, 18.9752 E	Yes	2011	This study
Aldegondabreen	Spitsbergen	CS	77.9778 N, 14.1148 E	Yes	2008	This study
Arnicabreen	Spitsbergen	CS	78.2345 N, 16.6694 E	Yes	2009	This study
Bjarmebreen	Spitsbergen	CS	78.0136 N, 18.1316 E	Yes	2011	This study
Brombreen	Spitsbergen	CS	78.0215 N, 15.6459 E	Yes	2011	This study
Buckfallet Isrosa	Spitsbergen	CS	78.1874N, 18.6711 E	Yes	2012	This study
Gleditschfonna	Spitsbergen	CS	77.9116 N, 14.7254 E	Yes	2010	This study
Høgsnytbreen	Spitsbergen	CS	78.9828 N, 15.5752 E	Yes	2011	This study
Janssonbreen	Spitsbergen	CS	77.8965 N, 14.4408 E	Yes	2008	This study
Jinnbreen	Spitsbergen	CS	78.1580 N, 17.4489 E	Yes	2009	This study
Kalvdalsbreen	Spitsbergen	CS	77.9173 N, 15.1252 E	Yes	2010	This study
Kolfjellbreen	Spitsbergen	CS	77.8127 N, 14.9914 E	Yes	2010	This study
Kvitryggfonna	Spitsbergen	CS	78.0292 N, 17.0000 E	Yes	2009	This study
Königsbergbreen	Spitsbergen	CS	78.3455 N, 18.6477 E	Yes	2012	This study
Lumpbreen	Spitsbergen	CS	78.2147 N, 18.0001 E	Yes	2012	This study

Lusitaniabreen	Spitsbergen	CS	78.2762 N, 16.7359 E	Yes	2009	This study
Nord Aurdalsbre	Spitsbergen	CS	77.8776 N, 14.5069 E	Yes	2008	This study
Oppdalsbreen	Spitsbergen	CS	78.0913 N, 17.4344 E	Yes	2011	This study
Passbreen	Spitsbergen	CS	78.0236 N, 17.9641 E	Yes	2011	This study
Plogbreen	Spitsbergen	CS	78.0800 N, 16.1838 E	Yes	2009	This study
Rabotbreen	Spitsbergen	CS	78.2837 N, 18.0932 E	Yes	2012	This study
Rieperbreen	Spitsbergen	CS	78.1186 N, 16.1142 E	Yes	2009	This study
Rypefjellbreen	Spitsbergen	CS	77.9000 N, 15.1808 E	Yes	2010	This study
Sagabreen	Spitsbergen	CS	77.7797 N, 14.4454 E	Yes	2008	This study
Samuelssonbreen	Spitsbergen	CS	77.9229 N, 16.1613 E	Yes	2011	This study
Slottsbreen	Spitsbergen	CS	78.1000 N, 17.1358 E	Yes	2009	This study
Stakkbreen	Spitsbergen	CS	78.9891 N, 17.0427 E	Yes	2009	This study
Tavlebreen	Spitsbergen	CS	77.9797 N, 15.1509 E	Yes	2011	This study
Tellbreen	Spitsbergen	CS	78.2564 N, 16.2209 E	Yes	2009	This study
Tronisen	Spitsbergen	CS	78.1150 N, 17.0055 E	Yes	2009	This study
Tufsbreen	Spitsbergen	CS	78.0466 N, 15.6924 E	Yes	2011	This study
Tungebreen	Spitsbergen	CS	77.9621 N, 14.9511 E	Yes	2010	This study
Vardebreen	Spitsbergen	CS	78.0748 N, 13.9212 E	Yes	2010	This study
Vassdalsbreen	Spitsbergen	CS	77.8975 N, 15.0000 E	Yes	2010	This study
Vråbreen	Spitsbergen	CS	78.0640 N, 17.7310 E	Yes	2011	This study
Åbreen	Spitsbergen	CS	77.9786 N, 18.1834 E	Yes	2012	This study
*** CS-1**	Spitsbergen	CS	78.1021 N, 17.2846 E	Yes	2011	This study
*** CS-2**	Spitsbergen	CS	78.0878 N, 17.2759 E	Yes	2011	This study
*** CS-3**	Spitsbergen	CS	78.0610 N, 16.3409 E	Yes	2009	This study
*** CS-4**	Spitsbergen	CS	78.0566 N, 15.5613 E	Yes	2011	This study
*** CS-5**	Spitsbergen	CS	77.9301 N, 15.0891 E	Yes	2010	This study
Akkarbreen	Spitsbergen	SS	77.1178 N, 16.5029 E	Yes	2011	This study
Antoniabreen	Spitsbergen	SS	77.4979 N, 14.9345 E	Yes	2011	This study
Aspelinbreen	Spitsbergen	SS	77.7626 N, 16.7114 E	Yes	2011	This study
Austre Torellbreen	Spitsbergen	SS	77.1731 N, 15.1419 E	Yes	2011	This study
Bautabreen	Spitsbergen	SS	76.9693 N, 16.4203 E	Yes	2010	This study
Belopol'skijbreen	Spitsbergen	SS	76.6707 N, 16.5639 E	Yes	2010	This study
Berrklettbreen	Spitsbergen	SS	77.6458 N, 15.1486 E	Yes	2011	This study
Bordbreen	Spitsbergen	SS	77.1180 N, 17.0485 E	Yes	2011	This study
Brattisen	Spitsbergen	SS	77.6053 N, 16.1581 E	Yes	2011	This study
Chomjakovbreen	Spitsbergen	SS	76.9534 N, 16.3985 E	Yes	2010	This study
Crammerbreane	Spitsbergen	SS	77.4546 N, 14.4658 E	Yes	2011	This study
Disbreen	Spitsbergen	SS	77.5338 N, 16.4424 E	Yes	2011	This study
Elektrobreen	Spitsbergen	SS	77.7755 N, 16.7168 E	Yes	2011	This study
Emil'janovbreen	Spitsbergen	SS	77.3832 N, 17.2875 E	Yes	2011	This study
Fiskarbreen	Spitsbergen	SS	77.0952 N, 16.5512 E	Yes	2011	This study
Frysjabreen	Spitsbergen	SS	77.6843 N, 15.5620 E	Yes	2011	This study
Goësbreen	Spitsbergen	SS	76.8914 N, 15.9534 E	Yes	2010	This study
Greenbreen	Spitsbergen	SS	77.6757 N, 15.7673 E	Yes	2011	This study
Gåsbreen	Spitsbergen	SS	76.9084 N, 15.9462 E	Yes	2010	This study
Hansbreen	Spitsbergen	SS	77.0486 N, 15.6380 E	Yes	2011	This study
Hassingerbreen	Spitsbergen	SS	77.4548 N, 15.7579 E	Yes	2011	This study
Heimbreen	Spitsbergen	SS	77.4861 N, 15.3577 E	Yes	2011	This study
Hyrnebreen	Spitsbergen	SS	77.0436 N, 16.2108 E	Yes	2011	This study
Høegh-Omdalbreen	Spitsbergen	SS	77.6687 N, 15.8628 E	Yes	2011	This study
Innifonna	Spitsbergen	SS	77.6630 N, 18.1762 E	Yes	2012	This study
Instebreen	Spitsbergen	SS	77.6637 N, 15.3099 E	Yes	2011	This study
Isingbreen	Spitsbergen	SS	77.1136 N, 16.6453 E	Yes	2011	This study
Iwobreen	Spitsbergen	SS	77.0933 N, 16.2366 E	Yes	2011	This study
Jensenbreen	Spitsbergen	SS	77.2671 N, 14.5261 E	Yes	2011	This study
Juvbreen	Spitsbergen	SS	77.6770 N, 16.2832 E	Yes	2011	This study
Kambreen	Spitsbergen	SS	77.0028 N, 17.1670 E	Yes	2010	This study
Kanebreen	Spitsbergen	SS	76.9782 N, 17.2169 E	Yes	2010	This study
Keilhaubreen	Spitsbergen	SS	76.6567 N, 16.9368 E	Yes	2010	This study

Kolkbren	Spitsbergen	SS	77.6676 N, 15.1724 E	Yes	2011	This study
Krohnbreen	Spitsbergen	SS	77.0741 N, 16.2424 E	Yes	2011	This study
Kronglebreen	Spitsbergen	SS	76.8242 N, 16.6841 E	Yes	2010	This study
Krylbreen	Spitsbergen	SS	77.7139 N, 15.6663 E	Yes	2011	This study
Kvitskarvbreen	Spitsbergen	SS	77.6672 N, 16.1636 E	Yes	2011	This study
Langkollbreen	Spitsbergen	SS	77.3007 N, 14.5654 E	Yes	2011	This study
Leinbreen	Spitsbergen	SS	77.4674 N, 15.3231 E	Yes	2011	This study
Libreen	Spitsbergen	SS	77.3494 N, 14.6228 E	Yes	2011	This study
Lundbreen	Spitsbergen	SS	77.6906 N, 16.1556 E	Yes	2011	This study
Lyngebreen	Spitsbergen	SS	76.6249 N, 16.6661 E	Yes	2010	This study
Løyndbreen	Spitsbergen	SS	77.7161 N, 16.0964 E	Yes	2011	This study
Lågryggfonna	Spitsbergen	SS	77.3968 N, 15.6876 E	Yes	2011	This study
Mathiasbreen	Spitsbergen	SS	76.6192 N, 16.8096 E	Yes	2010	This study
Matrosbreen	Spitsbergen	SS	77.1872 N, 17.3211 E	Yes	2011	This study
Mettebreen	Spitsbergen	SS	77.8202 N, 17.2623 E	Yes	2011	This study
Mikaelbreen	Spitsbergen	SS	77.0235 N, 16.7754 E	Yes	2011	This study
Morsnevbreen	Spitsbergen	SS	77.6382 N, 17.5714 E	Yes	2011	This study
Märjelenbreen	Spitsbergen	SS	77.4582 N, 15.4927 E	Yes	2011	This study
Nannbreen	Spitsbergen	SS	77.1354 N, 15.2816 E	Yes	2011	This study
Niplibreen	Spitsbergen	SS	77.6806 N, 15.3006 E	Yes	2011	This study
Nobelbreen	Spitsbergen	SS	77.7528 N, 16.7297 E	Yes	2011	This study
Odessabreen	Spitsbergen	SS	77.0091 N, 16.9035 E	Yes	2011	This study
Olsokbreen	Spitsbergen	SS	76.7176 N, 16.4603 E	Yes	2010	This study
Professorbreen	Spitsbergen	SS	77.0292 N, 16.8717 E	Yes	2011	This study
Randbreen	Spitsbergen	SS	76.7243 N, 17.0848 E	Yes	2010	This study
Raudfjellbreen	Spitsbergen	SS	77.2131 N, 15.0549 E	Yes	2011	This study
Reidbreen	Spitsbergen	SS	77.6207 N, 15.8472 E	Yes	2011	This study
Renardbreen	Spitsbergen	SS	77.5248 N, 14.4608 E	Yes	2011	This study
Revtannbreen	Spitsbergen	SS	77.4806 N, 15.1397 E	Yes	2011	This study
Ringbreen	Spitsbergen	SS	77.5928 N, 15.9045 E	Yes	2011	This study
Rokkbreen	Spitsbergen	SS	77.5705 N, 16.5884 E	Yes	2011	This study
Ryggkollbreen	Spitsbergen	SS	77.6608 N, 16.0459 E	Yes	2011	This study
Rånebreen	Spitsbergen	SS	77.7547 N, 16.2147 E	Yes	2011	This study
Saksbreen	Spitsbergen	SS	77.3649 N, 14.4618 E	Yes	2011	This study
Signybreen	Spitsbergen	SS	76.9661 N, 16.6736 E	Yes	2010	This study
Skarvisen	Spitsbergen	SS	77.6883 N, 15.7014 E	Yes	2011	This study
Skilryggbreen	Spitsbergen	SS	77.0850 N, 15.3946 E	Yes	2011	This study
Smaleggbreen	Spitsbergen	SS	76.9624 N, 16.4995 E	Yes	2010	This study
Smaubreen	Spitsbergen	SS	77.6561 N, 15.1541 E	Yes	2011	This study
Sotryggfonna	Spitsbergen	SS	77.4439 N, 15.9043 E	Yes	2011	This study
Steindolpbreen	Spitsbergen	SS	77.7111 N, 16.2880 E	Yes	2011	This study
Stepanovbreen	Spitsbergen	SS	77.1819 N, 17.3608 E	Yes	2011	This study
Suessbreen	Spitsbergen	SS	77.4324 N, 15.7623 E	Yes	2011	This study
Svalisbreen	Spitsbergen	SS	76.9884 N, 16.6974 E	Yes	2010	This study
Svartkuvbreen	Spitsbergen	SS	76.6765 N, 16.9399 E	Yes	2010	This study
Sveitssarfonna	Spitsbergen	SS	77.4336 N, 15.5423 E	Yes	2011	This study
Svingobreen	Spitsbergen	SS	77.8593 N, 17.0624 E	Yes	2009	This study
Synshovdbreen	Spitsbergen	SS	77.6860 N, 15.4203 E	Yes	2011	This study
Sysselmannbreen	Spitsbergen	SS	77.6185 N, 16.0496 E	Yes	2011	This study
Tarmbreen	Spitsbergen	SS	77.5528 N, 16.2809 E	Yes	2011	This study
Tirolarbreen	Spitsbergen	SS	77.4143 N, 15.7255 E	Yes	2011	This study
Toppbreen	Spitsbergen	SS	76.6358 N, 16.9046 E	Yes	2010	This study
Tromsøbreen	Spitsbergen	SS	76.9203 N, 17.0899 E	Yes	2010	This study
Turrsjøbreen	Spitsbergen	SS	77.2852 N, 14.5353 E	Yes	2011	This study
Tverrbreen	Spitsbergen	SS	77.4091 N, 14.0907 E	Yes	2011	This study
Tvillingbreane	Spitsbergen	SS	77.4345 N, 15.9563 E	Yes	2011	This study
Vallotbreen	Spitsbergen	SS	77.6365 N, 15.1698 E	Yes	2011	This study
Vestre Torellbreen	Spitsbergen	SS	77.2410 N, 14.7490 E	Yes	2011	This study
Vinkelbreen	Spitsbergen	SS	77.8099 N, 17.2694 E	Yes	2011	This study

Vitkovskijbreen	Spitsbergen	SS	76.7630 N, 16.2557 E	Yes	2010	This study
Werenskioldbreen	Spitsbergen	SS	77.0760 N, 15.2968 E	Yes	2011	This study
Zimmerbreen	Spitsbergen	SS	77.6598 N, 16.0995 E	Yes	2011	This study
Øydebreen	Spitsbergen	SS	76.8801 N, 16.7438 E	Yes	2010	This study
*** SS-1**	Spitsbergen	SS	77.8563 N, 17.1765 E	Yes	2009	This study
*** SS-2**	Spitsbergen	SS	77.8518 N, 18.1172 E	Yes	2012	This study
*** SS-3**	Spitsbergen	SS	77.8018 N, 18.3916 E	Yes	2012	This study
*** SS-4**	Spitsbergen	SS	77.7475 N, 16.9520 E	Yes	2011	This study
*** SS-5**	Spitsbergen	SS	77.7238 N, 18.3158 E	Yes	2012	This study
*** SS-6**	Spitsbergen	SS	77.7055 N, 18.1346 E	Yes	2012	This study
*** SS-7**	Spitsbergen	SS	77.6928 N, 15.3311 E	Yes	2011	This study
*** SS-8**	Spitsbergen	SS	77.6695 N, 15.9858 E	Yes	2011	This study
*** SS-9**	Spitsbergen	SS	77.6305 N, 15.4804 E	Yes	2011	This study
*** SS-10**	Spitsbergen	SS	77.6054 N, 15.4785 E	Yes	2011	This study
*** SS-11**	Spitsbergen	SS	77.5951 N, 18.2430 E	Yes	2012	This study
*** SS-12**	Spitsbergen	SS	77.5676 N, 16.3176 E	Yes	2011	This study
*** SS-13**	Spitsbergen	SS	77.5582 N, 18.0639 E	Yes	2012	This study
*** SS-14**	Spitsbergen	SS	77.5170 N, 17.4817 E	Yes	2011	This study
*** SS-15**	Spitsbergen	SS	77.5097 N, 16.4449 E	Yes	2011	This study
*** SS-16**	Spitsbergen	SS	77.4925 N, 16.7066 E	Yes	2011	This study
*** SS-17**	Spitsbergen	SS	77.4727 N, 14.4167 E	Yes	2011	This study
*** SS-18**	Spitsbergen	SS	77.4671 N, 16.6816 E	Yes	2011	This study
*** SS-19**	Spitsbergen	SS	77.4436 N, 17.5652 E	Yes	2011	This study
*** SS-20**	Spitsbergen	SS	77.4304 N, 14.6441 E	Yes	2011	This study
*** SS-21**	Spitsbergen	SS	77.4273 N, 17.4473 E	Yes	2011	This study
*** SS-22**	Spitsbergen	SS	77.4218 N, 16.5615 E	Yes	2011	This study
*** SS-23**	Spitsbergen	SS	77.4187 N, 16.0174 E	Yes	2011	This study
*** SS-24**	Spitsbergen	SS	77.4051 N, 17.2470 E	Yes	2011	This study
*** SS-25**	Spitsbergen	SS	77.3666 N, 17.4962 E	Yes	2011	This study
*** SS-26**	Spitsbergen	SS	77.3236 N, 17.3886 E	Yes	2011	This study
*** SS-27**	Spitsbergen	SS	77.3137 N, 14.6709 E	Yes	2011	This study
*** SS-28**	Spitsbergen	SS	77.1726 N, 17.2446 E	Yes	2011	This study
*** SS-29**	Spitsbergen	SS	77.1268 N, 17.1259 E	Yes	2011	This study
*** SS-30**	Spitsbergen	SS	77.0214 N, 16.7055 E	Yes	2011	This study
*** SS-31**	Spitsbergen	SS	76.6998 N, 17.0249 E	Yes	2010	This study
*** SS-32**	Spitsbergen	SS	76.6523 N, 16.5996 E	Yes	2010	This study
Aldousbreen	Nordaustlandet	NA	79.8053 N, 20.7918 E	Yes	2010	This study
Hårdardbreen	Nordaustlandet	NA	79.6950 N, 21.2342 E	Yes	2010	This study
Augnebreen	Barentsøya	BEØ	78.5325 N, 21.8003 E	Yes	2010	This study
Besselsbreen	Barentsøya	BEØ	78.5405 N, 21.5850 E	Yes	2011	This study
Isormen	Barentsøya	BEØ	78.4432 N, 22.0414 E	Yes	2010	This study
Willybreen	Barentsøya	BEØ	78.4666 N, 22.0169 E	Yes	2010	This study
Albrechtbreen	Edgeøya	BEØ	77.9308 N, 23.1531 E	Yes	2010	This study
Blåisen	Edgeøya	BEØ	78.0286 N, 21.7325 E	Yes	2010	This study
Gandbreen	Edgeøya	BEØ	77.7234 N, 22.8646 E	Yes	2010	This study
Hartmannbreen	Edgeøya	BEØ	77.3669 N, 23.0081 E	Yes	2010	This study
Kuhrbrenosa	Edgeøya	BEØ	77.5664 N, 21.9544 E	Yes	2010	This study
Philippibreen	Edgeøya	BEØ	77.7347 N, 21.8529 E	Yes	2010	This study
Rutenbergbreen	Edgeøya	BEØ	77.8904 N, 23.4136 E	Yes	2010	This study
Schwerdtbreen	Edgeøya	BEØ	77.7102 N, 21.7063 E	Yes	2010	This study
Seidbreen	Edgeøya	BEØ	77.7882 N, 22.8182 E	Yes	2010	This study
Skarvbreen	Edgeøya	BEØ	77.6066 N, 22.2214 E	Yes	2010	This study
Svingeldalebreen	Edgeøya	BEØ	78.1321 N, 21.5417 E	Yes	2010	This study
Sydowbreen	Edgeøya	BEØ	77.5741 N, 21.2093 E	Yes	2010	This study
Veidebreen	Edgeøya	BEØ	77.6632 N, 22.2904 E	Yes	2010	This study
Vestre Edgeøyjoøkul	Edgeøya	BEØ	77.8676 N, 22.7269 E	Yes	2010	This study
*** BEO-1**	Edgeøya	BEØ	78.1668 N, 21.6518 E	Yes	2010	This study
*** BEO-2**	Edgeøya	BEØ	78.1441 N, 21.6086 E	Yes	2010	This study
*** BEO-3**	Edgeøya	BEØ	78.1427 N, 21.8600 E	Yes	2010	This study

*** BEO-4**	Edgeøya	BEØ	78.1330 N, 21.9397 E	Yes	2010	This study
*** BEO-5**	Edgeøya	BEØ	78.1215 N, 21.9460 E	Yes	2010	This study
*** BEO-6**	Edgeøya	BEØ	78.1032 N, 21.3793 E	Yes	2010	This study
*** BEO-7**	Edgeøya	BEØ	78.1022 N, 21.8918 E	Yes	2010	This study
*** BEO-8**	Edgeøya	BEØ	78.0396 N, 21.7253 E	Yes	2010	This study
*** BEO-9**	Edgeøya	BEØ	78.0322 N, 21.3216 E	Yes	2010	This study
*** BEO-10**	Edgeøya	BEØ	77.9829 N, 22.0968 E	Yes	2010	This study
*** BEO-11**	Edgeøya	BEØ	77.9139 N, 21.9787 E	Yes	2010	This study
*** BEO-12**	Edgeøya	BEØ	77.8771 N, 22.5644 E	Yes	2010	This study
*** BEO-13**	Edgeøya	BEØ	77.8376 N, 22.4845 E	Yes	2010	This study
*** BEO-14**	Edgeøya	BEØ	77.7006 N, 21.6279 E	Yes	2010	This study
*** BEO-15**	Edgeøya	BEØ	77.6989 N, 22.2611 E	Yes	2010	This study
*** BEO-16**	Edgeøya	BEØ	77.6916 N, 23.0239 E	Yes	2010	This study
*** BEO-17**	Edgeøya	BEØ	77.6424 N, 22.9717 E	Yes	2010	This study
*** BEO-18**	Edgeøya	BEØ	77.6304 N, 23.0828 E	Yes	2010	This study
***BEO-19**	Edgeøya	BEØ	77.6227 N, 21.5578 E	Yes	2010	This study
*** BEO-20**	Edgeøya	BEØ	77.5949 N, 21.4996 E	Yes	2010	This study
*** BEO-21**	Edgeøya	BEØ	77.5875 N, 23.8217 E	Yes	2010	This study
*** BEO-22**	Edgeøya	BEØ	77.5508 N, 23.7258 E	Yes	2010	This study
*** BEO-23**	Edgeøya	BEØ	77.5084 N, 23.1169 E	Yes	2010	This study
*** BEO-24**	Edgeøya	BEØ	77.4752 N, 23.1380 E	Yes	2010	This study